Electrochemical Society

UNIVERSITY
JAN 17 1956
SALT LAKE CITY

LIBRARY
UNIVERSITY OF UTAH

AS PARTNERS
IN YOUR PROGRESS

OUR EXTENSIVE RESEARCH – is a *plus* factor!

Our extensive program in carbon and graphite research is conducted by highly qualified chemists, physicists and technicians.

The scope of their specialized knowledge is a significant *plus factor* in the reliability that distinguishes GLC electrodes, anodes and mold stock.

The high degree of integration between discoveries in our research laboratories, refinements in processing raw materials and improved manufacturing techniques is further assurance of excellent product performance.

ELECTRODE GLC® DIVISION

Great Lakes Carbon Corporation

GRAPHITE ELECTRODES, ANODES, MOLDS and SPECIALTIES

ADMINISTRATIVE OFFICE: 18 East 48th Street, New York 17, N.Y. PLANTS: Niagara Falls, N.Y., Morganton, N. C. OTHER OFFICES: Niagara Falls, Oak Park, Ill., Pittsburgh, Pa. SALES AGENTS: J. B. Hayes Company, Birmingham, Ala., George O. O'Hara, Wilmington, Cal. SALES AGENTS IN OTHER COUNTRIES: Great Northern Carbon & Chemical Co., Ltd., Montreal, Canada; Great Eastern Carbon & Chemical Co., Inc., Chiyoda-Ku, Tokyo, Japan

EDITORIAL STAFF

R. M. Burns, *Chairman*
Cecil V. King, *Editor*
Norman Hackerman, *Technical Editor*
Ruth G. Sterns, *Managing Editor*
U. B. Thomas, *News Editor*
Natalie Michalski, *Assistant Editor*
Eleanor Blair, *Assistant Editor*

DIVISIONAL EDITORS

W. C. Vosburgh, *Battery*
J. V. Petrocelli, *Corrosion*
John J. Chapman, *Electric Insulation*
Abner Brenner, *Electrodeposition*
H. C. Froelich, *Electronics*
Herbert Bandes, *Electronics—Semiconductors*
Sherlock Swann, Jr., *Electro-Organic*
Irvin R. Kramer, *Electrothermics and Metallurgy, I*
A. U. Seybolt, *Electrothermics and Metallurgy, II*
W. C. Gardiner, *Industrial Electrolytic*
C. W. Tobias, *Theoretical*

REGIONAL EDITORS

Howard T. Francis, *Chicago*
Joseph Schulein, *Pacific Northwest*
J. C. Schumacher, *Los Angeles*
G. W. Heise, *Cleveland*
G. H. Fetterley, *Niagara Falls*
Oliver Osborn, *Houston*
Earl A. Gulbransen, *Pittsburgh*
A. C. Holm, *Canada*
J. W. Cuthbertson, *Great Britain*
T. L. Rama Char, *India*

ADVERTISING OFFICE

Jack Bain
Advertising Manager
545 Fifth Avenue
New York 17, N. Y.
PHONE—*Murray Hill 2-3345*

Journal of the
Electrochemical Society

JANUARY 1956 VOL. 103 • NO. 1

CONTENTS

Editorial

The Inevitable Quiz. *Herbert H. Uhlig* 5C

Technical Papers

Further Studies on the Anodic Corrosion of Lead in H_2SO_4 Solutions. *J. J. Lander* 1

Theoretical Electromotive Forces for Cells Containing a Single Solid or Molten Chloride Electrolyte. *Walter J. Hamer, Marjorie S. Malmberg, and Bernard Rubin* 8

Lead- and Manganese-Activated Cadmium Fluorophosphate Phosphors. *Robert W. Wollentin* 17

Dielectric Behavior of Electroluminescent Zinc Sulfides. *Willi Lehmann* 24

The System Cadmium Oxide-Boric Oxide, I. Phase Equilibria. *E. C. Subbarao and F. A. Hummel* 29

Time-Average Electroluminescence Output of Some Zinc Sulfide Phosphors. *Sol Nudelman and Frank Matossi* 34

Reactions of Refractory Silicides with Carbon and Nitrogen. *Leo Brewer and Oscar Krikorian* 38

The Fracture of Brittle Chromium by Acid Etching. *W. H. Smith* 51

Temperature Dependence of Hardness of the Equi-Atomic Iron Group Aluminides. *J. H. Westbrook* 54

Mathematical Studies on Galvanic Corrosion, IV. Influence of Electrolyte Thickness on the Potential and Current Distributions over Coplanar Electrodes Using Equal Polarization Parameters. *James T. Waber and Bertha Fagan* 64

Technical Feature

Electrochemical Corrosion in Nearly Neutral Liquids (Palladium Medal Address). *U. R. Evans* 73

Feature Section

Ulick Richardson Evans. *R. B. Mears* 9C

Current Affairs

San Francisco Meeting—April 29 to May 3, 1956 ..... 11C
Highlights of the Meeting of the Board of Directors 12C
Pittsburgh in Retrospect 14C
Division News 15C
Section News 16C
News Items 18C
New Members 19C
Personals 21C
Letters to the Editor 22C
Employment Situations 22C
Literature from Industry
New Products

Published monthly by The Electrochemical Society, Inc., Mount Royal and Guilford Aves., Baltimore 2, Md., combining the JOURNAL and TRANSACTIONS OF THE ELECTROCHEMICAL SOCIETY. Editorial offices: 216 West 102nd Street, New York 25, N. Y Statements and opinions given in articles and papers in the JOURNAL OF THE ELECTROCHEMICAL SOCIETY are those of the contributors, and The Electrochemical Society assumes no responsibility for them. Nondeductible subscription to members $5.00; subscription to nonmembers $18.00. Single copies $1.25 to members, $1.75 to nonmembers. Copyright 1956 by The Electrochemical Society, Inc. Entered as second-class matter November 15, 1947, at the Post Office at Baltimore, Md., under the act of August 24, 1912.

420980

Johnsonburg, Pa.

Administration Building
St. Marys, Pa.

Canadian Stackpole
Toronto

Plant No. 1
Kane, Pa.

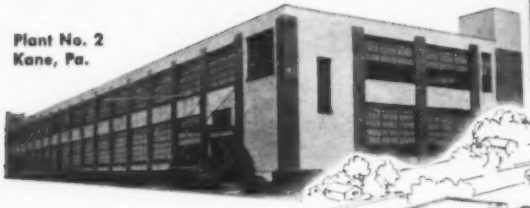

Plant No. 2
Kane, Pa.

Main plant
St. Marys, Pa.

Plant No. 2
St. Marys, Pa.

...THIS IS STACKPOLE

A dependable source for carbon, graphite, metal powder products

BRUSHES FOR ALL ROTATING ELECTRICAL EQUIPMENT
CARBON, GRAPHITE AND METAL POWDER CONTACTS
VOLTAGE REGULATOR DISCS • SEAL RINGS
POWER TUBE ANODES • CHEMICAL ANODES
PUMP VANES • FRICTION SEGMENTS • SPECTROGRAPHITE
CARBON RODS FOR SALT BATH RECTIFICATION
GROUND RODS • GRAPHITE NOZZLES
CARBON BEARINGS • CARBON MOLDS
WELDING AND BRAZING CARBONS . . . and specialties of all types.

FUTURE MEETINGS OF

The Electrochemical Society

San Francisco, April 29, 30, May 1, 2, and 3, 1956

Headquarters at the Mark-Hopkins Hotel

Sessions will be scheduled on

Corrosion (joint symposium with Theoretical),
Electric Insulation, Electronics (including Instrumentation, Luminescence,
Oxide-Cathodes, Phosphor Application, and Semiconductors),
Industrial Electrolytics, Electrothermics and Metallurgy,
and Theoretical Electrochemistry

* * *

Cleveland, September 30, October 1, 2, 3, and 4, 1956

Headquarters at the Statler Hotel

Sessions probably will be scheduled on

Batteries, Corrosion, Electrodeposition,
Electrothermics and Metallurgy, and Theoretical
Electrochemistry (joint with Electrodeposition)

* * *

Washington, D. C., May 12, 13, 14, 15, and 16, 1957

Headquarters at the Statler Hotel

* * *

Buffalo, October 6, 7, 8, 9, and 10, 1957

Headquarters at the Statler Hotel

* * *

New York, April 27, 28, 29, 30, and May 1, 1958

Headquarters at the Statler Hotel

* * *

Ottawa, September 28, 29, 30, October 1, and 2, 1958

Headquarters at the Chateau Laurier

* * *

Papers are now being solicited for the meeting to be held in Cleveland. Triplicate copies of each abstract (*not exceeding 75 words in length*) are due at the Secretary's office, 216 West 102nd Street, New York 25, N. Y., *not later than June 15, 1956* in order to be included in the program. *Please indicate on abstract for which Division's symposium the paper is to be scheduled.* Complete manuscripts should be sent in triplicate to the Managing Editor of the JOURNAL at the same address.

SARGENT SLOMIN

Motor-Stirred 5 Ampere

SARGENT HEAVY DUTY

Magnetically Stirred 15 Ampere

Designed for continuous trouble-free performance, these electrolytic analyzers, manufactured by E. H. Sargent & Co., are durably constructed of the highest grade materials and component parts, including stainless steel front panel, cast aluminum end castings and stainless steel fittings.

Completely line operated, the Sargent analyzers employ self-contained rectifying and filter circuits. The deposition voltage between the electrodes is adjusted by means of autotransformers, with meters indicating volts and amperes and controls on the panel. An easily replaceable fuse guards against circuit overload.

The Sargent-Slomin Analyzer stirs thorugh a rotating chuck operated from a capacitor type induction motor, motor having a fixed speed of 550 r.p.m. with 60 cycle A.C. current or 460 r.p.m. with 50 cycle A.C. current. Motors are sealed against corrosive fumes; are mounted on cast metal brackets, sliding on ½" square stainless steel rods, permitting vertical adjustment of electrode position over a distance of 4". Prelubricated ball-bearings support the rotating shaft.

The Sargent Heavy Duty Analyzer provides efficient stirring by the interaction between the cell current and the field established by a permanent magnet, tubular in shape and coaxial with the cell holder.

The Heavy Duty has recessed wells to hold the sample beakers, wells being 6¼" deep, designed to contain 250 ml electrolytic beakers. The wall of each well serves as an inner wall of the water jacket, for use in either heating or cooling. Two serrated nipples for rubber tubing connections for cooling or heating water are mounted on the right end casting. In plain copper analysis, 1 gram of copper may be deposited in 15 minutes with an accuracy of approximately 0.05% without the necessity of special techniques.

All electrolytic analyzers accommodate electrodes having shaft diameters no greater than 0.059 inch. Stainless steel spring tension chucks permit quick, easy insertion of the electrodes and maintain proper electrical contact. On the Heavy Duty Analyzer, the cathode chuck is eccentrically mounted, providing adjustability to accommodate electrodes up to 50 mm diameter. Special Sargent high efficiency electrodes are available for both analyzers.

Analyzers are complete with cord and plug for attachment to standard outlets. For operation from 115 volt, 50 or 60 cycle A.C. circuits.

	SARGENT-SLOMIN	HEAVY DUTY
Maximum D.C. current at each position	5 ampere	15 ampere
Maximum D.C. voltage at each position	10 volts	10 volts
Maximum power consumption	150* or 300 watts	400 watts
Height	18 inches	20¼ inches
Width	11¼* or 21 inches	21 inches
Depth	11¼ inches	11¼ inches
Net Weight	35* or 61 pounds	80 pounds
Shipping Weight	70* or 110 pounds	130 pounds

*One position unit

S-29459 ELECTROLYTIC ANALYZER — Motor Stirred, One Position, 5 Ampere, SARGENT-SLOMIN.....**$275.00**

S-29460 DITTO. But with adjustable sub-surface heater **$300.00**

S-29464 ELECTROLYTIC ANALYZER — Two Position, SARGENT-SLOMIN **$425.00**

S-29465 DITTO. But with two adjustable heaters, pilot lights and control knobs.....**$475.00**

S-29480 ELECTROLYTIC ANALYZER — Heavy Duty, Magnetically Stirred, Two Position, 15 Ampere, Sargent (illustrated top, right).....**$575.00**

SARGENT

SCIENTIFIC LABORATORY INSTRUMENTS • APPARATUS • SUPPLIES • CHEMICALS

Catalog No. 100 Now Available

E. H. SARGENT & COMPANY, 4647 W. FOSTER AVE., CHICAGO 30, ILLINOIS

MICHIGAN DIVISION, 8560 WEST CHICAGO AVENUE, DETROIT 4, MICHIGAN

SOUTHWESTERN DIVISION, 5915 PEELER STREET, DALLAS 19, TEXAS

SOUTHEASTERN DIVISION, 3125 SEVENTH AVE., N., BIRMINGHAM 4, ALA.

Editorial

The Inevitable Quiz

NUMEROUS PROBLEMS FACED regularly by all of us individually or collectively seem to have a never ending source. Each generation has had its full share of crises, so it appears, and this generation shows no signs of having been neglected. Whatever feeling of relief we may once have felt at school at the end of an examination period is tempered later by the knowledge that examinations continue long after graduation, the only difference being that the questions get more complex. As we face the New Year, for example, the problems presented to us on our "examination papers" certainly list many "stickers," some new and some old, and as usual there are no choices of answering a certain percentage of the whole; the choice is merely which one shall we answer first. It is of some significance to know that whatever progress we make as individuals, as a Society, or as nations depends on how effectively and conscientiously we solve each problem; there is also some comfort in knowing that with each adequate solution the rewards promise to be substantial.

In the current list of questions, the following stand out prominently:

1. How can atomic energy be used to improve the stature of mankind rather than to destroy him? (This is a hard one. Mankind did survive a similar problem ages ago when the use of fire was first discovered.)

2. What can be done to decrease the smog and noise hazards of modern cities? (Electrochemistry offers the promise of contributing toward the solution through future development of the fuel cell and improved storage batteries permitting smokeless power generation at much higher efficiencies, and the use of low-noise level, exhaust-free electric-driven automobiles and trucks.)

3. What steps should be taken for optimum use of our limited supplies of metals, water, wood, oil, and coal? How can we conserve the dwindling forest land upon which levels of rivers and lakes depend, and which alone remain as our primary source of clean drinking water? How can we convince industries and communities along waterways to preserve the assets which clean rivers provide for recreation and good health?

4. What steps can be taken to insure the continuation of sound business—will there be economic adjustments to present business levels, and, if so, how can we avoid serious unemployment? What is the magnitude of benefits to national business through helping our neighbors in foreign countries? What is the effect of the 200-fold increase in the national debt since 1900, and how will this debt eventually be satisfied without damaging our economy?

5. Will the United Nations succeed in uniting nations? How can we insure the evidence of peace on the horizon and avoid the murky skies of increased international tension? What language might we adapt and teach to everyone in order to improve international communication and understanding on the political and social levels comparable with reasonably good international understanding and faith among scientists and musicians?

(*Continued on next page*)

Editorial (*continued*)

6. What can be done to improve the education of our youth and to avoid the excess waste that characterizes particularly our secondary school educational system, and which deprives the world each year of many potential leaders and constructive thinkers? (See the pertinent editorials on this question in the November 1954 and April 1955 issues of the JOURNAL by the Chairman of our Publications Committee.)

There are many more questions after these are answered—the examination is not short or easy. All of us without exception are expected to contribute to the answers; there are no discounts offered to individuals on the basis of indisposure, headaches, or previous commitments. The answers can be postponed with a certain amount of calculated risk, but eventually the answers are demanded, and the possible consequences of default must be faced. The more the number of correct answers in good time, the better are the chances of lasting prosperity, good health, and general well being, if not hope for survival itself of the human race.

Electrochemistry offers important support in answer to several of the questions that are listed. In particular, it has already provided the electrostatic precipitator for eliminating the smoke nuisance, and has, furthermore, provided to some industries an additional source of income through recovery of stack wastes. Electrochemistry produces tons of chlorine for making water safe to drink. It offers substantial help to conservation programs through improved methods for corrosion control. By processes of electrorefining, it offers pure copper suitable for electrical conductors, and pure nickel for stainless steels and other corrosion resistant alloys. By processes of electrowinning, it promises almost unlimited supplies of aluminum and magnesium long after steel supplies may have dwindled and several of the nonferrous metals may have become too expensive as materials of construction or as electrical conductors. It will eventually make possible inexpensive supplies of titanium and zirconium for improved aircraft, nuclear power generators, and domestic hot water heaters and boilers. Electrochemistry, in other words, has made major contributions to our material standards of living and promises a great deal more in the future, all of which aids a world-wide sound economy.

The answers to purely social questions, which determine *how we shall use* rather than abuse the material advances that are placed at our disposal by science and engineering, must be answered by each of us as free thinking responsible individuals without regard to our profession, race, or nationality. Our moral obligation is consistently to cast our votes, direct and implied, without reservation and with full courage, for continuous social reforms that improve our surroundings, that support the brotherhood of man, and that cement world-wide peace and understanding.

—HERBERT H. UHLIG

Where voices are powered by the sun

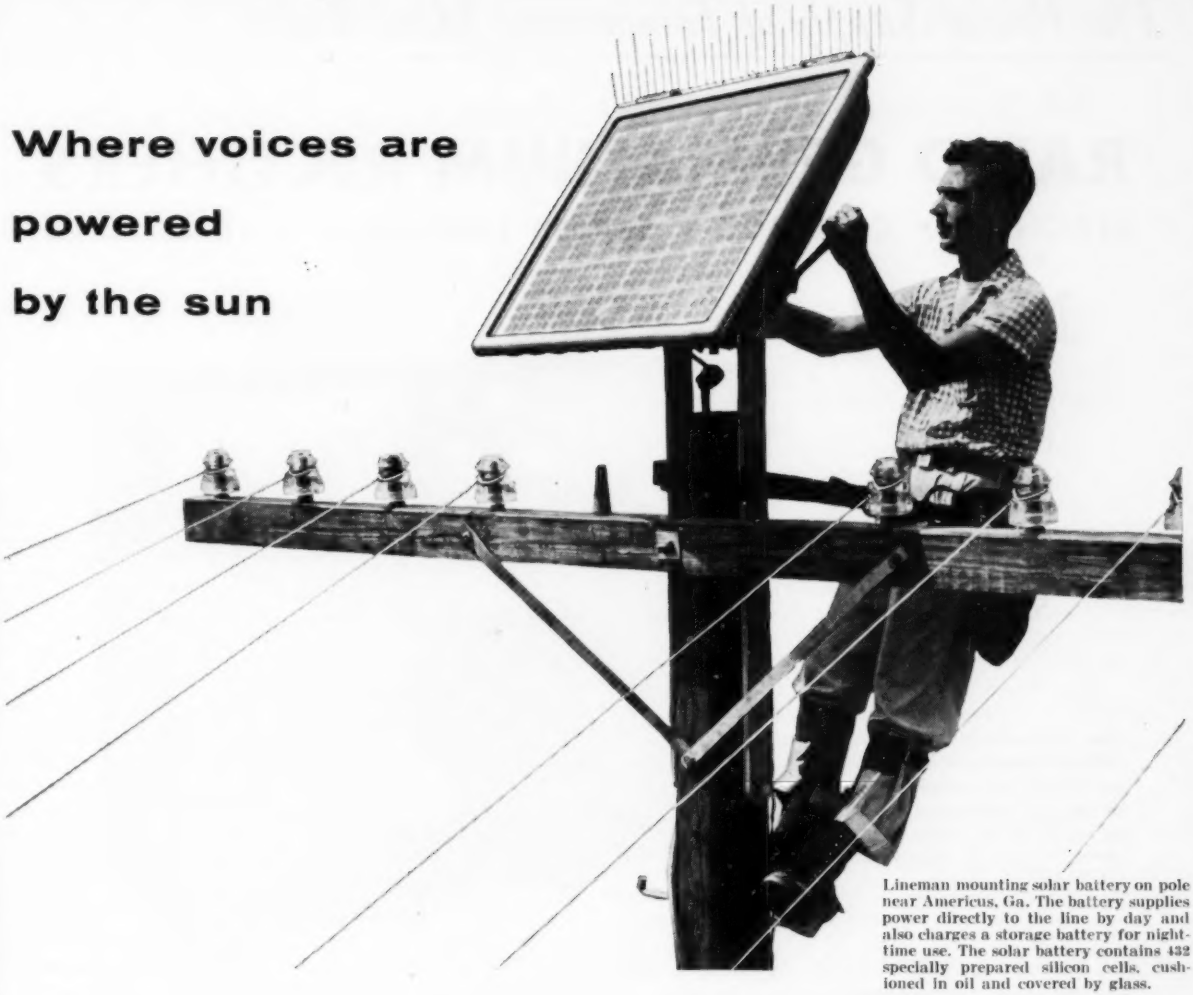

Lineman mounting solar battery on pole near Americus, Ga. The battery supplies power directly to the line by day and also charges a storage battery for night-time use. The solar battery contains 432 specially prepared silicon cells, cushioned in oil and covered by glass.

A new kind of telephone system developed by Bell Telephone Laboratories for rural areas is being operated experimentally by electric current derived from sunlight. Electric current is generated as sunlight falls on the Bell Solar Battery, which a lineman is seen adjusting in position.

The exciting achievement is made possible by two Laboratories inventions—the solar battery and the transistor. The new system uses transistors to the complete exclusion of electron tubes. Transistors require little power and this power can be easily supplied by the solar battery.

Compact and economical, the transistorized system can carry several voices simultaneously without interference. It has proved its ruggedness by standing up to heat, cold, rain and lightning. It promises more and improved telephone service for rural areas and it typifies the Laboratories' continuing efforts to make American telephony still better each year.

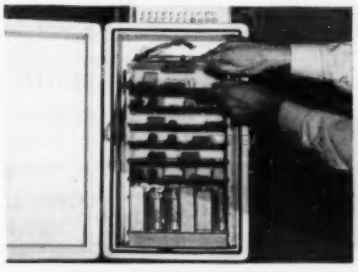

In sending and receiving terminals, transistors are used as oscillators, amplifiers and regulators, and for signaling.

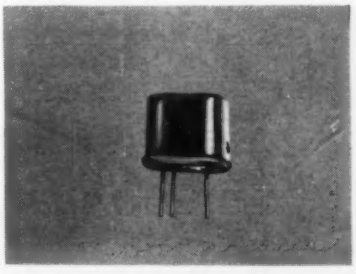

One of the transistors (actual size) used in the new system. New ideas, new tools, new equipment and new methods had to be developed for this project.

BELL TELEPHONE LABORATORIES

IMPROVING AMERICA'S TELEPHONE SERVICE PROVIDES CAREERS FOR CREATIVE MEN IN SCIENTIFIC AND TECHNICAL FIELDS

The Power Supply of Tomorrow—Here Today

RAPID GERMANIUM RECTIFIERS

EFFICIENT • COMPACT • SEALED JUNCTIONS • LONG LIVED

NOW!

New High Voltage Models
Up to 600 Volts
DC Output.

Higher Voltage on
Special Order.

The features of new Rapid GERMANIUM Rectifiers are proving to be the answer to many of the electrochemical industry's power problems. More than any other DC power supply, Rapid GERMANIUM Rectifiers answer the need for—

EFFICIENCY — 95% at full load

VOLTAGE STABILIZATION — ±1 volt from no load to full load

COMPACTNESS — require much less space than conventional units

SEALED JUNCTIONS — corrosion is kept out

PRECISE CONTROLS — oil immersed, fully motorized Inductrol controls, provide continuously variable control at the touch of a button

LONG-LIFE — no aging or change in characteristics even after accelerated full load tests

Find out more about RAPID GERMANIUM RECTIFIERS, "the power supplies of tomorrow — here today". Write to Rapid Electric Co., 2881 Middletown Road, New York 61, New York. Ask for Bulletin GE-2

THE NAME THAT MEANS *"More Power to You!"*

RAPID ELECTRIC COMPANY

Further Studies on the Anodic Corrosion of Lead in H_2SO_4 Solutions

J. J. Lander

Naval Research Laboratory, Washington, D. C.

ABSTRACT

Anodic corrosion of lead in sulfuric acid was studied in detail at potentials near the reversible $PbO_2/PbSO_4$ potential. Results indicate that the first step in the corrosion process was reaction of lead with water to form lead dioxide. The solid-phase reaction $Pb + PbO_2 = 2PbO$ probably occurred below a certain potential, and this reaction plus two electrochemical reactions rendered lead dioxide unstable at lower potentials. A potential was found at which the corrosion rate reached a sharp peak. Above this peak lead dioxide was found in the reaction product.

Kinetic treatment was only partially successful. In 30% acid, at potentials just below the reversible $PbO_2/PbSO_4$ potential, conversion of lead dioxide film to lead sulfate took place, and the rate of corrosion appeared to be controlled by diffusion of the electrolyte into the film. Above the reversible $PbO_2/PbSO_4$ potential, a protective lead dioxide film was formed, and a linear rate of corrosion was found which increased with increasing temperature and decreasing acid concentration.

Introduction

A previous paper showed results of corrosion of lead in sulfuric acid using constant potential techniques (1). The potential range of about 0.1–1.0 volt less noble than the reversible $PbO_2/PbSO_4$ potential was studied. More recently, corrosion was studied in detail at potentials near the positive plate potential, because at these potentials corrosion rates are more directly related to conditions of battery service. The primary aim of this work is to elucidate the thermodynamics and kinetics of the corrosion process, in the hope that results might indicate methods of preventing or slowing down corrosion, thus allowing longer positive grid life.

Theory

Thermodynamics

Standard electrode potentials for some reactions concerned in the electrochemistry of lead are given in Table I. The discussion to follow will tell what reactions are to be expected in the several potential ranges involved in the work.

The electrochemical couples H_2/H^+ and Hg/Hg_2SO_4 are included for reference. The oxidation of water to oxygen is theoretically reversible at 1.23 v, but actually it is subject to such a large overvoltage that oxygen production is not observed except at potentials several tenths of a volt more noble than the reversible potential for the $PbO_2/PbSO_4$ couple.

The potential limit of the reaction $Pb + PbO_2 = 2PbO$, which has been shown to take place in the solid phase (2), is placed at +1.58 v. It is believed that the occurrence of the reaction during anodization of lead and the potential at which it is limited may be inferred from the data of this paper. For purposes of discussion, it will be assumed here that the reaction does, in fact, occur below the potential given. Unlike electrochemical reactions, this potential is not a reversible one; it does not represent a point at which a net forward or reverse reaction begins. Rather, it may be rationalized that for the reaction to go, lead dioxide must take electrons away from the lead metal; if so, the possibility exists that lead can be polarized to some positive potential beyond which lead dioxide can no longer pull away electrons, effectively stopping the reaction. It is to be expected that this potential will not depend on the electrolyte concentration as do the reversible potentials for the other reactions.

The reaction $Pb + H_2SO_4 = PbSO_4 + 2H^+ + 2e$ occurs at the negative plate of the lead-acid cell. It has nothing to do with the corrosion process occurring at the positive plate of a battery, and it is given in the table for orientation purposes only. In a constant-current anodization process it would be the first reaction to occur.

The oxidation of lead to lead monoxide has been shown to occur at potentials more noble than +0.252 (1, 3), and lead monoxide (tetragonal) was found to be the principal reaction product up to potentials approaching the open-circuit value for the positive plate (1). Evidently, the lead sulfate coating formed on the outside protects the lead oxide film from rapid attack by the acid. At more noble potentials, the next reaction which can occur is the direct oxidation of lead to lead dioxide by water, $E_0 = +0.666$ v; and if the film is porous, the reaction would be expected to occur. It is to be noted that lead dioxide formation is possible a full volt below the reversible positive-plate potential. However, it is not stable below that potential, tending to react at the solution interface with sulfuric acid and hydrogen ion to give lead sulfate and lead monoxide, and at the metal interface to give lead monoxide by the solid-phase reaction. Above potential +1.100, corresponding to the reaction $PbO + H_2O = PbO_2 + 2H^+ + 2e$, lead dioxide would no longer be unstable due to reaction with hydrogen ion, but it would still be unstable on both the other counts. The fact that above this voltage

TABLE I. *Standard electrode potentials for various reactions*

Reaction	E_0
$Pb + H_2SO_4 = PbSO_4 + 2H^+ + 2e$	−0.355
$H_2 = 2H^+ + 2e$	0
$Pb + 2H_2O = Pb(OH)_2 + 2H^+ + 2e$	+0.242
$Pb + H_2O = PbO + 2H^+ + 2e$	+0.252
$2Hg + H_2SO_4 = Hg_2SO_4 + 2H^+ + 2e$	+0.616
$Pb + 2H_2O = PbO_2 + 4H^+ + 4e$	+0.666
$PbO + H_2O = PbO_2 + 2H^+ + 2e$	+1.100
$2H_2O = O_2 + 4H^+ + 4e$	+1.230
$Pb + PbO_2 = 2PbO$ (Solid phase, voltage limit of)	+1.58
$PbSO_4 + 2H_2O = PbO_2 + H_2SO_4 + 2H^+ + 2e$	+1.684

lead monoxide is found to be the chief product (1) shows that the corrosion process goes by direct oxidation to lead monoxide or by oxidation to lead dioxide followed by the solid-phase reaction. The possible reaction $PbO + H_2O = PbO_2 + 2H^+ + 2e$ does not go to any appreciable extent; otherwise, either lead dioxide would be found in the reaction product or lead sulfate would be the chief product. X-ray analysis indicates only lead monoxide and lead sulfate, and the reaction corresponds to Faraday's Law for $Pb = Pb^{++} + 2e$ (1).

At more noble potentials, if the primary reaction is oxidation of lead to lead dioxide, then lead dioxide should become evident in the reaction product as the potential passes the value +1.58. It should occur along with lead sulfate, lead oxide no longer being present. Finally, above the reversible $PbO_2/PbSO_4$ potential, PbO_2 should be the sole solid product.

Kinetics

When a nonporous film is formed, either a linear or a parabolic rate law may apply, depending on whether the rate is limited by reaction at one of the interfaces (4) or by migration of ions through the film (5).

Evans (6) considered mechanical breakdown of films growing in gaseous media and showed that if breakdown of a continuous film produces cracks too fine to allow the oxidizing medium to reach the metal surface, then migration of ions along the cracks should take place at an enhanced rate, the parabolic law being retained. If breakdown results because of blister formation, and the blister walls are impervious to the oxidant, then the flat cavities resulting constitute barriers to migration, and a logarithmic relationship between film weight and time is exhibited. In this case, it may be noted that breakdown results in a lower rate than a continuous film would provide. Analogous rate-controlling factors can be envisioned for electrochemical film-forming processes.

If the film is porous, the situation is by no means clear-cut, and rate laws are difficult to derive because they depend on the modes of crystallization and growth of the film substance. However, if the pore area becomes constant after a time, then the mathematical treatment is simplified, and linear or parabolic equations for the rate may be derived. A linear relation would be expected if the intrinsic rate of the reaction at the metal surface is controlling. In this case, the rate constant would be small enough that rates would not be limited by diffusion. Parabolic equations result if the rate is diffusion-controlled or if the film growth is limited by resistance of the electrolyte in the pores of the film.

Evidently, there are several mechanisms that can each lead to parabolic and linear w vs. t relationships; for data which fit either form, the form would not be sufficient to characterize the mechanism. Choice among mechanisms would have to be made on the basis of constants of the equations. This could be difficult because of lack of knowledge of the values of some of the constants concerned, e.g., pore area.

Experimental

Samples of lead were corroded at various constant potentials near the reversible $PbO_2/PbSO_4$ potential. The method, apparatus, and techniques employed have been described previously (1). Single samples were used for voltages below the $PbO_2/PbSO_4$ potential, and these were corroded for times up to 72 hr. Corrosion current was recorded, the films were stripped, and weight losses were determined. The weight-loss results were checked against values calculated from Faraday's Law and the current-time trace.

For rate determinations above the $PbO_2/PbSO_4$ potential, longer times were necessary to enable an estimate of the rate; furthermore, some of the current went to oxygen evolution so current could not be used to measure rates. Consequently, four or five samples were used. These were removed from the corrosion cell one at a time over a week or so, stripped in an alkali-hydrazine-mannitol bath, and weight losses were determined. Results were plotted against time, and slopes of the curves were measured to get rates.

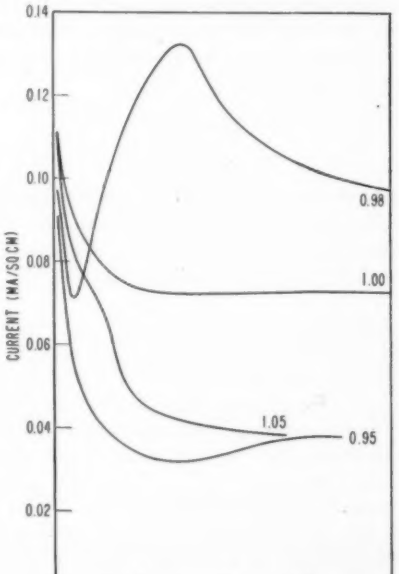

FIG. 1. Corrosion current vs. time in 30% acid at several potentials below the reversible $PbO_2/PbSO_4$ potential (1.100 volt).

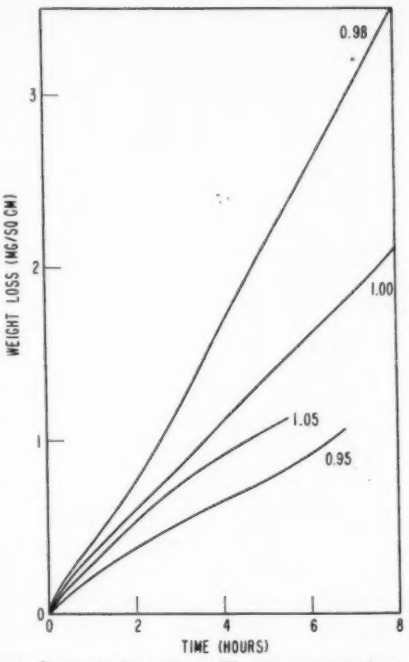

FIG. 2. Current data from Fig. 1 converted to weight loss.

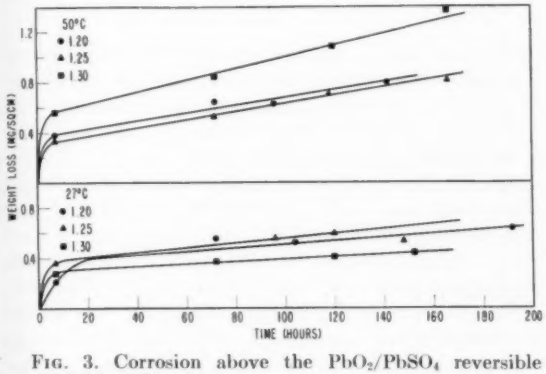

FIG. 3. Corrosion above the $PbO_2/PbSO_4$ reversible potential in 30% acid.

All potentials were measured against an Hg/Hg_2SO_4 reference electrode in the electrolyte of the anodizing cell.

RESULTS

Corrosion current data at room temperature were obtained at potentials ranging from about 0.2 v below the $PbO_2/PbSO_4$ reversible potential to as high as 0.20 v above, in acid strengths of 1%, 10%, 30%, and 40% by weight. Weight losses were obtained for these samples by stripping to check against those calculated from Faraday's Law. Fig. 1 shows a typical set of current curves at various potentials[1] for the 30% acid. At some potentials both divalent and tetravalent corrosion products were formed, in which case the weight loss measurement

[1] To save space, the data for each concentration of acid are not given. Complete data can be found in NRL Report 4475.

TABLE II. *Corrison rates above the* $PbO_2/PbSO_4$ *potential*

% Acid	Voltage	Penetration rate (cm/yr)	
		30°C	50°C
10	1.15	3.0×10^{-3}	3.5×10^{-3}
	1.20	4.2	4.3
	1.25	3.0	7.7
30	1.125	1.5	—
	1.20	1.2	2.1
	1.25	1.3	2.4
	1.30	0.9	3.9
40	1.25	0.4	1.5
	1.30	—	2.8
	1.35	0.9	3.3

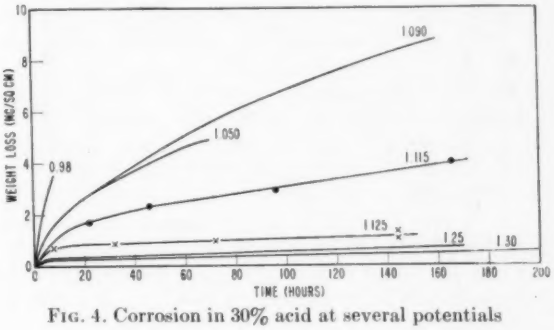

FIG. 4. Corrosion in 30% acid at several potentials

enabled estimation of current distribution between the two kinds of products. Weight loss curves calculated for Fig. 1 data are shown in Fig. 2. When lead dioxide is present only the final weight loss is exact, because the fraction of current going to each valence state was not constant with time, as was assumed in calculating the curves. This will be shown in subsequent data. Nevertheless, the weight-loss curves do give a good idea of the effect of potential.

A typical set of curves for corrosion above the $PbO_2/PbSO_4$ potential is shown in Fig. 3. Data were also obtained for 10% and 40% at both temperatures. The penetration rates calculated from slopes of the linear portions of the curves are given in Table II.

To obtain the corrosion rate vs. voltage relationship in still finer detail just above the $PbO_2/PbSO_4$ potential, additional runs were made in 30% acid at 1.115 and 1.125 v. Data are shown in Fig. 4, which includes data from Fig. 2 and 3 for comparison. This set of curves suggested the possibility of an inflection in the rate vs. potential curve just below the $PbO_2/PbSO_4$ potential, so this range was studied in greater detail for 30% acid.

In this case, several single samples were run for various times at a given constant potential and stripped to obtain weight loss. Current was measured vs. time to enable determination of the effect of time on the distribution of products between di- and tetravalent compounds. Fig. 5 shows a typical set of data for 1.100 and 1.108 v. Data were also obtained at potentials of 1.050, 1.075, and 1.090.

DISCUSSION

The data of this paper and the previous paper (1) may be combined to give a plot of corrosion rate vs. potential

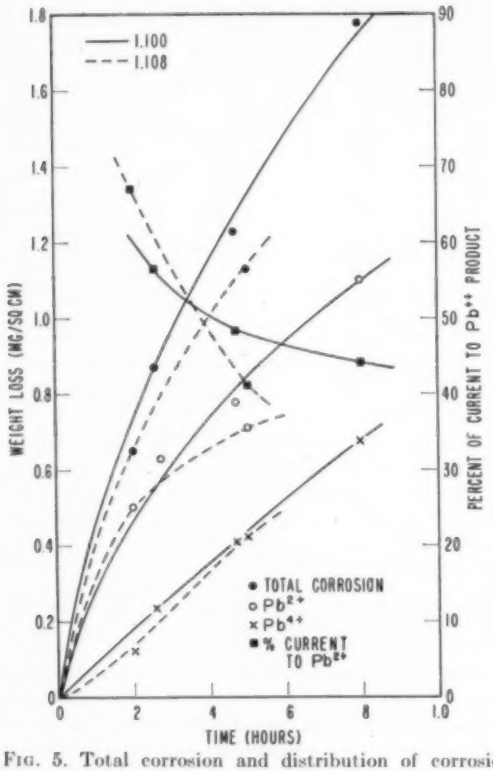

FIG. 5. Total corrosion and distribution of corrosion products in 30% acid at two potentials.

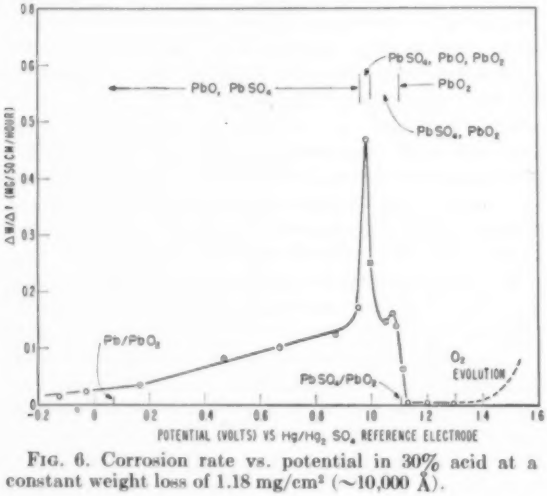

FIG. 6. Corrosion rate vs. potential in 30% acid at a constant weight loss of 1.18 mg/cm² (~10,000 Å).

over the range −0.134 to +1.30 v. This is shown for 30% acid at room temperature and a constant weight loss of 1.18 mg/cm² in Fig. 6. The reaction products found over the various potential ranges are also shown.

It was previously suggested (1) that corrosion below the peak of the curve was governed by an activated process and that the reaction involved was $Pb + H_2O = PbO + 2H^+ + 2e$. A different treatment of the data (7) indicated that the primary reaction is formation of lead dioxide above the potential +0.666 (on the hydrogen scale), and that polarization in the linear range above that point corresponds to *IR* drop through a porous lead monoxide film. Lead monoxide was formed because the lead dioxide is unstable on the several counts discussed in the theoretical section of this paper.

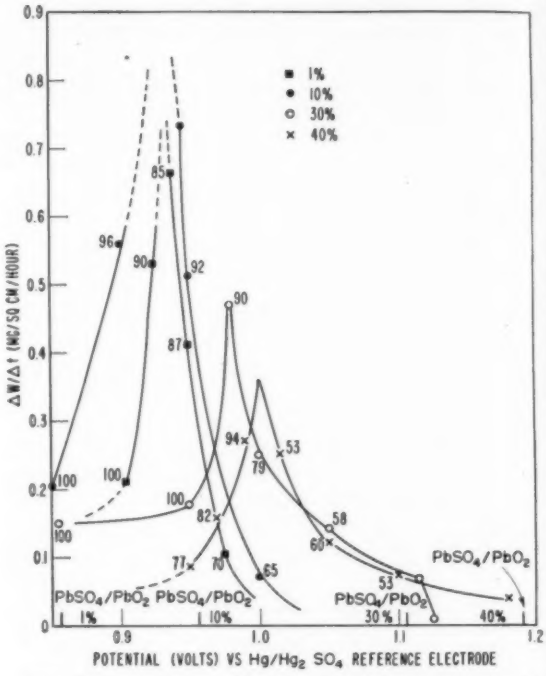

FIG. 7. Rate of corrosion vs. potential for several acid strengths at a constant weight loss of 1.18 mg/cm².

Actually, for a cell in any kind of service, the voltage range below some potential in the neighborhood of the peak of the curve is not of interest in the practical corrosion problem inasmuch as rates are not controlled by the same mechanism on either side of the peak. Positive-plate voltages, even in a cycling cell, do not drop below the voltage of the peak, except perhaps for short times only on a deep discharge or a high-rate discharge.

Data taken for the 1%, 10%, 30%, and 40% electrolytes, such as shown in Fig. 1 and 2, cover the voltage range of the peak of the corrosion curve. From that data, curves shown in Fig. 7 were obtained by plotting the slopes of the weight-loss curves at a constant value of weight loss against potential. The estimated per cent of current going to form divalent product is given by the number at each point. The reversible potential values for $PbO_2/PbSO_4$ couples are shown on the potential axis.

As voltage increased, a steep rise in the rate took place when lead dioxide became evident in the reaction product. It was not found in quantity, however, until the peak was passed and rates fell off sharply.

Attention may be directed to several features of these curves. First, the positions of the peaks have nothing to do with the location of the reversible $PbO_2/PbSO_4$ potentials, being found below by varying amounts in the stronger acids, but above in the 1% electrolyte. Second, the chief products of reaction on the low voltage side of

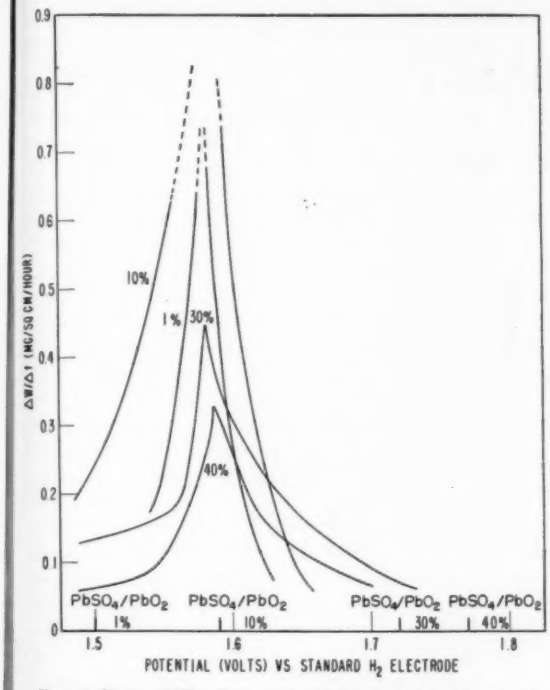

FIG. 8. Data of Fig. 7 vs. potential referred to the standard hydrogen electrode.

the peaks were lead monoxide and lead sulfate. Third, in the case of the 1% electrolyte, the chief reaction product was lead monoxide even at 0.1 v higher than the reversible $PbO_2/PbSO_4$ potential. Fourth, as shown in Fig. 8, positions of all the peaks fall at the same potential, regardless of acid concentration, when rate is plotted vs. potential referred to the standard hydrogen electrode; in other words, the position of the peaks does not vary with voltage.

It was shown in earlier work (2) that lead dioxide undergoes a solid-phase reaction with lead to form lead monoxide. It was suggested then that on discharge the lead dioxide formed during the previous charge might give this reaction with the grid metal and so contribute to corrosion in a cycling cell. It is now suggested that the maximum in the rate curves, illustrated in Fig. 8, corresponds very nearly to the potential above which the solid-phase reaction won't go, as discussed in the theory. Although no direct evidence is available to prove this, it seems to fit in with the experimental data,[2] especially the two facts that the potential of the peak does not vary with concentration, and that lead monoxide is the chief reaction product in 1% acid at voltages beyond the reversible $PbO_2/PbSO_4$ potential.

The picture now seems clear: lead dioxide is formed in the initial corrosion reaction at the metal surface at voltages well below the $PbO_2/PbSO_4$ reversible potential; being unstable, it goes to lead monoxide and lead sulfate at voltages below the peak, and to lead sulfate at voltages above the peak but below the $PbO_2/PbSO_4$ voltage, where the solid-phase reaction cannot go. Just below the peak the highly resistant lead monoxide film ceases to be the dominant rate-controlling factor, as lead dioxide begins to appear, breaking up the lead monoxide film.

It is now evident from Fig. 7, that the suggestion offered before (2), i.e., on discharge the solid-phase reaction contributes to the corrosion process, must be modified because polarization to the extent of 0.15–0.25 v is required. This does not occur except on high-rate discharges or discharges beyond the knee of the curve. Consequently, it is to be expected that, for cells in ordinary operation, lead dioxide will always be found next to the metal surface, and that the characteristics of this PbO_2 film will be important in determining corrosion rates.

The most important characteristic of the lead dioxide film is obvious from the thermodynamic and the corrosion rate vs. potential data: on discharge the lead dioxide film, which forms an effective barrier to corrosion during the previous charge, is converted to lead sulfate, and corrosion by the reaction $Pb + 2H_2O = PbO_2 + 4H^+ + 4e$ proceeds.

The factors which control rates at discharge potentials can be determined from data exemplified by Fig. 5, for the 30% acid. In Fig. 9, all the data taken at the several

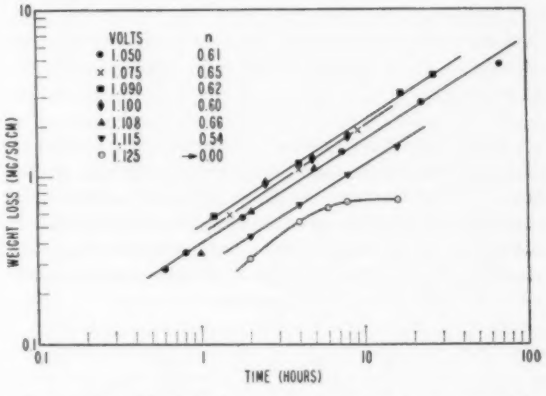

FIG. 9. Total weight loss vs. time at various potentials in 30% acid.

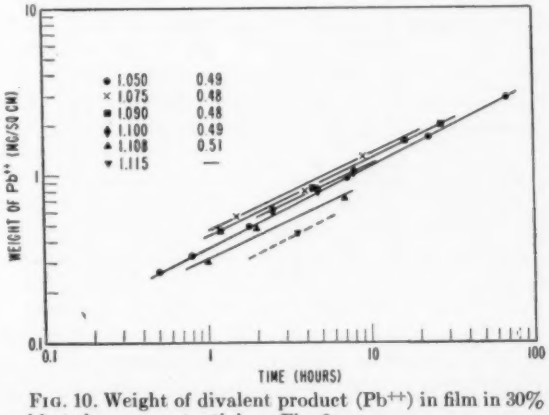

FIG. 10. Weight of divalent product (Pb^{++}) in film in 30% acid at the same potentials as Fig. 9.

[2] Additional evidence is given by our unpublished data which show that a 4½% tin alloy of lead does not exhibit the peak in the rate curve. This alloy does not undergo the solid-phase reaction to any appreciable extent.

potentials are plotted as total weight loss vs. time on a log log scale. Slopes of these curves all lie close to 0.6. Data for the formation of divalent product are plotted on a log log scale in Fig. 10. Slopes of these curves all lie close to 0.5, and the experimental equation for the formation of $PbSO_4$ is $w = kt^{1/2}$ and the data are accurately parabolic. This suggests that the rate of conversion of the underlying lead dioxide is diffusion-controlled. It has been shown (7) that a diffusion-controlled process fits the constants of the parabolic equation. It can be shown that control by a solid film or by the electrical resistance of a porous film results in unreasonable values for the constants in either case.

The conversion reaction tends to keep the lead dioxide from building up to thicknesses at which it becomes protective. At the same time, total corrosion proceeds somewhat faster than the conversion reaction because the latter actually undercuts some lead dioxide and isolates it electrically (Fig. 11), so it can not go to lead sulfate. This process allows quantities of lead dioxide larger than necessary for a protective film to be present in the reaction product, as can be seen by comparing Fig. 3 and 5. Therefore, it is not quite the rate of conversion of the lead dioxide film which limits the over-all rate, but, more exactly, it is the rate of penetration of the conversion process into the underlying film.

If the rate of corrosion at constant weight loss is plotted vs. potential, the curve shown in Fig. 12 is obtained. Numbers at the points show per cent of current going to divalent product. Ordinarily, the curve would be expected to follow the course of the dotted line as the concentration gradient of sulfate ion approaches the maximum value allowed by the concentration in the body of the solution. The rapid rise in the rates below about 1.025 v is indicative of a new reaction, i.e., the solid-phase reaction. The rate goes up because the underlying lead dioxide film is attacked from the metal side as well as the solution side, rendering the film more porous. The reason for the minimum at 1.050 v is not understood.

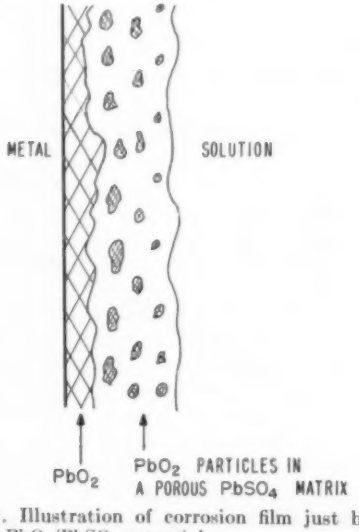

FIG. 11. Illustration of corrosion film just below the reversible $PbO_2/PbSO_4$ potential.

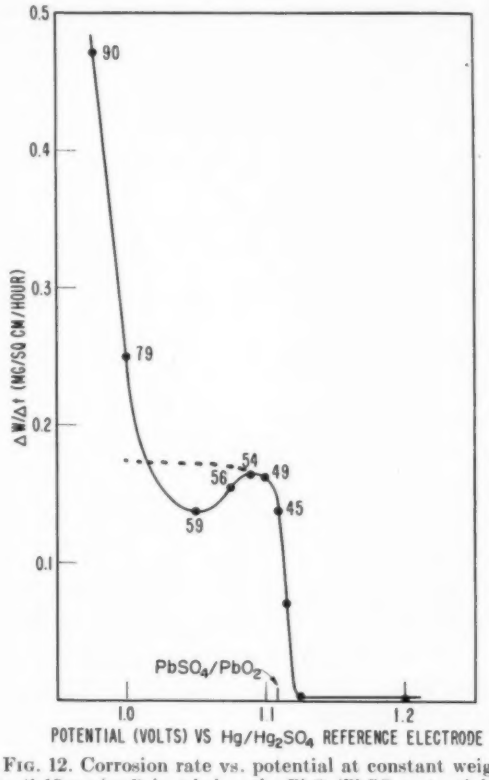

FIG. 12. Corrosion rate vs. potential at constant weight loss (1.18 mg/cm²) just below the $PbO_2/PbSO_4$ potential.

It seems that, above the $PbO_2/PbSO_4$ reversible potential, data are insufficient during the time of rapid film formation to characterize the mechanism definitely. Table II and Fig. 3 show the rates, determined from the linear portions of the curves, as a function of potential, acid strength, and temperature. There seems to be a trend toward higher rates at higher temperatures and lower acid concentrations. The effect of potential is uncertain, but must be small, from the data for 30% acid at 30°C.

Data of Fig. 3 show that something occurs in the lead dioxide film which slows down the rate quite sharply after an initial period of rapid film growth. This might be a case of blistering such as proposed by Evans (6). At any rate, the linear w vs. t curve and the very low rate for the thin films concerned imply ionic diffusion through a continuous film.

Discussion in Terms of Battery Service

Corrosion in cells on float may proceed at the very low rates of 1–3 × 10^{-3} cm penetration/year for pure lead. The data of Table II indicate that some life might be gained for batteries on float by changing to acids stronger than are usually employed (~30%). It is also indicated that the positive plate can be maintained over a rather wide range of potential (e.g., 1.125–1.30 for 30% acid at 30°C) without much effect on corrosion rate, so rigid voltage control might not be necessary. If these tests were extended to considerably longer times, however, small differences in rate might become apparent. These

could be appreciable in their effect on the life of a cell which is measured in terms of years.

In the past, antimonial alloys were used for grids of cells in float service, as for other types of service. Recently, it has been indicated that a binary alloy of calcium and lead might be more suitable for float service (8). With the antimonial alloys, float voltages were governed by the necessity for supplying enough current to the negative plates to keep them in good condition. With the calcium alloy the negative plate is no longer a problem, and, at the same float voltages, much smaller currents [of the order of $\frac{1}{10}$–$\frac{1}{70}$ (9)] will suffice for the negative plate. With lower currents, there may be danger that the positive-plate voltage will fall below the protective range. In such an event, higher float voltages than were used for the antimonial cells would be necessary to obtain the life increase expected of this alloy. Long-term tests should be run to determine whether a corrosion-rate minimum exists in the protective potential range.

Dropping down on the voltage scale, the next potential range for consideration is one in which the automobile battery operates. That is to say, it alternates between a stand condition and float, with short high-rate charge and discharge periods. The times on charge and discharge are relatively short and probably may be neglected in considering life.

It appears from Fig. 12 that the life of positive grids of automobile batteries should approach that of the same batteries on float, the life being shortened somewhat by the time spent on stand, during which time the positive-plate potential will be located somewhere on the steep portion of the curve at the reversible $PbO_2/PbSO_4$ potential. If most of the stand time were spent at the bottom of this steep curve, then the reduction in life should be small—a likely condition for batteries of cars that are run daily, because it takes an appreciable time for the positive-plate voltage to fall to the open-circuit value after a charge.

A peculiarity of automobile-battery service may be expected to become important as the end of life approaches, i.e., the constant-voltage charge. As the cell gets older, the hydrogen overvoltage at the negative plate falls off for batteries with antimonial grids, which means that the positive-plate voltage increases proportionately; when this voltage gets in the gassing range, faster corrosion during the time the car is running will ensue, hastening the end of life. Furthermore, the time spent at these higher voltages will be longer because the negative-plate voltage come-up will be sluggish, with the same effect.

Batteries which operate under a cycling program, such as industrial truck and submarine batteries, spend an appreciable part of their life on discharge; and during discharge, positive-plate potentials will be well up on the steep portion of the curve. This is unquestionably the reason why batteries in cycling service have relatively short lives in comparison with batteries in other types of service.

Because corrosion during discharge is limited by the rate of diffusion of acid into the corrosion film, it is to be expected that, as the film builds up in thickness, the rate at which acid can diffuse to the corroding surface will slow down, until eventually it becomes less than the linear rate observed for stand conditions. Then the rate of corrosion under cycling conditions should become the same as that for the linear rate on float, which does not depend on film thickness. This has been observed (10).

The theory presents two obvious methods of attack on the problem; the diffusion coefficient can be made smaller by increasing the viscosity, and possibly the diffusion path could be made tortuous or the pore area smaller. Lowering the diffusion coefficient is not a solution, because it would result in lower rates and energies which could be drawn from the cell, inasmuch as the active material discharge depends on this factor. The viscosity of the electrolyte could be increased by increasing the acid strength, and lower initial corrosion rates are actually found in the stronger electrolytes (2, 10). However, such an expedient can be utilized to a limited extent only, before the negative plate begins to show decreased capacity (11). In addition, although initial corrosion rates are higher in low-gravity acids, they slow down much faster, and after a time the corrosion rate in the high-gravity acid becomes larger (10, 12). On the whole, it is concluded that not much is to be gained in this way. Methods of affecting pore area and path length are not immediately evident. Apparently, what must be found is some method or trick of selectively preventing the normal discharge reaction from taking place at the lead dioxide coating on the grid.

Summary

Anodic corrosion of lead in sulfuric acid was studied in detail near the positive-plate reversible potential using constant-potential techniques. In general, it is indicated that the electrochemical reactions expected on the basis of thermodynamic data occur at their proper potentials. There are several of these reactions, and in addition chemical reactions also occur.

Mechanisms governing rates have not been determined in all the potential ranges concerned; indeed, the whole picture is rather complicated because of the number of reactions occurring.

Data for the several voltage ranges may be interpreted more specifically to show:

1. Formation of lead dioxide by the reaction $Pb + 2H_2O = PbO_2 + 4H^+ + 2e$ is the first step in the corrosion process above the reversible potential for that reaction. It is unstable both on chemical and electrochemical grounds at the lower potentials and goes to lead monoxide and lead sulfate.

2. A voltage limit above which the solid-phase reaction $Pb + PbO_2 = 2PbO$ cannot go has been shown to be about +1.58 v to the standard hydrogen electrode. This voltage marks the appearance of lead dioxide in the corrosion product and is characterized by a peak in the corrosion-rate vs. potential curve which separates the kinetic behavior of the corrosion processes. At more noble potentials, just below the reversible positive-plate potential, corrosion rates are limited by penetration of the positive plate discharge reaction into an underlying lead dioxide

film. This penetration is controlled by diffusion of $SO_4^{=}$ through a porous film of mixed lead dioxide and lead sulfate. At slightly less noble potentials, diffusion control gives way to a relatively rapid process because the solid-phase reaction begins to take place and the lead dioxide film is attacked from both sides.

3. Above the reversible $PbO_2/PbSO_4$ potential, corrosion rates fall off very rapidly to extremely low values, because a protective lead dioxide film is built up. Rates in this potential range do not vary with potential at room temperature within experimental error, but they do increase with increasing temperature and decreasing acid concentration.

Gains in knowledge of the corrosion process resulting from this work do not appear to indicate definite means of slowing down corrosion for cells in cycling service. The possibility of slowing corrosion in floating cells by increasing the electrolyte concentration is indicated.

Manuscript received May 20, 1955. Most of the data in this paper was presented at the Boston Meeting, October 3 to 7, 1954.

Any discussion of this paper will appear in a Discussion Section to be published in the December 1956 JOURNAL.

REFERENCES

1. J. J. LANDER, *This Journal*, **98**, 213 (1951).
2. J. J. LANDER, *ibid.*, **98**, 220 (1951).
3. E. F. WOLF AND C. F. BONILLA, *Trans. Electrochem. Soc.*, **79**, 307 (1941).
4. N. E. MOTT AND R. W. GURNEY, "Electronic Processes in Ionic Crystals," p. 250, Clarendon Press, Oxford (1940).
5. C. WAGNER, *Z. Physik. Chem.*, **B32**, 447 (1936); T. P. HOARE AND L. E. PRICE, *Trans. Faraday Soc.*, **34**, 867 (1938).
6. U. R. EVANS, "An Introduction to Metallic Corrosion," Edward Arnold, London (1948). *See also* U. R. EVANS, *Trans. Electrochem. Soc.*, **91**, 547 (1947).
7. J. J. LANDER, NRL Report 4475, Jan. 31, 1955.
8. U. B. THOMAS, F. T. FOSTER, AND H. E. HARING, *Trans. Electrochem. Soc.*, **92**, 313 (1947).
9. J. F. RITTENHOUSE AND H. E. JENSEN, "The Lead-Calcium Battery," C. and D. Batteries, Inc., Conshohocken, Pa. (1953).
10. J. J. LANDER, *This Journal*, **99**, 467 (1952).
11. G. W. VINAL, "Storage Batteries," 3rd ed., p. 217, John Wiley & Sons, Inc., New York (1940).
12. J. J. LANDER, Unpublished data.

Theoretical Electromotive Forces for Cells Containing a Single Solid or Molten Chloride Electrolyte

WALTER J. HAMER, MARJORIE S. MALMBERG AND BERNARD RUBIN

National Bureau of Standards, Washington, D. C.

ABSTRACT

From thermodynamic data, electromotive forces have been calculated for reversible galvanic cells of the type $M/MCl_n/Cl_2(z)$ where M is a metallic element in the solid, liquid, or gaseous state and MCl_n is the corresponding chloride in the solid or liquid state. Results are given for temperatures from 25° to 1500°C.

The chlorides are listed in a series and compared with the electromotive force series of the elements in aqueous solutions. Comparisons are given with results obtained from galvanic cells with fused chlorides or from measurements of decomposition voltages.

INTRODUCTION

Standard oxidation-reduction potentials are available for numerous electrochemical reactions in aqueous systems at 25°C (1). These potentials refer to the potentials when all solid or dissolved substances taking part in the oxidation-reduction processes are at unit activity and all gases are at a fugacity of one atmosphere. When the potentials of the elements alone are arranged in series in decreasing or increasing order of magnitude, relative to the conventional hydrogen electrode as reference, the series is generally referred to as "the electromotive force series of the elements."

A similar series for molten or fused systems is unavailable at present. Such a series would differ fundamentally from a series for aqueous systems in that a different standard state is involved for each electrolyte since the molten phase is a pure ionic fluid of one component. Potentials for half-cell reactions are, therefore, within present knowledge not feasible. However, a series may be established based on the free energies of formation of the electrolytic phase, these phases being of like type, such as chlorides, bromides, oxides, etc. These values would correspond to the decomposition voltages of fused salts, assuming the decomposition voltages as determined experimentally contain no ohmic voltages and are free of effects of polarization.

The theoretical decomposition voltages of fused electrolytes would correspond to the reversible electromotive force (emf) of galvanic cells composed of the electrolyte and two electrodes, one of which is reversible to the anion and the other to the cation of the fused electrolyte, the

fused electrolyte and the two electrodes being in their standard states of unit activity or unit fugacity. This reversible electromotive force is also related to the free energy of formation of the fused electrolyte through the relation

$$E^0 = -\Delta F_f^0/n\mathbf{F} \qquad [1]$$

where ΔF^0 is the standard free energy of formation of the electrolyte, E^0 is the standard emf, **F** the faraday constant, and n the number of faradays involved in the electrochemical reaction.

Although experimental measurements of decomposition voltages usually do not agree with theoretical values, owing to several factors, including the chemical interaction of the electrodes with the electrolyte, the production of electrodes in a nonstandard state, deviations from isothermal conditions, and electrode polarization, it is nonetheless important to know the theoretical values for the systems under study. These values aid in elucidating mechanisms and in interpretations of experimental observations on fused electrolytes.

It is the purpose of this paper to present the theoretical standard electromotive forces of cells containing a single solid or molten (fused) chloride electrolyte for which the necessary thermodynamic data are available. Data used were obtained from Kelley (2), from Brewer (3), and from the National Bureau of Standards (4). When estimates of heat capacity were required, the rule of Kelley (5) was used, namely, 7.0 cal/°/mean gram-atom for solid compounds, 8.0 for liquid compounds, 7.3 for solid metals, and 7.5 for liquid metals, or the method of Shomate (6) using values of heat content and heat capacity given by National Bureau of Standards (4) was employed. For this paper no attempt was made to review critically or include thermodynamic data other than those contained in the above references. Delimarski (7) conducted a somewhat similar investigation. He determined the potential of 21 metals in their respective chlorides relative to sodium, assigning to the latter a potential of zero, and formulated an electrochemical series on this basis at 500°, 700°C, and the fusion temperature of each chloride. Within the experimental uncertainties his series agrees, as to order, with that presented herein.

No attempt is made to evaluate the accuracy of the quantities used. This phase is discussed in each of the above references; in Table I are listed the uncertainties in emf at 25°C corresponding to the uncertainties in the heat of formation of the chlorides at 298.16°K quoted by Brewer (3), which uncertainties were assumed to apply also to the data in the National Bureau of Standards Circular (4) since the values listed agree closely and their sources are the same. The uncertainties in entropy values are, in general, small compared to those in heats of formation; thus, the uncertainties in emf here listed are based on uncertainties in heats rather than on free energies of formation. Furthermore, the authors are concerned more with the relative values (or order of the chlorides) than with actual values, and in all probability the order (*see* Table I) will remain the same whether the uncertainties are based on heats or free energies of formation.

Method of Evaluation of Standard EMF's

The method of evaluating the standard reversible emf of cells composed of a solid or molten chloride and two electrodes, one of which is reversible to the anion and the other to the cation of the fused chloride, follows well-known thermodynamic relations, considered most elementary by the thermodynamicist. The emf of such cells, namely,

metal/metallic chloride/chlorine gas[1] [*A*]

is related to the free energy change for the chemical reaction:

metal + chlorine gas → metallic chloride [*B*]

According to convention this free energy change is the free energy of formation, ΔF_f^0, of the chloride when the chloride, metal, and gas are in their standard states, and is related to the heat of formation, ΔH_f^0, by the equation

$$\Delta F_f^0 = \Delta H_f^0 - T\Delta S^0 \qquad [2]$$

where ΔS^0 is the difference in the entropy of the products and the reactants of the chemical reaction. Tables of thermodynamic data give ΔF_f^0 and/or ΔH_f^0 for 298.16°K.

To obtain ΔF_f^0 at temperatures above 298.16°K use is made of the equation

$$\frac{d\left(\frac{\Delta F_f^0}{T}\right)}{dT} = -\frac{\Delta H_f^0}{T^2} \qquad [3]$$

However, ΔH_f^0 is a function of temperature, and depends on the difference between the heat capacities of the products and reactants, as expressed by

$$\Delta H_f^0 = \Delta H_0^0 + \int_{T_1}^{T_2} \Delta C_P \, dT \qquad [4]$$

where ΔH_0^0 is evaluated from the heat of formation at 298.16°K as shown below, and ΔC_P represents the sum of the heat capacities of the products of a reaction less the sum of the heat capacities of the reactants and is usually expressed as a function of temperature by an equation of the empirical form:

$$\Delta C_P = \Delta a + (\Delta b)T + \frac{\Delta c}{T^2} \qquad [5]$$

[1] It is assumed that chlorine gas is adsorbed on an inert electronic conductor.

TABLE I. *Standard electromotive forces for single solid or molten metallic chlorides**

Order 25°C	Metal ion	E^0														
		25°C (aqueous)	25°C (solid)	Uncertainty (25°C)	100°C	200°C	300°C	350°C	400°C	450°C	500°C	550°C	600°C	800°C	1000°C	1500°C
		volts	volts	volts	volts	volts	volts	volts	volts	volts	volts	volts	volts	volts	volts	volts
1	Ra^{+2}	4.28	4.336	±0.07	4.272	4.189	4.108	4.068	4.029	3.990	3.952	3.913	3.876	3.723	3.569	3.098
2	K^{+1}	4.285	4.232	±0.01	4.158	4.056	3.954	3.904	3.854	3.805	3.755	3.707	3.658	3.441	3.155	2.598
3	Sm^{+2}	<4.52	4.206	±0.15	4.147	4.071	3.998	3.962	3.926	3.891	3.856	3.822	3.787	3.661	3.559	3.317
4	Ba^{+2}	4.26	4.202	±0.01	4.139	4.056	3.975	3.935	3.888	3.848	3.808	3.768	3.728	3.568	3.412	3.079
5	Cs^{+1}	4.283	4.189	±0.01	4.109	4.002	3.896	3.843	3.791	3.739	3.692	3.645	3.599	3.362	3.078	2.667 (1300V)
6	Rb^{+1}	4.285	4.177	±0.04	4.101	3.998	3.897	3.846	3.795	3.745	3.695	3.645	3.595	3.314	3.001	2.428 (1381V)
7	Sr^{+2}	4.25	4.048	±0.01	3.987	3.909	3.832	3.794	3.757	3.720	3.684	3.648	3.612	3.469	3.333	2.977
8	Li^{+1}	4.405	4.011	±0.09	3.955	3.881	3.800	3.761	3.722	3.684	3.646	3.608	3.571	3.457	3.352	3.122 (1382V)
9	Na^{+1}	4.074	3.980	±0.004	3.910	3.810	3.712	3.663	3.615	3.566	3.519	3.471	3.424	3.240	3.019	2.366 (1465V)
10	Ca^{+2}	4.230	3.888	±0.02	3.830	3.754	3.680	3.643	3.607	3.570	3.534	3.498	3.462	3.323	3.208	2.926
11	La^{+3}	3.88	3.565	±0.03	3.504	3.426	3.350	3.313	3.277	3.241	3.205	3.170	3.134	2.997	2.876	2.607
12	Ce^{+3}	3.84	3.517	±0.03	3.456	3.378	3.303	3.266	3.229	3.193	3.157	3.121	3.086	2.945	2.821	2.540
13	Pr^{+3}	3.83	3.481	±0.01	3.420	3.342	3.266	3.229	3.192	3.156	3.120	3.085	3.049	2.911	2.795	2.523
14	Nd^{+3}	3.80	3.430	±0.01	3.369	3.291	3.215	3.177	3.140	3.103	3.067	3.030	2.994	2.856	2.736	2.455
15	Pm^{+3}	3.78	3.410	±0.03	3.353	3.279	3.208	3.173	3.139	3.105	3.072	3.038	3.006	2.884	2.784	2.554
16	Sm^{+3}	3.77	3.380	±0.10	3.322	3.249	3.178	3.143	3.109	3.075	3.041	3.008	2.975	2.861	2.763	2.712 (1107D)
17	Eu^{+3}	3.77	3.340	±0.10	3.283	3.210	3.139	3.104	3.070	3.036	3.002	2.969	2.936	2.828	2.815 (>827D)	—
18	Gd^{+3}	3.76	3.317	±0.01	3.260	3.187	3.116	3.081	3.047	3.013	2.979	2.946	2.913	2.807	2.709	2.483
19	Tb^{+3}	3.75	3.261	±0.03	3.204	3.130	3.059	3.025	2.990	2.956	2.923	2.890	2.858	2.754	2.657	2.433
20	Dy^{+3}	3.71	3.206	±0.03	3.149	3.075	3.004	2.970	2.935	2.901	2.868	2.835	2.802	2.690	2.599	2.359
21	Y^{+3}	3.73	3.163	±0.04	3.106	3.032	2.961	2.926	2.892	2.858	2.824	2.791	2.758	2.643	2.548	2.329
22	Ho^{+3}	3.68	3.134	±0.01	3.077	3.003	2.932	2.897	2.863	2.829	2.796	2.762	2.729	2.610	2.511	2.283
23	Er^{+3}	3.66	3.119	±0.01	3.062	2.989	2.918	2.883	2.849	2.815	2.781	2.748	2.715	2.589	2.488	2.257 (1497V)
24	Tm^{+3}	3.64	3.086	±0.01	3.029	2.956	2.884	2.850	2.815	2.781	2.748	2.715	2.682	2.553	2.447	2.221 (1487V)
25	Yb^{+3}	3.63	3.075	±0.10	3.017	2.944	2.873	2.838	2.804	2.770	2.736	2.703	2.670	2.542	2.434	2.449 (1027D)
26	Mg^{+2}	3.73	3.070	±0.004	3.006	2.922	2.840	2.800	2.760	2.720	2.680	2.641	2.602	2.460	2.346	1.974 (1418V)
27	Lu^{+3}	3.61	3.049	±0.01	2.988	2.909	2.834	2.796	2.760	2.723	2.687	2.652	2.616	2.478	2.356	2.108 (1477V)
28	Sc^{+3}	3.44	2.946	±0.01	2.885	2.807	2.731	2.694	2.657	2.621	2.585	2.549	2.514	2.375	2.264 (967V)	—
29	Zr^{+2}	—	2.905	±0.43	2.847	2.772	2.699	2.664	2.629	2.594	2.560	2.526	2.508 (577D)	—	—	—
30	U^{+3}	3.16	2.846	—	2.788	2.713	2.639	2.602	2.566	2.530	2.494	2.458	2.423	2.280	2.162	1.886
31	Th^{+4}	3.26	2.840	±0.05	2.779	2.699	2.622	2.584	2.546	2.509	2.472	2.435	2.399	2.264	2.208 (921V)	—
32	Zr^{+3}	—	2.790	±0.29	2.736	2.668	2.603	2.571	2.540	2.509	2.492 (477D)	—	—	—	—	—
33	Hf^{+4}	3.06	2.537	±0.32	2.481	2.409	2.340	2.328 (3178)	—	—	—	—	—	—	—	—
34	U^{+4}	2.86	2.493	—	2.436	2.362	2.289	2.252	2.217	2.181	2.146	2.111	2.078	1.974	1.953 (827V)	—
35	Be^{+2}	3.21	2.435	±0.11	2.382	2.315	2.252	2.222	2.192	2.167	2.144	2.122 (547V)	—	—	—	—
36	Mn^{+2}	2.54	2.287	±0.02	2.235	2.166	2.098	2.065	2.032	1.999	1.967	1.935	1.902	1.807	1.725	1.649 (1190V)
37	Zr^{+4}	2.89	2.266	±0.22	2.209	2.135	2.063	2.041 (3318)	—	—	—	—	—	—	—	—
38	Ti^{+2}	2.99	2.255	±0.22	2.202	2.134	2.069	2.037	2.006	1.975	1.945	1.914	1.885D	—	—	—

37	Zr^{+4}	2.89	2.266	±0.22	2.209	2.135	2.063	2.041 (3318)	—	—	—	—	—	—	—	—
38	Ti^{+2}	2.99	2.255	±0.22	2.202	2.134	2.069	2.037	2.006	1.975	1.945	1.914	1.885D	—	—	—
39	$(Al^{+3})_2$	3.02	2.200	±0.01	2.150	2.097 (1808)	—	—	—	—	—	—	—	—	—	—
40	Ti^{+3}	ca 2.57	2.154	±0.14	2.097	2.024	1.954	1.919	1.886	1.852	1.836 (475D)	—	—	—	—	—
41	V^{+2}	ca 2.54	2.103	±0.43	2.044	1.970	1.898	1.863	1.828	1.794	1.761	1.727	1.695	1.566	1.441	1.269 (1377V)
42	Tl^{+1}	1.696	1.916	±0.02	1.865	1.798	1.732	1.696	1.660	1.629	1.606	1.583	1.561	1.473	1.470 (806V)	—
43	Zn^{+2}	2.123	1.914	±0.01	1.854	1.776	1.706	1.680	1.655	1.629	1.603	1.577	1.552	1.476 (756V)	—	—
44	Cr^{+2}	2.27	1.846	±0.06	1.795	1.729	1.664	1.632	1.600	1.568	1.537	1.505	1.474	1.352	1.262	1.137 (1302V)
45	$(Si^{+3})_2$	—	1.778	±0.07	1.736	1.713 (145V)	—	—	—	—	—	—	—	—	—	—
46	Cd^{+2}	1.763	1.775	±0.01	1.715	1.637	1.560	1.521	1.481	1.442	1.403	1.364	1.331	1.193	1.002 (980V)	—
47	Ti^{+4}	—	1.748	±0.11	1.700	1.678 (136V)	—	—	—	—	—	—	—	—	—	—
48	V^{+3}	ca 2.23	1.735	±0.43	1.674	1.596	1.576 (227D)	—	—	—	—	—	—	—	—	—
49	Ga^{+2}	ca 1.81	1.713	±0.22	1.659	(200D)	—	—	—	—	—	—	—	—	—	—
50	In^{+1}	ca 1.61	1.709	±0.22	1.654	1.581	1.520	1.492	1.465	1.439	1.414	1.389	1.364	1.360 (609V)	—	—
51	Cr^{+3}	2.10	1.706	±0.07	1.646	1.567	1.489	1.451	1.412	1.374	1.336	1.299	1.261	1.113	1.006 (947S)	—
52	In^{+2}	ca 1.66	1.657	±0.06	1.601	1.528	1.464	1.435	1.407	1.380	1.361 (485V)	—	—	—	—	—
53	In^{+3}	1.702	1.641	±0.04	1.588	1.519	1.451	1.417	1.384	1.352	1.321 (498S)	—	—	—	—	—
54	Pb^{+2}	1.486	1.627	±0.01	1.569	1.493	1.420	1.383	1.345	1.307	1.271	1.243	1.215	1.112	1.039 (954V)	—
55	Ga^{+3}	1.89	1.619	±0.01	1.572	1.528 (200V)	—	—	—	—	—	—	—	—	—	—
56	Sn^{+2}	1.496	1.607	±0.02	1.556	1.490	1.428	1.400	1.373	1.346	1.320	1.295	1.270	1.259 (623V)	—	—
57	Fe^{+2}	1.80	1.565	±0.02	1.516	1.451	1.388	1.357	1.327	1.297	1.267	1.237	1.207	1.118	1.050	1.041 (1026V)
58	Si^{+4}	—	1.484	±0.005	1.466 (57V)	—	—	—	—	—	—	—	—	—	—	—
59	Co^{+2}	1.637	1.464	±0.02	1.408	1.337	1.269	1.236	1.203	1.171	1.140	1.109	1.079	0.977	0.900	0.881 (1050V)
60	Ni^{+2}	1.610	1.412	±0.04	1.355	1.282	1.210	1.174	1.139	1.104	1.070	1.036	1.003	0.875	0.763 (987V)	—
61	V^{+4}	—	1.323	±0.32	1.281	1.253 (152V)	—	—	—	—	—	—	—	—	—	—
62	Cu^{+1}	0.839	1.232	±0.02	1.191	1.140	1.093	1.071	1.050	1.035	1.024	1.013	1.003	0.970	0.943	0.862
63	Sn^{+4}	1.35	1.228	±0.01	1.184	1.176 (113V)	—	—	—	—	—	—	—	—	—	—
64	Ge^{+4}	—	1.225	±0.16	1.190 (83V)	—	—	—	—	—	—	—	—	—	—	—
65	Fe^{+3}	1.396	1.197	±0.06	1.147	1.084	1.023	1.016 (319V)	—	—	—	—	—	—	—	—
66	Ag^{+1}	0.560	1.137	±0.01	1.093	1.037	0.984	0.959	0.935	0.911	0.896	0.883	0.870	0.826	0.784	0.665
67	Sb^{+3}	—	1.122	—	1.077	1.028	1.019 (221V)	—	—	—	—	—	—	—	—	—
68	Bi^{+3}	—	1.102	—	1.051	0.986	0.926	0.896	0.867	0.844 (441V)	—	—	—	—	—	—
69	$(Hg^{+1})_2$	0.571	1.092	±0.01	1.022	0.930	0.840	0.800	0.730	0.663	0.597	0.540 (543D)	—	—	—	—
70	As^{+3}	—	1.019	—	0.986	0.973 (130V)	—	—	—	—	—	—	—	—	—	—

TABLE 1.—*Continued*

Order 25°C	Metal ion	E^0														
		25°C (aqueous)	25°C (solid)	Uncertainty (25°C)	100°C	200°C	300°C	350°C	400°C	450°C	500°C	550°C	600°C	800°C	1000°C	1500°C
		volts	*volts*	*volts*	*volts*	*volts*	*volts*	*volts*	*volts*	*volts*	*volts*	*volts*	*volts*	*volts*	*volts*	*volts*
71	Hg^{+2}	0.506	0.952	±0.02	0.892	0.814	0.743	0.741 (304V)	—	—	—	—	—	—	—	—
72	Cu^{+2}	1.023	0.846	±0.11	0.791	0.721	0.654	0.621	0.589	0.558	0.528	0.506 (537D)	—	—	—	—
73	Ir^{+1}	—	0.794	±0.13	0.751	0.699	0.650	0.626	0.603	0.580	0.558	0.536	0.515	0.433 (799D)	—	—
74	Pd^{+2}	0.373	0.768	±0.06	0.714	0.646	0.581	0.549	0.518	0.487	0.457	0.427	0.397	0.331 (737D)	—	—
75	Mo^{+2}	—	0.759	±0.06	0.711	0.651	0.593	0.566	0.538	0.511	0.485	0.471 (527D)	—	—	—	—
76	Sb^{+5}	—	0.742	—	0.701	0.665 (172V)	—	—	—	—	—	—	—	—	—	—
77	Ir^{+2}	<0.26	0.733	±0.06	0.685	0.625	0.567	0.539	0.512	0.485	0.458	0.432	0.406	0.320 (771D)	—	—
78	Mo^{+3}	1.56	0.723	±0.07	0.669	0.602	0.536	0.519 (327D)	—	—	—	—	—	—	—	—
79	Ir^{+3}	ca 0.21	0.665	±0.04	0.610	0.539	0.472	0.439	0.406	0.374	0.342	0.311	0.280	0.180 (765D)	—	—
80	Mo^{+4}	—	0.650	±0.05	0.600	0.582 (127D)	—	—	—	—	—	—	—	—	—	—
81	W^{+2}	—	0.629	±0.11	0.581	0.521	0.463	0.435	0.408	0.393 (427D)	—	—	—	—	—	—
82	Mo^{+5}	—	0.597	±0.02	0.550	0.491	0.463 (268V)	—	—	—	—	—	—	—	—	—
83	Rh^{+3}	ca 0.56	0.593	±0.04	0.539	0.471	0.406	0.374	0.343	0.312	0.281	0.251	0.221	0.104	0.020 (948D)	—
84	Rh^{+2}	ca 0.76	0.575	±0.06	0.524	0.460	0.398	0.368	0.339	0.310	0.281	0.253	0.225	0.142	0.093 (958D)	—
85	Pt^{+1}	—	0.572	±0.13	0.525	0.465	0.407	0.380	0.353	0.326	0.300	0.274	0.257 (583D)	—	—	—
86	Pt^{+2}	ca 0.16	0.564	±0.06	0.513	0.449	0.387	0.357	0.328	0.299	0.270	0.242	0.225 (581D)	—	—	—
87	W^{+4}	—	0.564	±0.03	0.513	0.449	0.432 (227D)	—	—	—	—	—	—	—	—	—
88	Ru^{+2}	—	0.546	±0.04	0.494	0.428	0.364	0.333	0.303	0.273	0.243	0.214	0.185	0.170 (627D)	—	—
89	W^{+5}	—	0.538	±0.03	0.491	0.431	0.392 (276V)	—	—	—	—	—	—	—	—	—
90	Rh^{+1}	ca 0.76	0.520	±0.13	0.478	0.425	0.376	0.352	0.328	0.305	0.282	0.260	0.238	0.153	0.084 (965D)	—
91	W^{+6}	—	0.513	±0.03	0.464	0.401	0.343	0.325 (337V)	—	—	—	—	—	—	—	—
92	Pt^{+3}	—	0.484	±0.07	0.426	0.351	0.279	0.243	0.209	0.185 (435D)	—	—	—	—	—	—
93	Pt^{+4}	—	0.465	±0.03	0.412	0.344	0.278	0.261 (327D)	—	—	—	—	—	—	—	—
94	Au^{+3}	−0.140	0.211	±0.03	0.162	0.101	0.043	0.021	−0.001	—	—	—	—	—	—	—
95	Au^{+1}	ca −0.320	0.182	±0.04	0.138	0.082	0.037 (287D)	—	—	—	—	—	—	—	—	—
96	C^{+4}	—	0.178	±0.005	0.147 (77V)	—	—	—	—	—	—	—	—	—	—	—

S = sublimation; V = vaporization; D = decomposition.

* Values listed at the sublimation, vaporization, or decomposition temperatures obviously apply to cells with the solid or molten electrolyte, that is, slightly below the sublimation, vaporization, or decomposition temperatures.

where a, b, and c are known numerical values. Substitution of equation [5] in equation [4] and integration gives

$$\Delta H_0^0 = \Delta H_f^0 - (\Delta a)T - \frac{(\Delta b)T^2}{2} + \frac{\Delta c}{T} \qquad [6]$$

Substitution then of equation [6] in equation [3] and integration gives

$$\Delta F_f^0 = \Delta H_0^0 - (\Delta a)T \ln T - \frac{(\Delta b)T^2}{2} - \frac{\Delta c}{2T} + IT \qquad [7]$$

which gives ΔF_f^0 as a function of temperature. If ΔF_f^0 and ΔH_f^0 (or ΔH_0^0) are known at some temperature, usually 298.16°K, the integration constant I may be evaluated. Equation [7] is then valid for the calculation of values of ΔF_f^0 from 25°C up to temperatures for the first change in state for the chloride or metal, i.e., for the first transition, fusion, or vaporization of the products (metallic chloride) or reactants (metal and chlorine gas). At this point, the heat change for the transition, fusion, or vaporization must be added for products, subtracted for reactants, to the ΔH_f^0 at the temperature in question. Then, from this revised ΔH_f^0 and the new ΔC_P values resulting from the change in state, a new ΔH_0^0 and a new integration constant, I', must be calculated. This procedure is followed for each change in state of the products or reactants.

Values of ΔF_f^0 are then calculated for selected temperatures by equation [7] and values of the reversible emf are calculated from these ΔF_f^0 by equation [1]. The temperatures selected for the purpose of this paper were 25°, 100°, 200°, 300°, 350°, 400°, 450°, 500°, 550°, 600°, 800°, 1000°, and 1500°C. In these calculations 23060.5 cal/abs. volt g-equiv. was used for $\mathbf{F}$ and t°C + 273.16 for T [4].

The complete evaluation of 96 chlorides was done with the aid of the Standard Eastern Automatic Computer (SEAC) of the National Bureau of Standards, maximum operating time being 30 sec. The necessary data on the metals (or nonmetals) and chlorides used in these computations are not listed here since they are readily available in references (2), (3), and (4). Chlorine gas is common to all the systems and its heat capacity as a function of temperature is given by equation [8], namely (8):

$$\Delta C_P(\mathrm{Cl_2, gas}) = 8.79 + 0.00022\ T - 66{,}000/T^2 \qquad [8]$$

Results

The electromotive forces thus calculated when the chloride is solid or molten are given in decreasing order in Table I. A vertical line in the table indicates that the values to the left of the line are for solid chlorides and those to the right for molten or fused chlorides. The higher the emf value, the greater is the reducing power of the metal in a chloride system. For example, if magnesium were placed in fused zinc chloride it would displace zinc with the formation of magnesium chloride (i.e., zinc ions are reduced) thus

$$\mathrm{Mg + ZnCl_2 \rightarrow Zn + MgCl_2} \qquad [C]$$

This follows from the most elementary fact that the free energies of formation may be added or subtracted, hence at 400°C, for example:

$$\mathrm{Mg + Cl_2 \rightarrow MgCl_2} \qquad \Delta F_1 = -127{,}300 \text{ cal}, \quad E_1 = 2.76 \text{ v} \qquad [9]$$

$$\mathrm{Zn + Cl_2 \rightarrow ZnCl_2} \qquad \Delta F_2 = -76{,}300 \text{ cal}, \quad E_2 = 1.66 \text{ v} \qquad [10]$$

Then, subtracting [10] from [9] one has reaction [C] for which E = 1.10 v and ΔF^0 = −51,000 cal, and reaction [C] would be a spontaneous one.

The question next arises as to whether or not reaction [C] goes to completion, or proceeds only part way to an equilibrium state. From thermodynamic relations it is known that

$$-n\mathbf{F}E^0 = \Delta F^0 = -RT \ln K \qquad [11]$$

where K is the equilibrium constant of a chemical reaction under study, and for reactions [9] and [10] is, respectively:

$$K_{\mathrm{MgCl_2}} = \frac{a_{\mathrm{MgCl_2}}}{a_{\mathrm{Mg}}\, a_{\mathrm{Cl_2}}} \qquad [12]$$

and

$$K_{\mathrm{ZnCl_2}} = \frac{a_{\mathrm{ZnCl_2}}}{a_{\mathrm{Zn}}\, a_{\mathrm{Cl_2}}} \qquad [13]$$

where a represents the activity in the equilibrium mixture (not the standard state) of the species denoted by subscripts. For reaction [C] the equilibrium constant is

$$K_C = \frac{a_{\mathrm{MgCl_2}}\, a_{\mathrm{Zn}}}{a_{\mathrm{Mg}}\, a_{\mathrm{ZnCl_2}}} = \frac{K_{\mathrm{MgCl_2}}}{K_{\mathrm{ZnCl_2}}} \qquad [14]$$

Using the ΔF^0 values given above in equations [9] and [10], $K_{\mathrm{MgCl_2}}$ and $K_{\mathrm{ZnCl_2}}$ are, respectively, 2.133×10^{41} and 5.903×10^{24}. Then $K_C = 3.6 \times 10^{16}$ which means for all intents and purposes reaction [C] goes to completion.

For free energy changes when the reactants and products are not in their standard states, thermodynamics gives:

$$\Delta F_{\mathrm{MgCl_2}} = \Delta F^0_{\mathrm{MgCl_2}} + RT \ln \frac{a_{\mathrm{MgCl_2}}}{a_{\mathrm{Mg}}\, a_{\mathrm{Cl_2}}} \qquad [15]$$

$$\Delta F_{\mathrm{ZnCl_2}} = \Delta F^0_{\mathrm{ZnCl_2}} + RT \ln \frac{a_{\mathrm{ZnCl_2}}}{a_{\mathrm{Zn}}\, a_{\mathrm{ZnCl_2}}} \qquad [16]$$

and $\Delta F = \Delta F^0$ only when the a's are unity (the standard state). When one is dealing with the pure fused salt and the pure electrode phases, the activities are all unity and the last terms in equations [16] and [17] are zero. However, when reaction [C] proceeds, the zinc chloride originally present as a pure phase becomes diluted with magnesium chloride as it forms during the chemical reaction, and the

* Values listed at the sublimation, vaporization, or decomposition temperatures obviously apply to cells with the solid or molten electrolyte, that is, slightly below the sublimation, vaporization, or decomposition temperatures.

fused electrolyte and each electrode may or may not be mutually soluble in each other, and the activities of the fused phases (or phase) can no longer be taken as unity. When the system [*C*] attained equilibrium, each phase (electrode and electrolyte) could be analyzed. The activity of each component in each phase would be given by

$$a_{Zn} = N_{Zn}f_{Zn};\ a_{Mg} = N_{Mg}f_{Mg};\qquad a_{ZnCl_2} = N_{ZnCl_2}f_{ZnCl_2}$$

and $a_{MgCl_2} = N_{MgCl_2}f_{MgCl_2}$ where N represents mole fraction and f the activity coefficient. Analysis will give N but not f, but the latter is obtained from the expression

$$\frac{f_{Zn}f_{MgCl_2}}{f_{Mg}f_{ZnCl_2}} = \frac{K_{MgCl_2}N_{Mg}N_{ZnCl_2}}{K_{ZnCl_2}N_{Zn}N_{MgCl_2}} \qquad [17]$$

which follows from the substitution in equation [14] of the relations $a = Nf$ with the appropriate subscripts. To obtain values of each activity coefficient separately would be extremely involved and would entail information on each phase separately. If magnesium and zinc did not dissolve in the fused phase or the fused phase dissolve in them, their activities would be unity and equation [17] would reduce to

$$\frac{f_{MgCl_2}}{f_{ZnCl_2}} = \frac{K_{MgCl_2}N_{ZnCl_2}}{K_{ZnCl_2}N_{MgCl_2}} \qquad [18]$$

involving only the fused phase. Since the term on the right side of this equation is known, the ratio of the activity coefficients could be evaluated. However, for the present case we are concerned only with the relative position of the solid elements in a series (i.e., the values of K, the equilibrium constant) and the added refinement of determining the activity coefficients is unnecessary.

In this connection it should also be stressed that many cells, when constructed, would not give the theoretical electromotive forces as listed in Table I. For example, a cell made with a sodium electrode and a chlorine electrode in molten sodium chloride would not give the theoretical values because of the solubility of sodium in molten sodium chloride and of sodium chloride in molten sodium [*see* reference (9)], and the activities of sodium and molten sodium chloride would not be unity, and ΔF rather than ΔF^0 applies (*see* equations [15] and [16]).

Discussion

Solid and Aqueous States

Reference to Table I shows that the relative position of the elements is nearly the same whether the electrolyte phase is solid or molten. Values of aqueous systems at 25°C are also listed in Table I. The values obtained for the solid electrolyte, providing the solid phase is anhydrous, and aqueous systems differ in the free energy associated with the process of dilution of the saturated solution of the electrolyte to a solution of unit mean activity, $a_\pm$. The difference in free energy between a solid phase and a solution saturated with the solid phase is zero. Thus,

$$\Delta F^0_{aqueous} - \Delta F^0_{solid} = -RT \ln a_\pm^r \text{ (in sat. sol.)} \qquad [19]$$

or

$$\Delta F^0_{aqueous} - \Delta F^0_{solid} = -rRT \ln [(r_+^r + r_-^r)]^{1/r}\,\gamma m \qquad [20]$$

where m and y are, respectively, the molality and activity coefficient of the saturated aqueous solution, and r = the sum of the number, r_+ ions and the number, r_- ions into which the electrolyte dissociates. Therefore, since $\Delta F^0 = -nE\mathbf{F}$ one has

$$E^0_{aqueous} - E^0_{solid} = \frac{2.303RT}{n\mathbf{F}} \log a_\pm^r \qquad [21]$$

or

$$E^0_{aqueous} - E^0_{solid} = \frac{2.303RTr}{n\mathbf{F}} \log[(r_+^r + r_-^r)]^{1/r}\,\gamma m \qquad [22]$$

Thus, E^0_{aq} is higher than E^0_s for most highly soluble salts. For example, Owen (10) from potentiometric measurements and Gledhill and Malan (11) from conductometric measurements obtained 1.334×10^{-5} g-equiv/liter and 1.337×10^{-5} g-equiv/liter, respectively, for the solubility of silver chloride in water at 25°C, or an average value of 1.778×10^{-10} for the solubility product. When this value is substituted for $a_\pm$ in equation [21] and 0.05916 is used for $2.303\ RT/n\mathbf{F}$ one finds that $E^0_{aq} - E^0_s$ is -0.577 volt. The data of Table I give -0.577 volt in excellent agreement. Scatchard, Hamer, and Wood (12) give an activity of 6.1870 and 2.8248 for the saturated solutions of sodium chloride and potassium chloride, respectively. When these values are substituted in equation [21] one obtains, respectively, 0.0936 volt and 0.0533 volt between E^0_{aq} and E^0_s for sodium chloride and potassium chloride, whereas the data of Table I give 0.094 volt and 0.053 volt, in excellent agreement. In other cases, the agreement is not so good; however, the disagreements are in general well within the uncertainties listed in column 5 of Table I.

Molten State

Comparison of the data of Table I with data reported in the literature for those cases where the electrolyte is in the molten state could be most extensive. As an illustration, we shall compare the data with those reported in the literature for $PbCl_2$ and $ZnCl_2$, only, and for which a number of investigations have been made. These comparisons will suffice for the purpose of this paper.

Data for fused lead chloride have been obtained over a considerable range of temperature by Wachter and Hildebrand (13), Weber (14), Hildebrand and Rule (15), Czepinski (16), and Lorenz and Velde (17). These experimenters made observations on cells of the type, $Pb/PbCl_2/Cl_2$, C and all except Czepinski took special care to remove air

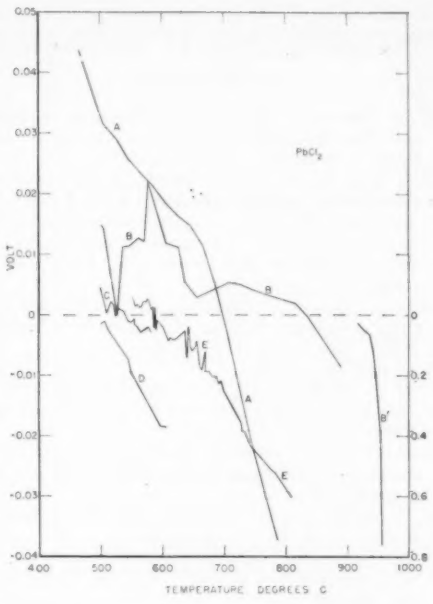

FIG. 1. Deviations of observed emf values for lead chloride from those calculated from thermodynamic quantities: curve A—Czepinski + 0.06 v; curve B—Weber (ordinate scale at left); curve B′—Weber (ordinate scale at right); curve C—Wachter and Hildebrand; curve D—Hildebrand and Rule; curve E—Lorenz and Velde.

and moisture from their cells; Weber removed air only, and all except Wachter and Hildebrand subjected their electrodes to polarization prior to the measurements of emf. For the temperature range 771°–1227°K, the data of this paper give

$$E^0 = 1.9049 + (5.796 \times 10^{-4})T \log T - (2.3950 \times 10^{-9})T^2 + 0.71551/T - (2.4934 \times 10^{-3})T \quad [23]$$

for the emf as a function of temperature. For the range 772.26°–855.26°K Wachter and Hildebrand, for the range 825.66° and 1082.56°K Lorenz and Velde, and for the range 779.16°–1063.16°K Weber gave, respectively,

$$E^0 = 1.2730 - 0.000625(t - 500°C) \quad [24]$$

$$E^0 = 1.2467 - 0.00065(t - 550°C) \quad [25]$$

and

$$E^0 = 1.2818 - 0.000584(t - 506°C) \quad [26]$$

Hildebrand and Rule, and Czepinski did not give equations for the emf as a function of temperature, nor did Weber for his data above 890°C. In Fig. 1, deviations of results of the various authors from the theoretical values, i.e., those calculated from thermodynamic data, are shown as a function of temperature. The data of Wachter and Hildebrand agree quite well with the theoretical values, within a few millivolts, over the temperature range studied. Data of Hildebrand and Rule agree well with the theoretical values from 500° to 545°C, but become increasingly lower than the theoretical values at the higher temperatures. Data of Lorenz and Velde show similar increasingly lower values at the higher temperatures. This falling off of the observed emf data at the higher temperatures is probably due to increased polarization or electrode-electrolyte interaction at the higher temperatures. Czepinski's values are lower than the theoretical values by 0.019 v at 466°C and by 0.097 v at 786°C; his values were undoubtedly affected by polarization and show the effects of the presence of air and moisture on the emf's.

Data for fused zinc chloride have been obtained by Wachter and Hildebrand (13), Lorenz and Velde (17), Czepinski (16), and Kirk and Bradt (18). Kirk and Bradt obtained their results at 400°C only and by means of measurements of decomposition voltages using platinum cathodes and graphite anodes. Their value of 1.96 v is much higher than the theoretical value of 1.655 v (*see* Table I); their results apparently indicate that electrode phenomena, other than the primary ones, occurred at either or both of their electrodes, or that the techniques involved in measuring decomposition voltages lead to incorrect values. The other experimenters made their observations on cells of the type $Zn/ZnCl_2/Cl_2(g)$, C and with the exception of Czepinski took special care to eliminate water and air from the cell system and only Wachter and Hildebrand worked with unpolarized electrodes. For the temperature range 692.7°–1029°K, the data of this

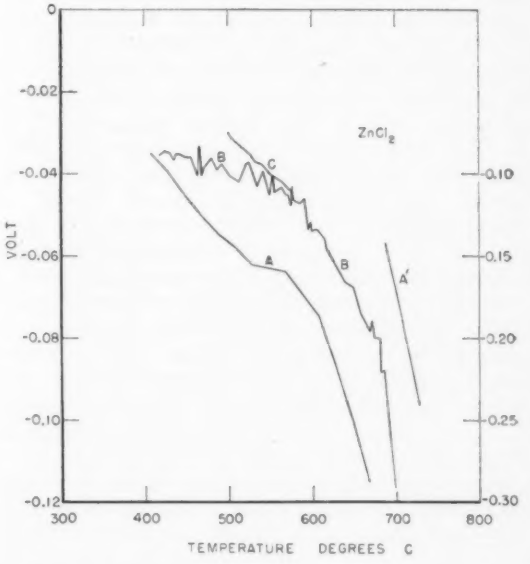

FIG. 2. Deviations of observed emf values for zinc chloride from those calculated from thermodynamic quantities: curve A—Czepinski (ordinate scale at left); curve A′—Czepinski (ordinate scale at right); curve B—Lorenz and Velde; curve C—Wachter and Hildebrand.

paper give

$$E^0 = 2.1310 + (3.8492 \times 10^{-4})T \log T - (2.385 \times 10^{-9})T^2 + 0.71551/T - (1.7941 \times 10^{-3})T \quad [27]$$

for the emf as a function of temperature. In Fig. 2 the deviations of the results of the various authors from the thermodynamic values are shown as a function of temperature. The observed data of Wachter and Hildebrand and of Lorenz and Velde lie approximately 0.03–0.04 v below the thermodynamic values at moderate temperatures; deviations become successively more marked at the higher temperatures. The reason for the differences between the observed emf and the thermodynamic value is not apparent. The fact that the observed emf values are low suggests that the galvanic cell $Zn/ZnCl_2/Cl_2(g)$, C is subject to polarization or electrode-electrolyte interactions.

The above two examples illustrate the agreement that may be expected between the theoretical values (Table I) of cells of the type (A) and those obtained either with galvanic cells or from measurements of decomposition voltages.

Acknowledgments

Acknowledgment is gratefully given to Miss Genevie Hawkins, Mrs. Ethel Marden, and Milton Abramowitz of the Computation Laboratory, Applied Mathematics Division, National Bureau of Standards for their assistance and the use of the Standard Eastern Automatic Computer (SEAC) during the course of this investigation.

Manuscript received July 11, 1955. This paper was prepared for delivery at the Boston Meeting, October 3 to 7, 1954.

Any discussion of this paper will appear in a Discussion Section to be published in the December 1956 Journal.

References

1. W. M. Latimer, "The Oxidation States of the Elements and Their Potentials in Aqueous Solutions," 2nd ed., Prentice-Hall, Inc., New York (1952).
2. K. K. Kelley, Bulletin 476, U. S. Dept. of the Interior, (1949); *also* Bulletins 383 (1935) and 393 (1936).
3. L. Brewer, "The Chemistry and Metallurgy of Miscellaneous Materials, Thermodynamics," L. L. Quill, Editor, McGraw-Hill Book Co., Inc., New York (1950).
4. "Selected Values of Chemical Thermodynamic Properties," National Bureau of Standards Circular 500 (1952); *also* Series III (1948–53).
5. Reference (2), p. 206.
6. C. H. Shomate, *J. Am. Chem. Soc.*, **66**, 928 (1944).
7. Y. K. Delimarskii, *Ukranian Khim. Zhur.*, **16**, 414 (1950).
8. D. D. Wagman, Private communication; equation given is better representation than that of K. K. Kelley, reference (2).
9. M. A. Bredig, J. W. Johnson, and W. T. Smith, Jr., *J. Am. Chem. Soc.*, **77**, 307 (1955).
10. B. B. Owen, *ibid.*, **60**, 2229 (1938).
11. J. A. Gledhill and G. McP. Malan, *Trans. Faraday Soc.*, **48**, 258 (1952).
12. G. Scatchard, W. J. Hamer, and S. E. Wood, *J. Am. Chem. Soc.*, **60**, 3061 (1938).
13. A. Wachter and J. H. Hildebrand, *ibid.*, **51**, 4655 (1930).
14. O. H. Weber, *Z. anorg. Chem.*, **21**, 305 (1899).
15. J. H. Hildebrand and G. C. Rule, *J. Am. Chem. Soc.*, **49**, 722 (1927).
16. V. Czepinski, *Z. anorg. Chem.*, **19**, 208 (1899).
17. R. Lorenz and H. Velde, *ibid.*, **183**, 81 (1929).
18. R. C. Kirk and W. E. Bradt, *Trans. Electrochem. Soc.*, **70**, 231 (1936).

Lead- and Manganese-Activated Cadmium Fluorophosphate Phosphors

ROBERT W. WOLLENTIN

Lamp Division, Westinghouse Electric Corporation, Bloomfield, New Jersey

ABSTRACT

The characteristics of lead- and manganese-activated cadmium fluorophosphates and homologous materials containing aluminum, barium, calcium, strontium, magnesium, zinc, sodium, and potassium as partial replacements for cadmium are described. With low activator concentrations in cadmium fluorophosphate, a double band emission is obtained with peaks at 4500 Å and 5900 Å. At high activator concentrations the blue peak is suppressed.

The luminous output and spectral emission of the mixed phosphors are dependent upon activator concentration, the amount of halide relative to the cadmium phosphate portion of the phosphor, the amount of phosphorus relative to cadmium, and the cation which replaces cadmium. Substitutions of sodium, potassium, and zinc for cadmium shift the emission and excitation spectra toward longer wave lengths. The x-ray patterns of these phosphors are quite complex and vary from sample to sample. However, they are all similar to an apatite configuration with the exception of the alkali modified phosphors which display quite different and unidentified patterns. In the case of the double band emission of the unmodified phosphor, the yellow band is suppressed at low temperatures and phosphorescence is enhanced. Above room temperature the fluorescence and phosphorescence of all the phosphors are decreased almost to extinction at 150°C.

INTRODUCTION

Manganese-activated cadmium phosphate phosphors have been described by several investigators. McKeag (1) and McKeag and Ranby (2, 3) described the influence of small amounts of lead and fluorine and various proportions of sodium fluoride on the fluorescence and phosphorescence of manganese-activated cadmium phosphate. Prener (4) described the influence of zinc fluoride on the emission spectrum of manganese-activated cadmium phosphate and found that 5–20% of zinc fluoride incorporated in the phosphor caused a substantial shift of the emission wave lengths toward the red end of the spectrum.

In the course of an investigation of the cadmium phosphate phosphors for consideration in fluorescent lamp applications, it was found that lead and manganese combinations, in proper proportions, acted as double activators for cadmium phosphate containing a substantial amount of fluorine. These materials were characterized by a double-band emission, with both peaks in the visible under 2537Å ultraviolet excitation. The relative heights of the two peaks, one in the blue and one in the orange-red, were dependent upon the concentration of activators.

This paper presents some of the luminescence and structural properties of a group of phosphors herein referred to as lead- and manganese-activated cadmium fluorophosphates and homologous materials where portions of the cadmium constituent are replaced by a variety of other cations. The experimental results are grouped into five sections as follows: (*a*) cadmium fluorophosphate, (*b*) mixed fluorophosphates, (*c*) excitation spectra, (*d*) structure studies, and (*e*) some observations on the temperature dependence of the luminescence. The implications of some of these results are given in a later section.

EXPERIMENTAL PROCEDURES

The chemical reagents used as raw materials in the preparation of cadmium fluorophosphates consisted o reagent grades of cadmium oxide, diammonium phos phate, manganous chloride or manganous carbonate, lead nitrate, and luminescent grades of cadmium fluoride and other fluorides. The powdered raw materials were mixed in about 40 g quantities in an acetone slurry, dried at 100°C, and ground thoroughly in a mortar. Firing of the mixes was performed in covered silica crucibles in an air atmosphere in an electric wire-wound furnace. The firing temperature was selected to provide maximum reaction of the raw materials without excessive sintering according to the composition of the phosphor.

Relative luminous output measurements were made on powdered samples under 2537Å ultraviolet excitation. A photronic cell corrected to eye sensitivity by suitable filters, a bridge circuit, and a sensitive galvanometer were used to compare the brightness relative to a standard 3500° white calcium halophosphate set at a value of 87 on an arbitrary scale.

Spectral emission measurements were obtained on powdered samples employing an automatic recording G.E. Spectroradiometer and a filtered 2537Å ultraviolet source for excitation. The curves so obtained were normalized to a peak height of 100.

Excitation measurements were obtained by means of a recording spectroradiometer employing a Beckman Model DU monochromator and a hydrogen discharge lamp as the exciting source. The luminescence of the sample was

detected by a photomultiplier circuit and automatically plotted against wave length of exciting energy. The curves were adjusted to correct for the energy distribution of the hydrogen source and the dispersion of the monochromator according to data supplied by the manufacturer. No correction was applied for the scattering of light in the instrument. Curves were finally normalized to a peak value of 100.

Structural studies were made employing a recording North American Philips Geiger Counter x-ray diffractometer.

Qualitative examination of the influence of temperature on luminescence was obtained by observation of the emission characteristics of the phosphor under filtered 2537Å ultraviolet excitation at −196°C, +21°C (room temperature), +100°C, and higher temperatures by means of a laboratory hot plate.

Experimental Results

Cadmium fluorophosphate.—When lead is introduced into a base material of cadmium fluorophosphate, which may be represented by the hypothetical formula: $3Cd_3(PO_4)_{2.5}\cdot 2.5CdF_2$,[1] a weak but detectable blue emission composed of a single band peaked at about 4500Å is obtained. The position of the peak is relatively independent of the lead concentration. An optimum amount of lead for maximum luminous output occurs at about 1.0%.[2] In the case of activation by manganese alone, a weak emission occurs which is characterized by a prominent peak at about 6000Å and a smaller secondary peak at about 4000Å. The relative height of the latter is decreased with respect to the 6000Å peak on increasing the manganese concentration.

The simultaneous addition of lead and manganese results in phosphors displaying a plurality of emission spectra dependent upon activator concentration. In the series of curves presented in Fig. 1, manganese was held constant at about 0.035% and the lead was varied from 0.5 to 10.0%. When increasing amounts of lead are added, the 4500Å peak is reduced relative to the longer wavelength peak near 5900Å, the 4500Å peak shifts to a new position at 4600Å, and the manganese peak is also shifted slightly toward longer wave lengths. In the case of higher manganese concentrations, the same influence on the relative peak height occurs; however, in this case the relative height of the blue peak is less than for the corresponding case with lower manganese concentration. With still higher manganese concentration, 0.35% and greater, the emission spectrum is relatively independent of the lead concentration as shown in Fig. 2.

The luminous output of the doubly activated cadmium fluorophosphate is dependent upon the activator, fluoride, and phosphate concentrations. In order to demonstrate the influence of the activator concentrations on the powder brightness of the phosphor, the concentration of

[1] All compositions are stated in terms of the number of moles present in the unfired mix. An explanation of the phosphate proportion follows later in this same section.

[2] All activator concentrations are expressed in per cent by weight of the cadmium orthophosphate portion of the phosphor.

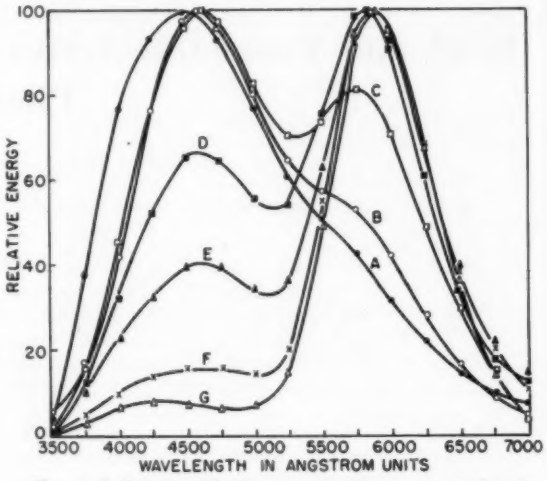

Fig. 1. Influence of lead concentration on spectral emission of $3Cd_3(PO_4)_{2.5}\cdot 2.5CdF_2$:0.035% Mn, xPb; firing temp, 750°C. Curve A, 0.5% Pb; curve B, 1.0% Pb; curve C, 2.0% Pb; curve D, 4.0% Pb; curve E, 6.0% Pb; curve F, 8.0% Pb; curve G, 10.0% Pb.

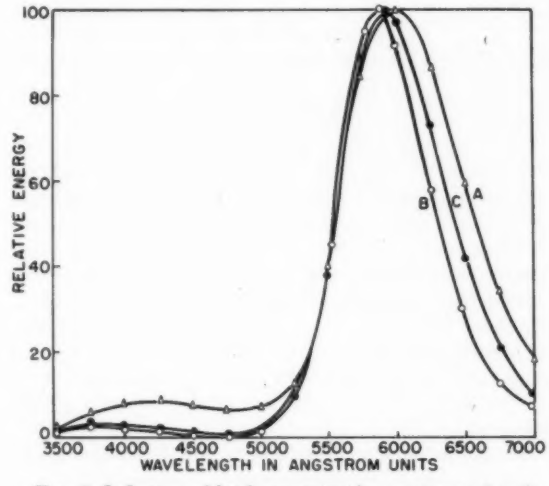

Fig. 2. Influence of lead concentration on spectral emission of $3Cd_3(PO_4)_{2.5}\cdot 2.5CdF_2$:0.35% Mn, xPb. Curve A, 0.1% Pb; curve B, 4.0% Pb; curve C, 10.0% Pb.

lead was varied from 0.05 to 10.0% and manganese from 0.035 to 1.40%. Experimental results indicate that the optimum manganese concentration is 0.70% while the concentration of lead is not critical above 2.0% and should amount to between 4.0 and 6.0%. The brightness value for the optimum formulation is of the same order of magnitude as for a well-made 3500° white halophosphate (87 on the scale used), but there is a considerable difference, of course, between the spectral distributions of the two phosphors.

The dependence of brightness upon the fluoride concentration is shown in Fig. 3, curve A, for the case where the cadmium fluoride of the raw mix was introduced in amounts up to 5.0 moles per 3.0 moles of cadmium orthophosphate. A clearly defined optimum occurs at 3.0

moles of cadmium fluoride. The spectral emission of the phosphor is shifted about 100Å toward shorter wave lengths on increasing the amount of cadmium fluoride from 1 to 5 moles per 3.0 moles of $Cd_3(PO_4)_{2.5}$.

The brightness of the phosphor is also dependent on the amount of phosphate relative to cadmium. When the phosphate is increased from the proportion of exact stoichiometry of the orthophosphate, a broad maximum occurs at a mixture of about 7.5 atoms of phosphorus to 9.0 atoms of cadmium in the brightness curve, Fig. 4. This amounts to a 25.0 mole % excess of phosphate over that required to form cadmium orthophosphate. Because of the benefit on brightness derived therefrom, all compositions reported here contain a 25.0% excess of phosphate in the prefired mixture.

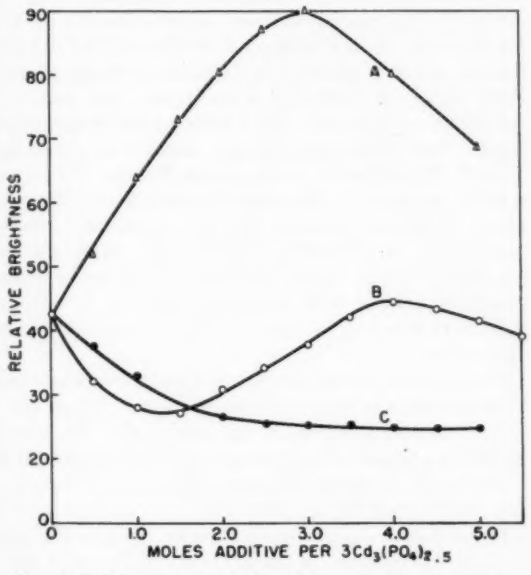

FIG. 3. Brightness of cadmium fluorophosphate phosphors

Curve	Composition	Firing Temp, °C
A	CdF_2 in $3Cd_3(PO_4)_{2.5}\cdot x CdF_2$:1.0% Mn, 4.0% Pb	750
B	NaF in $3Cd_3(PO_4)_{2.5}\cdot x NaF$:0.70% Mn, 6.0% Pb	650
C	KF in $3Cd_3(PO_4)_{2.5}\cdot x KF$:1.0% Mn, 4.0% Pb	600

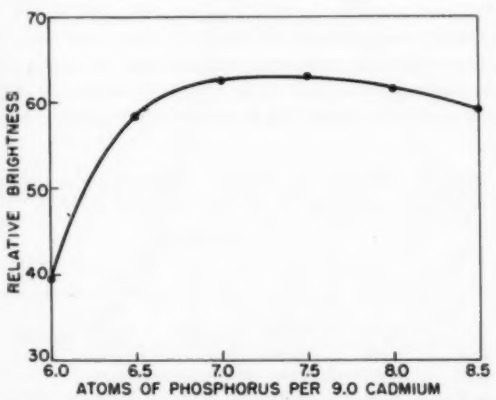

FIG. 4. Dependence of brightness on mole ratio of phosphorus to cadmium in $3Cd_3(PO_4)_x\cdot 2.5CdF_2$:1.0% Mn, 4.0% Pb prepared at 750°C.

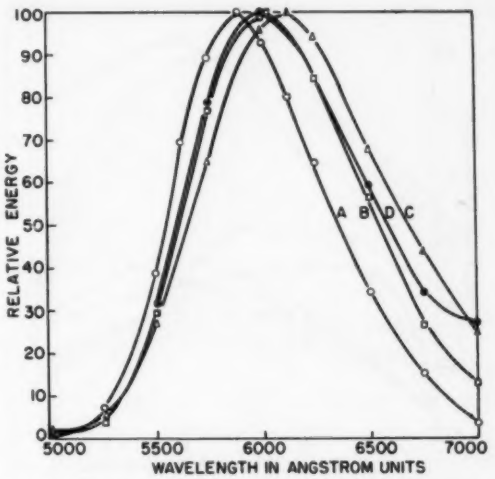

FIG. 5. Influence of partial cation substitution on spectral distribution of $3Cd_3(PO_4)_{2.5}\cdot 1.3CdF_2\cdot 1.2xF_2$:0.7% Mn, 6.0% Pb.

Curve	Substituent	Firing Temp, °C
A	AlF_3	800
	BaF_2	800
	SrF_2	800
	CaF_2	750
B	NaF	650
	MgF_2	750
C	KF	600
D	ZnF_2	800

Mixed fluorophosphates.—Fluorides of the elements aluminum, calcium, strontium, barium, zinc, magnesium, potassium, and sodium influence the luminescence characteristics of the doubly activated cadmium fluorophosphate. Partial replacement of the cadmium fluoride in the formulation $3Cd_3(PO_4)_{2.5}\cdot 2.5CdF_2$:0.70% Mn, 6.0% Pb by the fluorides mentioned above resulted in decreased brightness in all instances. In this respect, substitutions of the monovalent cations were most detrimental in that small amounts caused a large loss in luminous efficiency and 2.5 moles resulted in a drop of 70.0%, while the same amounts of the divalent substituents caused losses between 30.0 and 45% and the same concentration of trivalent aluminum resulted in only an 18.0% loss.

The effect of these partial substitutions on the spectral emission of the phosphor is shown graphically in Fig. 5 where 1.2 moles of cadmium fluoride in the formulation: $3Cd_3(PO_4)_{2.5}\cdot 2.5CdF_2$:0.70% Mn, 6.0% Pb are replaced by the fluorides of the cations previously mentioned. In the cases of aluminum, strontium, barium, and calcium, the emission spectrum remains unaltered with the peak wave length at about 5900Å. Sodium, magnesium, and zinc cause the peak wave length to shift to about 6000Å, while potassium causes the peak to shift to about 6130Å.

When the above-mentioned fluorides are added to the phosphor in various amounts in the absence of cadmium fluoride, the brightness vs. additive concentration curves, Fig. 6 and 3, display maxima at different concentrations, dependent upon the substituent cation. The optimum

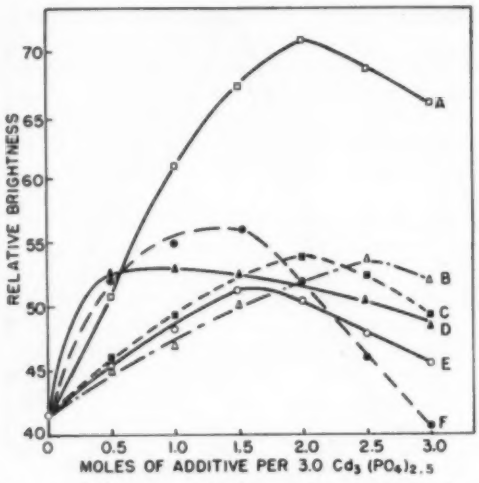

FIG. 6. Influence of foreign cation concentration on brightness of $3Cd_3(PO_4)_{2.5}\cdot nxF_2$:0.7% Mn, 6.0% Pb.

Curve	Substituent	Firing Temp, °C
A	AlF_3	800
B	SrF_2	800
C	MgF_2	750
D	ZnF_2	800
E	CaF_2	750
F	BaF_2	800

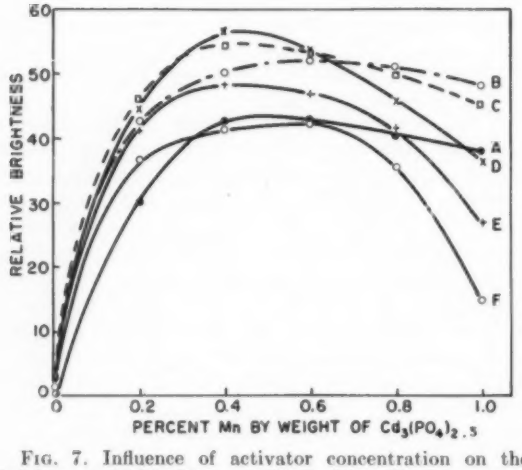

FIG. 7. Influence of activator concentration on the brightness of $3Cd_3(PO_4)_{2.5}\cdot 4.0NaF:xMn, yPb$, firing temp, 650°C. Curve A, 0% Pb; curve B, 0.5% Pb; curve C, 2.0% Pb; curve D, 4.0% Pb; curve E, 6.0% Pb; curve F, 8.0% Pb.

molar contents, for 3.0 moles of $Cd_3(PO_4)_{2.5}$, are as follows: aluminum and magnesium fluorides, 2.0 moles; strontium fluoride, 2.5 moles; calcium and barium fluorides, 1.5 moles; zinc fluoride, about 1.0 mole; sodium fluoride, 4.0 moles; and potassium fluoride, no apparent optimum.

Spectral distribution measurements of phosphors containing 2.0 moles of the various fluorides per 3.0 moles of cadmium orthophosphate showed the same pattern of emission shift as for the case where cadmium fluoride was present, except that without the cadmium fluoride the influence is more pronounced. Aluminum, calcium, barium, and strontium still show very little effect. The presence of sodium causes the peak to shift 200Å and potassium 300Å toward the red, while magnesium causes only a slight shift toward the red. Zinc not only shifts the emission peak 200Å toward longer wave lengths, but also increases the red tail of the emission.

The orange-red emitting cadmium-sodium fluorophosphate was examined more closely, since red or near-red emitting materials are of considerable interest with respect to fluorescent lamp applications. The brightness of the phosphor is strongly dependent on the activator concentration. The optimum activator concentrations for maximum luminous output in $3Cd_3(PO_4)_{2.5}\cdot 4NaF$ are 4.0% lead and 0.40% manganese as shown in Fig. 7, curve D. The spectral emission of the phosphor is dependent upon the activator concentration and the sodium fluoride content relative to cadmium orthophosphate. With regard to activator concentration, the emission consists of a single peak which shifts toward longer wave lengths with increasing activator contents as shown in Table I. The influence of the sodium fluoride content on spectral emission is illustrated graphically in Fig. 8, where the sodium fluoride was introduced into a base composition of $3Cd_3(PO_4)_{2.5}$:0.70% Mn, 4.0% Pb in amounts up to 5.0 moles. The shift toward longer wave lengths is gradual with increasing amounts of sodium fluoride up to 4.0 moles, curve C, above which no further shift occurs.

The phosphor system consisting of cadmium-potassium fluorophosphate is somewhat similar to the system containing sodium. However, in the case of the potassium-containing phosphor, the luminous output of the phosphor is continually decreased with increasing amounts of potassium fluoride (see Fig. 3, curve C).

The influence of potassium fluoride content on the spectral distribution of $3Cd_3(PO_4)_{2.5}\cdot nKF$:1.0% Mn, 4.0% Pb is shown in Fig. 9. The emission peak is shifted continuously toward longer wave lengths to about 6280Å with amounts up to 2.0 moles potassium fluoride. Greater amounts do not influence the emission spectrum.

Variation of activator concentration in two formulations containing 2.0 and 4.0 moles potassium fluoride per 3.0 moles cadmium orthophosphate, Fig. 10, shows an optimum concentration of 2.0–4.0% lead, but does not indicate that an optimum concentration of manganese was reached. The body color of the phosphor becomes more pink with increasing amounts of manganese, which

TABLE I. *Influence of activator concentration on spectral emission peak of* $3Cd_3(PO_4)_{2.5}\cdot 4.0NaF:xMn,yPb$

% Lead	% Manganese				
	0.2	0.4	0.6	0.8	1.0
	Å	Å	Å	Å	Å
0	6140	6180	6200	6200	6200
0.5	6160	6180	—	6200	—
2.0	6160	—	—	6200	—
4.0	6160	6200	6220	6250	6230
6.0	6190	—	—	6250	—
8.0	6190	6200	6220	6250	6250

indicates an absorption band extending into the visible region of the spectrum. The emission spectrum is also dependent upon activator concentration. Increasing amounts of activators cause a gradual shift toward longer wave lengths, as shown in Table II.

Excitation spectra.—The normalized excitation spectra for some of the mixed cadmium fluorophosphates are shown in Fig. 11. All of the phosphors for these curves contained 0.70% manganese and 6.0% lead except for the sodium- and potassium-containing phosphors, which contained 1.0% manganese and 4.0% lead.

The excitation spectrum of unmodified cadmium fluorophosphate (Fig. 11, curve E) is characterized by two maxima, one at 2350Å and a secondary one at about 2500Å, and a rather rapid fall-off on the long wave-length edge. When strontium or aluminum fluorides (Fig. 11, curves B and C, respectively) replace cadmium fluoride, the 2350Å peak is shifted to 2300Å and the 2500Å peak is decreased. The substitution of sodium fluoride (Fig. 11, curve D) causes a similar shift of the 2350Å peak, a lowering of the 2500Å peak, and also extends the long wavelength edge to longer wave lengths. Zinc fluoride (Fig. 11, curve F) increases the relative sensitivity to longer wave lengths without influencing the position of the maxima. Potassium fluoride (Fig. 11, curve G) increases the 2500Å peak and also increases the sensitivity to longer wave lengths without influencing the 2350Å peak. Barium fluoride (Fig. 11, curve A) shifts the 2500Å peak to about 2700Å and the 2350Å peak to 2300Å.

X-ray diffraction studies.—The x-ray diffraction pat-

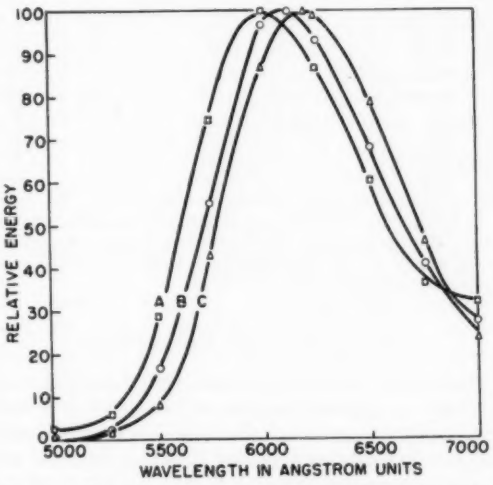

FIG. 8. Influence of sodium fluoride concentration on the spectral emission of $3Cd_3(PO_4)_{2.5}\cdot nNaF$:0.70% Mn, 4.0% Pb; firing temp, 650°C. Curve A, 0.5 mole NaF; curve B, 2.0 moles NaF; curve C, 4.0; 5.0 moles NaF.

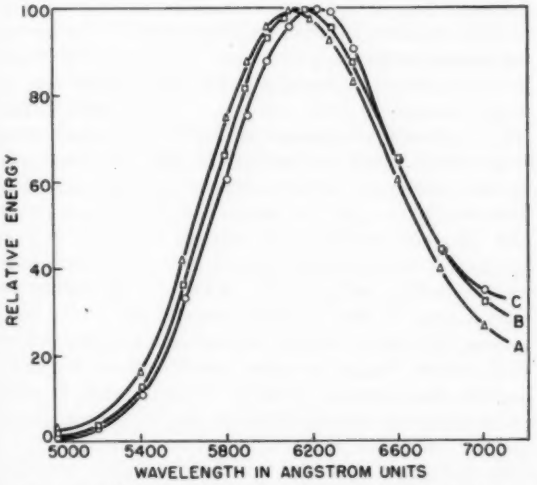

FIG. 9. Influence of potassium fluoride concentration on spectral emission of $3Cd_3(PO_4)_{2.5}\cdot nKF$:1.0% Mn, 4.0% Pb; firing temp, 600°C. Curve A, 0.5 mole KF; curve B, 1.0 mole KF; curve C, 2.0; 3.0; 5.0 moles KF.

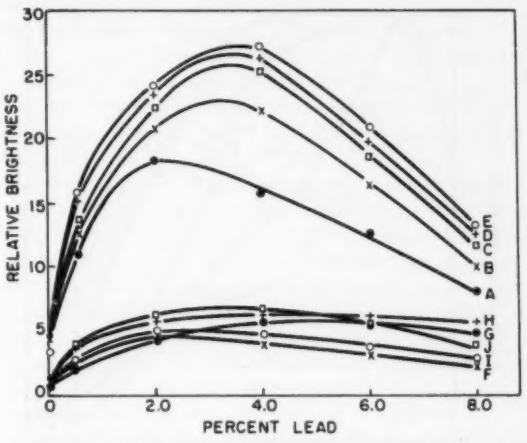

FIG. 10. Influence of activator concentration on brightness of lead- and manganese-activated cadmium-potassium fluorophosphates, firing temp, 600°C.

% Mn	2.0 KF	4.0 KF
0.2	A	F
0.4	B	G
0.6	C	H
0.8	D	I
1.0	E	J

TABLE II. *Influence of activator concentration on the emission peak of* $3Cd_3(PO_4)_{2.5}\cdot nKF$:$x$%Mn, y%Pb

(A) 2.0 KF

% Lead	% Mn			
	0.2	0.4	0.6	1.0
	Å	Å	Å	Å
0	6120	6150	6180	6200
0.5	6120	6160	6180	6230
2.0	6150	6160	6190	6250
4.0	6150	6180	6200	6260
8.0	6150	6180	6200	6280
(B) 4.0 KF				
0	6200	6210	6240	6260
0.5	6200	6210	6240	6260
2.0	6200	6220	6260	6280
4.0	6210	6220	6260	6280
8.0	6210	6240	6280	6300

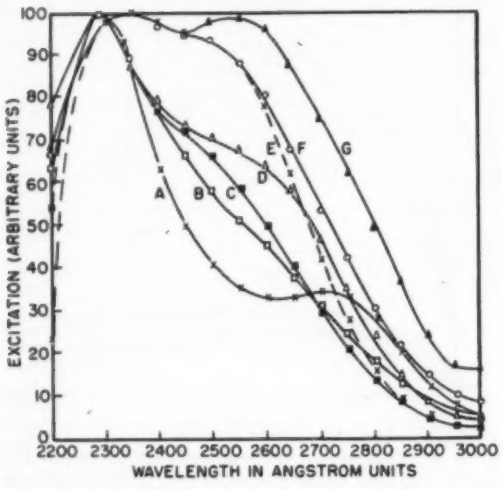

FIG. 11. Excitation spectra of mixed cadmium fluorophosphates

Curve	Composition	Firing Temp, °C
A	$3Cd_3(PO_4)_{2.5}$·2.0 BaF_2:0.70% Mn, 6.0% Pb	800
B	$3Cd_3(PO_4)_{2.5}$·2.0 SrF_2 :0.70% Mn, 6.0% Pb	800
C	$3Cd_3(PO_4)_{2.5}$·2.0 AlF_3 :0.70% Mn, 6.0% Pb	800
D	$3Cd_3(PO_4)_{2.5}$·2.0 NaF :1.0% Mn, 4.0% Pb	650
E	$3Cd_3(PO_4)_{2.5}$·2.0 CdF_2:0.70% Mn, 6.0% Pb	750
F	$3Cd_3(PO_4)_{2.5}$·2.0 ZnF_2:0.70% Mn, 6.0% Pb	800
G	$3Cd_3(PO_4)_{2.5}$·2.0 KF :1.0% Mn, 4.0% Pb	600

terns of a number of these phosphors show a number of variations. In some instances, the patterns contain more than forty lines, which vary in order of line intensity from sample to sample. In general, however, the patterns may be roughly classified into four groups as shown in Table III. One of these groups, designated A in the table, agrees closely with the apatite structure reported by Rooksby and McKeag (5). Another of these groups (A_1) is quite similar with respect to line position but differs slightly in line intensities. The third group (B) departs radically in the order of line intensities from the apatite pattern, and the fourth group (D) consists of a miscellaneous group of patterns all differing from one another and from an apatite pattern.

Some observations on the temperature dependence of the luminescence.—A qualitative examination showed the fluorescence and phosphorescence to be influenced by temperature. Unmodified cadmium fluorophosphate, with low activator concentration and hence having a double-band emission, is most noticeably influenced. At −196°C the orange band is considerably suppressed while the blue band is relatively unaffected. Above room temperature the orange emission appears to shift toward the yellow, and practically all emission is suppressed at +150°C. The phosphorescence is yellow at all temperatures and is more persistent at low temperatures. In the case of higher activator concentrations in the unmodified cadmium fluorophosphate and also in the mixed fluorophosphates, where the emission spectra consist of single bands, lowering the temperature enhances phosphorescence and causes a slight shift of the emission toward the yellow. Above room temperature, phosphorescence and fluorescence are decreased to extinction at about 150°C.

TABLE III. *X-ray diffraction patterns of cadmium fluorophosphates*

Moles halide per $3Cd_3(PO_4)_{2.5}$	% Mn	% Pb	Pattern type*
1.0 CdF_2	0.70	6.0	B
3.0 CdF_2 (opt.)	0.70	6.0	A_1
5.0 CdF_2	0.70	6.0	A_1
2.5 CdF_2	0.35	6.0	A
2.5 CdF_2	0.70	6.0	A
2.5 CdF_2	1.40	6.0	A
2.5 CdF_2	0.035	0.1	B
2.5 CdF_2	0.035	4.0	B
2.5 CdF_2	0.035	10.0	A
1.0 AlF_3	0.70	6.0	B
2.0 AlF_3 (opt.)	0.70	6.0	A
3.0 AlF_3	0.70	6.0	A_1
0.5 BaF_2	0.70	6.0	B
1.5 BaF_2 (opt.)	0.70	6.0	A
3.0 BaF_2	0.70	6.0	D_1
0.5 NaF	0.70	6.0	D_2
1.5 NaF	0.70	6.0	D_3
4.0 NaF (opt.)	0.70	6.0	D_4
5.5 NaF	0.70	6.0	D_5
0.5 KF	0.70	6.0	B
1.5 KF	0.70	6.0	B
3.0 KF	0.70	6.0	B
3.0 ZnF_2	0.70	6.0	D_6

* A, apatite structure; A_1, similar to apatite structure, but differing in order of intensities; B, pattern different from A and A_1; D, miscellaneous patterns different from B and A and each other.

DISCUSSION AND CONCLUSIONS

The double activation of cadmium fluorophosphate by lead and manganese is another addition to the growing list of sensitized phosphors. The cadmium fluorophosphate matrix is inefficiently activated by either activator alone, but in combination these activators provide a phosphor of high efficiency. While the more efficient phosphors of the system lack the double-band emission necessary to produce white, they possess other worthy characteristics which make them of use in blends and in theoretical considerations on the mechanism of luminescence.

Data on the influence of the concentration of activators on spectral emission, Fig. 1, are of particular interest at low activator concentrations. On the introduction of small amounts of lead, emission is predominantly blue. This indicates preferential excitation of blue-emitting lead centers which are sufficiently removed from manganese centers to prevent efficient transfer of energy between the two kinds of centers and, hence, gives rise to the blue lead emission. An increase of either lead or manganese concentration places some of the manganese centers within sufficient proximity to lead centers to permit some transfer of energy from the lead to the manganese, and thus gives rise to excitation and emission of both centers. Higher activator concentrations, therefore, provide the necessary proximity of both centers to allow efficient transfer of energy from the lead to the manganese to give rise to the preferred manganese emission.

In the mixed phosphors and the unmodified cadmium fluorophosphate, the structure studies (Table III) throw some light on the appearance of optima in the brightness vs. concentration curves of Fig. 3 and 6. In the case of cadmium fluorophosphate, there appear to be three

separate patterns dependent upon the halide content. Here, and also for the other fluorides studied, with the exception of sodium and potassium fluorides, maximum brightness occurs when the basic structure is most similar to the apatite configuration. The second pattern (B) which is also common to all but the sodium fluoride modification is present at concentrations of the fluoride below optimum. This pattern probably represents a mixture of cadmium phosphates and halides. Positive identification of this phase and others is complicated by the lack of published data and standard x-ray patterns on cadmium phosphates and related compounds. However, further consideration of this problem is being given and will be reported at a later date. The pattern group (A_1) in the unmodified cadmium fluorophosphate occurs for higher than optimum concentrations of cadmium fluoride and also in the case of aluminum fluoride, and closely resembles the apatite pattern. The difference in line intensities between this and the apatite pattern may be caused by further substitutional solid solution by the fluorine ion into sites which differ from the lattice position normally occupied by the fluorine in forming the apatite configuration. The sodium-containing phosphors seem to involve a slightly different structure which is not definable in the light of presently available data.

In those phosphors where the emission spectrum is located further in the red portion of the spectrum than the unmodified cadmium fluorophosphate, excitation spectra peaks show either a shift toward wave lengths longer than 2537Å or an increase in the relative height of the long wave-length tail of the excitation spectrum. The cadmium-barium fluorophosphate (Fig. 11, curve A) is peculiar in that the excitation spectrum contains a secondary peak at 2750Å, but the emission spectrum does not differ materially from the unmodified cadmium fluorophosphate.

Summary

A system of phosphors composed of lead- and manganese-activated cadmium fluorophosphates and homologous materials formed by the substitution of aluminum, barium, strontium, calcium, magnesium, zinc, sodium, and potassium for portions of the cadmium have been described.

The luminous output and spectral distribution of the phosphors under 2537Å ultraviolet excitation were shown to be dependent on concentration of activators, fluoride content, the specific cation selected to replace cadmium, and the amount of phosphorus relative to cadmium.

The spectral emission of the unmodified cadmium fluorophosphate consists of one band at high concentration, and two bands at low concentrations of lead and manganese. The two bands are peaked at about 4500Å and 5900Å.

Substitutions of aluminum, barium, strontium, and calcium fluorides for the cadmium fluoride portion of the phosphor result in products of lowered luminous output, essentially the same emission spectrum, and different excitation spectra dependent on the cation present. Replacements of cadmium fluoride by sodium and potassium fluorides cause the emission peak to shift to about 6200Å. Replacements of cadmium fluoride by magnesium and zinc fluorides cause the emission peak to shift to 5950Å and 6000Å, respectively.

X-ray diffraction studies established a direct correlation between the apatite configuration and optimum proportions of halide for maximum luminous output, except for the case of sodium and potassium fluoride modifications. Besides the apatite pattern, a number of other patterns occur dependent on the concentration of the particular cations present. Identification of the various patterns obtained on these fluorophosphates is in progress and will be reported at a later date.

The fluorescence and phosphorescence of the cadmium fluorophosphates are dependent on temperature. At −196°C the yellow or red emission is greatly suppressed and the phosphorescence increased. Above room temperature, phosphorescence and fluorescence are decreased to extinction at about 150°C.

Manuscript received May 16, 1955. This paper was prepared for delivery before the Cincinnati Meeting, May 1 to 5, 1955.

Any discussion of this paper will appear in a Discussion Section to be published in the December 1956 Journal.

REFERENCES

1. A. H. McKeag, (To General Electric Co.) U. S. Pat. 2,214,643, Sept. 10, 1940.
2. A. H. McKeag and P. W. Ranby, (To General Electric Co. Ltd.) Brit. Pat. 581,778, Oct. 24, 1946.
3. A. H. McKeag and P. W. Ranby, (To General Electric Co.) U. S. Pat. 2,476,676, July 19, 1949.
4. J. S. Prener, (To General Electric Co.) U. S. Pat. 2,636,010, April 21, 1953.
5. H. P. Rooksby and A. H. McKeag, *General Electric Co. Journal, England*, **17**, 89 (1950).

Dielectric Behavior of Electroluminescent Zinc Sulfides

WILLI LEHMANN

Lamp Division, Westinghouse Electric Corporation, Bloomfield, New Jersey

ABSTRACT

The complex dielectric factor of electroluminescent zinc sulfides was measured as a function of the voltage and frequency applied to the electroluminescent cell. Both the real and the imaginary part of the dielectric factor obey the law: $k = k_0 +$ function of (L/f), where L is the time average of the electroluminescent emission and f is the frequency. For low and moderate voltages, this expression becomes $k = k_0 + c(L/f)^{1/2}$, where k_0 may depend on frequency f, but c is a constant independent of voltage and frequency.

INTRODUCTION

During measurements concerning the efficiency (lumens per watt) of several electroluminescent phosphors it was necessary to determine the complex dielectric factor of the phosphors as accurately as possible. These measurements produced several unexpected results which may help in understanding the mechanism of electroluminescence. It should be mentioned that it is somewhat misleading to speak about a "dielectric constant" in the present case. The designation "dielectric factor" is preferred here since this factor is, at least in electroluminescent phosphors, not constant but dependent on field strength and frequency.

The results given in this report are mainly related to a zinc sulfide phosphor activated with 0.3 mole % copper and 0.05 mole % lead (amounts added before firing). This phosphor emits green light for applied frequencies up to about 500 cps and turns blue for higher frequencies. The phosphor is mainly cubic and has an average particle size of about 4 μ. This phosphor is given here as a typical example. Other zinc sulfides gave similar results, however.

Measurements of the complex dielectric factor of an electroluminescent zinc sulfoselenide have been made by Roberts (1). However, his results are quite different from those reported here. Roberts found that the dielectric factor first decreased then increased with increasing field strength, while the results given here show only an increase of the dielectric factor with the field strength. The reasons for these differences are not clear.

EXPERIMENTAL ARRANGEMENT AND PROCEDURE

The phosphor was mixed with castor oil and placed in a cell consisting of an aluminum back electrode and a front electrode of conducting glass (Fig. 1). The distance between the two electrodes was about 60 μ, and the area of the cell was 11 cm^2. The sinusoidal voltage applied to this cell could be varied between 0 and 600 rms volts and the frequency between 20 and more than 20,000 cps. It must be noted that the electrical and optical properties of the cell are somewhat variable, since the phosphor particles can move in the viscous liquid dielectric (the castor oil). However, after applying a high voltage to the cell for several minutes the phosphor reaches a geometrical arrangement which is stable for some time; therefore, if the measurements are made carefully and not too long after the "stable" condition is reached, it is possible to obtain reproducible results. Three types of measurements were made, the electroluminescent brightness, the electrical capacity of the cell, and the phase angle of the cell, all as a function of voltage and frequency. All measurements were made only at room temperature.

The light emitted from the cell was detected by a photomultiplier. The voltage drop produced by the photocurrent across a resistor was measured by a vacuum tube electrometer (Keithley Model 200). Precautions were taken to avoid the photocurrent becoming too high with increasing cell brightness and also to avoid any effect of the stray electric field from the electroluminescent cell upon the photomultiplier. With this arrangement it was possible to measure the electroluminescent brightness over a range of more than seven orders of magnitude with an accuracy of better than $\pm 10\%$.

The capacity $\vec{C}$ of the cell is complex. The real part C' of the capacity gives a current which is 90° out of phase with the applied voltage; the imaginary part C'' of the capacity gives a current in phase with the voltage. The magnitude, $C = [(C')^2 + (C'')^2]^{1/2}$, of the capacity is directly measured by comparison with a standard capacitor (General Radio Type 505) of about the same capacity by measuring the currents through both (Fig. 2a). Thus C can be obtained with an accuracy better than $\pm 1\%$.

The phase angle, $\varphi = \tan^{-1}(C''/C')$, of the cell has been measured in a bridge with four standard capacitors as shown in Fig. 2b. Here the capacity of C_a is about the same as that of the cell, while C_b is about 100 times larger, so that about 99% of the voltage from the power supply appears across C_a and only about 1% across C_b. Since the phase angle of the cell is not very dependent on voltage, this deviation of 1% is unimportant. The electronic phase angle meter (Advance Electronics Model 405) used in connection with the bridge permits readings of phase angle differences with an accuracy of about $\pm 0.2°$. A calculation of the electrical behavior of the bridge shows that the phase angle meter does not measure the true phase angle φ of the cell, but a slightly smaller angle ψ, where

$$\tan \varphi = (1 + C/C_b) \cdot \tan \psi \qquad \text{(I)}$$

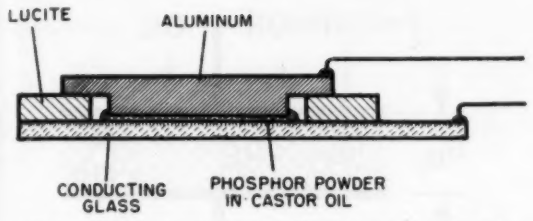

FIG. 1. Electroluminescent cell used for measurements

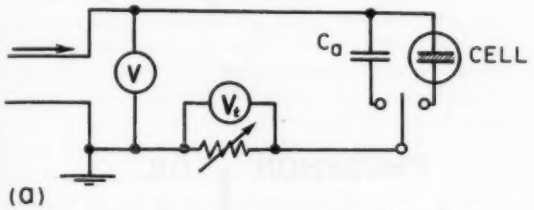

FIG. 2a. Circuit for measurements of cell capacitance. C_a = standard capacitor, V_t = vacuum tube voltmeter.

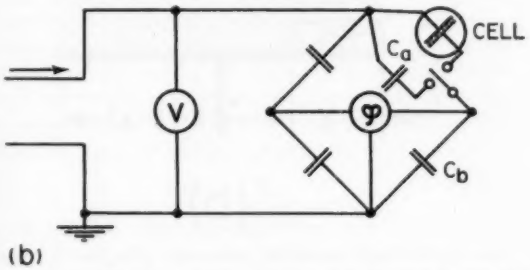

FIG. 2b. Circuit for measurement of phase angle of the cell.

Since C_b is about 100 times greater than C, this correction, in general, can be neglected.

The following results are indicated with the index 0 relating to air, with 1 relating to the castor oil, with 12 relating to the mixture of oil and phosphor, and with 2 relating to the phosphor itself. For example, C'_{12} means the real part of the capacity of the whole cell containing oil and phosphor.

RESULTS OF MEASUREMENTS

The electroluminescent cell filled only with castor oil (without phosphor) has a very small phase angle φ_1, so that practically here $C_1 = C'_1$. By dividing this real capacity C'_1 by the real capacity C'_0 (here $C_0 = C'_0 = 154$ $\mu\mu f$) of the cell containing only air, the real dielectric factor k'_1 of the castor oil is obtained. The value of k'_1 varies between 3.78 for 20 cps and 3.70 for 40,000 cps and is practically independent of voltage. The phase angle φ_1 of the castor oil was found to be roughly $45/f$ where f = the applied frequency, e.g., f = 20 cps, $\varphi_1 = 2.2°$. This phase angle is practically independent of voltage and is always much smaller than the phase angle φ_{12} of the mixture of phosphor and oil. The imaginary part, k''_1, of the dielectric factor of the castor oil is

$$k''_1 = k'_1 \tan \varphi_1 \qquad \text{(II)}$$

or approximately

$$k''_1 = 2.95/f \qquad \text{(III)}$$

The same cell is next filled with a mixture of 80% by volume of castor oil and 20% of phosphor. Now the magnitude C_{12} of the cell capacity and the phase angle φ_{12} of the whole cell are greatly dependent on voltage and frequency. Both C_{12} and φ_{12} increase with increasing voltage and with decreasing frequency. Maxima or minima for certain voltages or frequencies are not observed, and in general the behavior agrees with that reported by Jerome and Gungle (2). Some typical values are given in Table I below.

TABLE I

V (volts rms)	f (cps)	C_{12} ($\mu\mu f$)	φ_{12} (degrees)
50	20	1270	9.5
300	20	3140	53
50	1000	960	6.5
300	1000	1205	15.4

From these measured data of C_{12} and φ_{12} the real dielectric factor of the phosphor-oil mixture can be found from the equation

$$k'_{12} = (C_{12}/C_0) \cos \varphi_{12} \qquad \text{(IV)}$$

and the imaginary dielectric factor from the equation

$$k''_{12} = (C_{12}/C_0) \sin \varphi_{12} \qquad \text{(V)}$$

The emission intensity L of the phosphor used here is shown graphically in Fig. 3. These intensity values are not those measured directly, but they have been corrected for the influence of the change in color of the emission when the frequency is varied and for the spectral response of the

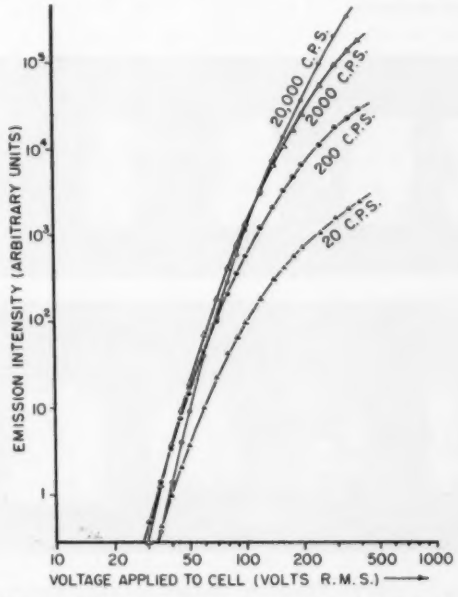

FIG. 3. Electroluminescent quantum emission as a function of voltage and frequency.

photocell. Values given in Fig. 3 are thus proportional to the number of emitted light quanta for all voltages and frequencies.

Methods of Determining the Dielectric Factor of the Phosphor

From the measured data for the dielectric factor of the oil and of the mixture of phosphor and oil it should be possible to determine the dielectric factor of the phosphor itself. This determination is possible, however, only under the assumption that the phosphor particles are essentially uniform as regards dielectric properties and, furthermore, it depends greatly on the geometrical arrangement of the phosphor in the cell. Three different geometrical arrangements are possible.

1. The phosphor has settled down on the surface of one electrode and is there essentially separated from the castor oil.

2. The phosphor is uniformly distributed throughout the insulating oil.

3. Under the influence of the strong electric field the phosphor particles form bridges between the electrodes

Fig. 4. Experimental cell to show phosphor bridges between electrodes.

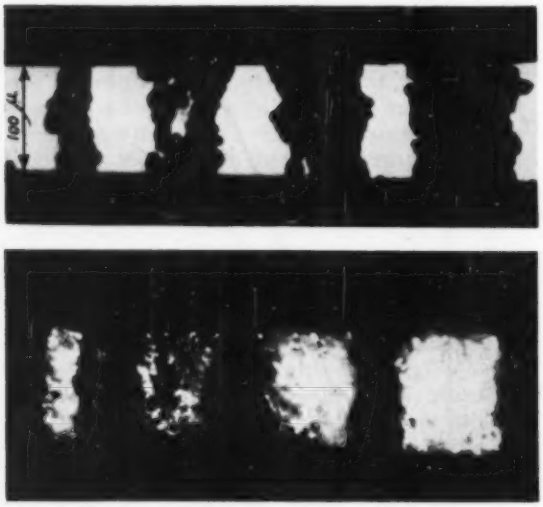

Fig. 5. (*Above*) Phosphor bridges between electrodes, illuminated with white light; (*below*) phosphor bridges in their own electroluminescent light.

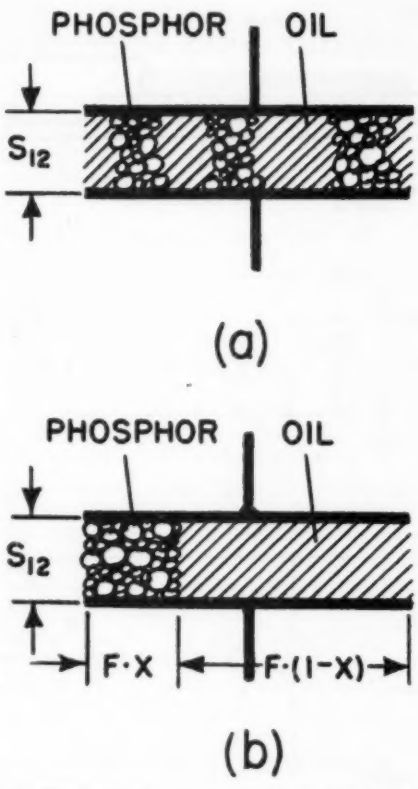

Fig. 6a. Electroluminescent cell with phosphor bridges between the electrodes; b, the equivalent capacitor.

like iron powder between the poles of a magnet. This effect is well known and has been reported in a similar case by Pearce (3).

Actually, it is observed that case 3 most nearly describes the situation in the castor oil cells used. The effect is so distinct that it can be seen even with the unaided eye.

A separate experiment was made in order to show the phosphor bridges as clearly as possible. Two pieces of metal of about 140 μ thickness were mounted with a separation of about 100 μ on a piece of plexiglass, as shown in Fig. 4. The space between the two metal electrodes was filled with the usual mixture of an electroluminescent phosphor in castor oil, and this mixture was observed microscopically. Before a voltage was applied, the phosphor particles were randomly distributed as might be expected. After application of 600 volts rms (of any frequency) the phosphor particles form close bridges between the two metal electrodes. These bridges are shown in two photomicrographs, in Fig. 5a illuminated with white light, and in Fig. 5b in their own electroluminescent light.

Considering the electrical behavior of an electroluminescent cell with bridges between the electrodes, the actual particle distribution, as shown in Fig. 6a, can be simplified to that of Fig. 6b. This system can be considered as two parallel connected capacitors, C_1 and C_2, which have the same thickness S_{12}, but different areas, $(1 - x) \cdot F$ and xF, and different dielectric factors, k_1 and

k_2. Then simply $C_{12} = C_1 + C_2$ with

$$C_{12} = \frac{Fk_{12}}{4\pi S_{12}}; \quad C_1 = \frac{(1-x)Fk_1}{4\pi S_{12}}; \quad C_2 = \frac{xFk_2}{4\pi S_{12}} \qquad \text{(VI)}$$

Combining these formulas and separating k_2 gives the result

$$k_2 = \frac{k_{12} - (1-x)k_1}{x} \qquad \text{(VII)}$$

Of course, this equation can be only an approximation, since the particle bridges in Fig. 6a are still different from the close packed solid phosphor, as assumed in Fig. 6b. But the particles in the bridges between the electrodes are packed very closely; therefore, the approximation seems to be good. Equation (VII) is valid for both the real and the imaginary part of the dielectric factor.

The observed phenomenon of phosphor bridges between the electrodes provides a convenient method of determining the average electric field strength across the phosphor particles. Normally this determination is dependent on the dielectric constant of the phosphor and of the embedding oil, and, therefore, is dependent in a complicated way on the voltage and frequency applied to the cell. But in the case of the phosphor bridges shown in Fig. 5 and 6 there is, in effect, only phosphor between the electrodes; therefore, the average electric field strength E across the phosphor particles is simply given by

$$E = V/S_{12} \qquad \text{(VIII)}$$

where S_{12} is the electrode separation and V the voltage applied to the cell. Equation (VIII) is independent of all changes in the dielectric factors of the phosphor and of the oil. In practice, however, equation (VIII) is only an approximation.

The Imaginary Dielectric Factor of the Phosphor

By use of equation (VII), the imaginary part of the dielectric factor of the phosphor itself can easily be determined. The result for a typical electroluminescent zinc sulfide activated with copper (as described above) is shown graphically in Fig. 7.

It is obvious that there must be some connection between the appearance of electroluminescent emission and the increase of the imaginary part of the dielectric factor (which is responsible for the power absorbed) with increasing voltage. A quantitative correlation between the measured output, L, and the measured increase of the imaginary dielectric factor should then be expected. To consider only this increase of k_2'', it is split into two parts:

$$k_2'' = k_{20}'' + \Delta k_2'' \qquad \text{(IX)}$$

Here the constant k_{20}'' has nothing to do with electroluminescence and may be due to other losses of energy in the phosphor. k_{20}'' can be determined for each frequency by graphical extrapolation to zero voltages as shown in Fig. 7. The other part, $\Delta k_2''$, may be plotted as a function of the emission intensity, L, in a diagram with logarithmically calibrated axes. It is found empirically that the curves obtained in this way are identical within the accuracy of the measurements if $\Delta k_2''$ is plotted not simply as a function of L but as a function of L/f. This is shown in Fig. 8 for the phosphor considered here. Similar diagrams have been obtained also for other electroluminescent phosphors of the type ZnS:Cu. It may be seen in Fig. 8 that all points of measurements approach a straight line with the slope 1:2, except the points for high values of $\Delta k_2''$ (i.e., for high applied voltages). Therefore, within the accuracy of the measurements, the dependence of $\Delta k_2''$ on L/f can be described by

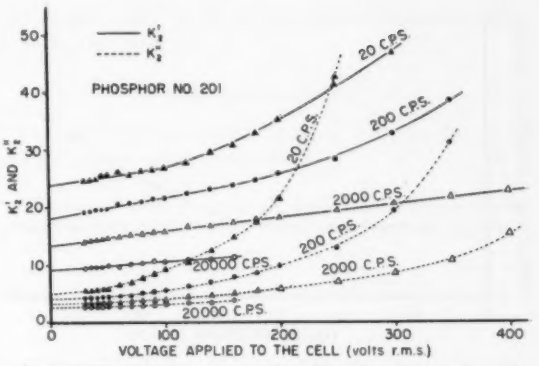

FIG. 7. Variation of the real and imaginary parts of the dielectric factor with voltage and frequency.

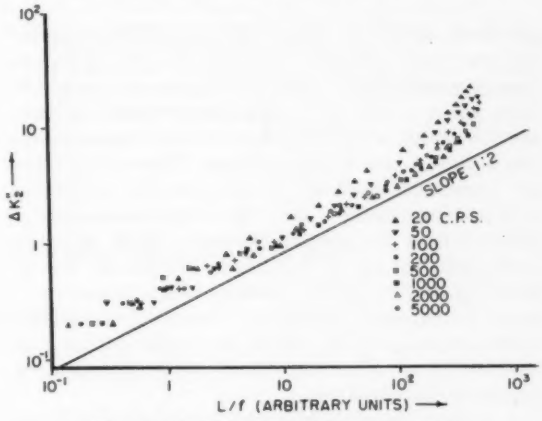

FIG. 8. $\Delta k_2''$ plotted as function of L/f

$$\Delta k_2'' \propto (L/f)^{1/2} \qquad \text{(X)}$$

It is possible to interpret this result by the assumption that the concentration of free carriers in the phosphor is responsible for both the electroluminescent emission and the increasing imaginary dielectric factor. Considering a constant applied frequency, this increase in k_2'' is proportional to the conductivity and, therefore, proportional to the carrier concentration, n, and the average mobility of the carriers, μ:

$$\Delta k_2'' \propto n\mu \qquad \text{(XI)}$$

Introducing (XI) into (X) for the case f = const. gives

$$n^2\mu^2 \propto L \qquad \text{(XII)}$$

The emission mechanism of photoluminescence in these

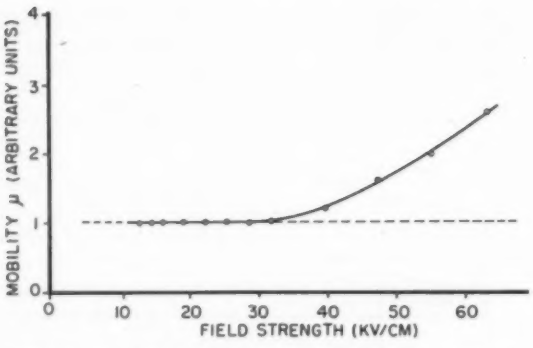

FIG. 9. Possible dependence of the effective mobility on the electric field strength.

phosphors can be described roughly by a bimolecular law (4) (this is a simplification, however; the real mechanism is more complicated). Equation (XII) now shows directly that, within the accuracy of the measurements, the emission mechanism of electroluminescence obeys a bimolecular law, at least for not too high voltages. This result confirms the assumption, made already in practically all theories of electroluminescence, that the electroluminescence is different from the photoluminescence in its excitation mechanism, but not in its emission mechanism. The influence of the frequency in relations such as equation (X) is not yet rigorously understood, however. This influence of the frequency exists without any doubt and has been observed in all other electroluminescent phosphors examined in this laboratory.

A distinct deviation from the straight line with the slope 1:2 in Fig. 8 is to be observed, however, for high values of $\Delta k_2''$ (i.e., for high applied voltages). Several explanations of this deviation have been attempted. It might be assumed that the deviation results from an inaccurate determination of k_2'' caused by the fact that the bridges of phosphor particles in the cell (Fig. 5 and 6a) are not identical with the solid phosphor (Fig. 6b). This assumption cannot be true as shown by the following consideration: equation (VII) is linear in k_2'' and in k_{12}''. Further, the imaginary dielectric factor k_1'' of the castor oil is relatively small compared to that of the phosphor. Therefore, $\Delta k_{12}''$ should be dependent upon L in the same way as $\Delta k_2''$ is. This is indeed the case. A plot of $\Delta k_{12}''$ as a function of L gives a diagram similar to that of Fig. 8 for $\Delta k_2''$. Since the imaginary part of the dielectric factor of the whole cell, k_{12}'', can be directly measured without any calculations, the conclusion must be drawn that the values of k_2'' determined with equation (VII) are relatively accurate.

A further proof that Fig. 6b describes the geometrical situation in the castor oil cell used can be found in the fact that the values of k_2'' determined with equation (VII) are independent (within the limit of error) over a wide range of the ratio phosphor:oil in the cell. This has been checked by measurements. Table II gives some data for a particular phosphor, at a constant voltage of 400 volts rms and a constant frequency of 500 cps, but for various phosphor concentrations x in the cell.

TABLE II. *Variation of the dielectric factor, k_2'', with phosphor concentration, x*

x	0.02	0.03	0.04	0.06	0.10	0.15	0.20	0.30
k_2''	1.4	1.3	1.4	1.3	1.4	1.6	1.4	1.2

Also other possibilities of error have been considered, such as a mechanical deformation of the cell under the influence of electrostatic forces, or the influence of selective polarization of the phosphor particles, but they cannot explain the observed deviation for very high field strengths. One possibility has been found by considering equations (X) and (XI), with the conclusion that the mobility μ in the region of very high field strengths is no longer constant. If so, then the mobility is constant for an average field strength up to about 30 kv/cm and increases strongly for higher field strengths. An example of this possible behavior of the mobility as a function of the average alternating field strength across the cell is given in Fig. 9. It cannot be decided by these experiments whether this assumed increase is due to the mobility of free electrons in the conduction band, or to holes in the valence band, or to both. Furthermore, this dependence of the mobility on the field strength is only a possibility and not a rigorous conclusion.

The Real Dielectric Factor of the Phosphor

The real part of the dielectric factor of the phosphor itself can also be determined by means of equation (VII). Results are given in Fig. 7. As in the case of the imaginary part, the real part k_2' also increases with increasing voltage and decreasing frequency, but these variations, in general, are relatively less than those of the imaginary part. The behavior of the real part of the dielectric factor has also been examined as a function of L/f and found to agree with that of the imaginary part as shown in Fig. 10. The reason for this agreement may be found in an electrical polarization of the phosphor particles due to free carriers, so that the same carrier concentration plays the major role as in the case of the imaginary part. This assumption agrees with results on nonelectroluminescent phosphors obtained by Dropkin (5) who showed that the dielectric dispersion at lower frequencies is due to grain conductivities.

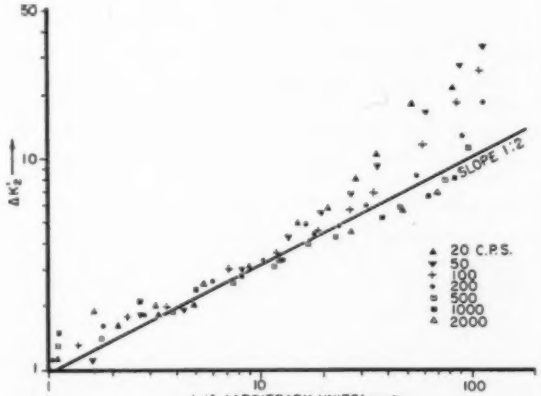

FIG. 10. $\Delta k_2'$ plotted as function of L/f

However, independent of any theoretical explanation, the behavior of the dielectric factor of the phosphor can now be described with two similar equations:

The real part:

$$k_2' = k_{20}' + a(L/f)^{1/2} \qquad \text{(XIII)}$$

The imaginary part:

$$k_2'' = k_{20}'' + b(L/f)^{1/2} \qquad \text{(XIV)}$$

Here k_{20}' and k_{20}'' may be dependent on frequency, but they are independent of the voltage, while a and b are two constants, both independent of frequency and voltage. These two equations (XIII) and (XIV) are valid only in the region of low and moderate electric field strengths. For higher field strengths, $(L/f)^{1/2}$ has to be replaced by a more complicated expression, but it seems that this new expression is dependent only on the ratio L/f, as can be seen in Fig. 8 and 10.

A dielectric behavior similar to that described here is observed also on many other electroluminescent zinc sulfides. The assumption is made, therefore, that equations (XIII) and (XIV) hold for all electroluminescent phosphors of this type.

ACKNOWLEDGMENT

The author is indebted to Dr. H. F. Ivey for discussion and for aid in instrumentation.

Manuscript received May 16, 1955. This paper was prepared for delivery before the Cincinnati Meeting, May 1 to 5, 1955.

Any discussion of this paper will appear in a Discussion Section to be published in the December 1956 JOURNAL.

REFERENCES

1. S. ROBERTS, *J. Opt. Soc. Amer.*, **42**, 850 (1952).
2. C. W. JEROME AND W. C. GUNGLE, *This Journal*, **100**, 34, (1953).
3. C. A. R. PEARCE, *Brit. J. Appl. Phys.*, **5**, 136 (1954).
4. G. F. J. GARLICK, "Luminescent Materials," p. 15 ff, Clarendon Press, Oxford (1949).
5. J. J. DROPKIN, "Photoconduction in Phosphors," Final Report, Contract N6onr-26313, Polytechnic Institute of Brooklyn, June 30, 1954.

The System Cadmium Oxide-Boric Oxide

I. Phase Equilibria

E. C. SUBBARAO AND F. A. HUMMEL

Department of Ceramic Technology, College of Mineral Industries, The Pennsylvania State University, University Park, Pennsylvania

ABSTRACT

Phase relationships in the system CdO-B_2O_3 were investigated by the quench method and by differential thermal analyses. A large region of liquid immiscibility extends from practically 100% B_2O_3 to about 46% B_2O_3. The compounds $2CdO \cdot 3B_2O_3$ (44.86% B_2O_3), and $3CdO \cdot 2B_2O_3$ (26.55% B_2O_3) both melt congruently near 1000°C and form a simple eutectic system. The compound $2CdO \cdot B_2O_3$ (21.33% B_2O_3) undergoes a rapid, reversible inversion near 900°C and melts congruently at 980°C. A large volume change attends a polymorphic transition in the compound $3CdO \cdot B_2O_3$ (15.31% B_2O_3) at 875°C and it melts at 1020°C. The compounds and polymorphs were characterized by x-ray diffraction, optical and thermal data. Some experiments on the solid solubility of MnO in the C_2B_3, C_3B_2, and C_2B [1] compounds are described.

INTRODUCTION AND LITERATURE SURVEY

Many investigators (1–4) have reported on the luminescence of manganese-activated cadmium borate compositions, but very little documented information has accumulated on the number or thermal behavior of compounds which exist in the system CdO-B_2O_3. Likewise, the phase diagram (Fig. 1) of Mazetti and deCarli (5a) appears to be incomplete in view of more recent work on binary borate systems such as CaO-B_2O_3, ZnO-B_2O_3, BaO-B_2O_3, etc.

The present work was undertaken to clarify the phase relationships in the system and to provide a substantial background for further work on the luminescent behavior of the cadmium borates.

[1] C = CdO, B = B_2O_3.

EXPERIMENTAL PROCEDURE

Raw Materials and Methods

The chemically pure raw materials boric acid, cadmium carbonate, and manganous carbonate were used in the preparations. The quench method (6) was used to investigate that part of the system from 44–100 mole % B_2O_3 (30–100 wt % B_2O_3). When using the quench method it is customary to melt each composition and use the glass as a starting material for the determination of liquidus and solidus temperatures. In this system homo-

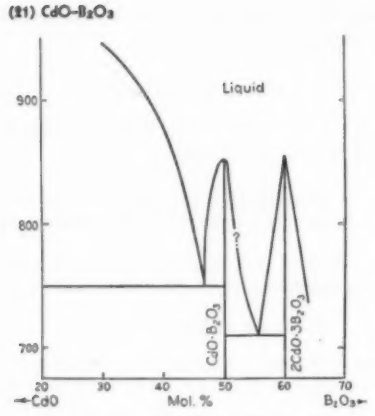

FIG. 1. The system CdO-B_2O_3 (from Hall & Insley, "Phase Diagrams for Ceramists," p. 25, Fig. 49, drawn from the data of Mazetti and deCarli, reference 5b).

geneous glasses can be obtained only in the range 44–51 mole % B_2O_3 (30–46 wt % B_2O_3). Compositions richer in B_2O_3 develop immiscible liquids, while those richer in CdO than the 1:1 mole ratio crystallize so rapidly from the fused condition that glasses cannot be obtained.

At least two previous investigators examined the range of glass formation in the system CdO-B_2O_3 and the present results are in good agreement with both sources. Kordes (9) melted binary cadmium borate glasses with the following results:

Wt % B_2O_3	Density	N_D *
44.2	3.842	1.672
38.3	4.159	1.705
33.8	4.434	1.732
29.4	4.696	1.750

* Refractive index.

More recently Dale and Stanworth (10) claimed a region of glass formation between 31 and 33 wt % B_2O_3, but these compositions seem to be very near to the low B_2O_3 limit of the glass-forming range according to the present work.

In the CdO-rich portion of the system it is necessary to use the method of Differential Thermal Analysis (D.T.A.) and high temperature x-ray diffraction data to determine the phase relationships. These two techniques have been described in previous papers (7, 8). Copper Kα radiation from a wide angle Norelco Geiger counter unit or from a G.E. XRD-3 unit was used in all diffraction work. Platinum ware was used throughout the investigation for fusions, calcinations, D.T.A., and high temperature x-ray work.

Compositions

Table I shows the analyzed compositions which were investigated and the refractive indices of those compositions which could be obtained as glasses. Many supplemental compositions were prepared during the course of the work, but they were not analyzed. The molecular compositions C_2B_3, C_3B_2, C_2B, and C_3B are included in the table as reference points, since they were found to be true compounds. In preparing glasses for the quench work, ten-gram batches were mixed with ethyl alcohol, dried at 110°C, and fused at 1100°C. For solid-state reactions, thermal expansion, and D.T.A. measurements, 60-gram batches were prepared.

TABLE I. *Analyzed compositions and refractive indices of glasses*

No.	% B_2O_3	Refractive index of glass (±0.003)
1	46.09	1.670
$2CdO \cdot 3B_2O_3$	44.86	—
2	44.13	1.676
3	43.73	1.677
4	37.82	1.715
5	34.93	1.726
6	33.34	1.736
7	29.15	1.765
8	27.32	—
$3CdO \cdot 2B_2O_3$	26.55	—
9	26.38	—
10	22.49	—
11	21.44	—
$2CdO \cdot B_2O_3$	21.33	—
12	20.16	—
13	19.00	—
$3CdO \cdot B_2O_3$	15.31	—

RESULTS

The system divides rather naturally into three regions, (*a*) the immiscible liquid region, (*b*) the region between the C_2B_3 and C_3B_2 compounds, and (*c*) the cadmium oxide-rich region ranging from the compound C_3B_2 to the end member, CdO.

In the following discussion, reference should be made to Fig. 2 which shows the entire binary system including the two-liquid region, and Fig. 3 which shows an enlargement of the region lying between the compound C_2B_3 and CdO. The latter diagram contains the compositions o greatest interest with respect to luminescent properties. The interval in which homogeneous glass can be obtained is also indicated on this diagram.

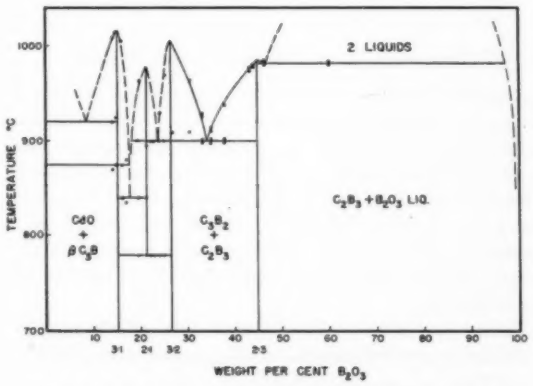

FIG. 2. The system CdO-B_2O_3—C = CdO, B = B_2O_3

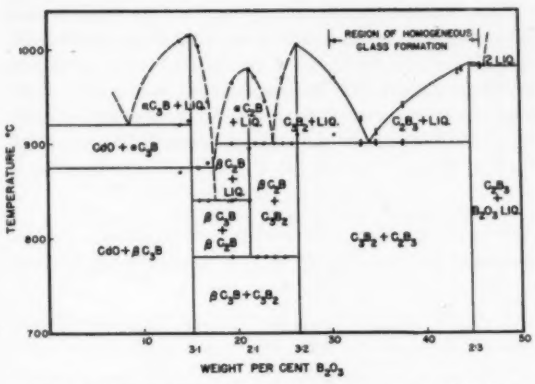

FIG. 3. The system $CdO\text{-}2CdO\cdot3B_2O_3$—C = CdO, B = B_2O_3.

The Immiscible Liquid Region

A very extensive region of liquid immiscibility was established which ranges from 46.4% B_2O_3 to nearly 100% B_2O_3, in agreement with that found in other $RO\text{-}B_2O_3$ systems such as MgO-, CaO-, and BaO-B_2O_3. The liquid separation took place readily in platinum crucible melts giving a light layer with a refractive index of 1.455, very close to that of pure B_2O_3 glass. The refractive index of the heavy layer was about 1.67 (Table I).

All preparations under the immiscibility gap when heated in the range 600°–980°C, gave only the C_2B_3 phase when examined petrographically and by x-rays. The second phase which should be present in compositions in this area is B_2O_3 glass, but its detection is difficult or impossible when present in small quantities or as thin films surrounding the C_2B_3 crystals. Since manganese-activated phosphor compositions of a 1:2 and 1:3 ratio have been mentioned in the literature, it was thought that the presence of manganese might promote the formation of compounds of these molecular ratios. Extensive investigation of manganese-containing compositions lying between the 2:3 compound and 100% B_2O_3 proved that only $2CdO\cdot3B_2O_3$ existed below 980° in this region.

It is interesting to compare the extent of experimentally determined liquid immiscibility in the system $CdO\text{-}B_2O_3$ with that in the systems discussed recently by Shartsis and Capps (11). These authors related the ionic potential (z/R) to the mole per cent of monovalent or divalent oxide present in the heavy liquid in nine borate systems shown in Table II. It is obvious that the data obtained in the present work allow CdO to fall into the anticipated position in the series as indicated.

TABLE II. *Ionic potential and immiscibility in simple borate systems (after Shartsis and Capps)*

Ionic radius R(a.u.)	Valence (Z)	Ionic potential (Z/R)	Immiscibility gap mole % of oxide
K 1.33	1	0.75	0
Na 0.98	1	1.02	0
Li 0.78	1	1.28	0
Ba 1.43	2	1.40	16
Pb 1.32	2	1.51	19
Sr 1.27	2	1.57	21
Ca 1.06	2	1.89	27
Cd 1.03*	2	1.94	39
Zn 0.83	2	2.41	49
Mg 0.78	2	2.56	50

* Data from this paper.

The Region Between the Compounds C_2B_3 *and* C_3B_2

Compounds C_2B_3 *and* C_3B_2.—The compound $2CdO\cdot3B_2O_3$ has been shown to melt congruently at 980° ± 5° by both quench and D.T.A. data. The crystals are highly birefringent with N_{max} = 1.630 and N_{min} = 1.617. A

TABLE III. *X-ray data on cadmium borates*

2:3		3:2		2:1		β3:1		α3:1	
d	R.I.	d	R.I.	d	R.I.	d	R.I.	d	R.I.
5.53	65	6.15	7	6.14	10	4.33	7	4.95	22
5.38	75	5.98	7	5.98	10	4.23	40	4.33	20
4.57	12	5.15	6	4.64	50	3.74	18	4.21	20
4.16	30	4.64	50	4.41	10	3.53	6	4.13	20
4.12	30								
3.73	85	4.41	6	4.33	27	3.41	10	4.03	45
3.67	65	4.19	6	4.05	30	3.36	7	3.60	20
3.56	55	3.50	5	3.62	15	3.24	6	3.57	20
3.21	100	3.37	5	3.42	30	2.99	43	3.49	12
3.00	30	3.21	20	3.24	60	2.87	100	3.41	55
2.93	70	3.07	30	3.22	60	2.81	8	3.27	15
2.75	30	3.02	13	3.14	5	2.68	50	3.23	55
2.69	20	2.97	44	3.07	25	2.56	8	2.98	100
2.56	85	2.84	100	3.00	90	2.44	47	2.90	60
2.46	18	2.77	25	2.97	50	2.39	15	2.86	30
2.38	25	2.72	25	2.92	60	2.25	4	2.79	45
2.34	8	2.58	10	2.82	100	2.11	4	2.75	10
2.29	80	2.40	10	2.80	15	1.936	7	2.72	30
2.20	7	2.29	4	2.77	60	1.868	30	2.57	25
2.18	40	2.24	6	2.71	30	1.843	5	2.56	20
2.06	13	2.22	6	2.58	35	1.786	35	2.46	10
2.02	50	2.09	35	2.47	5	1.703	20	2.44	10
1.971	75	1.961	10	2.40	30	1.688	10	2.41	25
1.920	18	1.886	7	2.33	30	1.660	15	2.38	40
1.856	18	1.847	8	2.23	20	1.641	5	2.35	40
1.847	5	1.789	7	2.16	15	1.493	7	2.32	45
1.834	40	1.776	9	2.09	50	1.468	11	2.31	10
1.797	25	1.732	20	2.02	5	1.458	11	2.11	20
1.792	35	1.723	20	2.00	8	1.416	36	2.07	14
1.781	45	1.703	5	1.886	5	1.407	10	1.996	30
1.757	6	1.694	5	1.850	17	1.388	6	1.955	15
1.732	40	1.682	5	1.806	3	1.363	9	1.870	25
1.691	8	1.641	20	1.776	10	1.341	6	1.847	30
1.676	8	1.617	4	1.729	16	1.267	6	1.812	10
1.660	18	1.592	12	1.705	10	1.199	6	1.799	10
1.604	14	1.534	4	1.657	5	1.195	4	1.773	20
1.571	12	1.509	6	1.641	10	1.123	4	1.760	15
1.524	16	1.474	5	1.611	5	1.117	5	1.744	20
1.520	15	1.430	6	1.594	17	1.110	8	1.703	25
1.461	19	1.416	4	1.431	7	1.094	5	1.688	40
1.422	10	1.407	5	1.394	10			1.657	40
1.403	12	1.358	50	1.352	5			1.609	10
1.370	10	1.348	5	1.344	8			1.591	30
1.353	13	1.241	10	1.232	6				
1.303	10	1.185	5						
1.277	8								
1.265	9								
1.168	6								
1.161	6								
1.157	6								
1.148	6								
1.131	8								
1.128	8								

few of the crystals develop sharp hexagonal outlines. The compound can be formed by solid-state reaction at any temperature ranging from 600°C up to its melting point or by recrystallization of a quenched glass between 600° and 980°C. The x-ray pattern is given in Table III.

The compound $3CdO \cdot 2B_2O_3$ has been shown to melt congruently at 1005° ± 5° by D.T.A. data only. Well-grown crystals are elongated and highly birefringent with $N_{max} > 1.790$ and $N_{min} = 1.745$, but the crystals generally do not show any characteristic shape or cleavage under the microscope. The compound can be prepared by solid-state reaction between 600°–1000°C or by recrystallization from fusions. The x-ray pattern is given in Table III.

Solid-state reactions.—All compositions lying between the C_3B_2 and C_2B_3 compounds reacted to give these two phases when heated between 600° and 900°. Both compounds could be distinguished in these intermediate mixtures by optical and x-ray methods.

The liquidus region.—The range of glass formation in this area did not extend beyond compositions containing less than 30% B_2O_3 if the following criterion was used: A 10-gram batch fused in a 20 cc platinum crucible at 1100°C for 10–15 min must yield a clear, homogeneous glass when the outside of the crucible is water-quenched. Using this criterion, the part of the system lying between the C_3B_2 compound (26.55% B_2O_3) and a composition containing about 30% B_2O_3 is not a glass-forming region. However, small batches (ca. 0.2 gram) will yield glasses in this compositional range when quenched rapidly, but they cannot be used to obtain dependable liquidus data (*see* section on Compounds C_2B_3 and C_3B_2).

Data for quenched samples upon which the liquidus curve in Fig. 2 and 3 is based are shown in Table IV.

TABLE IV. *Quench data for cadmium borates*

Composition No.	% B_2O_3	Temp, °C	Time, min	Phases present
0	60.00	982	20	2 Liquids
		980	20	C_2B_3 + B_2O_3 liquid
1	46.09	982	20	Glass
		980	15	Glass + C_2B_3
2 (2:3)	44.13	980	25	Glass
		978	15	Glass + C_2B_3
3	43.73	977	15	Glass
		975	15	Glass + C_2B_3
4	37.82	942	15	Glass
		940	15	Glass + C_2B_3
		902	20	Trace glass
		898	15	No glass
5	34.93	914	25	Glass
		910	20	Glass + C_2B_3
		901	20	Trace glass
		899	20	No glass
6	33.34	927	25	Glass
		923	15	Glass + trace C_2B_3
		901	20	Trace glass
		899	15	No glass

Since Botden and Kroger (1) and Mazetti and deCarli (5b) claimed the existence of the compound $CdO \cdot B_2O_3$, special care was taken in the examination of compositions in this neighborhood. Both solid-state and quench work failed to reveal a compound of this composition, so additional work was done with a high temperature x-ray diffraction furnace to test for a possible limited existence

TABLE V. *D.T.A. data for cadmium borates*

Composition No.	% B_2O_3	Previous heat treatment, temp, °C	hr	Temp of differential thermal peaks, °C			
14(2:3)	44.8	760	20	900	990		
15	30.4	700	3	910	970		
16(3:2)	26.5	780	12	910	1005		
17	25.0	700	1	780	903	970	
18	24.0	700	1	780	900	930	
19	23.0	700	1	775	900	945	
20	22.0	700	1	780	900	970	
21(2:1)	21.5	700	1	780	840	895	980
22	19.5	830	20	780	840	900	965
23	17.0	800	18	835	880	945	
24	16.0	700	1	835	880	1005	
25(3:1)	15.0	700	1	875	925	1015	
26	14.0	630	4	870	920	1010	

TABLE VI. *Thermal expansion data for cadmium borates*

Composition	Temp range, °C	Coefficient of linear thermal expansion $\times 10^7$
C_2B_3	25–700	53.6
C_3B_2	25–700	66.7
βC_2B	25–700	57.2
βC_2B	25–700	92.3
C_2B_3 glass	25–500	63.7 (interferometer)

TABLE VII. *Solid solubility of* MnO *in cadmium borates*

	Sintered			Fusion (1100°C)	
	Concentration of MnO, %	Temp, °C	Result	Temp of recrystallization, °C	Result
C_2B_3	5	800	No color		
	8	800	No color		
	10	800	Very slight brown color	620	No color
	12			650	Considerable brown color
C_3B_2	1	800	No color	600	Practically no color
	3	800	No color	600	Slight brown color on crystals
	5	800	Thin brown coating on crystals		
C_2B	0.015			550	No color
	0.0286			700	No color
	0.06			710	Brown color on crystals
	0.5	800	No color		
	2	800	Very slight brown color on crystals		

near the liquidus. However, diffraction data obtained in the temperature range 750°–860°C gave no evidence for a CB compound.

On the basis of both quench and D.T.A. data the eutectic between the C_2B_3 and C_3B_2 compounds has been placed at 900°C and approximately 34 wt % B_2O_3.

The Cadmium Oxide-rich Region

This portion of the system was the most difficult to investigate experimentally since glasses could not be obtained and the deduction of all high temperature events had to be based on D.T.A. and high temperature x-ray data. In addition, volatility problems arose when compositions were held near the liquidus for more than 10–30 min. Hence this portion of the system is drawn in dashed lines in Fig. 2 and 3, indicating some uncertainty in the relationships. X-ray data for the low form of C_2B compound and the low and high forms of the C_3B compound are shown in Table III.

The C_2B *compound.*—This compound appears to have a lower temperature limit of stability at 780°C. When the composition is held at 700°, only the βC_2B and C_3B_2 compounds appear. At 780°C the composition gives an intense nonreversible D.T.A. peak which signals the formation of the βC_2B compound. Further heating then yields a reversible D.T.A. peak at 900° (β-α inversion), and final melting takes place at 980°. Although the formation of the βC_2B compound from βC_3B and C_3B_2 is very rapid on heating to 780°, the reverse dissociation does not occur on cooling. Samples which have been heated between 780° and 980° (or samples which have been fused) cool to room temperature as the βC_2B phase. If the compound is held at 725° for 20 hr, it begins to show the dissociation products in the x-ray pattern. The αC_2B phase was detected by D.T.A. and by a high temperature x-ray pattern taken at 930°.

The absence of x-ray lines at d values of 4.05 and 2.00Å is characteristic of the α form of C_2B. On the other hand, the α form has prominent lines at d values of 2.45 and 2.35 which do not appear in the pattern of the β form.

It is very difficult to distinguish the βC_2B and C_3B_2 compounds by x-ray patterns. Likewise, it is difficult to differentiate between the compounds optically, since the βC_2B crystals are highly birefringent with $N_{max} > 1.790$ and $N_{min} = 1.775$.

The C_3B *compound.*—The C_3B compound melts congruently at 1020°C, and exists in two polymorphic forms. The reversible inversion occurs at 870°C. The high temperature form on cooling from fusion reverts to the low temperature form with a very large change in volume, causing the sample to fall to dust, reminiscent of the well-known β to γ "dusting" of dicalcium silicate, one of the constituents of cement clinker. Table V gives the principal D.T.A. data upon which the CdO-rich portion of the diagram was constructed.

Thermal Expansion Data

The linear thermal expansions of the four compounds and the C_2B_3 glass were measured with the results shown in Table VI.

The four crystalline compounds had been sintered at 800°–830° for 20 hr prior to the dilatometric thermal expansion determination.

Solid Solubility of MnO *in Cadmium Borates*

The solid solubility of MnO in the three compounds C_2B_3, C_3B_2, and βC_2B was estimated by adding varying amounts of MnO and heating in the solid state or by fusing the sample and then observing the crystals under the microscope. The appearance of brown specks or surface discolorations on the crystals would indicate the presence of oxidized manganese and the limit of the solid solubility. This method can only give a rough approximation of the solubility, but some interesting observations were made as summarized in Table VII.

It appears from these data that the solid solubility of MnO in the sintered βC_2B and C_3B_2 compounds is relatively low (approx. 1–3%). In contrast, the C_2B_3 compound can probably take about 5–8% MnO into solid solution. The fused samples are in general agreement with the solubility data for sintered samples, but in this case it is very unlikely that only divalent manganese is present, since the fusions always yield purple crystalline masses or pink to purple glasses.

The luminescent properties of the compounds $2CdO \cdot B_2O_3$, $3CdO \cdot 2B_2O_3$, and $2CdO \cdot 3B_2O_3$ are being investigated and will be reported at a later date.

Manuscript received June 6, 1955. This paper was prepared for delivery before the Cincinnati Meeting, May 1 to 5, 1955. Contribution #54-58 from the Dept. of Ceramic Technology, College of Mineral Industries, Pennsylvania State University, University Park, Pa.

Any discussion of this paper will appear in a Discussion Section to be published in the December 1956 JOURNAL.

REFERENCES

1. TH. P. J. BOTDEN AND F. A. KROGER, *Physica*, **13**, 216 (1947).
2. R. NAGY AND C. K. LUI, *J. Opt. Soc. Amer.*, **37**, 37 (1947).
3. F. A. KROGER, "Some Aspects of the Luminescence of Solids," p. 60, Elsevier Publishing Co., New York (1948).
4. H. W. LEVERENZ, "An Introduction to Luminescence of Solids," pp. 175 and 234, John Wiley & Sons, Inc., New York (1950).
5a. F. P. HALL AND H. INSLEY, *J. Am. Ceram. Soc.*, **30**, 25 (Fig. 49) (1947).
5b. C. MAZETTI AND F. DECARLI, *Gazz. chim. ital.*, **56**, 19 (1926).
6. E. S. SHEPHERD, G. A. RANKIN, AND F. E. WRIGHT, *Am. J. Sci.* (4th series), **28** (4), 293 (1909).
7. R. M. GRUVER, *J. Am. Ceram. Soc.*, **31** (12), 323 (1948).
8. R. ROY, E. T. MIDDLESWARTH, AND F. A. HUMMEL, *Am. Mineralogist*, **33**, 458 (1948).
9. E. KORDES, *Z. anorg. u. allgem. Chem.*, **241**, 1 (1939); *Glastech. Ber.*, **17**, 67 (1939).
10. A. E. DALE AND J. E. STANWORTH, *J. Soc. Glass Technol.*, **33**, 167 (1949).
11. L. SHARTSIS AND W. CAPPS, *J. Am. Ceram. Soc.*, **35**, 169 (1952).

Time-Average Electroluminescence Output of Some Zinc Sulfide Phosphors

SOL NUDELMAN

U. S. Naval Ordnance Laboratory, White Oak, Maryland, and University of Maryland, College Park, Maryland

AND

FRANK MATOSSI

U. S. Ordnance Laboratory, White Oak, Maryland

ABSTRACT

Dependence of time-average electroluminescence output on field strength and frequency is observed for frequencies up to 20 kcps for green and blue emission. The field dependence can be described either by a power law or by an exponential law. The frequency dependence is discussed in terms of theoretical relations connecting the light output to recombination characteristics or to polarization effects. The polarization effects are of minor importance. Light outputs from sinusoidal and square wave excitation are compared.

INTRODUCTION

Dependence of time-average light output on field strength and frequency is one of the fundamental properties of electroluminescent phosphors. In several papers (1–3), the general increase of light output with field strength and frequency has been reported. In some cases, a saturation at high frequencies was observed. Furthermore, it was established that these properties are different in different spectral regions. Most of this work was restricted to frequencies up to about 3 kcps and to phosphors used in the Sylvania Panelescent Lamp.

The purpose of this paper is to extend the experimental material to higher frequencies as well as to other phosphors, and to compare the output of sinusoidally excited electroluminescence to that excited by square wave fields. The results will be discussed, as far as possible, in the light of several theoretical expressions (4).

EXPERIMENTAL PROCEDURE

Phosphors were embedded in Parlodiun[1] and used in cells of about 5 cm² area and about 0.2 mm thickness, as described previously (5). Sylvania lamps were used as delivered. Resistance of the conducting glass electrode of the cells was constant in the frequency range 10 cps-100 kcps. For typical cells it was about 600 ohms. The capacitance of the cells was of the order of 100 $\mu\mu$f, varying slightly for different cells because of different phosphor materials and different thicknesses of the phosphor-plastic layer. Cell impedance at 1000 cps was of the order of 5×10^5 ohms. Phosphors were of the zinc sulfide type and were copper-activated. Some of them were commercial products;[2] some were made in the laboratory according to the methods of Homer and co-workers (6). These include phosphors No. 23, ZnS(Cu, Pb), cubic, and No. 11, ZnS(Cu, Pb, Mn), cubic. Phosphor No. 23 was of the same type as that used in the Green Sylvania Lamp, giving results very similar to those obtained with the panel. Phosphor No. 11 is similar to a Sylvania yellow phosphor.

The light output passed through a Wratten filter No. 21 (transmitting above 5300 Å) or through a Wratten filter No. 3 and a Corning filter 5850 (transmitting from 4300 to 4800 Å) in order to separate the green and blue regions of the emission spectrum. Thus, the central part of the emission spectrum was excluded so that overlapping of the two bands found in the green Sylvania type phosphors (2) was minimized.

The luminescence output was received by a 1P21 photomultiplier. The output of the photomultiplier consisted of a periodic ripple superimposed on a steady background. Its time-average was measured with a vacuum tube voltmeter in an appropriate averaging circuit.

A sinusoidal signal generator and power amplifier produced the fields, which could be varied from 0 to 500 v in the frequency range of 100–10,000 cps. For higher frequencies, the output voltage dropped so that at 20 kcps only 200 v were available. For a few measurements, the frequency range could be extended down to 10 cps, with a voltage of only 100 v. All voltages refer to rms values, if not stated otherwise.

The cells were operated well below breakdown voltages and showed no signs of heating. In addition, since the impedance of the cell is so much greater than the resistance of the conducting film on the glass surface, any voltage drop across the phosphor plastic layer will be large compared to that across the film. Thus, in the investigation of the frequency dependence of the phosphor light output, constant voltage applied to the cell is es-

[1] A highly purified form of nonexplosive cellulose nitrate manufactured by Mallinckrodt Chemical Works.

[2] No. 3-310, General Electric Co., ZnS, Se(Cu), cubic; No. Q 62-2666, E. I. du Pont de Nemours and Co., ZnS (Cu), hexagonal; Sylvania Green Panelescent Lamp, Sylvania Electric Products Inc., ZnS(Cu, Pb), cubic.

sentially equivalent to constant voltage applied to the phosphor plastic layer.

Because of appreciable fatigue of the cells in the first 24 hr of use, all cells were aged before usage by applying a potential difference of 300 v at 5000 cps for at least 24 hr before measurements were started. If necessary, measurements could be corrected for changes occurring after that time. Blue emission seemed to fatigue faster than green. Decay during fatigue could be described by power laws (intensity proportional to t^{-n}), with n ranging from 0.1 to 0.2.

Results and Discussion

Frequency Dependence

Fig. 1 shows typical results for the frequency dependence of the time-average light output B. Most phosphors follow the behavior shown for phosphors 3–310. Qualitatively, different curves were obtained only for phosphor No. 23, where the green emission reaches an intermediate quasi-saturation after going through a small maximum. The width of this plateau decreases with increasing applied voltage, and its beginning shifts to higher frequencies. This plateau cannot be associated with any electrical property of the cell, since it would then also appear in the blue emission. Phosphor No. 23 is similar to that in the Green Sylvania Lamp, so the saturation in the green luminescence reported for that phosphor (1) may in reality be only such a plateau. Unfortunately, this lamp was too great a load for the equipment, so it was not possible to obtain the frequencies and voltages necessary to investigate the lamps for such a plateau.

If the data are plotted as in Fig. 2, i.e., as $1/B$ vs. $1/f$ (f = frequency), there is for all phosphors an extended linear region ranging from 100 cps (the low-frequency limit

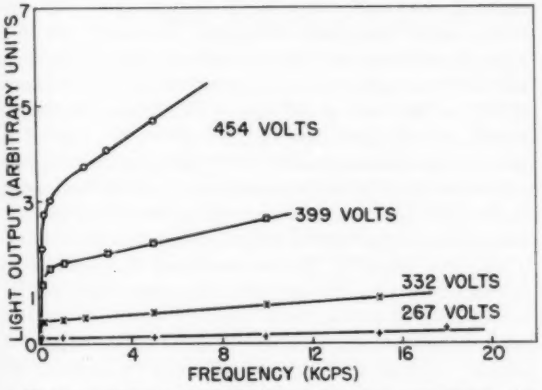

Fig. 1a. Time-average light output vs. frequency. The parameters indicate electrode potential differences in rms values. Phosphor 3–310, green emission.

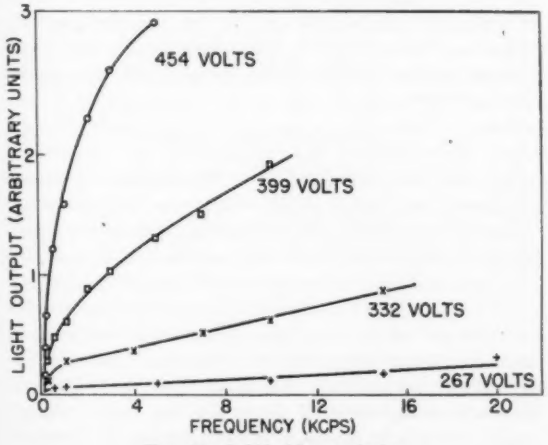

Fig. 1b. 3–310, blue emission

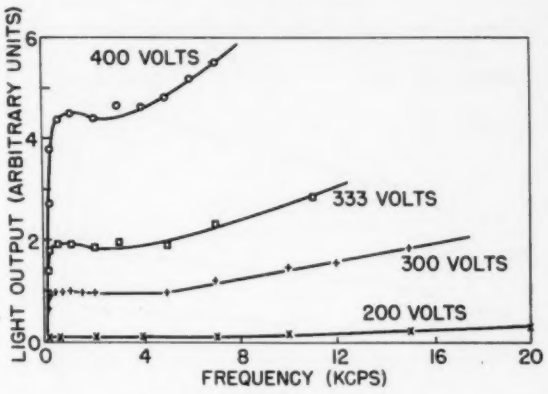

Fig. 1c. 23, green emission

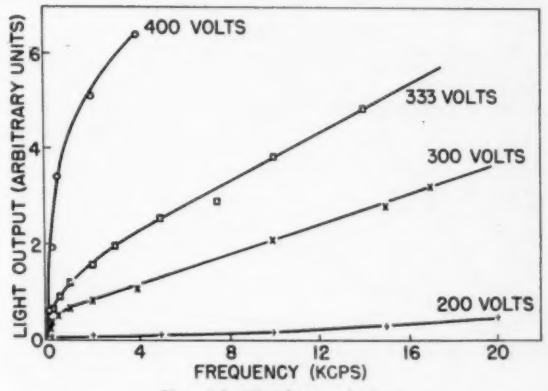

Fig. 1d. 23, blue emission

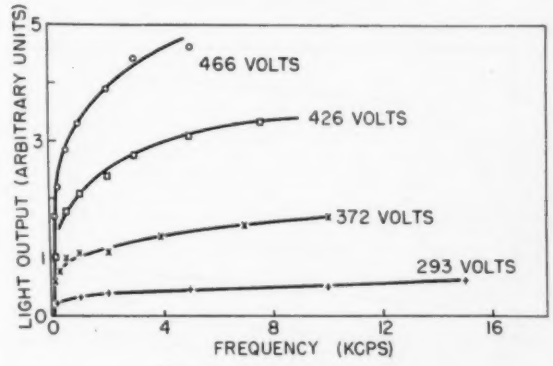

Fig. 1e. 11, green emission

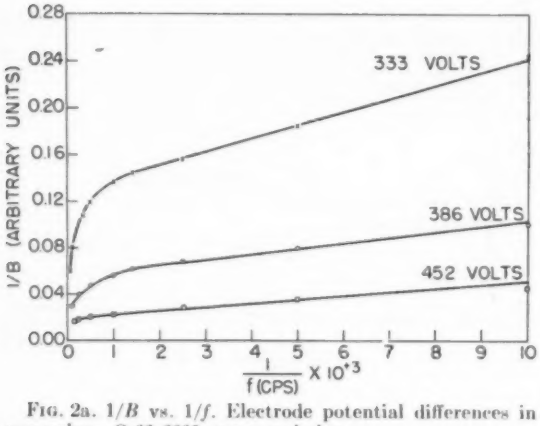

FIG. 2a. $1/B$ vs. $1/f$. Electrode potential differences in rms values. Q 62-2666, green emission.

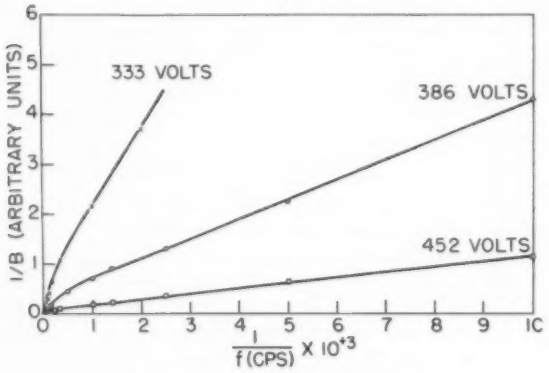

FIG. 2b. Q 62-2666, blue emission

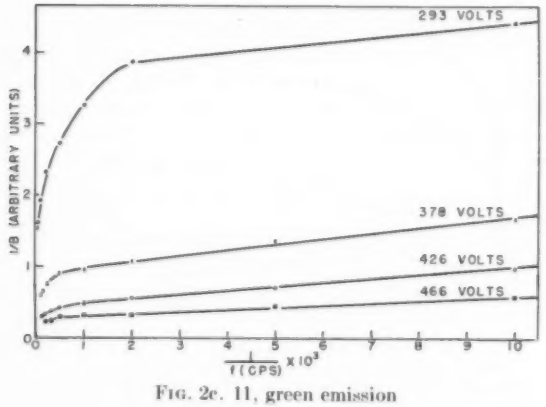

FIG. 2c. 11, green emission

of most of the measurements) to about 1000 cps, except for the green band of the green Sylvania phosphors, according to the irregular shape of the curves of Fig. 1c. The linear region was, in general, larger at higher fields.

For the linear regions of the curves of Fig. 2, Curie (4) derived an approximate formula, according to which

$$1/B = (1/Cn_0^2\alpha)(1 + n_0\alpha/2f) \qquad (I)$$

where C is a constant and α describes the decrease of the number of electrons in the conduction band from its maximum n_0 at the beginning of the decay. Equation (I) thus describes the light output in terms of recombination characteristics, for which Curie assumed, as an approximation, the equation $dn/dt = -\alpha n^2$ with n being the number of conduction electrons. Equation (I) is presumably valid for frequencies for which polarization effects may be neglected. At high frequencies, the observed curves deviate from the linear relation of $1/B$ vs. $1/f$. This is to be expected since n_0 was assumed to be independent of frequency, which may not be true at higher frequencies, as Curie points out.

From the slopes and the intercepts at $1/f = 0$ of the linear parts of the $1/B$ vs. $1/f$ relations, numerical values for $n_0\alpha$ can be obtained. These are smallest for the green band of phosphor No. 23, where they vary from about 10 sec^{-1} at 100 v to about 200 sec^{-1} at 400 v. This is consistent with the existence of the quasi-saturation plateau, since equation (I) reduces to $B = constant$ for $n_0\alpha \ll 2f$. The higher values of $n_0\alpha$ at higher fields are also consistent with the shift of the quasi-saturation plateau at such fields.

For α and n_0 separately, only relative values can be obtained because of the unknown constant C. For the blue luminescence of phosphor No. 23, α turns out to be constant within 2% between 300–400 v, for which the most accurate measurements are available, while n_0 increases with field strength. ($n_0\alpha$ = 415 sec^{-1} at 293 v, 600 sec^{-1} at 333 v, 1260 sec^{-1} at 400 v; α = 56, 54, and 55, respectively, in arbitrary units.) This behavior would be expected, and similar qualitative results are also obtained with other phosphors with one exception: the blue emission of the 2666-phosphor yields α-values that definitely decrease with increasing field while n_0 still increases.

Although equation (I) describes well the qualitative aspects of the time-average light output as evidenced by the linearity of the curves of Fig. 2, it should be kept in mind that it is of approximate character only, and that it may be oversimplified because of the law for dn/dt which actually is more complicated than has been assumed. Therefore, it cannot be expected to yield exact numerical values for the parameters n_0 and α.

For low frequencies, where polarization effects are assumed to be important, Curie (4) has suggested another relation, which considers the influence of polarization charges on the effective field. For very low frequencies, Curie obtains

$$B = \text{const}\, f \exp(-b'/Ef) \qquad (II)$$

where E is the applied field and b' a constant. Equation (II) would require that $dB/df = 0$ for $f = 0$. This contradicts the observations. Measurements with the Sylvania Lamp at frequencies below 100 cps down to 10 cps ruled out any possibility of a horizontal tangent to the frequency axis. On the contrary, equation (I) describes the green as well as the blue light output adequately even at these low frequencies. Another discrepancy between observations and equation (II) is the fact that $b'/f = b$ is nearly independent of frequency (*see* next section), while it should be inversely proportional to f if equation (II) is valid.

This analysis, in connection with the discussion of the previous paragraphs, indicates that polarization effects are of minor importance for the frequency dependence of the time-average light output. The principal factor governing this output is, rather, the number of electrons in the conduction band. However, the specific equation accounting for this effect, viz., equation (I), needs refinement. Observations with nonsinusoidal fields (7) have also shown that the polarization field alone cannot account for the frequency dependence of luminescence intensity, but that the decay characteristics of the phosphor are essential even at low frequencies, although polarization charges play an important role in other respects.

Field Dependence

The measurements were not primarily intended to test different laws of the field dependence of the brightness, but, as a by-product of the measurements of frequency dependence at different field strengths, some data on field dependence were obtained. Within the restricted range of voltages covered, both a power law, $B = aE^n$, with n ranging from 4 to 8, and an exponential law, $B = aE^2 \exp(-b/E)$, with b ranging from 500 to 900 v, agree well with the observations. The constants n and b vary, if at all, only very little with frequency. Only one phosphor (No. 11) showed appreciable deviations from the exponential law at low fields, but the output of this phosphor could well be described by $B = aE \exp[-b''/(E + E_0)]$, where $E_0 = 11$ v and $b'' = 700$ v at 1000 cps, while b had the value 550 v. A law of this kind was recently proposed (8) on an empirical basis, and generally offers better agreement at lower voltages. A definite decision among the different laws proposed cannot be made. The authors' observations disagree, however, with exponential laws of the form (9) $B = aE \exp(-b/E^{1/2})$.

Sinusoidal and Square Wave Output

Fig. 3a and 3b give characteristic examples of the dependence of the time-average light output excited by square wave and sinusoidal fields on frequency. At low frequencies, the light output excited by square wave fields rises faster than that excited by sinusoidal fields. Similar results have been reported by Schwertz (10), but the quantitative details are somewhat different. The maximum of the Sylvania Lamp square wave light output at about 3000 cps agrees well with the expectation derived from the measurements of peak heights and the continuous background of square wave excited brightness waves (7). The maximum for the sinusoidal light output in the vicinity of 6000 cps is consistent with the work of Schwertz (10) in that he found at low field strengths similar maxima below 20 kcps for a variety of phosphors. At higher field strengths, such maxima do not appear (*see* Fig. 1a–1e). They apparently shift to higher frequencies with increasing voltage.

Another characteristic feature of Fig. 3 is the crossing of corresponding curves for sinusoidal and square wave excitation at some characteristic frequency. This frequency shifts with the "rise time" of the square wave field, which actually should be described as an "exponential" field. For rise times of 25 μsec and 100 μsec (time to obtain 95% of maximum field strength), this frequency was observed at about 15 kcps and about 4.5 kcps, respectively. The crossing occurs, therefore, when the half period is of the order of the rise time.

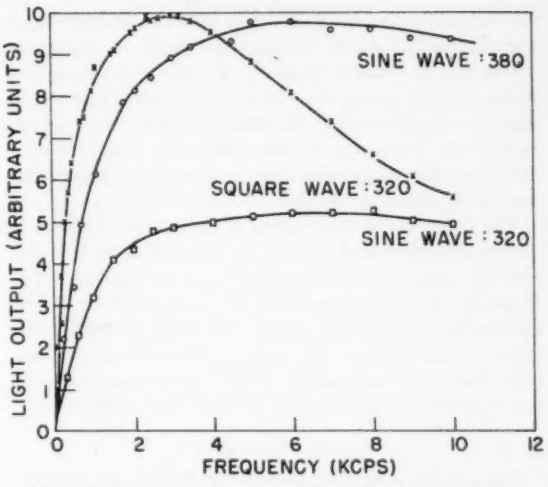

FIG. 3a. Time-average output vs. frequency. The parameters give peak voltage of electrode potential difference. Blue emission of Green Sylvania Lamp, rise time of square wave field 25 μ sec.

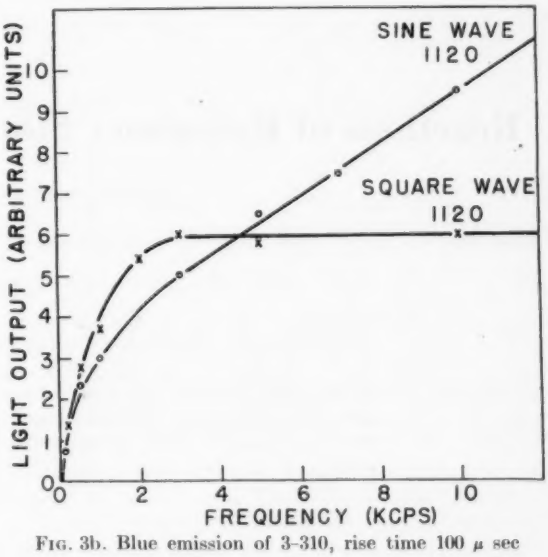

FIG. 3b. Blue emission of 3-310, rise time 100 μ sec

The larger output with square wave fields at low frequencies is probably due to the fact that the amplitudes of the brightness waves generally increase with decreasing field rise times, since the influence of polarization charges that weaken the effective field needs time to develop. The crossover point and its dependence on rise time can be related to the relative rate of field change from square wave and sinusoidal fields as the frequency is increased. Exponential fields with rise times much shorter than the half period rise faster than sinusoidal fields of the same frequency. However, for half periods much smaller than

the rise time, the sinusoidal field becomes steeper, since the exponential waves assume the shape of triangular waves with increasing frequency. Therefore, corresponding to the change in slope of the sinusoidal wave relative to that of the square wave, the intensity ratio of the outputs is expected to reverse at some frequency related to the rise time. An exact definition of the characteristic frequency in terms of rise time is, however, difficult.

The frequency of the crossing point was dependent only on the rise time and not on the kind of phosphor, the spectral region, or other details of the luminescence. However, in accordance with the interpretation of the amplitude maximum of square-wave-induced light emission as being related to decay characteristics and polarization effects (7), the position of the output maximum was not appreciably influenced by the rise time of the field.

Acknowledgment

The authors wish to thank Dr. J. F. Waymouth, Sylvania Electric Products, for information about the Sylvania panel and Dr. Meschter, du Pont Company, for providing wo electroluminescent phosphors. They also wish to hank Dr. D. R. Frankl, Sylvania Electric Products, and Dr. F. A. Schwertz, Mellon Institute, for kindly sending reports on unpublished results.

Manuscript received June 6, 1955. This paper is based on a dissertation submitted by Sol Nudelman to the University of Maryland in partial fulfillment of the requirements for the Ph.D. degree.

Any discussion of this paper will appear in a Discussion Section to be published in the December 1956 JOURNAL.

REFERENCES

1. C. JEROME AND W. GUNGLE, *This Journal*, **100**, 34 (1953).
2. J. F. WAYMOUTH, *ibid.*, **100**, 81 (1953).
3. P. ZALM, G. DIEMER, AND H. A. KLASENS, *Philips Research Repts.*, **9**, 81 (1954).
4. D. CURIE, *J. Phys. Radium*, **14**, 672 (1953).
5. F. MATOSSI AND S. NUDELMAN, *Phys. Rev.*, **89**, 660 (1953).
6. H. H. HOMER, R. M. RULON, AND K. H. BUTLER, *This Journal*, **100**, 566 (1953).
7. S. NUDELMAN AND F. MATOSSI, *ibid.*, **101**, 546 (1954).
8. B. T. HOWARD, H. F. IVEY, AND W. LEHMANN, *Phys. Rev.*, **96**, 799 (1954).
9. F. A. SCHWERTZ, J. J. MAZENKO, AND E. R. MICHALIK, *ibid.*, **98**, 1133 (1955).
10. F. A. SCHWERTZ, Private communication.

Reactions of Refractory Silicides with Carbon and Nitrogen

LEO BREWER AND OSCAR KRIKORIAN

Department of Chemistry and Chemical Engineering and Radiation Laboratory, University of California, Berkeley, California

ABSTRACT

Silicides of Ti, Zr, Ce, and Nb were investigated to determine the phases present at temperatures around 2000°K. Ce-C and Nb-C systems were also investigated to a limited extent. Reactions of silicides of Ti, Zr, Ce, Nb, Ta, Mo, and W with carbon were studied at these temperatures. Also, a limited amount of work was done on the reactions of some silicides with nitrogen. The data have been used to establish ternary phase diagrams for the systems and to obtain upper and lower limits for heats of formation of the silicides.

Introduction

Silicides of titanium, zirconium, cerium, niobium, tantalum, molybdenum, and tungsten were investigated to fix their thermodynamic stabilities and thus determine their importance as refractories. These metals are expected to form the most stable silicides from a comparison with the carbide stability region in the periodic table.

Combustion calorimetry and solution calorimetry are not easily applicable in determining heats of formation of silicides due to their inertness toward oxidation and solvents. Dissociation pressure measurements would probable be the most applicable in determining their stabilities. Searcy and McNees (1) determined the stabilities of rhenium silicides by studies of this type. In order to undertake such studies on other refractory silicides, information on the phases present, their approximate stabilities, and suitable containers are of great importance.

In this work high temperature equilibrium studies involving silicides are used to obtain useful information about their stabilities. Equilibrium studies involved the systems M-Si, M-Si-C, M-Si-N_2, and M_1-M_2-Si. By comparing the stabilities of the silicides with the corresponding carbides and nitrides it was possible to set upper and lower limits to the stabilities of many of the silicides. The M_1-M_2-Si equilibria gave information about the relative stabilities of the silicides.

Experimental Procedure

M-Si, M-Si-C, and M_1-M_2-Si reactions were carried out by mixing together 140–400 mesh powders of the reactants and heating them to about 2100°K for 15–60 min in the inductively heated equipment already described (2). Argon, at 0.75 atm, was used to suppress volatilization of the silicon. Molybdenum crucibles were found to be satisfactory containers since molybdenum silicides were less stable than most of the other silicides studied. When

sample silicides were less stable than the molybdenum silicides, crucible attack still did not occur, providing the samples did not fuse. A protective silicide layer on the surface of the molybdenum evidently prevented further attack. Graphite crucibles were used when samples contained excess graphite. Usually, equilibrium was rapidly established between the reactants which then sintered and drew away from the container.

M-Si-N_2 systems were studied by allowing metal and silicon powder mixtures to come into equilibrium with N_2 at about ¾ atm pressure and at various temperatures. Molybdenum containers were again used for most of the heatings, although they were not satisfactory with titanium and zirconium systems because of crucible attack. ZrO_2 containers were also used for these systems.

Samples were quenched by turning off the induction heater and cooling with the gas in the system. About 3 min were required to cool from 2100° to 1200°K.

Temperatures were measured with an optical pyrometer. X-ray powder diffraction patterns were taken of the resulting samples. The new phases found and x-ray data for the various phases will be given in a forthcoming paper (3). All compositions of samples are given in atomic per cent and all temperatures are expressed in °K unless otherwise indicated.

Starting materials.—Silicon metal[1] was ground to finer than 140 mesh with a steel mortar and pestle. Spectroanalysis showed the main impurities to be: titanium less than 1%, chromium 0.1–1%, and aluminum and iron approximately 0.1%. X-ray analysis showed a very weak unidentified second phase.

Zirconium metal was obtained in the form of high purity, hafnium-free sponge from K. K. Kelley of the U. S. Bureau of Mines at Berkeley. X-ray analysis of the titanium metal powder ($a = 2.950 \pm 0.003$ *A*, $c = 4.692 \pm 0.005$ *A*) indicated that it contained roughly 4.5 at. % oxygen (4). Cerium metal obtained in the form of rods contained 4.5 at. % carbon as the main impurity. All other metals were of 99.9% or greater purity.

Binary Systems

The Ta-Si, Mo-Si, and W-Si systems at the temperatures of interest here have already been studied (5). The following phases were found: $TaSi_2$, $TaSi_{0.6}$, $TaSi_{0.4}$, $TaSi_{0.2}$; $MoSi_2$, $MoSi_{0.65}$, Mo_3Si; WSi_2, $WSi_{0.7}$. The $MoSi_{0.65}$ and $WSi_{0.7}$ phases were recently shown to be isomorphous with the tetragonal Cr_5Si_3 phase (52).

In an x-ray investigation of Ta-Si system (6), structures were assigned to phases $Ta_{4.5}Si$, Ta_2Si, and Ta_5Si_3. The x-ray pattern found for $Ta_{4.5}Si$ was different than that for the $TaSi_{0.2}$ reported by Brewer and co-workers (2). These two phases may be high and low temperature forms of the same compound. Ta_2Si corresponds to the $TaSi_{0.4}$ of Brewer and co-workers. The Ta_5Si_3 pattern, however, is different from the $TaSi_{0.6}$ phase reported by them. The two phases may again be high and low temperature modifications or, as is discussed later, the Ta_5Si_3 phase may have been stabilized by carbon impurity.

In this work the systems Ti-Si, Zr-Si, Ce-Si, and Nb-Si were investigated for the phases present at high temperatures. The results of the Ti and Zr heatings are presented in Tables I and II. The cerium and niobium results are discussed in the text. The detailed tabulated data are given by Krikorian (45). The symbols s. (strong), m. s. (moderately strong), m. (moderate), m.w. (moderately weak), w. (weak), and v.w. (very weak) refer to observed x-ray intensities. Maximum temperature attained is given in the tables. Molybdenum containers were used for all heatings unless otherwise indicated. Any evidence of melting of the sample has also been indicated. In all cases where the samples fused, they had a silvery-gray metallic luster.

TABLE I. Ti-Si *system*

Atomic % Si	Temp (°K)	Description of sample	Phases observed
17.8	2105	Fused Cruc. attack	Mo (m.s.) + Ti_5Si_3 (m.w.)
20.2	1691	Fused	Ti_5Si_3 (s.) + Ti (v.w.)
30.0	2105	Fused	Ti_5Si_3 (s.) + Mo (v.w.)
33.5	2105	Sintered Porous	Ti_5Si_3 (s.)
37.5	2105	Partially fused	Ti_5Si_3 (s.)
50.5	1933	Partially fused	Ti_5Si_3 (m.) + TiSi (w.) + ? (v.w.)
50.5	2105	Fused	Ti_5Si_3 (s.) + TiSi (w.)
60.0	2141	Fused	Ti_5Si_3 (s.) + ? (v.w.)
60.2	2190	Fused Al_2O_3 cruc. Crystals above melt	$TiSi_2$ (s.) + Ti_5Si_3 (w.)
67.1	2105	Fused	$MoSi_2$ (s.) + Ti_5Si_3 (w.)
71.9	1618	Partially fused	$TiSi_2$ (m.) + Si (w.)

Ti-Si *system.*—In addition to $TiSi_2$, the Ti_5Si_3 phase already reported (7) was found. The Ti_5Si_3 lattice constants were found to vary with the silicon content of the sample from 20 to 60 at. % Si. Such an effect is not necessarily indicative of a wide homogeneity range in the binary system, but may be due to presence of oxygen in the sample from the titanium starting material, as well as possible solubility of the molybdenum container material in the Ti_5Si_3 lattice.

The reported TiSi phase (8) was not observed in pure

[1] Supplied by the J. T. Baker Chemical Co., Phillipsburg, N. J.

TABLE II. Zr-Si *system*

Atomic % Si	Temp (°K)	Description of sample	Phases observed
22.4	1952	Fused Condensate on walls	A phase (m.)
35.0	1952	Partially fused	Zr_2Si (m.) + Zr_5Si_3 (w.)
40.4	1952	Sintered	Zr_2Si (m.s.) + ? (v.w.)
40.4*	2156	Well-sintered Brown color on surface	Zr_5Si_3 (m.s.)
42.6	1952	Sintered	Zr_2Si (m.s.) + Zr_5Si_3 (w.) + ? (w.)
42.6*	2156	Slightly sintered Brown color on surface	Zr_5Si_3 (m.s.) + Zr_3Si_2 (w.)
45.4	1952	Sintered	Zr_2Si (m.s.) + ? (w.)
45.4*	2156	Not sintered	Zr_5Si_3 (m.) + Zr_6Si_5 (m.) + Zr_3Si_2 (w.)
45.4*	2156	Sintered	Zr_5Si_3 (m.) + Zr_6Si_5 (m.) + Zr_3Si_2 (w.) + ? (w.)
49.8	1952	Sintered	$ZrSi$ (m.s.) + Zr_2Si (m.w.)
49.8*	2156	Not sintered Brown color on surface	$ZrSi$ (m.) + Zr_6Si_5 (m.)

* Preceding sample reheated.

phase. Many weak lines appeared in the TiSi region along with Ti_5Si_3. $TiSi_2$ and Ti_5Si_3 were found together in a sample heated in an alumina crucible, indicating that the Ti_5Si_3 phase is sufficiently stabilized by oxygen to cause disproportionation of TiSi. The presence of oxygen in the starting Ti metal is undoubtedly responsible for the difficulty of the production of the TiSi phase even when molybdenum containers are used.

Attack of the crucible by a sample containing 67% silicon showed that molybdenum is capable of reducing $TiSi_2$ to Ti_5Si_3. Also its presence in fused samples of Ti_5Si_3 indicates that Ti_5Si_3 is stable in the presence of molybdenum.

Zr-Si *system.*—For the preparation of compounds of silicon with pure zirconium, small pieces of sponge zirconium were heated with silicon for an hour at 1952°K. Some samples were then powdered to 140 mesh or finer and reheated. Results of the x-ray analyses are given in Table II.

Samples of zirconium silicides have been prepared by others (9–11); the phases ZrSi, Zr_6Si_5, Zr_4Si_3, Zr_3Si_2, Zr_2Si, and Zr_4Si, in addition to the previously known $ZrSi_2$, were reported (9). Their identifications were based largely upon metallographic analysis. The phase Zr_5Si_3, with the Mn_5Si_3 structure, was said to be the only phase between Zr_2Si and ZrSi (10). McPherson (43) and Pietrokowsky (11) kindly supplied samples of all their phases for comparison with present samples.

X-ray examination of the samples received from McPherson showed characteristic x-ray patterns for each of the five lower silicides. Except for Zr_4Si, all of these phases appeared in the authors' samples. A sample containing 22.4 at. % Si fused at 1952°K without apparent crucible attack and appeared to contain a single phase different from the Zr_4Si of McPherson. Pietrokowsky obtained yet another diffraction pattern for Zr_4Si. The structure of none of these phases has been worked out. Pietrokowsky (11) determined the structure of Zr_2Si. In the present work Zr_2Si was obtained as a practically pure phase near 35 at. % Si. It appeared in small amounts in samples containing up to 50 at. % Si apparently due to incomplete attainment of equilibrium since the Zr_2Si disappeared upon powdering and reheating the samples.

The sample designated as Zr_3Si_2 by McPherson was found to have the Mn_5Si_3 structure and is designated here as the Zr_5Si_3 phase. This composition is consistent with the data reported in reference (9). Pietrokowsky prepared a single crystal of the phase designated as Zr_4Si_3 by Mc-

Pherson and found it to have the tetragonal U_3Si_2 structure reported by Zachariasen (12). This phase is designated here as Zr_3Si_2. The structures of the Zr_6Si_5 and ZrSi phases have not yet been determined. ZrSi does not index well on the hexagonal lattice reported by Lundin and co-workers (9).

Zr_5Si_3 shows a varying lattice constant depending upon the preparation, which may indicate a wide homogeneity range. Since the ternary diagram studies show that this phase takes up elements like carbon, nitrogen, and oxygen, the variation may be due to impurities.

To check the effect of impure zirconium, preparations were made using zirconium powder. Ignition of the zirconium powder indicated 21.4 at. % oxygen, assuming all the impurity was oxygen. X-ray analysis showed the presence of a pure zirconium phase plus a zirconium phase with a lattice constant corresponding to 22 at. % oxygen, assuming all the impurity to be oxygen (13). The preparations gave single-phase samples of ZrSi and Zr_5Si_3, but patterns of the Zr_3Si_2 and Zr_6Si_5 phases could not be positively identified. These results indicate that the absence of these phases in the work of Schachner and co-workers (10) may be due to the presence of oxygen, carbon, or nitrogen dissolving in and stabilizing the Zr_5Si_3 phase, thus causing the disporportionation of the Zr_3Si_2 and Zr_6Si_5 phases. The results presented below for the Zr-Si-C system confirm this. Heatings with 15–18 at. % oxygen and with less than 30 at. % silicon at temperatures above 1900°K yield only the phases Zr and Zr_5Si_3. The Zr lattice was expanded, indicating dissolved oxygen. Lowering of the zirconium activity by oxygen apparently causes the disproportionation of the Zr_4Si and Zr_2Si phases. Above 1900°K the impurity reduces the number of silicide phases to Zr_5Si_3, ZrSi, and $ZrSi_2$. As the temperature is lowered, reduction of the zirconium activity is not so great and it is possible to prepare Zr_2Si. The oxygen impurity also raises the eutectic temperature for the Zr-Zr_5Si_3 region. Samples were well sintered at 2000°K and were probably close to the eutectic temperature.

To check the effect of oxygen on the Zr-Si system, the composition triangles of the Zr-Si-O system were determined. A join was found between ZrO_2 and $ZrSi_2$. Thus, none of the other zirconium silicides can exist in equilibrium with zircon or any silicon oxide. There is also a join between $ZrSi_2$ and SiO_2. Thus, silicon reacts with ZrO_2. Most of the binary silicide phases below $ZrSi_2$ are of no importance in the ternary Zr-Si-O diagram because of the stabilization of the Zr_5Si_3 phase, and no phases are found between Zr and Zr_5Si_3 at 2000°K within the ternary diagram. Also, it appears that no phases are stable between Zr_5Si_3 and ZrSi at 2000°K within the ternary diagram. A ternary diagram is given in Fig. 1 to represent the probable behavior at 1950°K. At lower temperatures, where the solubility of oxygen in the Zr_5Si_3 phase decreases thus increasing its activity, the other binary phases appear to become important and joins should be drawn between the binary zirconium silicides and ZrO_2.

Ce-Si *system*.—Ce-Si samples were prepared by reacting small pieces of Ce rod with Si powder at about 1700°K. They all had the appearance of being fused or partially fused. It was not possible to determine visually the extent of the fusion. There was no evidence of crucible attack.

The samples were prepared for x-ray analysis by grinding them to 200 mesh in a dry box under argon and sealing the specimens in capillary tubes.

The x-ray patterns were rather poor and the samples were inhomogeneous mixtures; however, it was established that several lower silicides exist. These are provisionally assigned the formulas $CeSi_{0.35}$, $CeSi_{0.5}$, and $CeSi_{0.75}$.

The $CeSi_{0.35}$ phase appeared along with CeO_2 in all of its samples. In spite of precautions, the CeO_2 probably came from oxidation of Ce metal during preparation of the specimens for x-ray study. Therefore, it is believed that $CeSi_{0.35}$ is the lowest silicide.

The $CeSi_{0.5}$ appeared in samples containing 33–37 at. % Si, and $CeSi_{0.75}$ appeared in samples containing 40–50% Si. $CeSi_2$ was obtained in single phase and its lattice constants were measured: $a = 4.175 \pm 0.002$ *A*, $c = 13.848 \pm 0.006$ *A*. It is reported to have the tetragonal $\alpha ThSi_2$ type structure with the lattice constants $a = 4.16 \pm 0.03$ *A*, $c = 13.90 \pm 0.07$ *A* (12).

Nb-Si *system*.—The Nb-Si system showed the two lower silicides $NbSi_{0.55\pm0.1}$ and Nb_5Si_3. $NbSi_{0.55}$ is isostructural with the $TaSi_{0.6}$ phase reported earlier (5). It was obtained in equilibrium with niobium metal up to 36 at. % Si. Nb_5Si_3 has Mn_5Si_3 type structure. $NbSi_{0.55}$ and Nb_5Si_3 were not obtained together in equilibrium and the region should be more fully investigated.

It has been possible to set the Nb-$NbSi_{0.55}$ eutectic, or peritectic, temperature as greater than 2095°K and the Nb_5Si_3-$NbSi_2$ eutectic, or peritectic, at 2110° ± 30°K.

M-Si-C Systems

From heats of formation of the carbides in these systems it is possible to obtain limits on heats of formation of silicides. To make these calculations, use is made of the approximate relation:

$$\Delta F^{\circ}_{T} = \Delta H^{\circ}_{298} - T\Delta S^{\circ}_{298}$$

Assuming that ΔS°_{298} is zero when all reactants and products are solids, the heats of formation of the carbides directly

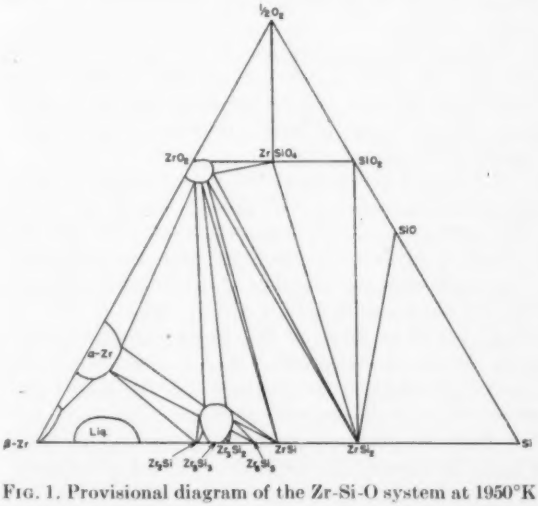

FIG. 1. Provisional diagram of the Zr-Si-O system at 1950°K

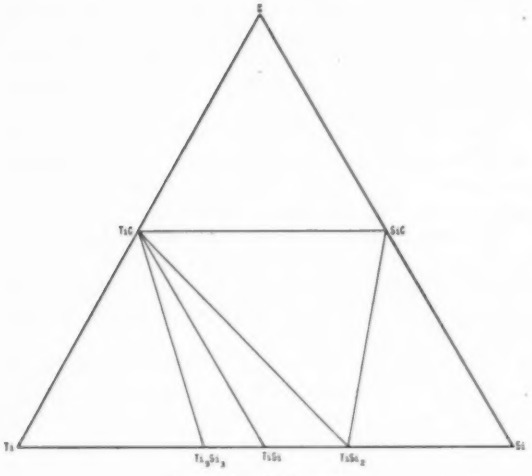

FIG. 2. Ti-Si-C system

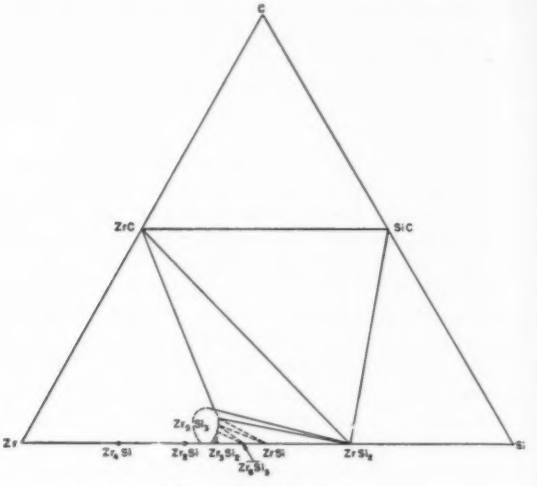

FIG. 3. Zr-Si-C system

set limits for heats of formation of the silicides. As an example:

$$\tfrac{1}{2}\ MSi_2 + \tfrac{3}{2}\ C \rightarrow \tfrac{1}{2}\ MC + SiC$$

$$\tfrac{1}{2}\ MC + \tfrac{3}{2}\ Si \rightarrow \tfrac{1}{2}\ MSi_2 + \tfrac{1}{2}\ SiC$$

If the ΔH^0_{298} of formation of SiC is -13.0 kcal (14) and that of MC is A, then ΔH^0_{298} of formation for MSi_2 must be greater than $(A - 26.0)$ kcal and less than $(A + 13.0)$ kcal for the reactions to go as written.

The calculations may be improved somewhat if the entropies of the silicides become available. Third law entropy values are available for SiC, TiC, and TaC (15). Entropies for the other carbides may be estimated by Latimer's method (16). One may assign an entropy contribution for carbon in a solid compound by subtracting the contribution of the metal from the known entropies of carbides (15). It is found that about -4.1 e.u. may be assigned to carbon for its contribution in a carbide of one to one metal to carbon ratio, about -7.2 e.u. in a carbide of two to one or three to one metal to carbon ratio and about -14 e.u. in a carbide of four to one metal to carbon ratio.

The absolute entropy of WC, for example, is estimated as $S^0_{298} = S^0_M + S^0_C = 15.0 - 4.1 = 10.9$ e.u. Using values of 8.04 and 1.36 e.u. (15) for the absolute entropies of W and C, respectively, ΔS^0_{298} of formation for WC is estimated as 1.5 ± 1 e.u.

The heat of formation of SiC is available (14), as are those for TiC and TaC (17, 18) and for WC (19). For NbC, $\Delta H^0_{298} = -33.7$ kcal was obtained from Kelley (51).

Heats of formation of Mo_2C and MoC were calculated from equilibrium constant data of Browning and Emmett (20) for the reactions $2Mo + CH_4 = Mo_2C + 2H_2$ and $Mo_2C + CH_4 = 2MoC + 2H_2$. In making these calculations the S^0_{298} for Mo_2C and MoC were estimated by the method described above. The heat capacity of MoC was estimated to be $\frac{2}{5}$ the heat capacity of Cr_3C_2 (21), that for Mo_2C was assumed to be $\frac{3}{10}$ the heat capacity of Cr_7C_3 (21). Estimated values were combined with thermodynamic data for the other substances (21, 15) involved in the reaction to tabulate $(\Delta F^0_T - \Delta H^0_{298})/T$ functions for the reactions. ΔH^0_{298} was found to be 13.67 ± 1.09 kcal for the first reaction and 18.11 ± 0.20 kcal for the second reaction. With the value of -17.89 kcal/mole for ΔH^0_{298} of formation for methane (22), ΔH^0_{298} of formation is -4.22 ± 1.09 kcal for Mo_2C and -2.00 ± 0.65 kcal for MoC. The respective ΔS^0_{298} values were estimated to be 2.4 ± 1 and 0.0 ± 1 e.u.

The ternary diagrams of Fig. 2 to 7 have been used to show phases resulting from M-Si-C heatings. Several of the diagrams were not completed, but the joins that were established are indicated. Other joins, boundaries, or homogeneity ranges that were inferred are indicated by dotted lines. For simplicity, homogeneity ranges for carbide phases have been omitted. In the Mo-Si-C system, an attempt was made to give the general form of the melting region along with several ternary eutectic temperatures. The melting diagram of the molybdenum-silicon system was given by Kieffer and Cerwenka (23) and also by Ham and Herzig (24). Results have been re-interpreted to obtain better agreement with the data. The Mo-Mo_2C eutectic temperature is given by Sykes, Van Horn, and Tucker (25) and the Mo_2C melting temperature by Agte and Alterthum (26).

After this work had been completed, word was received that the Mo-Si-C system had been determined in more detail (27). Results are in essential agreement with the authors except for an MoC phase in their samples. This phase is unstable at low temperatures and may have been retained by a faster quenching.

In the Mo-Si-C system a ternary compound was observed at about the composition Mo_4CSi_3. Considerable variation of lattice parameters with composition was observed for ternary compound. Evidently carbon replaces Mo in a Mo_5Si_3 lattice until the composition Mo_4CSi_3 is obtained on the high carbon side. Lattice constants for the composition Mo_4CSi_3 are $a = 7.285 \pm 0.007$ A and $c = 5.242 \pm 0.007$ A.

Using the lattice constants for Mo_4CSi_3 the calculated x-ray density is 6.62 g/cm³ for Mo_4CSi_3 and 7.94 g/cm³

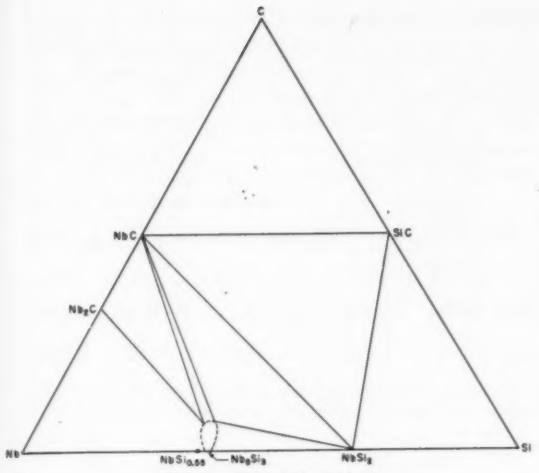

FIG. 4. Nb-Si-C system

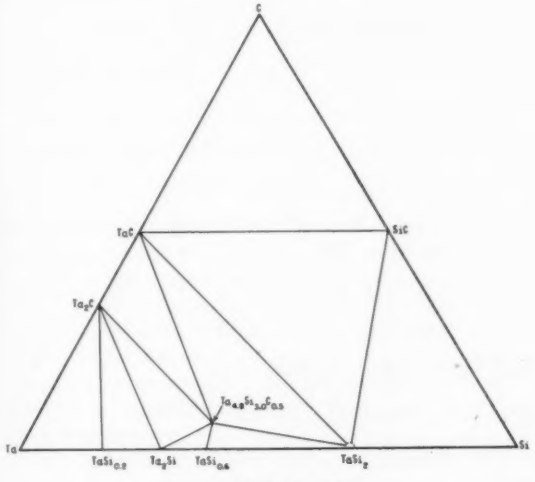

FIG. 5. Ta-Si-C system

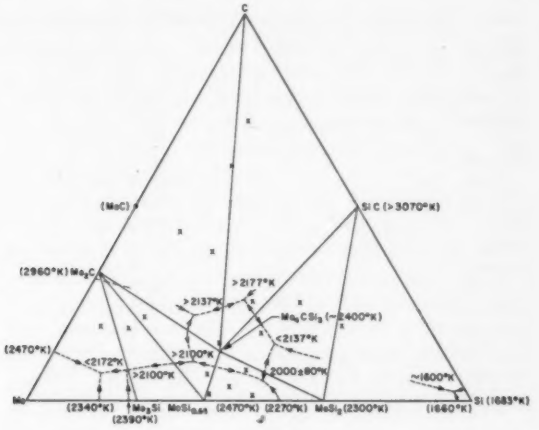

FIG. 6. Mo-Si-C system

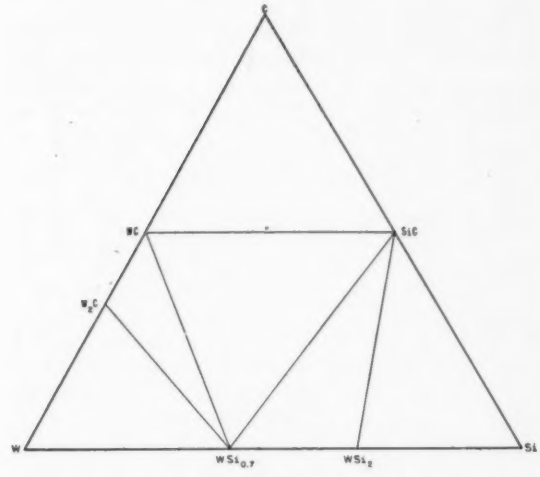

FIG. 7. W-Si-C system

for Mo_5Si_3. The measured density for a single-phase sample of Mo_4CSi_3 was found to be 6.9 g/cm³ which gives fair agreement with its composition. The homogeneity range for the compound is believed to extend to lower carbon contents but does not reach the binary Mo-Si region. Mo_4CSi_3 is the only molybdenum silicide phase found that is stable in the presence of graphite.

In the Ta-Si-C system a ternary compound appeared in single phase with the Mn_5Si_3 structure in a sample of composition $Ta_{4.8}Si_3C_{0.5}$ with parameters $a = 7.494 \pm 0.007$ *A* and $c = 5.242 \pm 0.007$ *A*. No variation in lattice constants was observed in the x-ray patterns, so that there is no evidence for an extended homogeneity range.

The Mn_5Si_3 structure has two molecules per unit cell. Assuming that the carbons in $Ta_{4.8}Si_3C_{0.5}$ are interstitial and the departure of the number of Ta's from 5 is due to vacancies in the lattice, the calculated x-ray density is 12.48 g/cm³ for $Ta_{4.8}Si_3C_{0.5}$. The density of the powder measured with a pycnometer using the volume displacement of CCl_4 gave 12.4 g/cm³.

A phase Ta_5Si_3, of the Mn_5Si_3 structure, has been reported (6) with lattice constants $a = 7.474$ *A* and $c = 5.225$ *A*. These values are close to those which obtained here for $Ta_{4.8}Si_3C_{0.5}$. In the work on the Ta-Si system (5), Ta_5Si_3 with the Mn_5Si_3 structure was not found, although a phase of composition $TaSi_{0.6}$ was found which did not have the Mn_5Si_3 structure. Nowotny and co-workers (6) also report that Ta_5Si_3 transforms to a new phase somewhere between 1600° and 1800°K. This high temperature phase may be the $TaSi_{0.6}$ reported by Brewer and co-workers. If $TaSi_{0.6}$ is stable only at high temperatures, it is easily quenched since the Ta_5Si_3 phase has not been observed in this work in binary Ta-Si samples. The Mn_5Si_3 type structure is stabilized by oxygen, carbon, and nitrogen impurities and was obtained with added nitrogen or carbon in the present ternary diagram studies. Thus, it is likely that the Ta_5Si_3 phase is unstable at all temperatures in the binary system and requires a third component for its existence. A variation of lattice constants was observed for $TaSi_2$ from the $TaSi_2$-SiC-Si region to the $TaSi_2$-SiC-TaC region, indicating solubility of carbon in $TaSi_2$.

Both Zr_5Si_3 and Nb_5Si_3 showed large homogeneity ranges in the presence of carbon. Other than this there was

TABLE III. ΔH°_{298} *of formation in kcal/gram atom* Si

$\frac{1}{2}TiSi_2$	−15.4 to −34.9	$\frac{5}{6}$ $TaSi_{0.6}$	−20 to −77.2
TiSi	−15.4 to −65.8	Ta_2Si	−20 to −90.1
$\frac{1}{5}Ti_5Si_3$	−20 to −86.1	$5TaSi_{0.2}$	<−20
$\frac{1}{2}ZrSi_2$	−30.5 ± 5	$\frac{1}{3}Ta_{4.8}Si_2C_{0.5}$	−20 to −74.7
ZrSi	−58 ± 10	$\frac{1}{2}MoSi_2$	−5.8 to −15.5
$\frac{1}{5}Zr_5Si_3$	−66 ± 10	$10/6.5MoSi_{0.65}$	−18.4 ± 1.6
$\frac{1}{2}Zr_2Si_2$	−70 ± 10	Mo_2Si	−20
$\frac{1}{3}Zr_2Si_3$	−72 ± 10	$\frac{1}{3}Mo_4CSi_3$	−19.6 ± 2
Zr_2Si	−74 ± 10	$\frac{1}{2}WSi_2$	−1.6 to −17.2
Zr_4Si	−76 ± 10	$10/7WSi_{0.7}$	−4.6 to −20
$\frac{1}{2}CeSi_2$	−16.6 to −34.4	$\frac{1}{2}ReSi_2$	−12.5*
$1/xCeSi_x$	<−16.6	ReSi	−11.6*
$\frac{1}{2}NbSi_2$	−8.5 to −28	Re_2Si	−6.2*
$\frac{1}{3}Nb_2Si_3$	−8.5 to −63		
$\frac{20}{11}NbSi_{0.55}$	−8.5 to −68		
$\frac{1}{2}TaSi_2$	−12.8 to −32.3		

* Values for the Re silicides (1) have been recalculated using ΔH°_{298} = 105 kcal for the heat of sublimation of Si (41, 42).

no indication of ternary compound formation in the systems. A hexagonal phase (a = 3.117 ± 0.003 A, c = 4.969 ± 0.005 A) isomorphous with Ta_2C was observed in the Nb-Si-C system, indicating the presence of an Nb_2C phase (28, 29, 30). To confirm this, a powder mixture of 67% Nb and 33% carbon was held at 2130°K for 38 min in a Mo crucible under vacuum. The phases Nb_2C and NbC were obtained. Similar treatment of a mixture of 75% Nb and 25% carbon at 1920°K yielded Nb_2C as the principle phase with a very small amount of NbC present.

In the Ce-Si-C system a sample containing 25% Ce, 50% Si, and 25% carbon was held at 1605°K for 44 min. X-ray analysis showed $CeSi_2$, plus an unidentified phase. The sample was gray-brown and gave off an acetylene odor. An investigation of the Ce-C system in the range between 50% and 67% carbon showed the phases CeC, Ce_2C_3, and CeC_2, plus several unidentified phases. None of these could be identified in the Ce-Si-C sample. The Ce_2C_3 (body-centered cubic Pu_2C_3 type) lattice constant was a = 8.455 ± 0.008 A (31); the CeC (NaCl type) lattice constant was a = 5.130 ± 0.002 A (31); the Ce-C samples were golden brown.

Details of calculations of the stabilities of silicides of Mo and Zr from data of the M-Si-C systems follow. Calculations for the other systems are similar. Pertinent results are summarized in Table III. The numbers below each species are the values for ΔH°_{298} of formation expressed in kilocalories.

Mo-Si-C *system.*—Recent studies (32) on the vapor pressure of Si over Mo + Mo_2Si give a preliminary value of −20 kcal for ΔH°_{298} of Mo_2Si.

$$0.71\,Mo_2Si + 0.29\,SiC \rightarrow \frac{10}{6.5}\,MoSi_{0.65} + 0.29\,Mo_2C$$

$$-14.2 \qquad -3.8 \qquad <-16.8 \qquad -1.2$$

$$\frac{10}{6.5}\,MoSi_{0.65} + \frac{19}{13}\,Mo \rightarrow Mo_2Si$$

$$>-20 \qquad -20$$

Therefore, ΔH°_{298} for $10/6.5\ MoSi_{0.65}$ = −18.4 ± 1.6 kcal.

$$\frac{10}{6.5}\,MoSi_{0.65} + \frac{17}{39}\,C \rightarrow \tfrac{1}{3}\,Mo_4CSi_3 + \frac{4}{39}\,Mo_2C$$

$$-18.4 \qquad <-18.0 \qquad -0.4$$

$$\tfrac{1}{3}\,Mo_4CSi_3 + \tfrac{7}{3}\,Mo \rightarrow Mo_2Si + \tfrac{1}{3}\,Mo_2C$$

$$>-21.4 \qquad -20 \qquad -1.4$$

Therefore, ΔH°_{298} for Mo_4CSi_3 = −19.7 ± 2 kcal.

$$\tfrac{1}{2}\,MoSi_2 + \tfrac{3}{4}\,C \rightarrow \tfrac{1}{8}\,Mo_4CSi_3 + \tfrac{5}{8}\,SiC$$

$$>-15.5 \qquad -7.4 \qquad -8.1$$

$$\tfrac{1}{8}\,Mo_4CSi_3 + \tfrac{3}{4}\,Si \rightarrow \tfrac{1}{2}\,MoSi_2 + \tfrac{1}{8}\,SiC$$

$$-7.4 \qquad <-5.8 \qquad -1.6$$

Zr-Si-C *system.*—From the Zr-Si-O system, using oxide heats of formation (33)

$$\tfrac{1}{2}\,ZrO_2 + \tfrac{3}{2}\,Si \rightarrow \tfrac{1}{2}\,ZrSi_2 + \tfrac{1}{2}\,SiO_2$$

$$-130.9 \qquad <-25.8 \qquad -105.1$$

The carbide ternary diagram yields

$$\tfrac{1}{2}\,ZrSi_2 + \tfrac{3}{2}\,C \rightarrow \tfrac{1}{2}\,ZrC + SiC$$

$$>-35.2 \qquad -22.2 \qquad -13.0$$

Therefore, ΔH°_{298} for $\frac{1}{2}\ ZrSi_2$ = −30.5 ± 5 kcal. The Zr-Si phase diagram established by Lundin and co-workers (9) shows that all of the zirconium silicides except Zr_6Si_5 have incongruent melting points. Thus, at the $ZrSi_2$ peritectic there are $ZrSi_2$, ZrSi, and a Si rich melt in equilibrium; at the ZrSi eutectic ZrSi, Zr_6Si_5, and a Si rich melt in equilibrium; and so on to Zr_2Si, Zr_4Si, and a Zr rich melt in equilibrium.

If the activity of Si or of Zr in the melt at the peritectic points can be estimated, then heats of formation of all of the other zirconium silicides can be calculated from the heat of formation of $ZrSi_2$. The activity of Si in the melt is estimated to be roughly equal to the mole fraction of Si between the stable solid compound and pure Si, when working on the Si rich side of the diagram. The free energy of solution of Si from its standard state can then be calculated.

$$Si\ (s) \rightarrow Si\ (l);\ \Delta F^\circ_T = \Delta H^\circ_f - T\Delta S^\circ_f$$

$$Si\ (l) \rightarrow Si\ (sol'n);\ \overline{\Delta F}_T = RT \ln a_{Si}$$

$$Si\ (s) \rightarrow Si\ (sol'n);\ \overline{\Delta F}_T = \Delta H^\circ_f - T\Delta S^\circ_f + RT \ln a_{Si}$$

On the Zr rich side of the diagram a similar calculation is made referring to the activity of Zr rather than Si. For the fusion process ΔS_f^0 is taken as 6.6 e.u. for Si (34) and 2.3 e.u. for Zr (34), ΔH_f^0 is taken as 11.1 kcal for Si (34) and calculated as 4.9 kcal for Zr from the melting point of Zr given by Lundin and co-workers (9). In the calculations that follow, the numbers below the Si and Zr solutions represent the $\overline{\Delta F}_T$ of solution.

$ZrSi_2 = ZrSi + Si(sol'n, a_{Si} = 0.47); \quad T = 1790$

$-61 \quad -57.6 \quad -3.4$

$6ZrSi = Zr_6Si_5 + Si(sol'n, a_{Si} = 0.108); \quad T = 2370$

$-345.6 \quad -330.6 \quad -15.0$

$5Zr_3Si_2 = 2Zr_6Si_5 + 3Zr(sol'n, a_{Zr} = 0.084);$

$-700.5 \quad -661.2 \quad -39.3 \quad T = 2500$

$2Zr_5Si_3 = 3Zr_3Si_2 + Zr(sol'n, a_{Zr} = 0.147);$

$-430.5 \quad -420.3 \quad -10.2 \quad T = 2480$

$3Zr_2Si = Zr_5Si_3 + Zr(sol'n, a_{Zr} = 0.352); \quad T = 2380$

$-220.8 \quad -215.3 \quad -5.5$

$Zr_4Si = Zr_5Si + 2Zr(sol'n, a_{Zr} = 0.601); \quad T = 1900$

$-76.4 \quad -73.6 \quad -2.8$

M-Si-N_2 Systems

The M-Si-N_2 systems can yield information about the stabilities of silicides of Ti, Zr, Ce, Nb, and Ta since these elements form stable nitrides at high temperatures. The nitrides of these metals are more stable than the silicides at lower temperatures, but at high temperatures the nitrides become less stable due to their negative entropy of formation. Determination of the temperature at which this reversal of stabilities occurs would be very valuable in fixing the stabilities of the silicides.

ΔH_{298}^0 values for Si_3N_4 and CeN are available (35) as is ΔS_{298}^0 of formation of Si_3N_4 (15). The other entropies have been estimated.

From the observations of Schönberg on the Ta-N system (36) the phases prepared and investigated by earlier workers can be identified. Neumann, Kröger, and Kunz (37) have determined the heat of combustion of tantalum nitride. Their method of preparation indicates the compounds are $TaN_{0.846}O_x$ and $TaN_{0.955}O_y$. In order to interpret the results, x is assumed to be 0.060. $TaN_{0.846}O_{0.060}$ is treated as being a solid solution of 0.012 Ta_2O_5 in 0.976 $TaN_{0.867}$ with zero heat of solution. Thus -199.3 kcal is obtained as the ΔH_{298}^0 of combustion for $TaN_{0.867}$. Combining this value with the heat of formation of Ta_2O_5 (33) the ΔH_{298}^0 of formation is -59.2 ± 2 kcal per equivalent of N for $TaN_{0.867}$.

Slade and Higson (38) have studied the dissociation pressure of a tantalum nitride. From their method of preparation, they were probably studying the equilibrium $2\ TaN_{0.8} = Ta_2N + \frac{3}{10}\ N_2$. The dissociation pressure leads to $\Delta H_{298}^0 = 29.6 \pm 2$ kcal for this reaction. Combining this with the above value for $TaN_{0.8-0.9}$ yields a ΔH_{298}^0 of -65.2 ± 5 kcal for Ta_2N.

An experimental difficulty was encountered in attaining equilibrium in the M-Si-N_2 systems. As some of the samples nitrided, they sintered and formed a crust on the surface so that the samples were not homogeneous in nitrogen throughout. More useful results would be obtained by introducing nitrogen into the system in the form of a metal nitride. Preparation of Si_3N_4 and Ta_2N was investigated for this purpose.

To prepare Si_3N_4, Si metal powder was heated in a Mo crucible under about $\frac{3}{4}$ atm of N_2. The rate of the nitriding reaction was very slow below 1600°K while, above 1900°K, Si_3N_4 showed considerable decomposition. The sample was first heated to 1660°K. The temperature was then gradually increased to 1800°K over a period of an hour. Sintered portions of the resulting sample were crushed and the sample was reheated. The final product was grayish white. X-ray analysis showed a strong Si_3N_4 pattern plus weak Si.

Ta_2N was prepared by heating Ta powder contained in a Mo crucible to 2100°K for 33 min under $\frac{3}{4}$ atm of N_2. From the weight gain the composition was calculated to be $Ta_{1.96}N$. The x-ray diffraction pattern showed Ta_2N as a single phase.

Work on the M-Si-N_2 systems was concentrated on the Ta-Si-N_2 system with only a few reactions in the other systems being studied. A summary of the reactions studied is presented in Table IV. Heatings at 1600°K in the Ta-Si-N_2 system show that $TaSi_2$ is unstable in the presence of N_2 and reacts to give $Ta_{5-x}Si_{3-y}N_z$. Si_3N_4 would also be expected to form, however it was not picked up by x-ray analysis. When samples of Si content 38% and lower were heated in N_2 at 1600°K they showed a considerable gain in weight. The phase Ta_2N appeared in equilibrium with $Ta_{5-x}Si_{3-y}N_z$. Some weak unidentified lines were also present. These lines may be due to $TaN_{0.8\ 0.9}$ and TaN. From these data a provisional form of the Ta-Si-N_2 diagram has been constructed at 1600°K (*see* Fig. 8).

At 2109°K $TaSi_2$ was found to be stable in the presence of N_2. This means that the following reaction can proceed as written:

$$\underset{-5.6}{\frac{1}{4}\ Ta_2N} + \underset{-2.4}{\frac{1}{3}\ Si_3N_4} = \underset{-8.0}{\frac{1}{2}\ TaSi_2} + \frac{19}{24}\ N_2(g)$$

The ΔF_T^0 of formation of Ta_2N and Si_3N_4 have been indicated in the equation. Thus, ΔH_{298}^0 of formation for $TaSi_2$ is less than -8.0 kcal. This does not improve the limits set by the carbide equilibria; however, a study of the equilibrium at a lower temperature would give additional data.

The Nb-Si-N_2 system appears to be similar to the Ta-Si-N_2 system. Joins were established between $Nb_{5-x}Si_{3-y}N_z$ and N_2 and between $Nb_{5-x}Si_{3-y}N_z$ and $NbSi_2$.

From the gain in weight and physical appearance of a sample of Ce + 2Si heated in N_2, it is evident that $CeSi_2$ is unstable in the presence of N_2. The x-ray pattern was too poor to reveal anything. Providing no ternary compounds are formed in the Ce-Si-N_2 system, the following reaction can proceed at 1610°K. From a calculation of ΔF_T^0 for CeN and Si_3N_4, ΔH_{298}^0 of formation of $CeSi_2$ is greater than -34.4 kcal/equivalent of Si

$$\underset{>-34.4}{\frac{1}{2}\ CeSi_2} + \frac{11}{12}\ N_2 = \underset{-18.4}{\frac{1}{2}\ CeN} + \underset{-16.0}{\frac{1}{3}\ Si_3N_4}$$

TABLE IV. M-Si-N_2 *systems*

Reactants	Cruc.	Temp (°K)	Weight change	Description of sample	Phases observed
Ti + 0.61 Si + N_2	ZrO_2	2109	−4.0%	Not sintered Gold color	TiN (s.)
Ti + 2.18 Si + N_2	Mo	2146	Unknown	Partially fused Gold color Crucible attack	? (m.s.) + TiN (m.s.)
Zr + 2.04 Si + N_2	Mo	2146	Unknown	Partially fused Gold color Crucible attack	$MoSi_2$ (v.s.) + ZrN (s.) + $ZrSi_2$ (w.) + ? (v.w.)
Zr + 13.1 Si_3N_4 + N_2	ZrO_2	2109	−54%	Not sintered	? (s.) + Si (m.s.)
Ce + 2.23 Si + N_2	Mo	1610	13.5%	Black brittle solid. Strong odor of NH_3	? (v.w.)
Nb + 0.60 Si + N_2	ZrO_2	2109	−0.2%		$Nb_5Si_3N_x$ (m.s.)
Nb + 1.17 Si + 0.28 Si_3N_4 + N_2	Ta	2365	Unknown	Fused Crucible attack	(Ta, Nb)Si_2 (m.s.) + (Ta, Nb)$_5Si_3N_x$ (m.s.) + (Ta, Nb)$Si_{0.6}$ (w.)
Nb + 2.01 Si + N_2	Mo	2146	Unknown	Partially fused Crucible attack	$NbSi_2$ (m.) + $Nb_5Si_3N_x$ (m.) + ? (w.)
Ta + 0.20 Si + N_2	Mo	1602	+4.2%	Sintered	$Ta_5Si_3N_x$ (m.) + ? (m.w.)
Ta + 0.40 Si + N_2	Mo	1602	+3.7%	Sintered	$Ta_5Si_3N_x$ (m.s.) + Ta_2N (m.w.) + ? (v.w.)
Ta + 0.61 Si + N_2	Mo	1602	+4.3%	Sintered	$Ta_5Si_3N_x$ (m.s.) + $TaSi_2$ (m.) + ? (w.)
Ta + 1.07 Si + 0.30 Si_3N_4 + N_2	Ta	2365	Unknown	Fused Crucible attack	$TaSi_2$ (m.) + $Ta_5Si_3N_x$ (m.) + $TaSi_{0.6}$ (v.w.)
Ta + 1.13 Si + 1.72 Si_3N_4 + N_2	Mo	1651	+5.5%	Not sintered	$TaSi_2$ (m.) + $Ta_5Si_3N_x$ (m.) + Ta_2N (w.)
Ta + 2.20 Si + N_2	Mo	2146	Unknown	Partially fused	$TaSi_2$ (v.s.)
Ta + 2.30 Si + N_2	Mo	1602	+7.1%	Not sintered Top of sample	$TaSi_2$ (s.) + Si (m.) + ? (v.w.)
Ta + 2.30 Si + N_2	Mo	1602	+7.1%	Not sintered Bottom of sample	$TaSi_2$ (s.) + $Ta_5Si_3N_x$ (m.)
$TaSi_{2.20}N_{1.24}$ + N_2	Mo	1651	+3.0%	Not sintered Previous sample	$TaSi_2$ (s.) + $Ta_5Si_3N_x$ (m.s.) + Ta_2N (w.)
Ta_2N + 0.81 Si_3N_4 + N_2	Mo	2109	−14.1%	Sintered	$TaSi_2$ (s.) + $Ta_5Si_3N_x$ (m.s.)

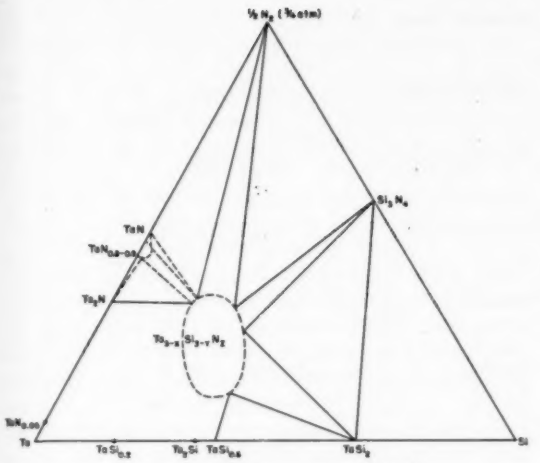

FIG. 8. Ta-Si-N system at 1600°K

Since there was no attack of the container by Si, it is assumed that a join exists between $CeSi_2$ and Si_3N_4, so that the reaction

$$\underset{-39.0}{\tfrac{1}{2}\ CeN} + \underset{<-16.6}{1\tfrac{1}{8}\ Si} = \underset{-22.4}{\tfrac{1}{2}\ CeSi_2} + \tfrac{1}{8}\ Si_3N_4$$

can go as written. Assuming $\Delta S^\circ_{298} = 0$ for this reaction, ΔH°_{298} of formation of $CeSi_2$ is less than -16.6 kcal/equivalent of Si. These calculations are, of course, provisional.

In the Ti-Si-N_2 system a sample containing 62% Ti and 38% Si reacted with N_2 to give TiN. No other phases were found, indicating a wide homogeneity range for TiN in the ternary system. A sample initially containing 69% Si showed considerable attack of the Mo container yielding TiN plus an unidentified phase.

When a sample containing 33% Zr and 67% Si was heated in N_2 in a Mo crucible it yielded $MoSi_2$, ZrN, $ZrSi_2$, plus weak unidentified lines. Crucible attack would be expected since $ZrSi_2$ was previously found to be unstable in the presence of Mo. When Zr metal was heated with excess Si_3N_4 in a ZrO_2 container in the presence of N_2 at 2100°K, an unidentified hexagonal (a = 7.603 ± 0.008 A, c = 2.906 ± 0.003 A) phase of strong intensity appeared along with Si metal.

M_1-M_2-Si Systems

In the M_1-M_2-Si systems it is difficult to obtain thermodynamic data from the phases observed because of extended solid solubilities in these systems. Nevertheless some useful data were obtained. The main region studied was that of low Si content. A summary of the heatings is given in Table V.

$TaSi_{0.6}$ and Ta_2Si were found to be stable in the presence of Mo, as was Ta_2Si in the presence of W.

A join was found to exist between Ta_2Si and Ti_5Si_3. The lattice constants of Ti_5Si_3 were expanded, indicating a solubility of Ta in Ti_5Si_3.

Mo reduces $TiSi_2$ to Ti_5Si_3 which is believed to be stable in the presence of Mo. It is believed that a join exists between Ti_5Si_3 and $MoSi_2$.

Mo_3Si was found to be stable in the presence of W with no apparent change in lattice constants of either phase.

A join exists between Zr_5Si_3 and Nb. Nb_5Si_3 and Zr_5Si_3 appear to be completely soluble in each other. X-ray analysis of the region showed a phase of the Mn_5Si_3 structure with lattice constants intermediate between Nb_5Si_3 and Zr_5Si_3.

The relative stabilities of the silicides may be summarized as follows: Ti_5Si_3, $TaSi_{0.6}$, Ta_5Si, $TaSi_{0.2}$ > Mo_3Si > $WSi_{0.7}$; Zr_5Si_3, Zr_2Si, Zr_4Si > $NbSi_{0.55}$.

Discussion of Results

The results of this investigation have been combined with available data in the literature and summarized as ternary phase diagrams given in Fig. 1 to 8, and summarized in terms of heats of formation of the various phases studied in Table III. These heats are consistent with the observations and, through thermodynamic calculations, may be used to reproduce the observations of this work as well as to predict the behavior of these materials under conditions not yet studied. Except for the Mo-Si-C diagram, the positions of the liquidus surfaces are not indicated and only the composition triangles are presented to indicate the phases at equilibrium with one another.

It is of interest to note that in the ternary systems involving carbon, no binary metal silicides were found to be stable in the presence of carbon, although one ternary compound Mo_4CSi_3 was stable in the presence of carbon. This is in contrast to the results presented by Brewer and Haraldsen (44) for the metal-carbon-boron systems where many borides are stable in the presence of carbon. Fig. 8 represents the Ta-Si-N system at 1600°K and shows that none of the silicides of tantalum is stable in the presence of nitrogen at this temperature, but a ternary Ta-Si-N compound is stable. However, at high temperatures, $TaSi_2$ does become stable in the presence of nitrogen and the solid solution range of the ternary compound becomes greatly reduced and might even disproportionate completely.

One of the purposes of this investigation, as well as that of the corresponding study of borides (44), was to obtain enough data to compare the bond strengths of these compounds with those of the carbides, nitrides, etc., of the transition metals. It was hoped that these data would yield some insight into the nature of the bonding and allow prediction of the stability of compounds for which no data exist. Bonding energies of the refractory compounds were calculated in the following way. The heats of formation (45) of the compounds from the elements at 298°K were combined with the heats of sublimation or dissociation to the gaseous atoms at 298°K to obtain the heats for the reaction MX(s) = M(g) + X(g). This heat which is needed to produce two gram-atoms of monatomic gaseous products from a mole of the solid MX compound is a measure of the bonding strengths and is referred to as the bonding energy. Evaluation of this quantity for borides, carbides, silicides, nitrides, oxides, sulfides, and halides was carried out for the MX compounds of the transition metals of the fourth row or period of the periodic table from calcium through the iron group metals and for the transition metals of the fifth and sixth rows from stron-

TABLE V. M_1-M_2-Si *systems*

Atomic % M_1	Atomic % M_2	Atomic % Si	Atomic % O	Temp (°K)	Description of sample	Phases observed
40.3-Ti	39.1-Zr	7.1	12.5	2071	Partially fused	? m.
34.0-Ti	32.7-Zr	22.8	10.5	1995	Partially fused	$(Ti, Zr)_5Si_3$ m. + ? v.w.
51.0-Ti	15.5-Ta	31.1	2.4	2142	Partially fused	$(Ti, Ta)_5Si_3$ s.
30.6-Ti	30.9-Ta	37.0	1.5	2071	Partially fused	Ti_5Si_3 s. + Ta_2Si m. + ? v.w.
29.4-Ti	53.5-Mo	15.6	1.5	1920	Sintered	Mo_3Si s. + Mo s. + ? v.w.
27.4-Ti	18.9-Mo	52.3	1.4	1920	Sintered	Ti_5Si_3 m.s. + $(Ti, Mo)Si_2$ m.
33.9-Zr	35.3-Nb	21.5	9.3	1995	Sintered	Zr_5Si_3 m. + Nb w.
29.7-Zr	31.1-Nb	31.2	8.0	2071	Partially fused	$(Nb, Zr)_5Si_3$ m. + Nb m.
26.4-Zr	27.7-Nb	38.9	7.0	2071	Sintered	ZrSi m.s. + ? m.
26.0-Zr	27.9-Ta	39.0	7.1	2071	Partially fused	Ta_2Si m.s. + Ta m. + ? m.
37.5-Zr	39.2-Mo	13.2	10.1	1995	Sintered	(Mo, Zr) m. + ? w.
33.5-Zr	34.6-Mo	23.0	8.9	2142	Sintered	(Mo, Zr) s. + ? m.
7.7-Ce	77.0-Ta	15.3		1920	Sintered	Ta_2Si m. + CeO_2 w. + ? v.w.
37.8-Nb	39.7-Mo	22.5		1995	Sintered	Mo_3Si s. + Mo_3Si_2 w.
29.2-Nb	29.4-Mo	41.4		2071	Sintered	(Mo, Nb) s. + ? m.
38.2-Nb	38.6-W	23.2		1995	Sintered	W s. + $WSi_{0.7}$ m.
45.0-Ta	45.9-Mo	9.1		1983	Sintered	(Mo, Ta) m.s. + Ta_2Si m.
41.1-Ta	41.2-Mo	17.7		2142	Well-sintered	Ta_2Si m.s. + (Mo, Ta) m. + ? v.w.
38.4-Ta	38.4-Mo	23.2		2142	Well-sintered	(Mo, Ta) s. + $(Mo, Ta)Si_{0.6}$ m.s.
44.25-Ta	46.75-W	9.0		1983	Sintered	W m.s. + Ta_2Si w. + ? v.w.
41.2-Ta	42.1-W	16.7		2142	Slightly sintered	W s. + (W, Ta) s. + Ta_2Si m.s.
33.2-Ta	33.2-W	33.6		2071	Well-sintered	W s. + $WSi_{0.7}$ m. + Ta_2Si w.
41.7-Mo	43.7-W	14.6		1983	Sintered	Mo_3Si s. + W m.

tium and barium through the platinum group metals. Where the MX compounds were thermodynamically unstable with respect to disproportionation or decomposition to other compounds, an upper limit was set to the stability of the MX compound. The conclusions that can be drawn from the examination of the bonding energies of the refractory compounds will be briefly reviewed.

Data were incomplete for some of the rows, but sufficient data were available to show that the bonding energy varies greatly with the metal within a row. For every type of compound a sharp maximum in bonding energy is found in the middle of the row with the bonding energy falling off rapidly to either side. To illustrate the behavior, curves are shown in Fig. 9 for the bonding energies of the carbides of the fourth row together with the bonding energies of the corresponding pure metals phase for comparison and for the bonding energies of the nitrides of the sixth row together with the energies for the metals of the same row. Complete data and other plots are given by Krikorian (45). To put the bonding energies of the refractory compounds and of the metals on the same basis, bonding energies of the metals are given as twice the heats of sublimation; so that two gram-atoms of gaseous products are formed in all cases.

Plots of bonding energy for the various refractory compounds were remarkably similar. For the oxides and nitrides, a maximum was found in the compounds of the fourth group of the periodic table in all three rows. Thus the compounds of Ti, Zr, and Hf have higher bonding energies than compounds of any other metals in the corresponding rows. When the compounds of maximum bonding energies are compared, the nitrides are found to be about 10 kcal higher than the oxides and the carbides about 20 kcal higher than the nitrides. Although TiC has a higher bonding energy than any other carbide of the fourth row, the maximum for the bonding energies of the carbides of the fifth and sixth rows occurs in the fifth group with Nb and Ta. Silicide bonding energies are about 50 kcal lower than those of the corresponding carbides, with the borides intermediate between the carbides and silicides.

There are several striking characteristics of the plots of bonding energies. One thing is that the bonding energies of these refractory compounds are close to and even greater than the values for the metals. Although the maximum bonding energy is found in the fourth group with nonmetals containing many valence electrons, the maximum shifts to the fifth group as the number of valence electrons of the nonmetal decreases and, finally, for the pure metals the maximum shifts over more to the right reaching the sixth group metal tungsten in the sixth row of the periodic table. It is striking that the maxima for the metals occur in that region of the periodic table where the maximum number of unpaired *d* electrons is found. The shift of the maximum to the left in the periodic table as nonmetals with increasing numbers of valence electrons are added seems to indicate that the nonmetals contribute electrons to the metallic bonding. Thus the optimum number of unpaired electrons occurs in a group with less valence electrons when nonmetals are added. An especially striking observation is that the bonding energies of the metals and refractory compounds all increase as the size

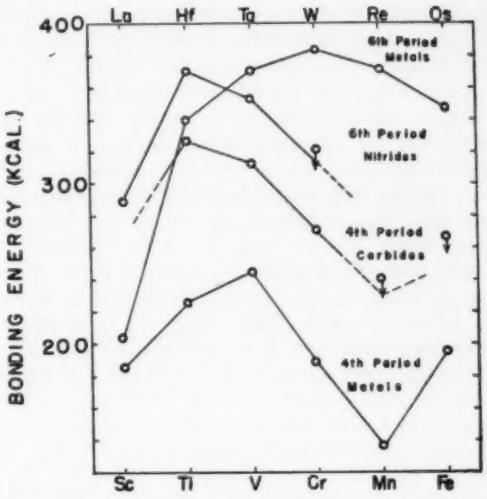

FIG. 9. Typical curves of bonding energies of metals and metallic type compounds in the fourth and sixth periods of the Periodic Table.

of the elements is increased from the fourth row to the sixth row. This is unusual, since bonding energies usually decrease in any series where the sizes of the bonding elements are increased. The close similarity of the bonding energy curves indicates that the type of bonding is similar in all the MX compounds from borides to oxides as well as in the pure metals for the transition elements. Similar calculations of bonding energies were carried out for some compounds of formula MX_2. Oxides show a maximum in bonding energy at the fourth group with a rapid drop as one moves to the right in the periodic table.

All of the plots of bonding energy for the compounds and pure metals of the fourth row showed a maximum at titanium or vanadium and a minimum at manganese. This is very suggestive as the bonding energies of the halides (46) of the dipositive oxidation state of these elements as well as the hydration energies (47–49) of the dipositive ions of these elements show a similar behavior and this has been attributed to stabilization of the ions in the electric field of the crystal by splitting the degeneracy of the free ion electron levels (46–48, 50). Thus, in the presence of the electric field of a crystal, dipositive manganese ion with a half-filled *d* electron shell retains spherical symmetry; whereas, other transition metal dipositive ions of the fourth row become asymmetric and highly polarized in the field and accommodate themselves to a lattice with a higher bonding energy than obtainable with the spherical ion. Splitting of *d* electron levels may occur for the divalent ions on either side of Mn^{+2} in the periodic table, and leads to stabilization due to lowering of the ground state energy of the ion. Mn^{+2} cannot partake in this stabilization due to nondegeneracy of its ground state.

The observation of a minimum in the bonding energies of the metals and refractory compounds at manganese suggests that a bonding model involving positive ions, i.e., metal atoms with *d* electron configurations the same as those of the dipositive ions, might be fruitful for further investigation. The possibility of accounting for the varia-

tion of the bonding energies of the refractory compounds of the transition elements by an ionic model was considered. A simple ionic model with only simple coulombic interactions that does not take into account polarizability is a good approximation for compounds like the alkali halides and the alkaline earth oxides. Such a model is quite unsatisfactory for the refractory compounds of the transition elements, since the effect of the strong force fields upon the *d* electron orbitals and other polarizability effects should be very large for these compounds. At present, these effects cannot be estimated, but it is hoped that absorption spectra and other similar measurements will be carried out for these compounds in an effort to gain further insight into the nature of their bonding.

From the practical point of view, immediate application of the plots of bonding energies can be made. From the rather similar behavior of the plots for the various compounds, it is possible to fill in missing values. In this way, one can estimate heats of formation of compounds for which values are not yet available. These estimated values are, of course, rather uncertain, but they can be of value. The following ΔH^0_{298} of formation values were estimated: $\frac{1}{2}$ $TiSi_2$, -28 ± 5; TiSi, -48 ± 10; $\frac{1}{3}$ Ti_5Si_3, -75 ± 20; $\frac{1}{3}$ Nb_5Si_3, -52 ± 20; $\frac{1}{2}$ $TaSi_2$, -25 ± 8; $\frac{5}{3}$ $TaSi_{0.6}$, -53 ± 20; $\frac{1}{2}$ WSi_2, -13 ± 5; and $\frac{10}{7}$ $WSi_{0.7}$, -18 ± 5 kcal.

Acknowledgment

The x-ray diffraction films were prepared by Mrs. Helena Ruben and interpreted by Mrs. Carol Dauben. The authors would like to express their appreciation for this help which was essential for this work. The authors would also like to thank Dr. John Conway for spectroanalyses.

This work was performed under the auspices of the U. S. Atomic Energy Commission.

Manuscript received January 31, 1955. This paper was prepared for delivery before the Wrightsville Beach Meeting, September 13 to 16, 1953, and was abstracted from the thesis of Oscar Krikorian in partial fulfillment of the Ph.D. degree in chemistry at the University of California.

Any discussion of this paper will appear in a Discussion Section to be published in the December 1956 JOURNAL.

REFERENCES

1. A. W. Searcy and R. A. McNees, Jr., *J. Am. Chem. Soc.*, **75**, 1578 (1953).
2. L. Brewer, L. A. Bromley, P. W. Gilles, and N. L. Lofgren, Declassified Atomic Energy Commission Report MDDC-367, August 4, 1945.
3. D. H. Templeton and C. H. Dauben, paper in preparation.
4. E. S. Bumps, H. D. Kessler, and M. Hansen, *Trans. Am. Soc. Metals*, **45**, 1008 (1953).
5. L. Brewer, A. W. Searcy, D. H. Templeton, and C. H. Dauben, *J. Am. Ceram. Soc.*, **33**, 291 (1950).
6. H. Nowotny, H. Schachner, R. Kieffer, and F. Benesovsky, *Monatsh. Chem.*, **84**, 1 (1953).
7. P. Pietrokowsky and P. Duwez, *J. Metals*, **3**, No. 9, 772 (1951).
8. M. Hansen, H. D. Kessler, and D. J. McPherson, *Trans. Am. Soc. Metals*, **44**, 518 (1951).
9. C. E. Lundin, D. J. McPherson, and M. Hansen, *ibid.*, Preprint No. 41 (1952).
10. H. Schachner, H. Nowotny, and R. Machenschalk, *Monatsh. Chem.*, **84**, 677 (1953); *see* also, R. Kieffer, F. Benesovsky, and R. Machenschalk, *Z. Metallkunde*, **45**, 493 (1954).
11. P. Pietrokowsky, Private communication.
12. W. H. Zachariasen, *Acta Cryst.*, **2**, 94 (1949).
13. R. F. Domagala, D. J. McPherson, and M. Hansen, "The Zirconium-Oxygen System," Armour Research Foundation of Illinois Institute of Technology, Report No. 4, Summary (COO-181), March 31, 1953.
14. G. L. Humphrey, S. S. Todd, J. P. Coughlin, and E. G. King, U. S. Bureau of Mines Report of Investigations 4888, July 1952.
15. K. K. Kelley, U. S. Bur. Mines Bull. No. 477 (1950).
16. W. M. Latimer, "The Oxidation States of the Elements and Their Potentials in Aqueous Solutions," 2nd ed., Prentice-Hall Inc., New York (1952).
17. G. L. Humphrey, *J. Am. Chem. Soc.*, **73**, 2261 (1951).
18. G. L. Humphrey, *ibid.*, **76**, 978 (1954).
19. G. Huff, E. Squitieri, and P. Snyder, *J. Am. Chem. Soc.*, **70**, 3380 (1948).
20. L. C. Browning and P. H. Emmett, *ibid.*, **74**, 4773 (1952).
21. K. K. Kelley, U. S. Bur. Mines Bull. No. 476 (1949).
22. F. D. Rossini, D. D. Wagman, W. H. Evans, S. Levine, and I. Jaffe, U. S. Bureau of Standards Circular 500 (1952).
23. R. Kieffer and E. Cerwenka, *Z. Metallkunde*, **43**, 101 (1952).
24. J. L. Ham and A. J. Herzig, Second Annual Report to Office of Naval Research, Misc-1951-132 (Climax Molybdenum Company of Michigan, 1951).
25. W. P. Sykes, K. R. Van Horn, and C. M. Tucker, *Am. Inst. Mining Met. Engr.*, Techn. Publ. No. 647 (1935).
26. C. Agte and H. Alterthum, *Z. Techn. Physik*, **11**, 182 (1930).
27. H. Nowotny, E. Parthé, R. Kieffer, and F. Benesovsky, *Monatsh. Chem.*, **85**, 255 (1954).
28. G. Brauer, H. Renner, and J. Weinet, *Z. anorg. u. allgem. Chem.*, **277**, 249 (1955).
29. J. S. Umanski, *Zhur. Fiz. Chim.*, **14**, 332 (1940).
30. G. F. Hardy and J. K. Hulm, *Phys. Rev.*, **93**, 1004 (1954).
31. C. H. Dauben, Private communication.
32. A. W. Searcy and A. G. Tharp, Private communications.
33. L. Brewer, *Chem. Rev.*, **52**, 1 (1953).
34. L. Brewer, National Nuclear Energy Series, Vol. 19B, Paper 3, L. L. Quill, Editor, McGraw-Hill Book Co., New York (1950).
35. L. Brewer, L. A. Bromley, P. W. Gilles, and N. L. Lofgren, *ibid.*, Paper 4.
36. N. Schönberg, *Acta Chem. Scand.*, **8** [No. 2], 199 (1954).
37. B. Neumann, C. Kröger, and H. Kunz, *Z. anorg. u. allgem. Chem.*, **218**, 379 (1934).
38. R. E. Slade and G. I. Higson, *Chem. News*, **108**, 166 (1913).
39. R. Kieffer, F. Benesovsky, H. Nowotny, and H. Schachner, *Z. Metallkunde*, **44**, 242 (1953).
40. R. Kieffer, F. Benesovsky, and E. Gallistl, *Z. Metallkunde*, **43**, 284 (1952).
41. R. E. Honig, *J. Chem. Phys.*, **22**, 1610 (1954).
42. R. F. Barrow and H. C. Rowlinson, *Proc. Roy. Soc. A*, **224**, 374 (1954).
43. D. J. McPherson, Private communication.
44. L. Brewer and H. Haraldsen, *This Journal*, **102**, 399 (1955).
45. O. Krikorian, Ph.D. Thesis, University of California (1955).
46. Z. Z. Hugus, Jr., Unpublished work.
47. O. Holmes, Ph.D. Thesis, University of California (1955).
48. L. E. Orgel, *J. Chem. Soc.*, **1952**, 4756.
49. D. S. McClure and R. E. Connick, Private communications.

50. J. H. van Santen and J. S. van Wieringen, *Rec. Trav. Chim.*, **71**, 420 (1952).
51. K. K. Kelley, Unpublished work.
52. C. H. Dauben, C. E. Meyers, D. H. Templeton, and A. W. Searcy, paper presented at the Amer. Cryst. Assoc. Meeting, Pasadena, Calif., June 27, 1955.

The Fracture of Brittle Chromium by Acid Etching

W. H. Smith

Research Laboratory, General Electric Company, Schenectady, New York

ABSTRACT

A mechanism is presented to explain the formation of transcrystalline cleavage cracks during the etching of brittle annealed chromium. The mechanism proposed is the formation of a face-centered-cubic chromium hydride on the surface which, due to its larger volume, initiates cracks in the brittle material beneath. These cracks may then propagate by a stress corrosion mechanism. Room temperature ductile material appears to be capable of taking up this volume expansion without cracks being initiated. X-ray data confirm the existence of the face-centered-cubic hydride.

Introduction

For many metals it has been found that embrittlement occurs because of hydrogen pick-up during etching (1). Two types of embrittlement are observed, one associated with the formation of a brittle hydride, and the other occurring as a result of solution of hydrogen in the metal, as in iron. In the first case, the formation of the hydride results in a lattice expansion which ruptures the brittle hydride. The source of brittleness in the second case is not completely understood. A number of theories have been proposed to explain the hydrogen embrittlement of iron and related materials, but none is entirely satisfactory.

Little information is available regarding the changes in mechanical properties brought about by hydrogen in chromium. The solubility of hydrogen in solid chromium is very small (2, 3), appreciably less than the solubility of hydrogen in iron or nickel. This small amount of hydrogen in solution appears to have very little effect on the mechanical properties of the metal; however, no detailed study has been made over a wide temperature range. Snavely in 1947 (4) confirmed the existence of face-centered-cubic and hexagonal-close-packed hydrides of chromium and described their properties, stabilities, and lattice structures.

Within the past few years it has also been established that room temperature brittle cold-worked chromium can often be made ductile by etching away the surface, either anodically in a bath consisting of 64% orthophosphoric acid, 15% sulfuric acid, balance water, or chemically in a hydrochloric acid solution (5–7). Experiments confirming this behavior have been performed here. No embrittling effect due to hydrogen occlusion in cold-worked chromium during acid etching has been observed. The most detailed analysis of this phenomenon has been made by Wain and Henderson (6). Their results showed conclusively that the etching process removed the badly nitrided surface layers formed during fabrication.

Room temperature brittleness of chromium has been shown to be due to the presence of nitrogen and possibly carbon as impurities (6, 8). It has been fairly well established that about 0.005 wt % nitrogen renders annealed chromium brittle at room temperature, while a nitrogen content above 0.02 wt % will render wrought chromium brittle. The critical limit for carbon is believed to be around 0.01%.

No information has been presented on the effects observed when annealed chromium of low and high nitrogen contents is etched in acid. Marked physical and mechanical changes have been found to occur when high-nitrogen-content, annealed chromium is etched in hydrochloric acid. This paper presents a description of the changes observed, along with evidence supporting the belief that they are brought about by the formation of face-centered-cubic chromium hydride.

Observations

In marked contrast to the behavior of cold-worked chromium, very severe transcrystalline cracking occurs when brittle annealed chromium (nitrogen content > 0.005%) is etched in hydrochloric acid (Fig. 1). Chromium which is ductile as annealed (nitrogen content < 0.005%) does not exhibit any tendency toward crack formation on etching (Fig. 2). If the etching of brittle annealed chromium is done anodically, and hence with no hydrogen evolution at the surface of the specimen, cracks are not observed (Fig. 3). In Fig. 4, a micrograph of the brittle annealed chromium before etching is presented. It can be seen that cracks are not present. Dye check of the specimen also failed to reveal any cracks.

Since etching cracks were formed in material which had been given a very thorough anneal, 24 hr at 1300°C in a dry hydrogen atmosphere and furnace cooled, it appeared unlikely that residual stresses in the material could account for the behavior. From these observations it

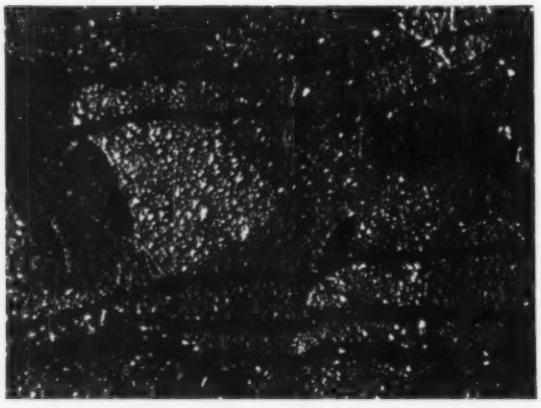

FIG. 1. Annealed chromium containing 0.022 wt % nitrogen, etched in HCl, showing transcrystalline cracks. ×22.

FIG. 2. Annealed chromium containing <0.005 wt % nitrogen, etched in HCl. No cracks are developed. ×22.

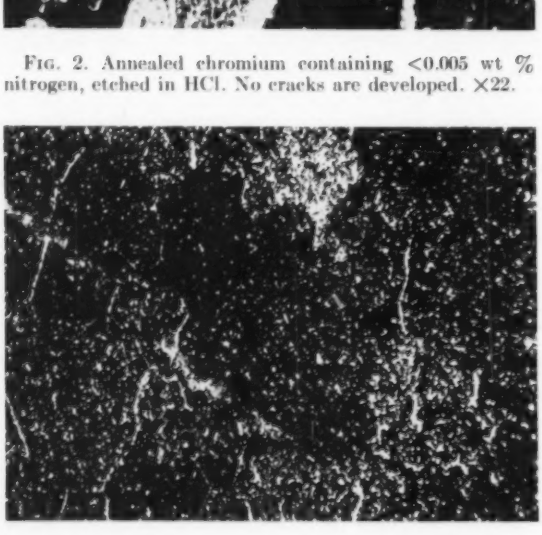

FIG. 3. Annealed chromium containing 0.022 wt % nitrogen, etched anodically. No cracks are developed. ×22.

seemed probable that cracks developed during etching were related to the liberation of hydrogen at the surface of the specimen. To establish the role of hydrogen more firmly, an annealed specimen containing 0.022% nitrogen

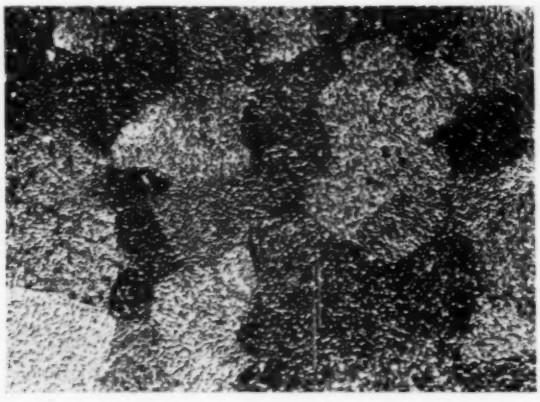

FIG. 4. Annealed chromium containing 0.022 wt % nitrogen, unetched. ×22.

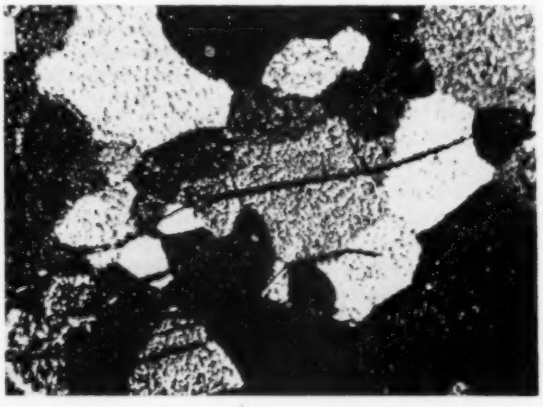

FIG. 5. Annealed chromium containing 0.022 wt % nitrogen made the cathode in an H_2SO_4 solution. Transcrystalline cracks developed. ×22.

was made the cathode in a sulfuric acid solution and a voltage applied to the cell, using a platinum anode. Rapid evolution of hydrogen was allowed to occur, and in a relatively short time transcrystalline cracks were developed (Fig. 5).

MECHANISM OF CRACK FORMATION

From the foregoing it appears that the following facts must be accounted for in any proposed mechanism of crack formation:

1. Evolution of hydrogen must occur at the chromium surface.
2. The chromium must be brittle, i.e., high in nitrogen (or possibly carbon) and in the annealed condition.
3. Annealing in a hydrogen atmosphere does not produce cracks.

Since the mechanism sought was one of initiating cracks in brittle material, it appeared that the idea of a hydride formation might account for the observed phenomena. Snavely (4) was able to show that both face-centered-cubic and hexagonal-close-packed chromium hydrides are formed during the electrodeposition of chromium from chromic

acid solutions. Chromium-hydrogen combinations in the formular range of from CrH to CrH_2 gave face-centered-cubic structures with the chromium atoms at the normal corner and face-centered-cubic positions. Hydrogen atoms occupy from one-half to all of the second-largest interstitial openings, the former giving a zinc-blend type of structure, the latter a fluorite structure. Metal-hydrogen ratios in the range Cr_2H to CrH crystallize in the hexagonal-close-packed arrangement. Hydrogen atoms again occupy the second-largest interstices, giving a lattice similar to an incomplete or complete wurtzite structure. Unfortunately, the hydrogen atoms do not produce x-ray diffraction lines and their positions can only be determined by deduction. It is now possible by neutron diffraction methods to check these proposed positions. Prior to the work of Snavely, it was generally believed that the face-centered-cubic and hexagonal-close-packed structures were allotropic modifications of chromium.

The lattice dimensions of the hexagonal-close-packed hydride of chromium are given as $a = 2.71(7)$ Å and $c = 4.41(8)$ Å; the face-centered-cubic hydride has an $a_o = 3.85$ Å. Snavely also demonstrated that these hydrides are relatively unstable at room temperature and revert quickly to normal body-centered-cubic structure by the evolution of hydrogen. He also showed that a volume expansion of about 16.4% could be expected in converting the metal to the face-centered-cubic hydride and a 15.6% expansion in going to the hexagonal-close-packed hydride. This would give linear expansions of about 5.5%.

To determine whether or not hydrides were being formed during acid etching, the following experiments were performed. A specimen of brittle annealed chromium containing 0.022% nitrogen and 0.0002% hydrogen was obtained. Dye check failed to reveal any surface cracks and x-ray diffraction patterns showed only normal body-centered-cubic chromium lines with an $a_o = 2.886$ Å (Handbook value 2.885 Å). Cracks were developed in this material by etching in (1:1) hydrochloric acid. Following the etch the specimen was immediately quenched in liquid nitrogen. An x-ray diffraction pattern obtained on this sample revealed body-centered-cubic lines with an $a_o = 2.885$ Å and a face-centered-cubic structure with an $a_o = 3.86$ Å. Comparison of the face-centered-cubic values with Snavely's pattern for face-centered-cubic chromium hydride showed excellent agreement. Nitrogen gas cooled by passing through liquid nitrogen was blown across the specimen while the x-ray diffraction pattern was being obtained. It is estimated that the specimen temperature never exceeded −100°C. On allowing this sample to stand at room temperature for eight hours and rerunning the diffraction pattern, it was found that only chromium lines were obtained. This confirms Snavely's remarks regarding the instability of the hydride. These particular experiments were repeated several times with the same results. No evidence for the formation of hexagonal hydride was obtained.

Patterns of face-centered-cubic chromium hydride were found in all cases in which the samples were etched in acid with the evolution of hydrogen or when the piece was made the cathode in an acid cell. A pattern for Cr_2O_3 was obtained when chromium was made anodic.

With identification of the hydride, it was possible to propose a mechanism for crack development in brittle annealed chromium. Since a volume expansion accompanies the formation of the hydride, it would be expected that brittle material might be stressed to the point where the fracture stress is exceeded and cracks could be initiated. The propagation of the cracks could then occur by a stress corrosion mechanism. Room temperature ductile material would be able to take up the linear expansion plastically, or crack propagation by a stress corrosion mechanism might not occur.

X-ray analysis of the crack orientation revealed that fracture was occurring on the (100) cleavage planes.

Acknowledgment

The author is indebted to Mrs. A. Cooper, who obtained the x-ray data presented. Helpful discussions with Dr. J. R. Low, Jr., H. C. Rogers, and Dr. A. U. Seybolt and many other members of the Metallurgy and Ceramics Research Department are also acknowledged.

Manuscript received July 28, 1955.
Any discussion of this paper will appear in a Discussion Section to be published in the December 1956 Journal.

REFERENCES

1. D. P. Smith, "Hydrogen in Metals," University of Chicago Press, Chicago (1948).
2. A. Sieverts and A. Gotta, *Z. anorg. u. allgem. Chem.*, **172,** 1 (1928).
3. L. Luckemeyer-Hasse and H. Schenak, *Arch. Eisenhüttenw.*, **6,** 209 (1932).
4. C. A. Snavely, *Trans. Electrochem. Soc.*, **92,** 537 (1947).
5. W. J. Kroll, *Metal Ind.*, **85,** 345 (1954).
6. H. L. Wain, F. Henderson, and S. T. M. Johnstone, *J. Inst. Metals*, **83,** 133 (1954).
7. H. Johansen and G. Asai, *This Journal*, **101,** 604 (1954).
8. W. H. Smith and A. U. Seybolt, Unpublished research.

Temperature Dependence of Hardness of the Equi-Atomic Iron Group Aluminides

J. H. Westbrook

Research Laboratory, General Electric Company, Schenectady, New York

ABSTRACT

A series of iron group aluminides, a typical group of intermetallic compounds, were prepared by arc melting and their hardness studied as a function of temperature and composition using a modified Bergh instrument. FeAl-, CoAl-, and NiAl-based materials were studied up to 800°C and over the entire homogeneity range of each compound. The results appear to be related to the defect structure in such materials.

Introduction

As a part of a general investigation of the strength of solids as a function of temperature, it was decided to study the temperature dependence of hardness of a group of intermetallic compounds. The literature on the mechanical properties of intermetallic compounds has been reviewed recently in some detail (1), and it will suffice here to state only the principal conclusions. While most compounds are hard and brittle at ordinary temperatures, all become at least somewhat ductile if the temperature is raised sufficiently. The homologous temperature[1] at which ductility becomes apparent is about the same for many compounds in a given test, but may vary widely with the type of test used. Few satisfying correlations have been established between fundamental parameters and the mechanical properties of intermetallic compounds or the temperature dependence thereof. The melting point, crystal structure, interatomic bond type, ionic charge, polarization parameters, atom size, and presence of ordering have been indicated to be important factors, but the details of their effects and possible interactions are not yet understood.

In selecting a particular group of compounds for study, it was thought wise to choose a group in which at least some of the above factors could be held constant. It was also considered helpful for this group to have a fairly rich literature covering the pertinent phase diagrams, physical properties, etc. Further, it was desirable that the group comprise compounds in which there is some practical interest. Such considerations led to the selection of the equi-atomic iron group aluminides—FeAl, CoAl, and NiAl.

The nickel aluminide has been of interest as a deleterious second phase in certain high temperature alloys and cermets (2–4), as a binder for a TiC base cermet (5), and recently has even been proposed as a base for high temperature materials (6–9). All three compounds, CoAl, FeAl, and NiAl, and certain of their binary and ternary combinations are important constituents in the class of permanent magnet alloys known as "alnico's" (10).

Probably as a result of these manifold practical interests, the literature on this triad of compounds is unusually rich. Their phase diagrams have been determined, crystal structures are known, diffusion rates and certain chemical properties measured, bond type established, atomic arrangements studied in exquisite detail by Bradley's group in England, and many other physical properties measured—electrical resistance, magnetic properties, thermal expansion, etc. Specific references to this literature are made later in connection with the results of the present investigation.

The triad of aluminides have in common a number of those factors which have been thought to be important in controlling the mechanical properties of intermetallic compounds. They are all Hume-Rothery phases or electron compounds and hence have essentially the same type of interatomic bonds. All have the ordered BCC or CsCl structure and are supposed to maintain this structure from room temperature up to the melting point.[2] NiAl and CoAl both form congruently from their melts at about 1650°C and thus have melting points in excess of those of both the component elements. FeAl has a considerably lower melting point than the other compounds, about 1270°C. The phase diagrams (11) for the three systems are shown in Fig. 1. Those for the nickel and cobalt systems are very similar. The current phase diagram for the Fe-Al system is somewhat different and shows FeAl as forming continuously from the alpha solid solution. It should be noted, however, that considerable uncertainty exists in the portion of the diagram near FeAl; the diagram as drawn is not compatible with modern views on the order-disorder transformation (12). All three compounds exist over rather wide ranges of composition which include the stoichiometric value. Finally, as shown in Table I, the the atomic parameters of all three transition elements are very similar but in distinct contrast to those of aluminum. Thus, the equi-atomic iron group aluminides appeared to be an excellent base for the proposed study.

Experiment

Preparation of Samples

Because of the refractory nature of the compounds, conventional melting methods were not convenient for the preparation of the alloys to be tested. Therefore, resort was made to arc melting. For this purpose a small multiple

[1] The homologous temperature is the ratio of the test temperature to the melting point when expressed in absolute degrees, $T_h = T/T^{mp}$ (°K).

[2] Recent work indicates that FeAl may disorder below its melting point. See further discussion in a later section of this paper.

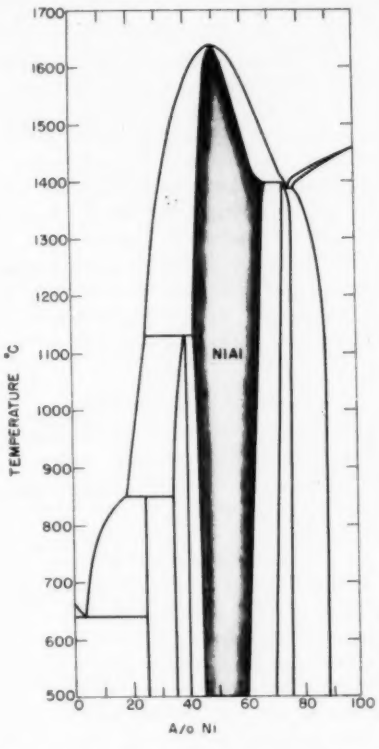

FIG. 1a. Phase diagram of the Ni-Al system

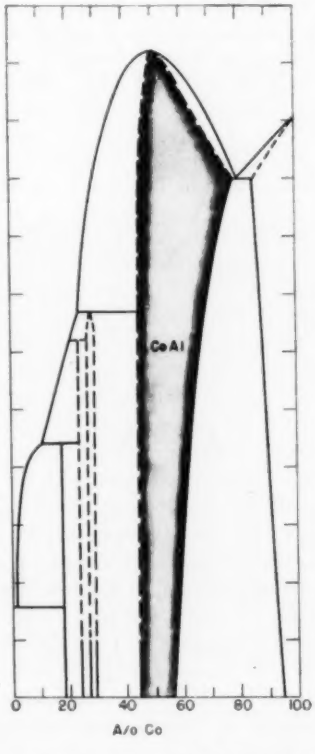

FIG. 1b. Phase diagram of Co-Al system

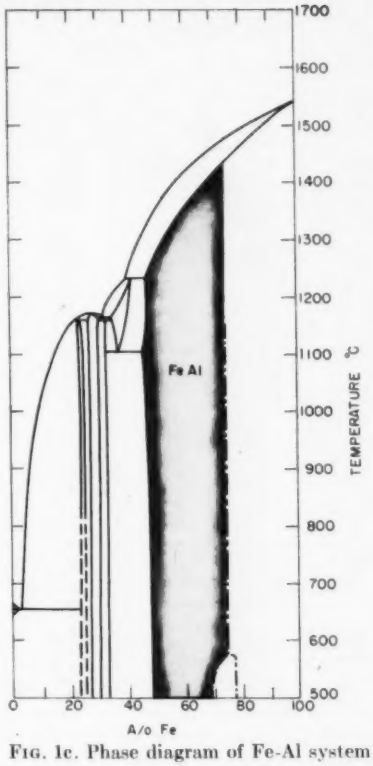

FIG. 1c. Phase diagram of Fe-Al system

TABLE I. *Some physical and chemical properties of iron, cobalt, nickel, and aluminum**

Element	Electron structure				Atomic radii Å	Standard electrode potential E_0 volts	Work of cohesion kcal/mole	Compressibility $\times 10^7$ kg/cm	Sat. Mom. β at 0°K
	3s	3p	3d	4s					
Iron	2	6	6	2	1.24	0.441	94	5.9	2.22
Cobalt	2	6	7	2	1.25	0.278	85	5.3	1.71
Nickel	2	6	8	2	1.24	0.231	85	5.4	0.61
Aluminum	2	1	0	0	1.43	1.70	55	13.7	—

* Except for aluminum, data were taken from a similar table published by Zackay (13).

hearth button furnace previously developed in this laboratory (14) was found to be quite suitable. This furnace utilized a water-cooled copper crucible and an argon atmosphere. Provision is made for electromagnetic rotation of the arc to ensure uniform melting.

The metals used for making up the alloys were as follows:

	Form	Source	Nominal purity %
Nickel	Pellets	Whitehead Metal Products	99.8
Cobalt	Rondelles	African Metals Corp.	99.4
Iron	Electrolytic plast iron	National Radiator Co.	99.95
Aluminum	Pig, swaged to $\frac{1}{8}$-in. rod and cut up	Aluminum Co. of America	99.99

TABLE II. *Nominal or intended composition*

Alloy No.	Atomic %				Weight %				Remarks
	Ni	Fe	Co	Al	Ni	Fe	Co	Al	
5815-9-25	45	—	—	55	64.0	—	—	36.0	Two phase
5815-22-1	45.4	—	—	54.6	64.7	—	—	35.3	
5815-22-37	46	—	—	54	65.0	—	—	35.0	
5815-21-34	47	—	—	53	65.8	—	—	34.2	
5815-22-38	48	—	—	52	66.8	—	—	33.2	
5815-7-2	49	—	—	51	67.6	—	—	32.4	
1459A	50	—	—	50	68.6	—	—	31.4	
1629C	50	—	—	50	68.6	—	—	31.4	Single phase
5815-16-6	51	—	—	49	69.4	—	—	30.6	
1702B	52	—	—	48	70.2	—	—	29.8	
5815-7-15	54	—	—	46	71.9	—	—	28.1	
5815-7-14	56	—	—	44	73.4	—	—	26.6	
1703B	58	—	—	42	75.1	—	—	24.9	
5815-16-4	61	—	—	39	77.3	—	—	22.7	
1843B	—	48	—	52	—	65.5	—	34.5	Two phase
5815-7-1	—	49	—	51	—	66.4	—	33.6	At phase boundary
1457A	—	50	—	50	—	67.4	—	32.6	
1844B	—	53	—	47	—	70.0	—	30.0	
5815-16-5	—	58	—	42	—	74.1	—	25.9	Single phase
1845B	—	63	—	37	—	78.0	—	22.0	
1922B	—	—	48	52	—	—	67.0	33.0	At phase boundary
5815-21-35	—	—	49	51	—	—	67.7	32.3	
1759B	—	—	50	50	—	—	68.6	31.4	
1852C	—	—	52	48	—	—	70.6	29.4	Single phase
1851C	—	—	54	46	—	—	72.6	27.4	
1860B	16.6	16.7	16.7	50	23.1	21.9	23.2	31.8	
1861B	—	25.0	25.0	50	—	33.1	34.9	32.0	
1862B	25.0	—	25.0	50	34.2	—	34.4	31.4	Single phase
1863B	25.0	25.0	—	50	34.9	33.1	—	32.0	

Table II lists all of the compositions melted. Previous experience had indicated that little loss would be experienced on melting, so the weighed amounts charged into the furnace corresponded exactly to the intended compositions. Checks were made of the resulting composition of several representative arc-melted buttons by wet analysis. Results are compared with the intended compositions in Table III. The differences are seen to be negligible, as had been expected; intended compositions are therefore used throughout the balance of this report. Little difficulty was experienced in the melting operation itself except for the susceptibility of the buttons of some compositions, particularly the alloys containing cobalt, to crack badly because of the unavoidably high thermal stresses induced on cooling.

TABLE III. *Intended composition*

Alloy No.	Atomic %	Weight %	Analyzed composition weight %
1457A	50.0 Fe	67.4	67.0
	50.0 Al	32.6	33.1
1759B	50.0 Co	68.6	68.8
	50.0 Al	31.4	31.1
1629C	50.0 Ni	68.6	67.8
	50.0 Al	31.4	31.4
1459A	50.0 Ni	68.6	68.4
	50.0 Al	31.4	31.5
1702B	52.0 Ni	70.2	70.4
	48.0 Al	29.8	29.3
1703B	58.0 Ni	75.1	74.8
	42.0 Al	24.9	24.8

Many of the buttons after arc melting were found by metallographic examination to be homogenous, single-phase, rather coarse grained materials. Any specimens not showing good homogeneity in either macro or micro examination were given a subsequent homogenization anneal at a temperature about 250°C below their melting points. Such treatment was usually successful, but, as indicated in Table II, certain of the compositions near the published phase boundaries apparently are two-phase in the equilibrium condition. This result is a consequence of the poor definition of phase boundaries in the existing literature. General dispersion of the second phase was found to raise hardness values significantly. On the other hand, if the second phase were restricted to grain boundaries, hardness values obtained for indentations falling within the grains apparently could be taken as truly representative of the saturated phase.

After the homogeneity of a particular button had been established, it was prepared as a hardness specimen. In some cases it was possible to grind the requisite disk-shaped samples (approximately $\frac{3}{16}$-in. thick by $\frac{3}{4}$ in. in diameter) directly from the buttons. In many other cases, however, where the thermal stress cracking mentioned above was severe, it was impossible to obtain pieces of sufficient size to yield the disk-shaped samples. In these instances it was found convenient to mount irregularly shaped fragments in copper by melting the copper in situ about the fragment held in an iron tube. Times at temperature were kept very short, and careful metallographic examination showed no significant amount of diffusion between the mounting

metal and the sample. Specimens so mounted were then surface ground on the faces on the disk.

All samples were given a metallographic polish prior to hardness testing. Metallographic preparation of these samples presented a curious anomaly. Despite their rather high hardness, which necessitated the use of diamond polishing techniques, the surface of the specimens flowed quite easily. This unfortunate situation has been noted previously in the literature in another connection (7, 15). It was necessary, therefore, to polish and etch repeatedly in order to secure an apparently undisturbed surface. Some experiments were done with electropolishing to avoid this tedious method of preparation, but only limited success was obtained and the technique was abandoned.

Experimental Procedure

Hardness values were obtained on the samples over the temperature range from room temperature to 800°C using a micro hot hardness tester of modified Bergh design (16, 17). Load is applied hydraulically by moving the specimen on an anvil against a fixed indenter; specimen and indenter are heated by a resistance furnace, and all components of the tester are enclosed within a large evacuated chamber. The sample was heated continuously during a test run and hardness impressions and thermocouple readings made at desired intervals. Preliminary experiments disclosed that the hardness of the aluminide specimens was independent of load from about 50 to 1000 grams. Most of the data herein reported were obtained at 200-grams load; a Vickers diamond indenter and a 15-sec load duration were used throughout the study. Measurement of the size of indentations was made at room temperature and the data expressed in the conventional Vickers fashion in terms of the impressed load divided by the contact area of the indentation in units of kilograms per square millimeter. The various precautions usual in microhardness testing were observed.

A portion of a typical hardness run is illustrated in Fig. 2. The small loads used and the coarse grain size of

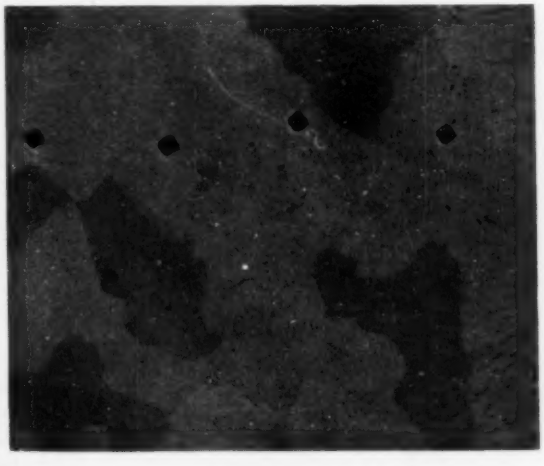

FIG. 2. Portion of a typical hardness-temperature run. 50×

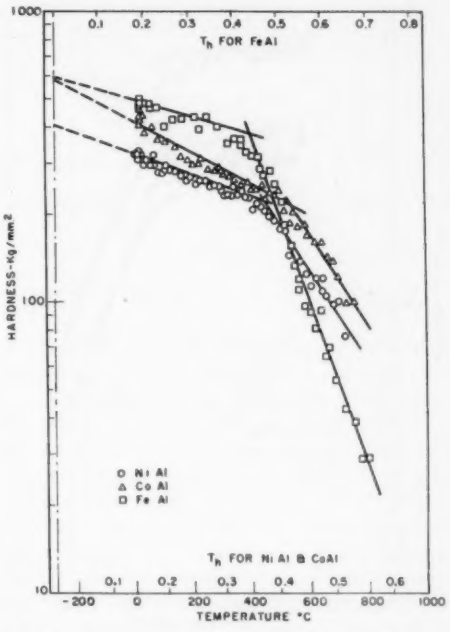

FIG. 3. Temperature dependence of hardness of the three equi-atomic iron group aluminides at the stoichiometric composition.

the specimens resulted in effect in a single crystal measurements. No significant effects of anisotropy were observed, however. Preliminary experiments established the reproducibility of duplicate runs on the same sample as well as on duplicate samples. Annealing following polishing was

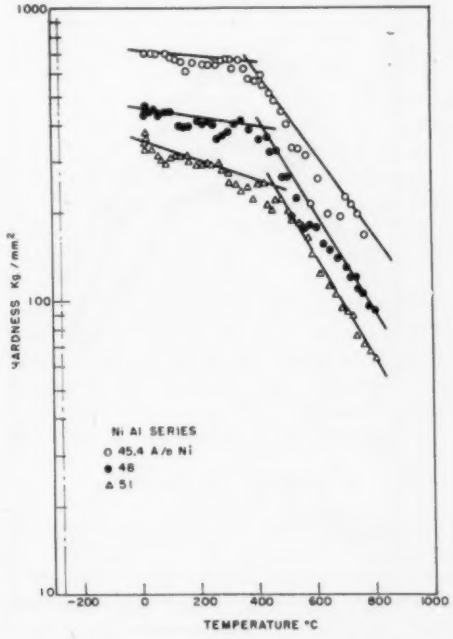

FIG. 4. Temperature dependence of hardness of some NiAl compositions.

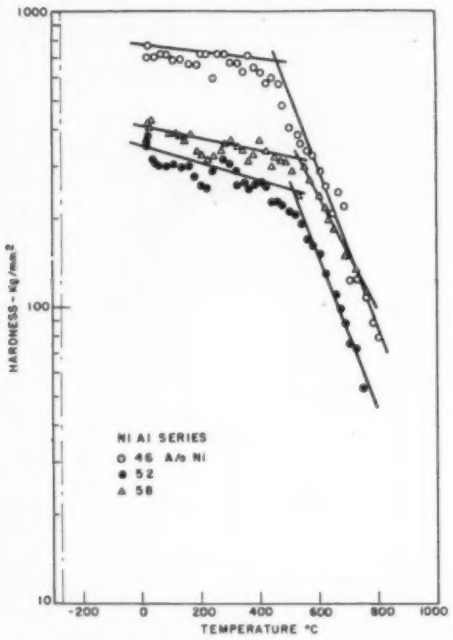

FIG. 5. Temperature dependence of hardness of some NiAl compositions.

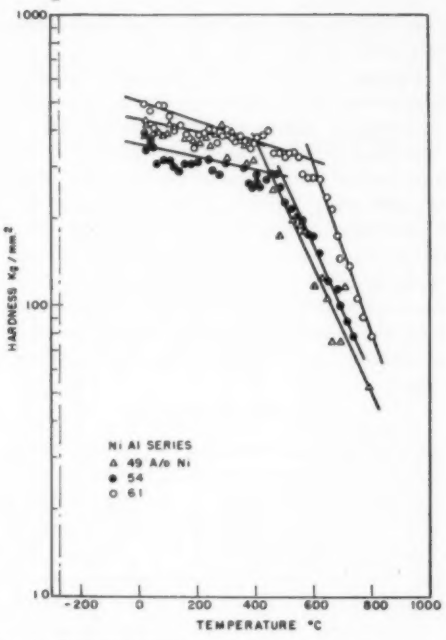

FIG. 7. Temperature dependence of hardness of some NiAl compositions.

frequently required to eliminate surface work hardening from the polishing operation.

Treatment of Data

Assessment of the possible scatter as well as subsequent detailed analyses of the data were facilitated by the use of a semilogarithmic method of plot. This procedure, in which the logarithm of hardness is plotted against temperature, has been demonstrated (17, 18) to yield a two-segmented linear plot for a wide variety of materials. This result implies a hardness-temperature relation of the sort $H = Ae^{-BT}$, where A and B have one set of values at low temperatures and another set at high temperatures.

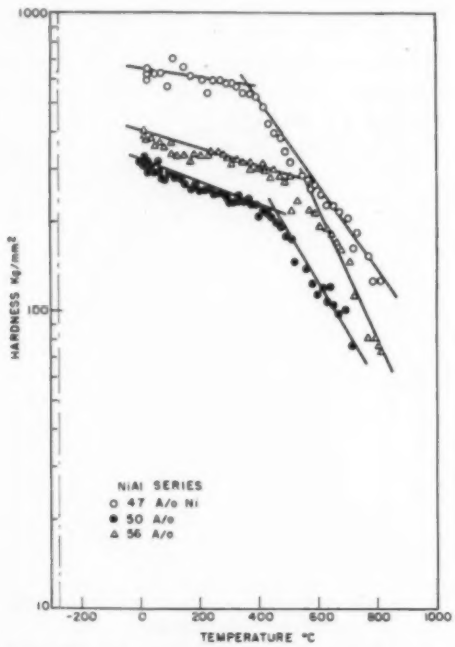

FIG. 6. Temperature dependence of hardness of some NiAl compositions.

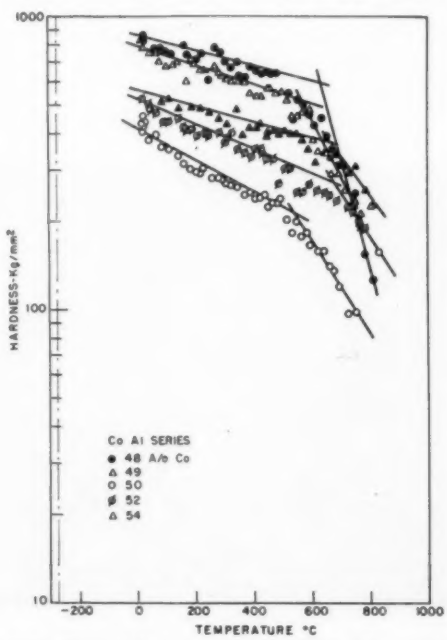

FIG. 8. Temperature dependence of hardness of some CoAl compositions.

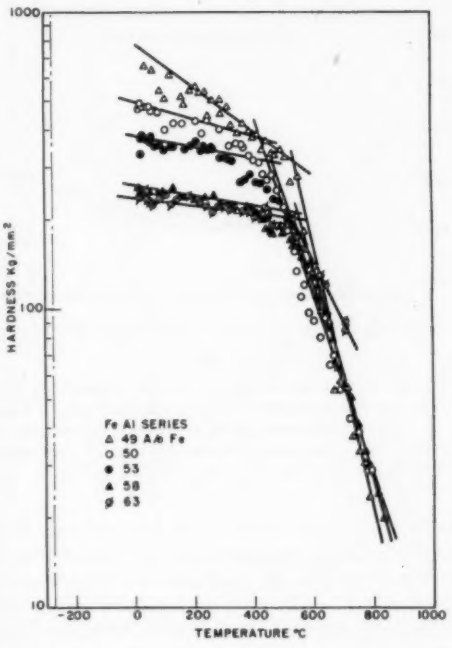

FIG. 9. Temperature dependence of hardness of some FeAl compositions.

Occasional points were found in hot hardness runs on the aluminides which deviated considerably from the normal scatter band. In almost every case these deviations could be associated with excessive cracking or with the presence of an inclusion, grain boundary, or other incidental defect in the material. Therefore, such points were not considered valid and have been eliminated from the plots shown in the figures. The usual procedure was to take 30 to 50 points over the 800°C temperature range, to plot all points for which visually acceptable impressions were obtained, and to represent the data by the best linear plot approximating the upper envelope of the scatter band. This procedure is in accord with the view of Winchell (19) in analyzing the results of room temperature microhardness tests on brittle materials.

The principal experimental results are shown in Fig. 3 through 9. Fig. 3 compares the three equi-atomic aluminides at the stoichiometric composition, i.e., 50 at. % aluminum. Fig. 4 to 7 show data for various compositions within the phase limits of the NiAl structure, while Fig. 8 and 9 represent similar studies on CoAl- and FeAl-based alloys, respectively.

DISCUSSION

Stoichiometric Compounds

As indicated above, a convenient method of analyzing hardness-temperature data is in terms of the constants describing the straight line segments of the semilogarithmic plot of the data. Table IV presents a comparison of such data for the low temperature branch of the stoichiometric aluminide curves with similar data for hypothetical pure metals of equivalent melting point derived from curves

TABLE IV

	A (kg/mm²)	$B \times 10^3$(°C⁻¹)	$T_b(T_h)$	T_{mp}(°C)
NiAl	410	0.863	0.38	1640*
CoAl	580	1.209	0.44	1625*
FeAl	600	0.663	0.46	1270*
Hypothetical pure metal	140	0.60	0.55	1630†
Hypothetical pure metal	100	1.00	0.55	1270†

* This study.
† Interpolation from (18).

of a previous study (18). Data are also listed for T_b, the break temperature or the temperature at which the change in slope occurs expressed as a homologous temperature.

Several important differences can be noted relative to the behavior of pure metals. First, the intrinsic hardness as given by the constant A is several times that for typical pure metals. This is not too surprising, however, considering the greater complexity of the cesium chloride structure as compared to those for the common metals. The slope or temperature coefficient B appears to be about the same as for the metals. On the other hand, break temperature data are rather unusual. Not only are all of the aluminide break temperatures significantly lower on the homologous scale than for the pure metals, but also the value for NiAl is even lower than those for FeAl and CoAl. It is also apparent from the tabulation that no correlation exists between A and B values and the melting points of the compounds, in contrast to the case of the isomorphous pure metals (18). Several other types of correlation were attempted without success. Therefore, it is already obvious that the behavior of these materials is both considerably different and more complex than for the pure metals.

The rather low hardness of NiAl at high temperatures is also worthy of note, particularly since this compound has been considered as a base for high temperature materials. Stern (6) and later his associate, Wachtell (7), reported good high temperature strengths for NiAl, but the hardness data of the present study as well as tensile experiments by McMullin (20) at this laboratory and by Maxwell and Grala (9) at NACA fail to confirm these results. It appears that the major reason for the difference in the behavior of the material produced by Stern and Wachtell at the American Electro Metallurgical Co. and that produced at this laboratory and at NACA lies in the fact that the former was hot pressed from powder, whereas the NiAl in the latter studies was prepared by melting. Oxide or other impurities introduced in powder processing have been known in other instances to result in substantial strengthening particularly at high temperatures (21, 22).

Effects of Composition

Effects of composition variation on the hardness of the single-phase aluminides observed in this study can be demonstrated in two ways, either through study of hardness-composition isotherms or by analysis of the effects of composition on the parameters A, B, and T_b. The first of these approaches was applied to the NiAl based compositions by cross plotting the data of Fig. 4 through 7. Results

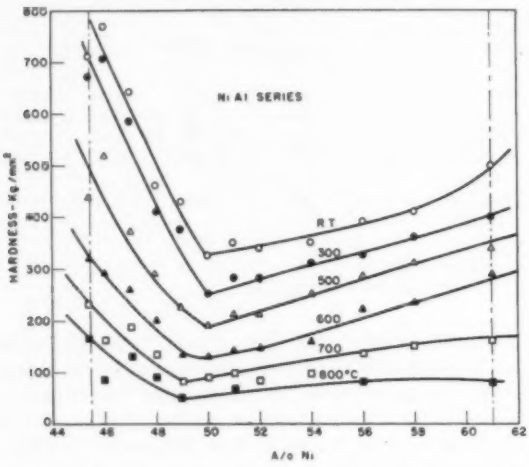

FIG. 10. Hardness-composition isotherms in the NiAl series.

of this cross-plot are shown in Fig. 10 and may be compared with atomic structure data derived from the work of Bradley and Taylor (23) in Fig. 11. The hardness minima exhibited at the stoichiometric composition are the most striking feature of the plot and correspond to the minimum density of defects as shown in Fig. 11.

Minima such as shown in Fig. 10 have been noted many times before for intermetallic compounds having a range of homogeneity, principally by the Russian group at the Leningrad Polytechnic Institute (24), but in only a few instances (25, 26) have temperatures other than room temperature been investigated. Furthermore, in these previous cases, only a very limited number of compositions was studied, and structural data for corresponding alloys were not available. In the cases cited, the Russians also observed the flattening of the minimum as the temperature is increased. The hardness increase on both sides of stoichiometry is of particular interest in the case of the nickel-aluminum system since it indicates that vacancies can be at least as potent a strengthening element as the substitution of solute atoms. Minima in the electrical resistivity (27) and in the diffusion of Co^{60} (28) at stoichiometry have also been noted. Both of these latter effects are not unexpected since the most perfectly ordered structure obviously exists at the stoichiometric composition. Diffusion data show that the deformation process is not diffusion-controlled within the temperature range studied (maximum homologous temperature $\sim$ 0.55). However, the flattening of the hardness minima with increasing temperature may be indicative of a trend in this direction. Possibly at some higher temperature or longer time the hardness-composition curves might invert to show maxima at stoichiometry as suggested by Kornilov (26).

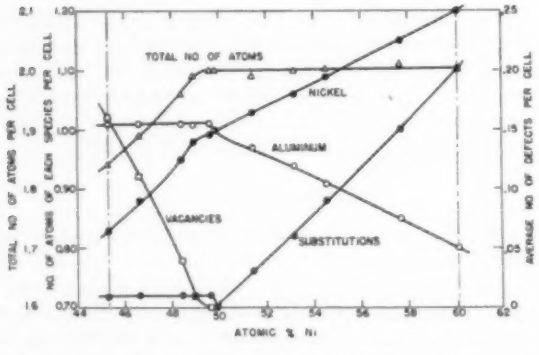

FIG. 11. Defect structure as a function of composition in NiAl (from Bradley and Taylor).

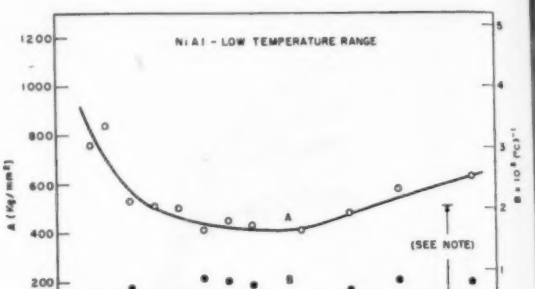

FIG. 12. Variation of the hardness parameters A and B for the low-temperature region as a function of composition in NiAl. (The arrow denotes the breadth of the scatter band for the B values for pure metals of corresponding melting point as previously determined.) (18)

Analysis of the constants A and B describing the linear segments of hardness-temperature curves was also made for the NiAl based compositions. The effect of composition on these constants for the low temperature segment is shown in Fig. 12. It is apparent that the primary effect of composition is on A, the intrinsic hardness of the materials; variations observed in the temperature dependence or B values are thought to be within the scatter of the data. Similar results were obtained for the high temperature segment except that the scatter was considerably greater.

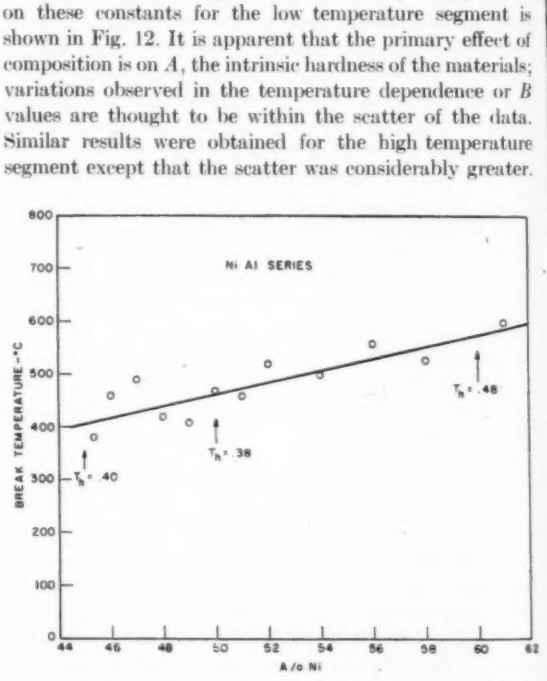

FIG. 13. Variation of break temperature with composition in the NiAl series.

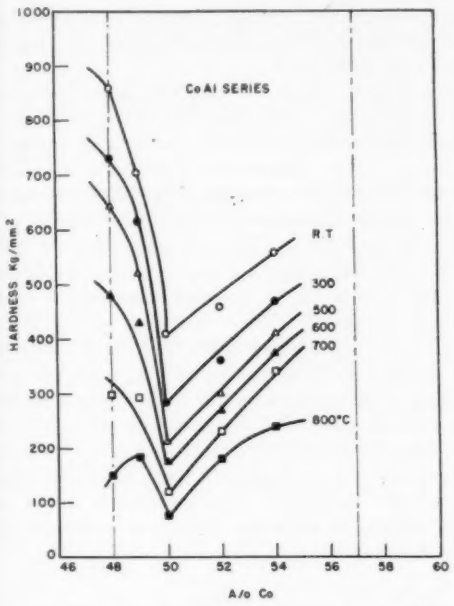

FIG. 14. Hardness-composition isotherms in the CoAl series.

Another, and perhaps more interesting, aspect of these results is presented in Fig. 13, which shows that there is a progressive increase in the break temperature with increasing nickel content over the whole composition range. This is rather surprising in view of the facts that the melting point, resistivity, lattice spacing, and diffusion constants show either maxima or minima at the stoichiometric composition. A possible interpretation of the behavior shown in Fig. 13 is that the compound becomes increasingly metallic with increasing nickel content.

The first few experiments on the cobalt aluminides gave results very similar to those for the nickel aluminides and consequently the CoAl-based compositions were not studied in great detail. A cross plot of the hardness isotherms is shown in Fig. 14. The similarity of the CoAl series with the NiAl group was perhaps to be expected in view of the marked similarity in the phase diagrams.

TABLE V

Property	NiAl	CoAl	FeAl
T_{mp} °C	1640 (13)	1625 (13)	1270 (13)
a_o Å	2.887 (23)	2.862 (29)	2.910 (30)
kx	2.881 (23)	2.856 (29)	2.903 (30)
% Contraction in atomic vol	15.3 (31)	15.8 (32)	13 (33)
ΔHf kcal/g atom	17.0 (34)	13.2 (34) 16 (35)	6.1 (34)
δ g/cc	5.92 (23)	6.08 (29)	5.59 (30)
$D_{Co^{60}}$ cm²/sec	0.2×10^{10} at 1150°C (36)	2.8×10^{10} at 1250°C (37)	
ρ μΩ cm	14.9 (27) 20–30 (7)		
$\frac{\partial \rho}{\partial T}$ μΩ cm/°C	0.0023 (27)		
α in./in./°C	15.1×10^{-6} (7)		

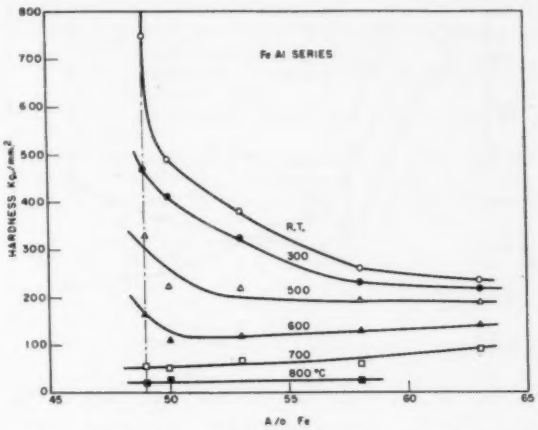

FIG. 15. Hardness-composition isotherms in the FeAl series.

Furthermore, x-ray studies by Bradley and Seager (29) show the defect structure to be of the vacancy type on the high aluminum side and substitutional on the high cobalt side, as in the case of NiAl. Further evidence of the close similarity of the NiAl and CoAl compounds is given by the comparison of property data in Table V. In view of the limited number of hardness data obtained and the close similarity with the nickel aluminides, no further analyses were carried out.

Iron-aluminides gave results which contrast sharply with those on the CoAl- and NiAl-based compositions. The cross plot of the hardness isotherms is given in Fig. 15. No sharp minimum is present at any temperature. At low temperatures hardness seems to decrease monotonically with increasing iron content. At the highest temperature used in the experiments there is no clear-cut effect of composition. These results may be compared with those of the x-ray structure studies by Bradley and Jay (30) replotted in Fig. 16. In contrast to the situation with NiAl and CoAl, no vacancy formation occurs on the high aluminum side; defects are substitutional on both sides of stoichiometry. Unlike the other two members of the triad, however, substitution of the iron group atoms at normal aluminum sites in FeAl lowers the hardness. This result is

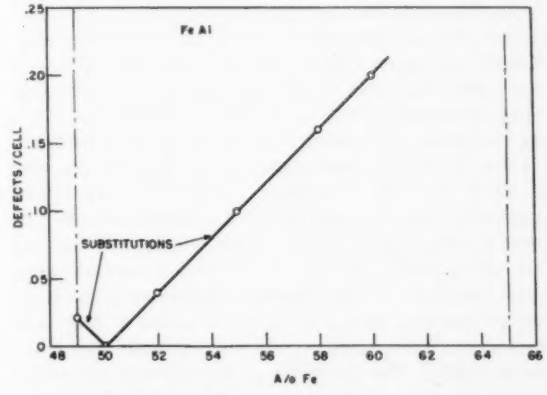

FIG. 16. Defect structure as a function of composition in FeAl (from Bradley and Jay).

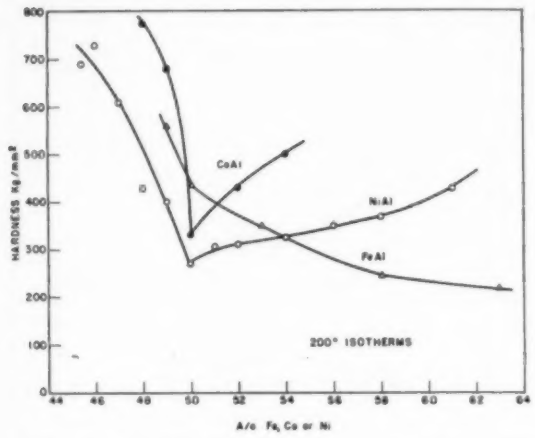

FIG. 17. Comparative hardness-composition isotherms for the three equi-atomic iron group aluminides.

most clearly illustrated in Fig. 17, which compares the 200°C isotherms for all three series. In addition, certain regular but not reproducible anomalies were sometimes encountered in the log hardness-temperature curves for FeAl compositions above about 700°C. No ready explanation for either of these effects is apparent. It is clear, however, from the phase diagram and the property data of Table V that the compound is considerably different from the other two, although it is isomorphous with them. It has been noted that the high temperature portion of the Fe-Al phase diagram as shown in Fig. 1 is rather uncertain in the vicinity of the compound FeAl. It is quite possible that a redetermination of this portion of the diagram might show a situation which would render the present hardness results more explicable (see further below).

Effects of Temperature on Degree of Order

It was thought at one time that perhaps some of the anomalies observed in the hardness data might result from a considerable decrease in the degree of order at a temperature within the range studied, although the phase diagrams represent all the aluminides as essentially completely ordered up to the melting point.

The literature shows several x-ray studies on NiAl conducted both at temperature and on quenched specimens. Results are contradictory. Isaichev and Mirekskii (38) claim that significant disordering and vacancy formation occur at temperatures as low as 900°C, although the ordering reaction is virtually insuppressible by quenching. Guseva (27) on the other hand finds no change in ordering at 900°C and only a negligible difference in the lattice parameter between quenched and annealed samples. In view of these contradictions, it was decided to test for disordering tendencies by an alternative method—electrical resistivity. A flat horseshoe-shaped strip specimen was ground from part of an annealed button of NiAl and its resistivity measured in the conventional manner to above 1200°C. The resistivity of the material was found to increase smoothly and not excessively over the entire temperature range. It is therefore unlikely that significant disordering takes place in NiAl within this temperature range, although the possibility cannot be dismissed that a resistance change below the sensitivity of the experiment occurs with disordering.

As indicated above, the published phase diagram as well as the present experimental results render the Fe-Al high temperature equilibria particularly suspect. In particular, in view of the shape of the solidus and liquidus curves it seems quite possible that the compound disorders before melting. Unfortunately, no further studies of this portion of the diagram have been made since the work of Bradley and Jay (30) over twenty years ago, and this extended to only 700°C. However, some results recently obtained by Bradley (39) on a section of the Fe-Ni-Al ternary led him to suspect that a different and more complex situation exists in the Fe-Al binary than had been indicated by his previous work. As a consequence of the anomalies encountered in the present study, some survey experiments have been initiated to re-examine this suspect portion of the binary diagram. Of these, only the resistance-temperature studies are complete as yet. Inconclusive results, similar to those for NiAl, were obtained. Other studies are in progress.

SUMMARY

This investigation has established that the temperature dependence of hardness of the equi-atomic iron group aluminides does not follow the empirical rules found previously to hold for the pure metals. The intrinsic hardness of the aluminides is considerably higher than would be expected for a pure metal of equivalent melting point, although the slope of the log hardness temperature curve is of the same order for both types of material. In addition, the change in slope of the log hardness temperature plot occurs at a lower homologous temperature for the aluminides than for the pure metals. Within the homogeneity range of any particular compound, hardness is controlled by the defect structure. For NiAl and CoAl, hardness minima are observed at the stoichiometric composition which flatten with increasing temperature. Knowledge of the details of the defect structure permits the further conclusion that either vacancies or substitutional defects can harden the material. Within the temperature range studied ($<0.55\ T_{mp}$) short-time hardness is not diffusion-controlled. The FeAl compounds are anomalous in that hardness at constant temperature decreases with increasing iron content on both sides of stoichiometry. This anomaly and the failure to obtain a satisfactory correlation for the relative hardness of the three stoichiometric aluminides indicates that factors other than those now known—melting point, crystal structure, and defect structure—are significant in the control of strength of pure intermetallic compounds. The possibility of significant disordering with increasing temperature was considered for certain compounds. No evidence was found for this in stoichiometric NiAl up to above 1250°C; it appears likely, however, that stoichiometric FeAl disorders between 700° and 1250°C.

ACKNOWLEDGMENTS

The assistance and advice of many members of the Metallurgy Research Department of the General Electric Research Laboratory aided materially in this research.

Mr. Arthur Peat contributed in a major way to all of the experimental phases of the work. The chemical analyses were made by Ledoux and Co., and the resistivity determinations on NiAl and FeAl by T. S. Jones. J. E. Burke, R. W. Guard, and W. R. Hibbard read and criticized the manuscript.

Manuscript received August 1, 1955. This paper was prepared for delivery before the Chicago Meeting, May 2 to 6, 1954.

Any discussion of this paper will appear in a Discussion Section to be published in the December 1956 JOURNAL.

REFERENCES

1. J. H. WESTBROOK, Report in preparation.
2. H. V. KINSEY AND M. T. STEWART, *Trans. Am. Soc. Metals*, **43,** 193 (1951).
3. H. V. KINSEY AND M. T. STEWART, *Can. J. Research*, **27,** No. 2-F (1949).
4. E. D. SAYRE, General Electric Report No. R54AGT115, March 1954.
5. C. C. MCBRIDE, H. M. GREENHOUSE, AND T. S. SHEVLIN, *J. Am. Ceram. Soc.*, **35,** 28 (1953).
6. G. STERN, Reported at the 1952 Air Force Conference on Cermets, Wright-Patterson Air Force Base, Oct. 6–8, 1952.
7. R. L. WACHTELL, Wright Air Development Center Report No. 52-291, Sept. 1953.
8. J. G. MCMULLIN, Unpublished research.
9. W. A. MAXWELL AND E. M. GRALA, NACA Tech. Note No. 3259, August 1954.
10. R. M. BOZORTH, "Ferromagnetism," Van Nostrand Co. Inc., New York (1951).
11. ASM Metals Handbook, 1948 Edition.
12. F. N. RHINES AND J. B. NEWKIRK, *Trans. Am. Soc. Metals*, **45,** 1029 (1953).
13. V. F. ZACKAY AND T. H. HAZLETT, *Acta Met.*, **1,** 624 (1953).
14. P. C. ROSSIN, *General Electric Research Lab. Memo*, **7,** 2 (1953).
15. H. V. KINSEY AND M. T. STEWART, Discussion of Ref. (2) p. 225.
16. P. S. BERGH, Tech. Rept. No. M-5, Silver Springs Lab., The Kellex Corp., December 1948.
17. J. H. WESTBROOK, GE Research Lab. Rept. No. RL-1029, February 1954.
18. J. H. WESTBROOK, *Trans. Am. Soc. Metals*, **45,** 221 (1953).
19. H. WINCHELL, *Ann. Mineralogist*, **30,** 583 (1945).
20. J. G. MCMULLIN, Unpublished research.
21. R. IRMANN, "Sintered Aluminum of High Resistance to Heat," *Rev. aluminum*, **28,** 269, 311 (1951).
22. R. IRMANN, *Metallurgia*, **46,** 125 (1953).
23. A. J. BRADLEY AND A. TAYLOR, *Proc. Roy. Soc.*, **A159,** 56 (1937).
24. N. KURNAKOW, S. ZEMCZUZNY, AND M. ZASEDATELEV, *J. Inst. Metals*, **40,** 305 (1916).
25. V. P. SHISHOKIN AND V. A. AGEEVA, *Tsvetnye Metal.*, **2,** 119 (1932).
26. I. I. KORNILOV, *Doklady Akad. Nauk. S. S. S. R.*, **86,** 721 (1952).
27. L. N. GUSEVA, *ibid.*, **77,** 415 (1951).
28. A. E. BERKOWITZ, F. E. JAUMOT, AND F. C. NIX, "Diffusion of Co^{60} in some NiAl Alloys Containing Excess Vacancies," paper presented at Am. Phys. Soc. meeting, March 1954.
29. A. J. BRADLEY AND G. D. SEAGER, *J. Inst. Metals*, **64,** 81 (1939).
30. A. J. BRADLEY AND A. H. JAY, *Proc. Roy. Soc. London*, **A136,** 210 (1937).
31. A. WESTGREN AND A. ALMIN, *Z. phys. Chem.*, **B5,** 14 (1929).
32. E. ZINTL AND G. BRAUER, *Z. physik. Chem.*, **B20,** 245 (1933).
33. W. EKMAN, *ibid.*, **B12,** 57 (1931).
34. W. OELSEN AND H. MIDDEL, *Mitt. Kaiser Wilhelm. Inst. Eisenforsch. Düsseldorf*, **19,** 101 (1937).
35. W. BILTZ, *et al.*, *Z. anorg. u. allgem. Chem.*, **134,** 25 (1924).
36. R. SMOLUCHOWSKI AND H. BURGESS, *Phys. Rev.*, **76,** 309 (1949).
37. F. C. NIX AND F. E. JAUMOT, *ibid.*, **33,** 1275 (1951).
38. I. ISAICHEV AND V. MIREKSKII, *J. Tech. Phys. USSR*, **10,** 316 (1940).
39. A. J. BRADLEY, *J. Iron Steel Inst.*, **163,** 19 (1949).

Mathematical Studies on Galvanic Corrosion

IV. Influence of Electrolyte Thickness on the Potential and Current Distributions over Coplanar Electrodes Using Polarization Parameters

JAMES T. WABER AND BERTHA FAGAN

University of California, Los Alamos Scientific Laboratory, Los Alamos, New Mexico

ABSTRACT

Extensive numerical evaluation was performed on a Fourier series derived for the potential distribution in an electrolyte lying above a plane containing infinitely long, narrow electrodes juxtaposed and arranged in an infinitely alternating array with even symmetry. In contrast to the previous studies in this series, the limitation that the electrolyte has finite depth was imposed. Four perspective drawings of the reduced potential function were made to scale to illustrate the potential variation throughout the solution. From this study a practical rule was established for deciding from the behavior of the electrochemical system what effectively is an "infinite thickness" of the electrolyte. Current density variation over the anode was evaluated for several different combinations of relative thickness b/c and of relative polarization parameter $\mathfrak{P}/c$. When b/c is small, the major part of the corrosion current is concentrated in the vicinity of the anode-cathode junction, provided that the electrical resistance of corrodent is not too high or the polarization too strong, i.e., provided that $\mathfrak{P}$ is relatively small in comparison with c. Several graphs of $C_a^*(x)$ were included to illustrate the effects of the dimensionless groups (a/c), (b/c), and $(\mathfrak{P}/c)$. Comparison with published experimental data was made, and the agreement is reasonably good. Detailed discussion of the influence of several factors is also presented.

INTRODUCTION

In any practical study of galvanic corrosion and of pertinent potential distributions, it is not possible to cover the electrodes with an infinitely thick layer of corrodent. The necessary condition of a finite liquid thickness requires modification of the mathematical analysis. In the cases discussed so far (1-3), it is assumed that a perpendicular erected on the plane of the electrodes lies entirely in the region of consideration and does not intersect a boundary, i.e., the electrolyte depth was assumed to be infinitely larger than the characteristic repeat distance of the alternating array of electrodes.

Experimentally, this condition can be realized only if the galvanic cell behaves "microscopically." As explained earlier (1-3), the absolute dimensions of a galvanic cell have no physical significance, but they must be compared with the size of the polarization parameter. A given electrochemical system behaves as though it were composed of microscopic elements if the critical dimension λ of the system is smaller than the polarization parameter. Such a system is called "microscopic." An important characteristic of such a microscopic system is that the distribution of corrosion attack is relatively uniform over the electrode surface.

In treating the general behavior of corroding metals, it is necessary to consider the dimensionless group $(b/\mathfrak{P}_i)$ where b is the perpendicular thickness or depth of the liquid and $\mathfrak{P}_i$ is the smaller of the two polarization parameters. That is, one should identify b in many cases as λ, as it very strongly affects current distribution over the electrodes.

Whenever $\mathfrak{P}$ is large in relation to the critical dimension, the potential distribution becomes uniform. Given $\mathfrak{P}$, if the width of the anodes, $2a$, is small enough in comparison with b, the depth of the corroding liquid has little if any influence on the potential value measured in the liquid. However, in treating thin or shallow electrolyte layers, b may be smaller than a or $\mathfrak{P}$, and b in these instances is correctly λ. The greatest corrosion attack occurs within a distance a few times larger than b of the anode-cathode junction. There is significantly less attack on the anodes, and less hydrogen evolution on the cathodes elsewhere.

The effect of "truncating" the infinite column of corrodent lying above the electrode plane is the subject of this report. In general, the liquid layer thickness will be similar to or less than the electrode widths. As a qualitative rule useful in designing experiments, the liquid is essentially "infinitely deep" if it is deeper than the sum of anode and cathode widths. Further increase in the depth contributes only 2 or 3% at most to the local corrosion current density.

The effect of very thin liquid films on corrosion is also amenable to the analysis presented here. On the basis of physical reasoning, one might expect that, as the thickness of the liquid becomes smaller than the polarization parameter, the corrosion current, i.e., the attack, would concentrate more toward the anode-cathode junction. Meanwhile, much of the liquid remote from the junction would approach a uniform potential value. This phenomenon would limit the total corrosion current. Decreas-

ing the liquid thickness has a similar effect on the total corrosion (4).

Boundary Conditions

The physical arrangement of electrodes is identical to that employed before (1–3). Coplanar, parallel, juxtaposed electrodes of finite width and great length are alternately arranged in an infinite array of even symmetry. The choice of even symmetry is equivalent to locating insulators at the edges of the cathodes away from the anode-cathode junction, thus limiting attention to one period. Location of the origin is indicated in Fig. 1. The important change in the boundary conditions is the assumption that an insulating plane is located parallel to the plane of the electrodes at a distance b units above. The specific boundary conditions are:

$$\lim_{y \to b} \frac{\partial P^*}{\partial y} = 0 \qquad \text{(I)}$$

$$\left.\frac{\partial P^*}{\partial x}\right|_{x=0} = \left.\frac{\partial P^*}{\partial x}\right|_{x=c} = 0 \qquad \text{(II)}$$

$$P^*(x, 0) - \mathfrak{L} \left.\frac{\partial P^*}{\partial y}\right|_{y=0} = E_a S_a(x) \qquad \text{(III)}$$

where $S_a(x)$ is the step function used previously (1–4), and E_a is the difference in potentials between the anode and cathode extrapolated to zero current flow. A more explicit definition of E_a has been given by Wagner (5). The definition and significance of $\mathfrak{L}$ has been discussed elsewhere (2–5). Since there are no sources or sinks for ions in the liquid phase, the polarized potential $P^*(x, y)$ satisfies Laplace's equation in two dimensions and in general must be real, finite, and continuous except on the boundaries of the liquid. The region under consideration is an infinite slab lying between the planes $x = c, x = -c, y = 0$ and $y = b$. Boundary values of the normal gradient, namely $\partial P^*/\partial y$, are obtained by approaching the boundary along paths lying wholly within the region. Because of the assumed even symmetry, boundary conditions (II) apply to either right or left handed derivatives. In contrast, at $x = a$ the limit approached by $\partial P^*/\partial y$ from the left applies to the anodic section and that approached from the right, to the cathodic section of the boundary. It is important to realize that these two limits differ in sign.

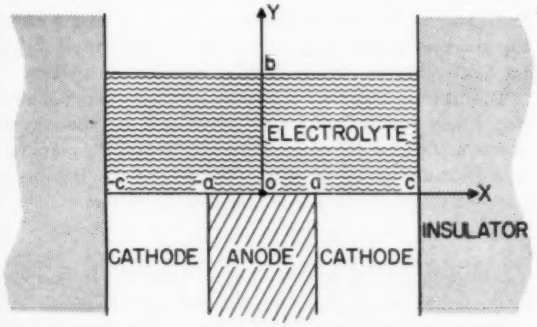

Fig. 1. Geometric relation of the electrodes and the location chosen for the origin.

Inasmuch as the interfacial potential $P^*(x, 0)$ is a periodic function of x, the potential at the interface and in the liquid is expressed by a Fourier series. It has been shown elsewhere (6), that

$$P^*(x,y) = \frac{E_a a}{c} + \frac{2E_a}{\pi} \sum_{n=1}^{\infty} \frac{\sin\left(\frac{n\pi a}{c}\right) \cos\left(\frac{n\pi x}{c}\right) \cosh\left[\frac{n\pi}{c}(b-y)\right]}{n\left[\cosh\left(\frac{n\pi b}{c}\right) + \left(\frac{n\pi\mathfrak{L}}{c}\right) \sinh\left(\frac{n\pi b}{c}\right)\right]} \qquad \text{(IV)}$$

and that P^* satisfies the several conditions imposed on it.

Interfacial Potential

The expression for the potential within the solution can be simplified in the event that $y = 0$:

$$P^*(x, 0) = \frac{E_a a}{c} + \frac{2E_a}{\pi} \sum_{n=1}^{\infty} \frac{\sin\left(\frac{n\pi a}{c}\right) \cos\left(\frac{n\pi x}{c}\right)}{n\left[1 + \left(\frac{n\pi\mathfrak{L}}{c}\right) \tanh\left(\frac{n\pi b}{c}\right)\right]} \qquad \text{(V)}$$

This equation was used to obtain the variation of the interfacial potential over the electrodes, and the variation in current density was obtained therefrom.

Equation (V) involves three adjustable parameters, and complete exploration of their effects would require evaluating this expression 50–100 times over the range of x. To minimize the time taken for computation, only two values of a/c were employed to analyze the effect of liquid thickness.

The values of the interfacial potential are tabulated elsewhere (7) and are graphically summarized for two cases in Fig. 2 and 3. When b/c is small, the curve of the interfacial potential approaches the ideal step function $S_a(x)$ despite the relatively large polarization parameter. As the ratio (b/c) becomes equal to the ratio (a/c), the full effect of polarization takes force.

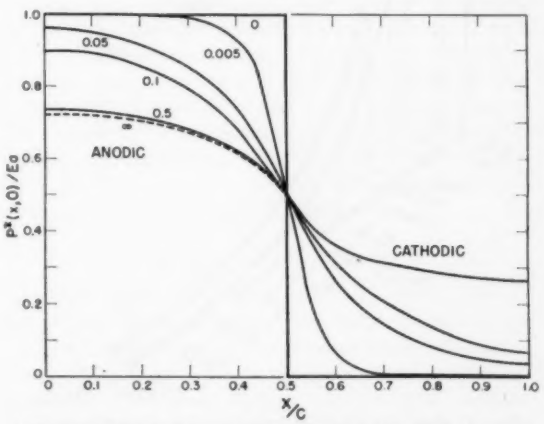

Fig. 2. Interfacial potential evaluated for $a/c = \frac{1}{4}$, $a/\mathfrak{L} = 1$, and for the b/c ratios 0.005, 0.05, 0.1, 0.5, and ∞.

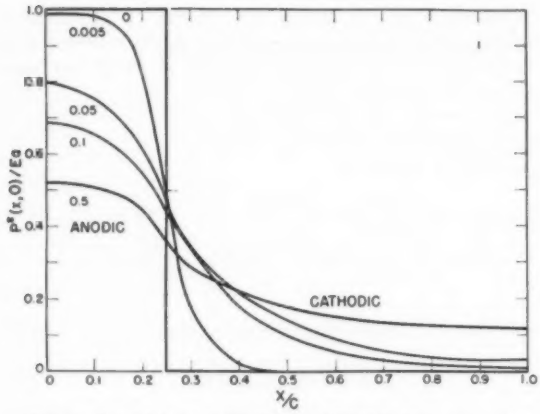

FIG. 3. Interfacial potential evaluated for $a/c = \frac{1}{4}$, $a/\mathfrak{L} = 1$, and for the b/c ratios 0.005, 0.05, 0.1, and 0.5.

Potential at the Outer Liquid Boundary

The expression used for series evaluation of the potential at the outer boundary of liquid was

$$P^*(x, b) = \frac{E_a\, a}{c} + \frac{2E_a}{\pi} \sum_{n=1}^{\infty} \frac{\sin\left(\frac{n\pi a}{c}\right) \cos\left(\frac{n\pi x}{c}\right)}{n\left[\cosh\left(\frac{n\pi b}{c}\right) + \left(\frac{n\pi \mathfrak{L}}{c}\right) \sinh\left(\frac{n\pi b}{c}\right)\right]} \qquad \text{(VI)}$$

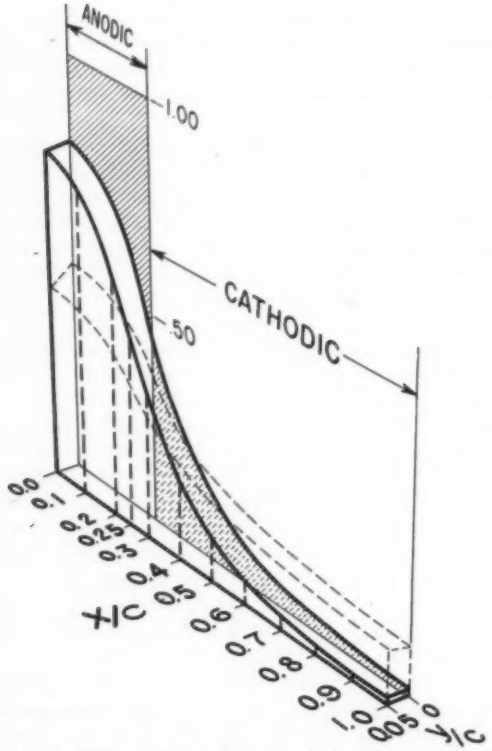

FIG. 4. Perspective illustration of the reduced potential function $P^*(x, y)/E_a$. Drawn for the relative liquid thickness of $b/c = \frac{1}{20}$ and for the ratio of anode to cathode widths of $\frac{1}{3}$.

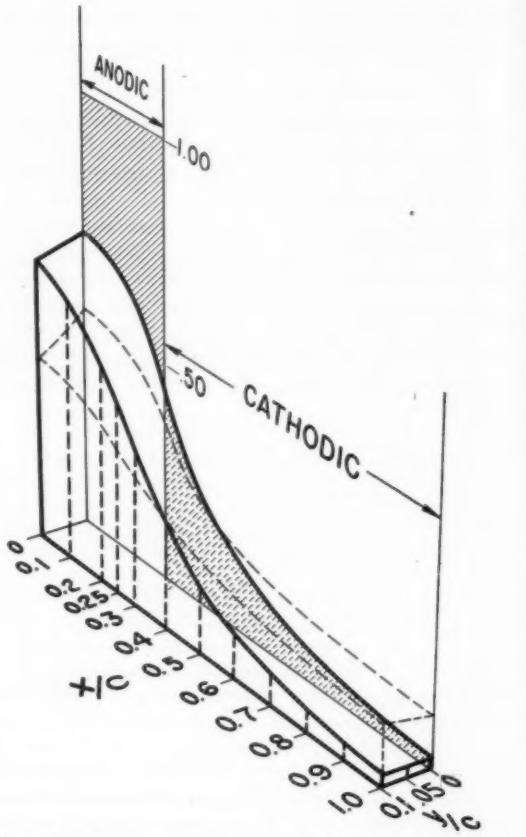

FIG. 5. Perspective illustration of the reduced potential function $P^*(x, y)/E_a$. Drawn for the relative liquid thickness of $b/c = \frac{1}{10}$ and for the ratio of anode to cathode widths of $\frac{1}{3}$.

From results tabulated elsewhere (7) it was seen that the potential does not have a constant value along this boundary.

A graphical summary of these potential evaluations was made in the form of four perspective illustrations drawn to scale. For reference, the potential distribution over the electrodes was evaluated for an infinite liquid depth at two y values, 0 and b, and is plotted as dotted lines on each perspective graph. As (b/c) approaches 1 there are only tiny differences between the curves for larger finite and for infinite (b/c) values. Fig. 4, 5, and 6 show the anodic fraction (a/c) of $\frac{1}{4}$. The curves are included for finite and infinite liquid thickness on each drawing.

To illustrate the effect of a small polarization parameter, Fig. 7 was prepared for $a/\mathfrak{L} = 500$ and for the special case $a/c = b/c = \frac{1}{2}$. When $a/\mathfrak{L}$ is very small, the potential is approximately $E_a(a/c)$ everywhere in the liquid, so perspective graphs were not prepared for this case.

CORROSION CURRENT

Corrosion current density can be calculated from interfacial potentials (2, 3). The dimensionless $C^*(x)$ group[1]

[1] This quantity is frequently written without subscripts. When a distinction between the cathodic $C_c^*(x)$ and the anodic $C_a^*(x)$ values is desirable, the appropriate subscripts are used.

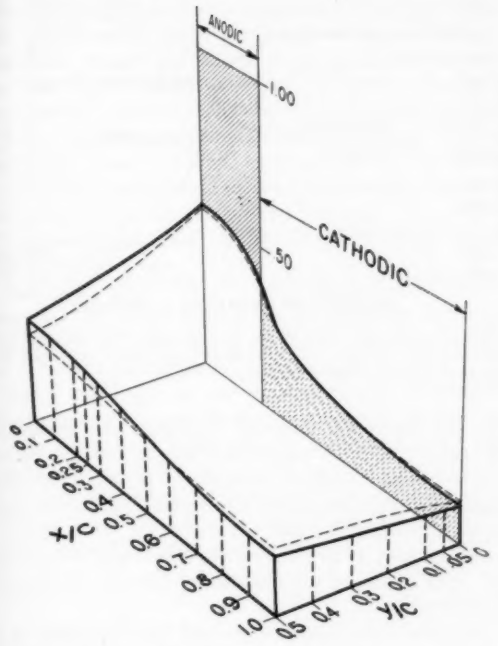

FIG. 6. Perspective illustration of the reduced potential function $P^*(x, y)/E_a$. Drawn for the reduced liquid thickness of $b/c = \frac{1}{2}$ and for the ratio of anode to cathode widths of $\frac{1}{3}$.

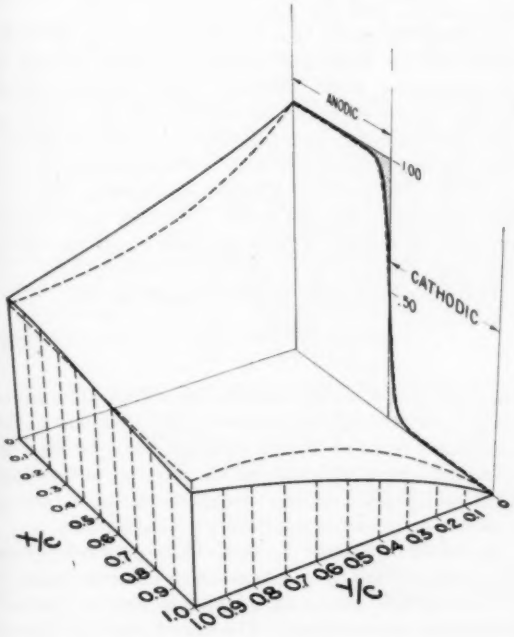

FIG. 7. Perspective illustration of the reduced potential function $P^*(x, y)/E_a$. Almost negligible polarization has been assumed. Drawn for the relative liquid thickness of $b/c = 1$, for equal anode and cathode widths and for $a/\mathfrak{L} = 500$. The dotted curve, appropriate to the interfacial potential for an infinite liquid thickness, has been separated from the curve for the finite liquid to facilitate illustration.

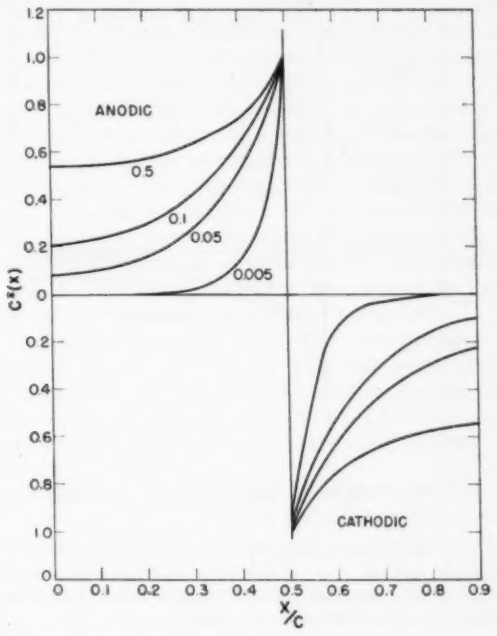

FIG. 8. Relative corrosion current parameter $C^*(x)$ evaluated for equal anode and cathode widths. Illustrates the effect of the various relative liquid thicknesses, $(b/c) = 0.005$, 0.05, 0.1, and 0.5.

representing current is defined as

$$C^*(x) \equiv \left(-\frac{2a}{E_a}\right)\left.\frac{\partial P^*}{\partial y}\right|_{y=0} \qquad \text{(VII)}$$

It can be shown from boundary condition (III) that

$$C^*(x) = \frac{2a}{\mathfrak{L}}\left[S_a(x) - \frac{P^*(x, 0)}{E_a}\right] \qquad \text{(VIII)}$$

The $C^*(x)$ values computed for 4 values each of the (b/c) ratio and for $(a/c) = \frac{1}{2}$ and $\frac{1}{4}$ are graphically summarized in Fig. 8 and 9. A single value of $\mathfrak{L}$ was employed so that $a/\mathfrak{L}$ was 1 for $a/c = \frac{1}{2}$ and $a/\mathfrak{L}$ was $\frac{1}{2}$ for $a/c = \frac{1}{4}$.

Fig. 10 illustrates the combined effects of polarization and electrolyte thickness on $C_a^*(x)$ for three $\mathfrak{L}/c$ values and for the respective relative thickness of $\frac{1}{10}$. Equal anode and cathode widths were assumed. Study elsewhere (7) shows that a reduction in thickness concentrates the current into the vicinity of the anode-cathode junction. When b/c and $\mathfrak{L}/c$ are small, the concentration is quite effective, and for a given b/c value of the order of $\frac{1}{10}$ or less, a maximum in $C_a^*(x)$ occurs as $\mathfrak{L}/c$ is increased. This phenomenon is discussed more fully later.

EXPERIMENTAL STUDIES

The principal value of this paper lies not in demonstrating the inadequacy of experimental studies or the large gap between theory and practice but in guiding an experimenter in selection of his experimental conditions. Particularly, it indicates that an "infinite depth" of liquid in any probable experiment is effectively equal to the sum of anode and cathode widths.

Qualitative results of Akimov and Golubev.—Akimov and

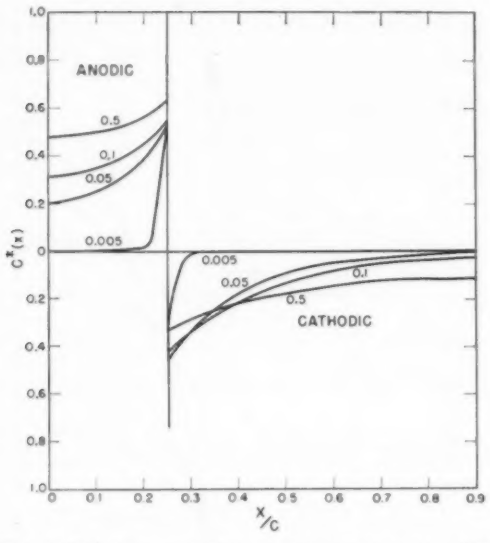

FIG. 9. Relative corrosion current parameter $C^*(x)$ evaluated for the ratio of anode to cathode widths of $\frac{1}{3}$. Illustrates the effect of various relative liquid thicknesses. Drawn for $b/c = 0.005, 0.05, 0.1$, and 0.5.

Golubev considered the question of potential distribution in the corrodent (9) and the distribution of corrosion attack (10) over the anode. They pointed out that in many earlier researches into the behavior of model local cells, e.g., (11–13), the experimenters employed models

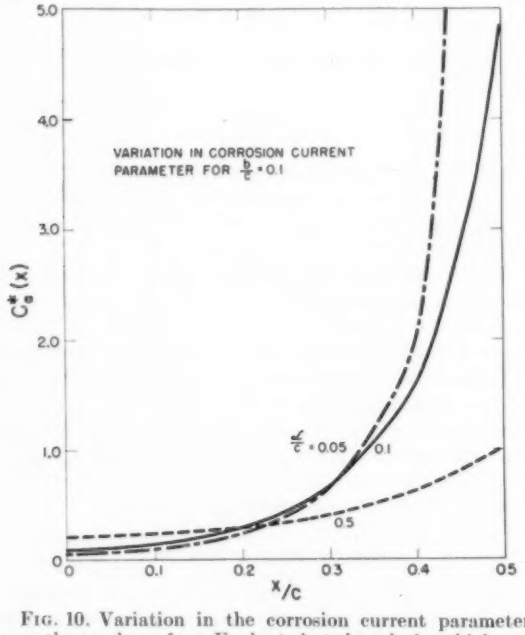

FIG. 10. Variation in the corrosion current parameter over the anode surface. Evaluated at the relative thickness $b/c = \frac{1}{10}$ and at various ℓ/c values. Illustrates the combined effects of these parameters in concentrating the current into the vicinity of the anode-cathode junction. Note that $C_a^*(x/c = 0.25)$ passes through a maximum as ℓ/c increases.

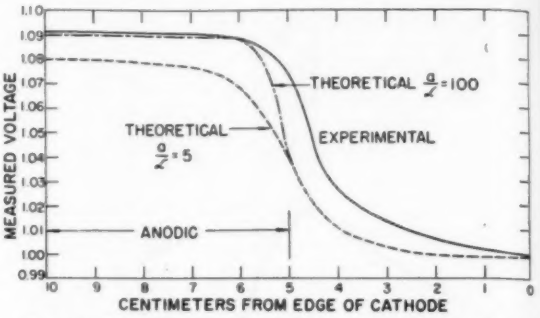

FIG. 11. Comparison between the experimental data of Akimov and Golubev for the Interfacial potential and the theoretically derived results.

with the electrodes physically separated and located in different planes. They emphasized the use and importance of short-circuited coplanar electrodes in trying to elucidate phenomena attending galvanic corrosion. Specifically, they employed rectangular and circular forms for both electrodes arranged to give several anode-cathode ratios. Further, they examined the influence of different thicknesses of electrolyte.

Their electrodes were copper and zinc immersed in a solution containing 3% sodium chloride, 0.06*N* hydrochloric acid and 0.24% hydrogen peroxide. They measured the anodic polarization curve of zinc in this solution as well as the cathodic polarization curve of copper. From these curves it is possible to estimate that $\ell_a \simeq 0.01\ \ell_c$. Thus the primary assumption in the present paper, that ℓ_a equals ℓ_c, does not apply.

Nevertheless these experimental results can be compared with the theoretical results to obtain some idea of the influence of widely differing polarization parameters. In Fig. 11, the experimental variation of the interfacial potential (estimated from their Fig. 1) is plotted together with the theoretical curve which was evaluated for $a/\ell = 5$. The abscissa that Akimov and Golubev used has been reversed so that the anodic portion of the electrode surface is on the left. This brings their graph into agreement with the location of electrodes employed here.

The differential form of Tafel's equation (5)

$$\left|\frac{\partial \Delta E_c}{\partial J_c}\right| = \frac{\mathbf{b}}{J_c} \qquad \text{(IX)}$$

where ΔE_c and J_c are the cathodic overvoltage and current density, respectively, and where **b** is the coefficient of the logarithmic term of Tafel's equation, may be used to estimate ℓ_c. From their data, it was probably in the range 0.4–2.5 cm. For convenience, the geometric mean value of 1 cm was employed in the theoretical calculations.

As defined by Wagner (5), E_a is not the open cell voltage but must be obtained by extrapolating tangents drawn to the polarization curves at appropriate current densities back to zero current density. The second paper by Akimov and Golubev (10) provides sufficient data for this procedure. The cathodic current density was found to be 6 ma/cm² from their Fig. 3. The value of E_a would be very large if the tangent were drawn at 6 ma/cm², since a new cathodic process sets in at approximately this value.

Note that as the current density is raised from 5 to 6 ma/cm², the overvoltage is raised from 0.4 to 1.2 v. By drawing a tangent to the final rising portion of the curve in their Fig. 1, and by drawing a tangent to the anodic polarization curve in their Fig. 2, a reasonable value of 100 mv was obtained. This voltage is compatible with the potential obtained from the curve appearing in their Fig. 6, after allowance is made for the polarization of the anode and cathode. It was somewhat arbitrarily assumed that the extrapolated value of the cathodic voltage $E_{c(0)}$ is 0.99 v on their scale.

Returning now to Fig. 11, the cathodic portion of their experimental curve approaches the present theoretical curve near the edge of the electrode. Near the junction ($x = 5$), the experimental curve is higher than the computed curve. This is not surprising since the slightly polarized anode is contributing significantly more current to the polarization of the cathode near the junction than would be possible if $\mathfrak{L}_a$ were equal to $\mathfrak{L}_c$ as assumed in the theoretical computation. In support of this argument, $C_a^*(x)$ for $a/\mathfrak{L} = 100$ is 3.27 at $x = 4$ cm and 74.2 at $x = 4.99$ cm, whereas $C_a^*(x)$ evaluated for $a/\mathfrak{L} = 5$ is 2.03 and 4.85 respectively (8). Since b/c is 0.6 in the Akimov and Golubev paper (9, 10), and $\mathfrak{L}$ only moderately large, use of the data calculated for an infinite thickness (8) is justified, and the data are approximately correct.

In the anodic portion of the experimental curve the behavior is not surprising. The anodic portion of the theoretical curve computed for $a/\mathfrak{L} = 100$ has been included. Thus, the potential on this surface remains essentially constant (to within 1 mv on the present voltage scale) up to within a centimeter of the anode-cathode junction. Substantial current can be tolerated on the anode without a large degree of polarization, so the change in potential at the junction is not large.

In Fig. 12, experimental variation of the potential at the outer boundary was plotted for two liquid thicknesses. These data were estimated from their Fig. 1. Two equivalent theoretical curves based on $b/c = \frac{1}{2}$ were computed for $a/\mathfrak{L} = 5$ and $a/\mathfrak{L} = 500$. These curves were included on Fig. 12 for comparison. It is somewhat surprising that the measured potential above the cathode approaches the values characteristic of the anodic region. The entire curve lies significantly above the theoretical curve. No simple explanation for this observation can be offered.

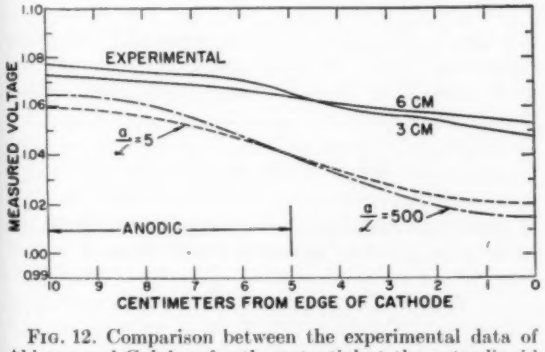

FIG. 12. Comparison between the experimental data of Akimov and Golubev for the potential at the outer liquid boundary and the theoretically derived results.

However, assumptions of the theoretical analysis differ from the experimental conditions in one further way. In the derivation, an array of galvanic cells was assumed so that edge effects could be ignored. In the case under discussion, a single pair of electrodes were immersed in a wider bath of corrodent. As a result, current flow lines were not as crowded as assumed in the theory, and the total current on both electrodes was larger than computed. Although this increased IR drop would have the effect of lowering the potential at the outer boundary above the anodic portion of the electrode surface and increasing it over the cathodic portion, it is not apparent that the effect should be as large as indicated by Fig. 12.

The general qualitative behavior is well illustrated by these two graphs, and it is gratifying that the agreement between theory and practice is this good, considering that experimental polarization parameters are not equal and that the liquid extends farther to each side than the electrodes.

Comparison with the Jaenicke and Bonhoeffer data.— An experimental variation in the relative current was estimated from Fig. 10 of Jaenicke and Bonhoeffer (14), and this is plotted as $J(x)/J(x = 1.6)$ in Fig. 13. Using equation (IX) to compute $\mathfrak{L}_c$, it was found to lie in the range 0.0225–0.2 cm. Thus, calculations of the theoretical curves were made for $\mathfrak{L}/c = 0.005$, 0.01, and 0.1, since the experimental range $\mathfrak{L}_c/c$ of values was covered by the latter two $\mathfrak{L}/c$ ratios. From their Fig. 9, $a = 2.05$ cm and $c = 2.30$ cm. Three theoretical curves, evaluated for $b = 2.5$ cm, are presented in Fig. 13. The fourth theoretical

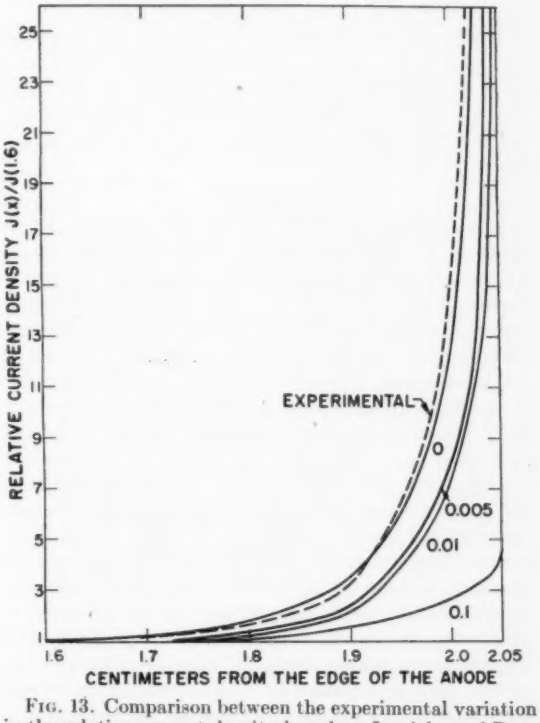

FIG. 13. Comparison between the experimental variation in the relative current density based on Jaenicke and Bonhoeffer's data and the theoretically derived variations for several $\mathfrak{L}/c$ values.

curve, for $\mathfrak{P} = 0$, was calculated from equation [4] of reference (1). Note that in equation (V) of the present paper when $\mathfrak{P} = 0$, the dependence on b drops out, and the equation reverts to equation [9] of (1) evaluated for $y = 0$. Thus the corrosion current parameter can be computed from the analytic expression [4] of (1).

As in the previous case, the experimental curve is not in agreement with the best theoretical estimates. Here the estimated curve lies above the curve computed for $\mathfrak{P} = 0$, i.e., for no polarization. Part of the difficulty could be removed by making the experimental $J_a(x = 1.6)$ somewhat larger or the x values slightly smaller. It is difficult to work accurately with their Fig. 10. However, it is possible that the actual current density is higher than computed because the liquid was not confined in width to the dimensions of the electrodes as required by the present analysis. This might be expected to contribute more to the remote portions of the electrodes than to the vicinity of the anode-cathode junction.

An important point is that Jaenicke and Bonhoeffer (14) used cylindrical, not plane, specimens. Thus, the present theoretical analysis cannot be expected to apply exactly. The boundary conditions and preliminary analysis for the RZ plane of the cylindrical coordinates (i.e., θ constant) is similar to that in the XY plane of the Cartesian coordinates employed in the present analysis. The physical separation between the RZ planes increases for two θ values as R increases. As a result, the current flow lines are not as crowded at appreciable distances above the electrodes in the cylindrical case. Thus, it would be expected that the current densities at the electrodes would be higher than if planar specimens were used.

For these reasons, agreement between the computed and the experimentally measured current densities is good. Further improvement can be made by modifying the experimental curve in either or both of the ways indicated. This would be arbitrary and would accomplish little.

Discussion

It is clear from the results presented that with increased ratios of a to $\mathfrak{P}$, local current densities as reflected by values of $C^*(x)$ become less uniform, and that the relative current density $C^*(x)/C^*(x = 0)$ becomes higher as x approaches the anode-cathode junction. That is, the galvanic system behaves more "macroscopically" as $a/\mathfrak{P}$ or $c/\mathfrak{P}$ is increased. This effect has been established earlier (1, 2). The novel and more interesting effect of the liquid layer thickness has been thoroughly examined for the first time, and it has been found that when b is small enough, the potential distribution over the electrodes at the metal-electrolyte interface approaches the limiting distribution found for negligible polarization in (1). Variation of current density over the electrode surface becomes increasingly sharp as the liquid layer becomes shallower. In compatability with the influence of the polarization parameter, the system behaves "macroscopically" when c/b is large. In certain instances, behavior of the galvanic system must be regarded as "macroscopic" even though there is sufficient polarization, because the liquid film is thin. In such instances the critical dimension λ is b, not a or c as it most frequently is.

When b is identified as the critical dimension λ and therefore is relatively small in comparison to the electrode size or the polarization parameter, the current density (dimensionless) parameter $C^*(x)$ is smaller in magnitude for a given set of a, c, $\mathfrak{P}$, and x values than it is when b is large. Thus, although the system appears to behave "macroscopically," which frequently connotes high current densities, the local current densities are limited and reduced by the corrodent thickness. In this sense, too, b may be regarded properly as the critical dimension.

Another interesting feature of this work is the determination of potential variation at the outer boundary of the corrodent as well as at the electrode boundary of the corrodent. Fig. 4 to 7 show that the potential variation is influenced by both c/b and $c/\mathfrak{P}$. When $c/\mathfrak{P} = 2$, the potential distribution approaches that obtained for an infinitely thick liquid when c/b becomes smaller than 2. However, when the polarization is slight or liquid conductivity high (for instance when $c/\mathfrak{P} = 1000$), and when $c/b = 2$, then the potential is significantly less uniform parallel to the electrode surface than in the case just mentioned. The relative thickness b/c must be further increased before the potential distribution can approximate that found for an infinite thickness of liquid. This combined effect of polarization and liquid thickness is of importance in designing a proper corrosion experiment. The liquid depth should be at least equal to the sum of the anode and cathode dimensions. This "rule" is supported by Fig. 6, 7, and 10.

Most of the statements made for potential distribution at the outer boundary apply equally well to potential distribution at the inner liquid boundary, i.e., to the interfacial potential. The influence of small b on increasing the variation of the interfacial potential is demonstrated by Fig. 2 and 3. The contrary influence of large $\mathfrak{P}$ on decreasing the variation for a given b can be shown.

The analytic results for corrosion current can be examined for limiting values. It is clear that the minimum current density should be found at $x = 0$ for any given set of a, c, $\mathfrak{P}$, and b values, and that the maximum current will be found adjacent to the junction, namely at $x = a - 0$. A simple expression for the limiting value of the maximum current density can be obtained from equation (VIII) for any nonzero value of $\mathfrak{P}$. Note that

$$\lim_{x \to a-0} P^*(x, 0) = {}^1\!/_2 E_a \qquad \text{(X)}$$

if $a/c = {}^1\!/_2$. This can be seen from equation (V) since the numerator of the summand vanishes for both odd and even values of n. Therefore, since in the anodic region $S_a(a - 0) = 1$,

$$\lim_{x \to a-0} C_a^*(x) = \max C_z^* = \frac{a}{\mathfrak{P}} \qquad \text{(XI)}$$

If then a/c is less than ${}^1\!/_2$, the value of $P^*(a, 0)/E_a$ lies between (a/c) and ${}^1\!/_2$ as seen in Fig. 3. Thus

$$\frac{a}{\mathfrak{P}} \leq \max C_a^* \leq \frac{2a}{\mathfrak{P}}\left(1 - \frac{a}{c}\right) \qquad \text{(XII)}$$

Similarly, if a/c is greater than ${}^1\!/_2$, it can be shown that

the value of $P^*(a, 0)/E_a$ lies between $\frac{1}{2}$ and a/c. Thus

$$\frac{a}{\mathfrak{L}} \geq \max C_a^* \geq \frac{2a}{\mathfrak{L}}\left(1 - \frac{a}{c}\right) \qquad \text{(XIII)}$$

These limits are independent of the relative thickness b/c if the latter is not zero. In the event that one has $b/c = 0$, then the dependence on polarization drops out as both equation (V) and equation (VI) show, and the interfacial function behaves like the step function. This would be expected if there were no liquid. Thus, the limit in equation [X] becomes E_a independent of a/c just as though $\mathfrak{L} = 0$. However, if the ratio b/c remains constant or greater than zero as c goes to infinity, the absolute upper limit on the current parameter for a finite width of anode is $2a/\mathfrak{L}$ as seen from equation (XII). This result agrees with that deduced in a different manner in equation [41] of (2). It has been pointed out previously (2, 3) that $P^*(x, 0)$ approaches $(a/c)E_a$ as $\mathfrak{L}$ becomes very large. This can be seen from equation (V).

The minimum current density is not well behaved in comparison to the maximum current density. The value of the minimum corrosion current parameter $C_a^*(0)$ is plotted in Fig. 14 as a function of both $\mathfrak{L}/2a$ and b/c for $(a/c) = \frac{1}{2}$. The reason for the maximum in this quantity as $\mathfrak{L}/2a$ increases can be understood on the basis of physical considerations. When $\mathfrak{L}$ is small, i.e., in a high resistance solution where little polarization occurs, the bulk of the reaction can occur only in the vicinity of the anode-cathode junction, or the resistance of the bath will be prohibitively high. The concentration of current lines into this region is increased when (b/c) is small, i.e., when a thin film is present. This statement is borne out by Fig. 8 and 9. The thinner the liquid film, the closer together the current lines, with an accompanying increase in total resistance. As conductivity of the corrodent increases or polarization increases, the current speads laterally from the anode-cathode junction, mainly over the cathode (when it is the larger electrode and vice versa). Thus, a higher current density occurs at the center of the anode, i.e., at $x = 0$.

However, when $\mathfrak{L}$ is large, i.e., when the system is behaving "microscopically" (since $a/\mathfrak{L}$ is small), the corrosion current parameter decreases, and it approaches the line $a/\mathfrak{L}$ on the right side of Fig. 14 whenever $\mathfrak{L}/a$ is greater than about one. As previously (2) current density becomes more uniform when $\mathfrak{L}$ is large, that is when the electrochemical system can be considered "microscopic." The minimum value of $C_a^*(x)$ converges toward the value $a/\mathfrak{L}$ and the maximum toward $(2a/\mathfrak{L})(1 - a/c)$ as the parameter $a/\mathfrak{L}$ becomes small.

In contrast, the minimum and maximum current density differ by several orders of magnitude on the left hand of Fig. 14, when b/c is large. The system is "macroscopic." However, if the relative thickness is small, the value of $C_a^*(x)$ over most of the electrode surface is approximately that of the minimum. The system would be regarded as completely "microscopic" if it were not for the fact that the current density in the immediate vicinity of the anode-cathode junction remains high and relatively independent of the electrolyte thickness. The difference between maximum and minimum is increased when b/c is small since the minimum is reduced. In the sense that the current density is uniform over most of the electrode surface when the thickness is small, the dimension b may be regarded as λ. When $b/\mathfrak{L}$ is small, the system can be regarded as "microscopic."

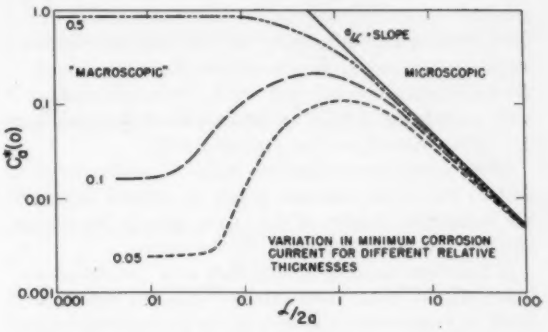

FIG. 14. Variation in the minimum corrosion current density parameter for several relative thicknesses of electrolyte.

Evidence for the a maximum current density, at a given location on the electrode, when b/c and $a/\mathfrak{L}$ take on certain values can be seen in Fig. 14. It can also be seen on the cathodic side of Fig. 9. At $x/c \simeq 0.35$ the parameter $C^*(x)$ increases as b/c is increased from 0.005 to approximately 0.1, and then decreases. $C^*(x)$ is still increasing at $x/c = 0.9$ for increasing values of b/c up to $\frac{1}{2}$. The phenomenon illustrated by Fig. 13 is not a special case, as it has been established with other a/c ratios. There is evidence in Fig. 10 to illustrate the fact that the current density parameter $C_a^*(x)$ passes through a maximum as $\mathfrak{L}/c$ increases. This phenomenon of a maximum holds for a range of x/c values as in Fig. 9 and 10. However, when b/c is as large as $\frac{1}{2}$, the minimum current remains fairly constant over a range of $\mathfrak{L}/c$ values, then decreases rapidly as $\mathfrak{L}/c$ exceeds one. This general phenomenon of concentration is more conclusively demonstrated by a detailed examination of the tables of $C_a^*(x)$ presented elsewhere (7).

Akimov and Golubev (10) concluded that the height of the field of forces is equal to about one-half the sum of lengths of the anode and cathode. This working rule is adequate if $a/\mathfrak{L}$ is one or smaller. However, the perspective drawings show that when $a/\mathfrak{L}$ is large, for instance in the absence of strong polarization, the potential at the outer boundary of a liquid with the relative thickness $b/c = \frac{1}{2}$ is significantly different from the potential at $y/c = \frac{1}{2}$ (i.e., at the same distance from the plane of the electrodes) in an infinitely thick electrolyte. Therefore, the rule suggested here that liquids in which b is greater than c can be considered "infinitely" thick would appear to be more reliable than that stated by Akimov and Golubev.

Conclusion

Many and detailed numerical evaluations of Fourier series (V) and (VI) have permitted elucidation of the opposing influences of the liquid depth and the polarization parameter. In relatively thin liquid films, the interfacial potential is forced toward the values expected with slightly

polarized electrodes, despite the fact that conductivity of the corrodent and its capacity for polarizing the electrodes would be high enough to polarize the electrodes strongly if the liquid layer were infinitely thick. One common effect of both parameters is that in general small b/c and large ℓ/c values reduce the local current density.

These numerical evaluations made it possible to show that in thin films corrosion attack is confined largely to the immediate vicinity of the anode-cathode boundaries, and that this region enlarges as ℓ/c increases.

It has been possible to establish as a "working rule" that a film of liquid is effectively "infinitely thick" if its depth is greater than the sum of the characteristic anode and cathode dimensions.

Acknowledgments

The authors are indebted to Andrew Dravnieks for the translation of the papers by Akimov and Golubev. John Morrissey contributed significantly to the success of this report by performing many numerical calculations. The authors would like to thank John Ruth for many helpful discussions and for checking the mathematics contained herein. The continuing interest and helpful guidance of Professor Carl Wagner was greatly appreciated.

Manuscript received December 27, 1954. This paper was prepared for delivery before the Cincinnati Meeting, May 1 to 5, 1955. Work done under the auspices of the Atomic Energy Commission.

Any discussion of this paper will appear in a Discussion Section to be published in the December 1956 JOURNAL.

REFERENCES

1. J. T. WABER, *This Journal*, **101**, 271 (1954).
2. J. T. WABER AND M. ROSENBLUTH, *This Journal*, **102**, 344 (1955).
3. J. T. WABER, *This Journal*, **102**, 420 (1955).
4. J. T. WABER, "Mathematical Analysis of Galvanic Corrosion. Part IV. Effect of Polarization and Liquid Thickness on the Total Corrosion Current," Los Alamos Scientific Laboratory Report LA-1686, June 1954.
5. C. WAGNER, *This Journal*, **99**, 1 (1951).
6. J. T. WABER, Report No. LA-1386, Los Alamos Scientific Laboratory, March 1952.
7. J. T. WABER, Unpublished report.
8. J. T. WABER, Report No. LA-1656, Los Alamos Scientific Laboratory, June 1954.
9. G. V. AKIMOV AND A. I. GOLUBEV, *Zhur. Fiz. Khim.*, **20**, 303 (1946).
10. A. I. GOLUBEV AND G. V. AKIMOV, *Zhur. Fiz. Khim.*, **20**, 309 (1946).
11. A. THIEL AND J. ECKELL, *Z. Elektrochem.*, **33**, 370 (1927).
12. M. STRAUMANIS AND M. CENTNERSWER, *Z. phys. Chem.*, **128**, 369 (1927).
13. G. V. AKIMOV, G. BRUSHEN, AND G. B. CLARK, *Zhur. Fiz. Khim.*, **6**, 1151 (1935).
14. W. JAENICKE AND K. F. BONHOEFFER, *Z. phys. Chem.*, **193**, 301 (1944).

Technical Feature

Electrochemical Corrosion in Nearly Neutral Liquids[1]

U. R. Evans

Department of Metallurgy, Cambridge University, Cambridge, England

Introduction

Two feelings are uppermost in your Lecturer's mind: first, appreciation of the honour which is being done him; second, the hopelessness of presenting in an hour any complete or convincing account of his subject. The best that can be hoped is that the lecture may arouse sufficient interest to encourage the reading, in the original journals, of papers about corrosion, and a habit of calm thinking on what has been read. If this is achieved, it will be something worth while, since reading and thought, once regarded as essential features of education and research, tend to be neglected today. It is impossible to open a scientific journal without feeling that some authors do not consult in the original the papers cited in their reference lists, nor even satisfy themselves that these represent the latest pronouncements of the scientists quoted. There is no need to take the situation too tragically, but it is certain that closer reading and clearer thinking would be in the interests of research. After this brief introduction—which combines gratitude, humility, and exhortation—it is time to approach the subject of the lecture.

Modes of Oxidation

A reaction can only occur spontaneously if it represents the passage from a less stable to a more stable state. The combination of a metal with oxygen frequently fulfills this condition, the stability of the final state being connected with two facts:

1. The capture of two electrons by an oxygen atom converts it to an anion possessing a stable structure comparable to that of an inert-gas atom.

2. The oxide formed consists of oxygen anions and metal cations with the particles of opposite charge placed closer together than those of like charge.

However, electron transfer from metal to oxygen can occur in two ways: the oxygen can gain electrons and the metal lose them at points separated by distances measurable in Angstrom units; or the gain and loss can occur at points separated, perhaps, by some millimeters. The first mechanism, which generally produces an oxide film, is commonly known as "simple oxidation," and the second, which generally requires the surface to be wetted with an aqueous solution (and often produces not an anhydrous oxide but a hydroxide), is called "electrochemical corrosion." The naming is imperfect; it is becoming evident that even the first mechanism is far from "simple," and, since it involves movement of electrons and ions through the film, it possesses some claim to be called "electrochemical." Nevertheless, it is convenient to retain the nomenclature, reserving the name "electrochemical corrosion" for cases involving the movement of ions over a liquid path. The length of that path is generally great compared to the thickness of an ordinary film, so that we may call the phenomenon "oxidation from a distance," perhaps even "tele-oxidation."

Simple Oxidation

This lecture is not concerned with the first mechanism, but it may be mentioned that simple oxidation has been studied lately in my Laboratory by Davies (1) using iron, Mills (2) using copper, and Hart (3) using aluminium; also that I have published, in response to an invitation from Australia (4), a simplified mathematical statement of the various oxidation-time laws. Moreover, if reminiscence is permissible, it may be recalled that my first American paper was devoted to film growth. It appeared, by invitation, in your Journal in 1924 (6)—the year following the appearance, in an English journal, of the classical work of the American investigators, Pilling and Bedworth (5); thus, two examples of transatlantic publication on the subject were provided within two years. It will be recalled that Pilling and Bedworth divided the metals into two classes: (*a*) the light metals, forming porous, nonprotective films which were believed to thicken (given constancy of temperature, a condition difficult to observe) by the rectilinear law with a velocity defined by the boundary reactions; and (*b*) the heavy metals forming compact relatively protective films, thickening by the parabolic law at a rate controlled by transport through the film. I ventured to propose (6), on theoretical grounds, a more general equation (now known as the "mixed parabolic equation") to cover cases where boundary reaction and transport both play their parts in controlling the oxidation rate; the rectilinear and simple parabolic equations became limiting cases of this more general equation. Afterwards Fischbeck (7) provided what I now regard as a more satisfactory derivation of the mixed parabolic equation and demonstrated that it was obeyed for the action of steam on iron; still later, Wagner and Grünewald (8) verified it for the oxidation of copper at low pressures.

Differences between Simple Oxidation and Electrochemical Corrosion

Disregarding very light metals, with their porous, nonprotective oxide films (5), it may be said that the rate of simple oxidation generally falls off as the oxide film thickens. In contrast, electrochemical corrosion in a salt solu-

[1] Palladium Medal Lecture delivered at the Pittsburgh Meeting, October 9 to 13, 1955.

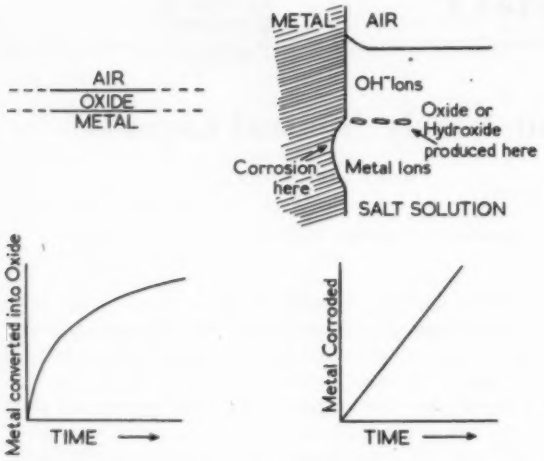

FIG. 1. Contrast between simple oxidation (*left*) and "electrochemical corrosion" ("oxidation from a distance") (*right*).

tion can, in absence of complicating factors, continue at an undiminished rate, provided that the immediate products are freely soluble (Fig. 1). Thus, on zinc partly immersed in sodium or potassium chloride solution, oxygen is readily renewed near the water line and captures electrons, becoming converted, not to O^{--} ions (which would be unstable in solution) but to OH^- ions; since this keeps removing electrons from the metal, cations (atoms short of electrons) can continuously enter the liquid without any accumulation of electric charge. The "anodic reaction"

$$Zn = Zn^{++} + 2e$$

occurs mainly on the lower part of the specimen, and the "cathodic reaction"—which is in effect—

$$O + H_2O + 2e = 2OH^-$$

at the water line. (In that region, a film is soon formed, ultimately thickening to produce interference tints, so that in the water line zone, there is no appreciable passage of cations into the liquid, at least in the early stage.) The Zn^{++} and OH^- ions, meeting near the junction of the cathodic and anodic areas, produce zinc hydroxide at a place where it cannot obstruct further attack;[2] thus the corrosion-time curves may be straight.

How straight the corrosion-time curves can be, if disturbances are avoided, is shown by curves (Fig. 2) produced in my laboratory by Borgmann (10), now President of Vermont University, and published in the Society's JOURNAL. Small amounts of copper or iron in the zinc caused a slight increase in the corrosion rate, while aluminium had the opposite effect; very pure zinc, kindly provided by American friends, gave rates appreciably slower than that of ordinary zinc, but in all cases the curves were straight.

[2] Oxide or basic salts may be formed under some conditions; corrosion products have been examined in detail in Feitknecht's laboratory at Berne (9).

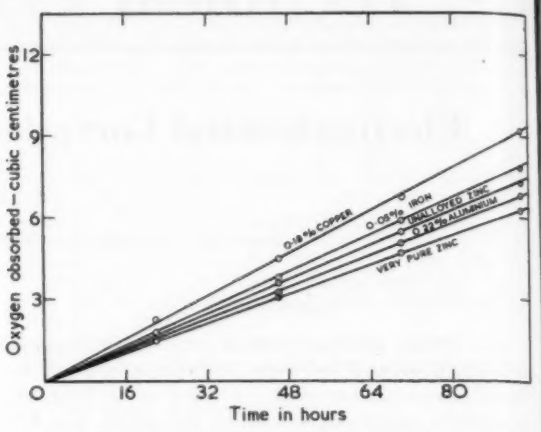

FIG. 2. Corrosion of zinc and its alloys in $N/10$ potassium chloride (C. W. Borgmann and U. R. Evans).

MEASUREMENT OF CORROSION CURRENT

That an electric current was really passing through the liquid between the anodic and cathodic regions on partly immersed zinc had been shown qualitatively in my early work (11). Just before the war stopped pure-science work in 1939, Agar (12) succeeded in measuring that current, and found that it corresponded to the corrosion rate in the sense of Faraday's law. He used (Fig. 3) zinc plates in sodium chloride (or sulphate) with two calomel (or mercurous sulphate) electrodes connected by tubuli, one (B) being fixed at an "infinite distance" from the zinc (a few inches sufficed), while the other (A) could be moved by racking in any of three directions; the three coordinates defining the position of the tubulus-tip were read off on three scales. In that way, equipotential surfaces in the liquid could be traced (Fig. 4), and, the conductivity of the liquid being known, the current flowing could easily be calculated on the basis of Ohm's law.

The corrosion of iron partially immersed in, say, sodium chloride solution is slightly more complicated, because the

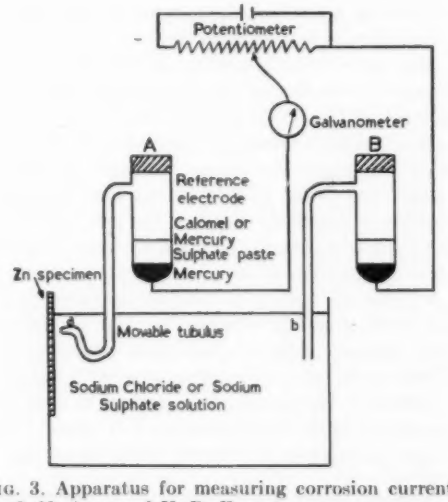

FIG. 3. Apparatus for measuring corrosion currents on zinc (J. N. Agar and U. R. Evans).

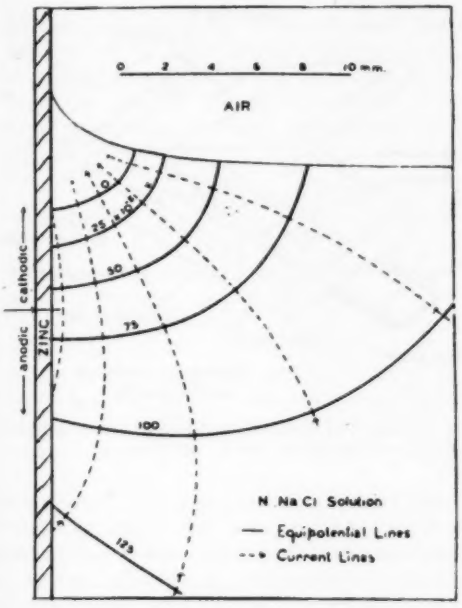

FIG. 4. Equipotential curves around zinc in *N* sodium chloride (J. N. Agar and U. R. Evans).

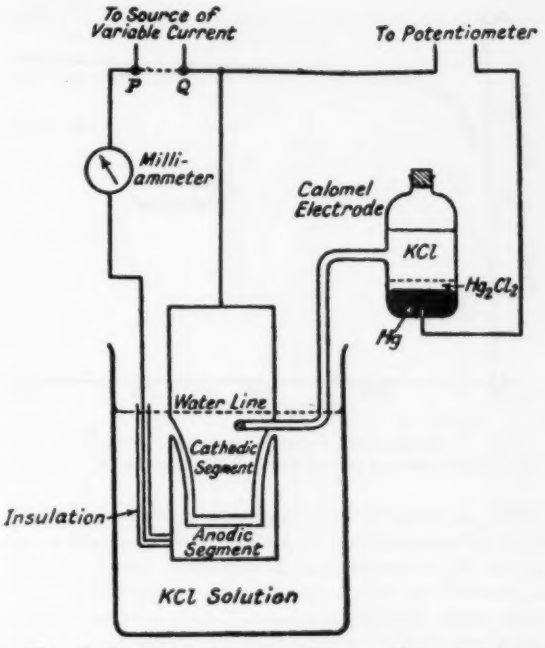

FIG. 5. Apparatus for measuring corrosion currents on iron (T. P. Hoar and U. R. Evans).

valency of iron is variable. Ferrous hydroxide is not precipitated as such, and the solid product obtained is, according to the oxygen-supply, red-brown FeO(OH), black magnetite, or sometimes green ferrous-ferric compounds. However, the accurate measurement of the corrosion currents was carried out earlier on iron than on zinc, being accomplished by Hoar (13) in 1932. Success was made possible by steel of special quality, provided by the late W. H. Hatfield, so uniform in composition that in concentrated salt solution the distribution of corrosion was always the same. Thus, specimens could be cut along the line separating what would be the corroded and uncorroded areas and the two parts mounted almost in their natural relative positions, but just out of contact. At some concentrations it was possible to measure the current directly by joining the two segments through a low-resistance milliammeter, but this procedure, although simple in principle, was not very accurate; nor could it be employed except within a limited range of concentration. A more satisfactory method was to join the segments to an external source of microcurrent (Fig. 5) and measure, by means of a tubulus opening close to the cathodic area and joined to a calomel electrode and potentiometer, the relation between cathodic potential and curent flowing; the curve obtained (Fig. 6) made it possible, by measuring the cathode potential on an uncut specimen, to read off the current flowing. Thus the corrosion rate obtained by application of Faraday's law could be compared with that measured directly from loss of weight; the agreement (Fig. 7) was surprisingly good.

On vertical specimens partly immersed in potassium or sodium chloride, the cathodic area is the zone lying just below the water line where oxygen needed for the cathodic reaction can readily be replenished; the anodic area, where attack occurs, is further down. On a horizontal, fully immersed surface, no part is specially favoured as regards oxygen supply (except that at the edges replenishment is somewhat better than elsewhere); the anodic and cathodic areas move about, so that in the end the whole area may become corroded, each point having been anodic at some time or other. The current here is much smaller than on partly immersed specimens, but Noordhof (14), by means of a tubulus consisting of two concentric tubes leading, respectively, to two silver chloride electrodes, succeeded in measuring it, after suitable amplification, and found that the electrically calculated corrosion rate was in reasonable accord with that observed directly. In the early stages, when only certain regions of the specimen were showing

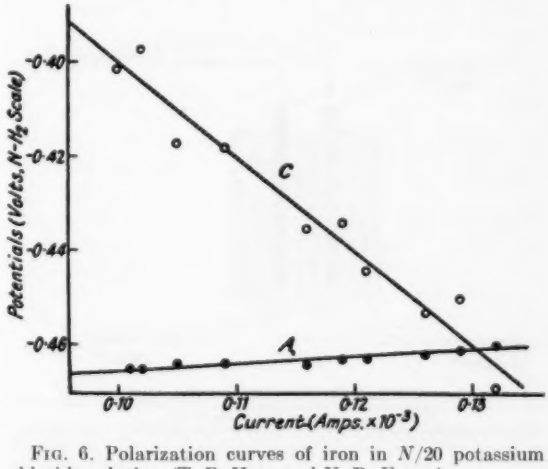

FIG. 6. Polarization curves of iron in *N*/20 potassium chloride solution (T. P. Hoar and U. R. Evans).

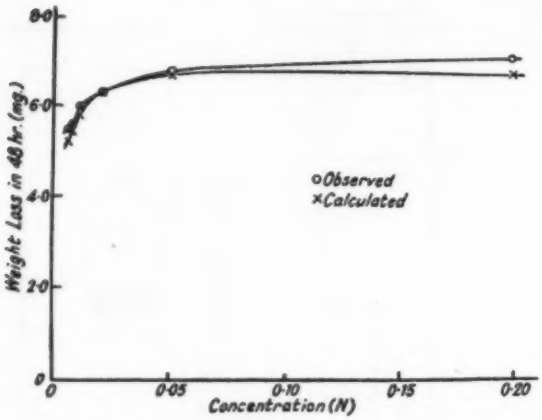

FIG. 7. Comparison between observed and electrically calculated values of corrosion (T. P. Hoar and U. R. Evans).

visible corrosion, it was found that these were identical with the regions shown by the electrical instrument to be anodic. It is believed that, in such cases, anodic polarity is generally dependent on physical looseness of structure rather than chemical differences. Groups of atoms, which can detach themselves most easily, pass into the liquid by an anodic reaction; when the loosened portion is exhausted, anodic attack shifts to another region.

In certain cases, however, the anodic regions seem to be connected with damage to an invisible oxide film. This is true of aluminium, which builds a very protective film. Brown and Mears (15), tracing scratch lines on aluminium, found that these were anodic to the rest, and that the current flowing corresponded to the corrosion rate. Unintentional blemishes, such as can be seen often on commercial aluminium sheet, were sometimes noticed to form the seats of anodic attack. Brown and Mears cut a piece of aluminium into two pieces, blocking out all the blemishes on one piece with a wax-resin mixture and applying the mixture to the whole surface of the other except for the blemishes. On joining the two pieces, immersed in liquid, through a milliammeter, the current flowing was found to be equivalent to the corrosion rate.

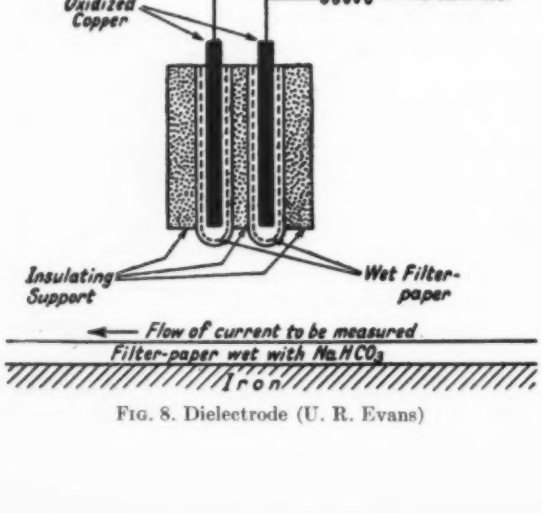

FIG. 8. Dielectrode (U. R. Evans)

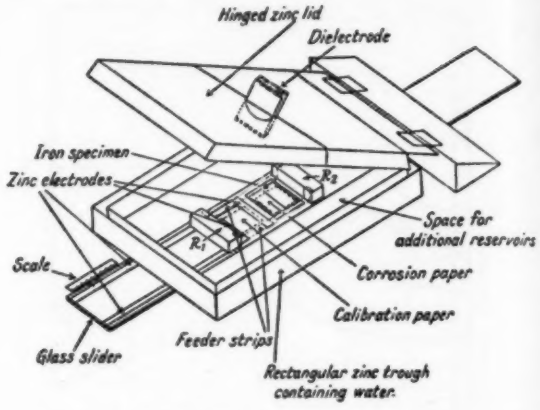

FIG. 9. Improved dielectrode apparatus with calibration circuit (R. S. Thornhill and U. R. Evans).

On iron, corrosion only occurs selectively at a scratch line if the liquid is made just sufficiently "inhibitive" to keep the main part of the film in repair (as explained later). If we engrave a scratch line on iron which has been exposed for some days to dry air after being cleaned by abrasion and then place upon it filter paper soaked in sodium bicarbonate solution of a concentration chosen as standing between the higher range (which produces passivity) and the lowest range (which produces corrosion), rust will generally appear along the scratch line, but not, on good specimens, elsewhere. In 1935 I proved (16) that current was really passing through the wet filter paper between the scratch line (as anode) and the uncorroding region on both sides (as cathodes) by bringing down the "dielectrode" shown in Fig. 8 into contact with the filter paper at some measured distance from the scratch line; the two Cu/Cu_2O electrodes were virtually nonpolarizing and a very small fraction of the current flowing horizontally along the filter paper was diverted through a central-zero microammeter. There was clearly a relation between the readings of that instrument and the current flowing through the filter paper. Thornhill (17), who evolved a greatly improved apparatus (Fig. 9), calibrated the dielectrode on a strip of wet filter paper through which known currents from an outside source were made to flow.

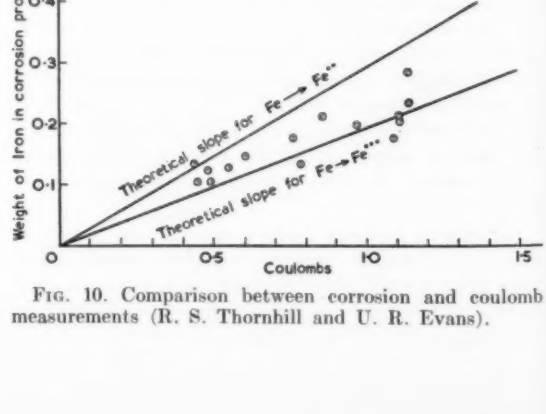

FIG. 10. Comparison between corrosion and coulomb measurements (R. S. Thornhill and U. R. Evans).

In that way the curves of Fig. 10 were obtained. The correlation between the total coulombs generated and the weight of iron corroded show that the former is greater than would be expected if the iron passed into solution merely in the ferrous state; the measurements indicate that not only the reaction

$$Fe = Fe^{++} + 2e$$

but also $$Fe^{++} = Fe^{+++} + e$$

can take an electrochemical course. It had hitherto been assumed that the anodic corrosion of iron to form ferrous products was electrochemical, but that the subsequent oxidation to the ferric state occurred "chemically" out of contact with the metal; probably the assumption was correct for iron immersed in liquid, but the stagnant conditions existing in sodden filter paper are favourable for the electrochemical oxidation of Fe^{++} to Fe^{+++}—explaining Thornhill's results.

Importance has been attached at Cambridge (England) to the measurement of the currents flowing over "naturally corroding" metal, since the comparison between calculated and observed values of the corrosion provide convincing quantitative evidence for the electrochemical mechanism. Not all of this work, however, was carried out in my laboratory; that of Brown and Mears was conducted at New Kensington after Dr. Mears had left Cambridge, and may perhaps be regarded as yet another friendly link between the American and British laboratories.

Influence of the Solubility of Primary Products

The rapid and persistent corrosion of zinc or iron in sodium or potassium chloride solution is clearly connected with the high solubility of the products formed at the anodes and cathodes; a solid corrosion product is ultimately formed, but, being precipitated well away from the site of corrosion, does not interfere with attack. Where the primary anodic product is sparingly soluble, corrosion is usually slow; the remarkable resistance of lead toward sulphate solutions, of silver toward chloride solutions, and of magnesium toward fluoride solutions is usually ascribed to the limited solubilities of lead sulphate, silver chloride, and magnesium fluoride.

Some measurements which I carried out (18) in 1924 with drops placed on a horizontal steel surface exposed to air at 29°C may serve to illustrate the influence of solubility. The corrosion, measured by a simple colorimetric method with thiocyanate, is shown in Table I. It may be remarked that the reproducibility was usually better in the short experiments than the long ones, especially with the potassium salt solutions, where during the longer periods the potassium hydroxide formed as cathodic product round the drop margin (where oxygen is best renewed) crept outward over the surface to an extent which varied from one drop to another.

Some apology is needed for putting forward measurements made thirty years ago, but even today they serve to illustrate certain features of the situation. With all those potassium salts which form a freely soluble cathodic product (potassium hydroxide) and a freely soluble anodic product (the appropriate ferrous salt), the corrosion rate is considerably greater than that produced by the distilled water used for making the solution (which probably contained traces of tin). The phosphate normally gave negligible corrosion, evidently due to the sparingly soluble anodic product, iron phosphate, but one exceptional specimen (probably carrying some abnormally weak point) suffered much attack. Zinc sulphate produced less corrosion than distilled water alone, evidently due to the sparingly soluble cathodic product, zinc hydroxide. [The fact that zinc sulphate retards the cathodic reaction was afterwards shown at Cambridge by Chyżewski (19) and has been confirmed by Cross and Hackerman (20).] Nickel sulphate caused considerable corrosion, and here the cathodic product may well have been metallic nickel, which would certainly not hinder the cathodic reaction; that explanation was not offered in the 1924 paper.

Two Cambridge researches of 1928 and 1929 on the corrosion of partially immersed steel plates provide a further example of the same principle. Magnesium sulphate solution (giving magnesium hydroxide as cathodic product,

TABLE I. *Corrosion on steel by single drops at 29°C, expressed in mg*

Time (hr)	5.5	18.5	24.0	48.7
Distilled water	0.26 0.30 0.25 0.25	0.73 0.77 0.75 0.70	1.0 1.05 0.95 0.95	0.95 1.47 1.47 1.40
N/10 KCl	0.65 0.65 0.66 0.66	1.91 2.10 2.00 1.94		3.50 2.57 3.25 5.12
N/10 K_2SO_4	0.71 0.73 0.77 0.77	2.22 2.07 2.15 1.97		3.25 3.27 4.35 3.05
N/10 KNO_3	0.80 0.75 0.82 0.77	2.08 2.64 2.32 2.35		3.00 3.02 3.57 3.07
N/10 (*M*/30) Na_2HPO_4			0.000 0.005 0.65 (Sic) 0.005* 0.006* 0.007*	
N/10 $ZnSO_4$			0.17 0.12 0.17 0.30 0.16	
N/10 $NiSO_4$			0.75 0.55 0.48 0.55 0.90 0.82	

* Temperature varied from 27° to 29°C in these three experiments.

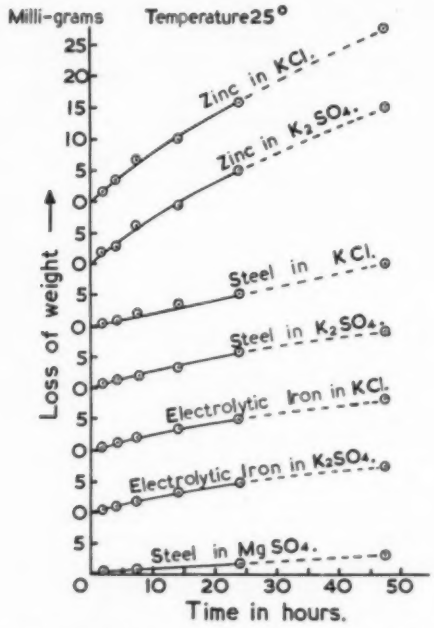

FIG. 11. Some early time-corrosion curves (U. R. Evans)

which afterwards undergoes transformation by interaction with anodic products) caused less attack than the distilled water employed to make it (21, 22). The curves of Fig. 11 show corrosion of partly immersed plates at 25.0°C. The zero points are off-set (otherwise many of the curves would fall on the top of each other), but the gradient of the curves provides a basis of comparison. Magnesium sulphate produces far less rapid corrosion than potassium sulphate, but there is little difference between potassium sulphate and chloride or between electrolytic iron and the steel then used [it was afterwards found by Hoar (13) that different steels corroded at significantly different rates]; the corrosion rate of zinc was much higher.

Starting Places of Attack

The 1929 observations on partly immersed plates brought out the fact that attack started locally on all the metals studied, but spread out on zinc, iron, and copper, while tending to remain localized on aluminium; later work suggested that the spreading was particularly rapid on iron.

The corrosion pattern on steel was rather similar to that on pure iron; actually there were more points of initiation of attack on the purer material which was attributed to greater frequency of rolling defects; however some of the initial attack on pure iron failed to develop. A sand-blasted steel behaved differently from the same steel with an abraded surface, developing a systematic distribution of corrosion spots each marked by a little tuft of rust.

In 1929, I devoted a second research (23) to the discovery of the nature of the starting points. In order to avoid complications due to local oxygen-exhaustion and to the interaction of cathodic and anodic products formed at contiguous points, the specimen was made entirely anodic in an oxygen-free solution of potassium chloride, by means of an external emf. Oxygen was removed by the passage of current between two auxiliary iron electrodes, giving a precipitate which was at first brown, then green, and finally white, indicating a satisfactory removal of oxygen. Passage of current between the auxiliary electrodes was then discontinued, and the experimental specimen was made the anode toward a 4th electrode as cathode. Experiments on pure iron, steel, zinc, and aluminium in different conditions always led to attack starting locally at points which were most numerous near the edges, where the metal had been stressed in cutting. On abraded specimens, the points lay on the major abrasion lines. On rolled specimens, they fell on lines following the rolling direction, even though the rolling had taken place some years earlier. It was suggested in 1929 that the sites of local corrosion represented weak spots where the protective film broke down, but that they could not in all cases be pre-existing gaps; they might be places of surface irregularity or regions where intense internal stresses left in the metal kept the oxide skin in a distended condition. In some instance, it was stated, weak spots undoubtedly coincided with cavities in the metal itself; but the existence of pores in the metal (as such) did not seem to be a necessary condition for localized corrosion. Weak places could be produced artificially in the laboratory, but the uniform groove left by a diamond point was less effective than the irregular scratch made by a steel file. Modern views on oxidation would suggest that, where groups of disarrayed atoms exist below an oxide film, they will possess sufficient energy to pass outward through a film sufficiently thick to resist passage by atoms from parts which are not disarrayed.

Importance of Physical and Chemical Peculiarities in Deciding Corrosion Patterns

All this seems to suggest that the starting points of attack are spots which are *physically*—rather than *chemically*—different from the rest of the surface. Traces of impurity in the metal, in the liquid, may, however, be important in deciding whether or not the starting places develop into pits. Aziz and Godard (24) find that the addition of iron to superpure aluminium increases the probability of pitting, although it has no effect on aluminium of commercial purity. Sometimes the pitting may be due to metal deposited from the water; Porter and Hadden (25) find that 0.02 ppm copper in water can cause trouble. Homer (26), studying localized attack on smooth iron surfaces in chloride-carbonate solutions, found it to take place at the sites of sulphide inclusions; on roughened surfaces, however, the effect of the roughening was more important than the effect of the inclusions. On the smooth specimens the hydrogen sulphide, formed by action of the anodically formed acidity on the sulphides, probably promoted anodic attack (by decreasing polarization), as suggested by statistical work of Hoar and his colleagues (27), as well as by that of Mears (28). On the other hand,

Davies (29) found that the pitting of pure zinc in very pure water followed the same general pattern as that of less pure zinc.

In potassium sulphate solution, I found (30) that two sides of the *same* piece of rolled zinc behaved differently, the duller sides showing *fewer* starting places than the brighter side; starting points were often connected with tiny scratches or rolling defects—where microscopic cavities probably existed; it was found that if the specimens were placed in a closed vessel, which was evacuated before the solution was introduced—a procedure which would facilitate entry of liquid into cavities—the starting of point-corrosion occurred much more quickly. Earlier Seligman and Williams (31) had produced pitting on aluminium by forming small depressions, closing them up with a hammer and placing the aluminium in hard water; they ascribed the pitting and blistering of certain aluminium vessels in hard water to the presence of microscopic cavities, closed over in the rolling process. Recently, Forsyth (32) has found that an aluminium surface, electropolished and then deformed sufficiently to produce gliding, suffers pitting in acid preferentially along the microledges produced where a gliding plane cuts the surface.

Two recent papers on tin suggest that physical and mechanical factors are all-important in deciding the starting points of corrosion. Britton and Michael (33) subjected three varieties of tin to cathodic cleaning and after minimal air exposure (about 25 sec) immersed them in *N* ammonia; all suffered rapid attack. Other specimens were exposed to air for 2 hr before they entered the ammonia; in two cases the corrosion rate was reduced to $^1/_{60}$th of its original value, but the third variety, which carried rolling defects, corroded at the same rate as before, suggesting that it is difficult to produce and maintain a protective oxide film on a defective surface.

Ross (34) transferred the invisible film from air-exposed tin to a sintered glass plate, connected to a manometer, by sticking the tin to the glass with shellac, leaving a central area (1 mm in diameter) free from shellac; the metal was then removed by ferric chloride or fusion in vacuo, leaving the film on the sintered glass. Such a film would normally withstand a small water pressure applied on the outside for 48 hr; but if sodium alkyl sulphate was added to the water, the film began to leak within about 5 min. Now metallic tin suffers pitting when placed in water containing sodium alkyl sulphate. More than one interpretation of Ross' results is possible, but the facts suggest that the oxide film, although normally able to withstand its internal strains, collapses under them in presence of the sodium alkyl sulphate. The criterion for any spontaneous collapse is that the decrease in strain energy brought about by fracture must exceed the increase in interfacial energy involved in the newly formed surface. That the sodium alkyl sulphate does decrease interfacial energy is shown by experiments on tin spheres (oxide-coated, it is presumed); the force needed to separate them in sodium alkyl sulphate is less than half that needed in water or sodium sulphate. The real existence of internal strains in oxide films has frequently been established, notably by the tendency to wrinkle or curl when transferrred to a soft basis such as vaselined glass (34). Thus the argument seems complete.

"Crack-heal"

In 1946 a research (36) on iron suggested that weak points keep appearing spontaneously in the invisible oxide film formed at ordinary temperatures. Heat-tinted steel specimens were inscribed with scratch lines, exposed to air for 5 min, and then immersed in a sodium carbonate-bicarbonate buffer solution, sufficiently inhibitive to confine attack to a few exceptional points situated on these scratch lines. At intervals the specimens were withdrawn in such a way that they came into contact with filter paper soaked in the same solution at the moment of emergence, and remained covered with the wet filter paper for 5 min in air; stains of rust were produced at places where the iron was corroding, and when the specimen was returned to the vessel containing the liquid, the filter paper was preserved as a permanent record of the pattern of rust spots. Five minutes later a fresh pattern was obtained and the specimen again returned to the liquid. This procedure was continued many times. So long as there was no direct exposure to air other than through the wet filter paper, the rusting always continued at the same points; the pattern of rust spots, produced on successive filter papers, remained practically unchanged (Fig. 12). If, however, the specimen was washed, dried, exposed to air for 5 min, and then put back, the same sequence of operations being followed, it was found that attack had ceased at most of the original spots; however, after further immersion in the liquid, new spots started at new points.

The best interpretation of these results is that weak places are developing spontaneously and sporadically in the film. If corrosion is already proceeding at several places along the lines, the new spots receive "cathodic protection," since the metal is being denuded of electrons owing to the corrosion already proceeding, and no fresh corrosion starts at the new points. If, however, most of the corroding points have disappeared because of direct exposure to air, new corrosion starts at some of the spontaneously forming weak points.

We thus get a picture of a process which is conveniently called "crack-heal," although it seems likely that the

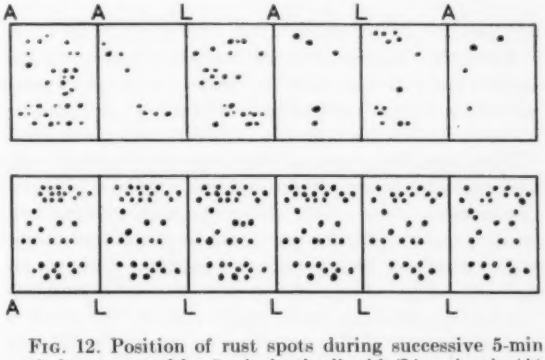

Fig. 12. Position of rust spots during successive 5-min periods, separated by 5 min in the liquid (L) or in air (A) (U. R. Evans).

spontaneous production of weak points is not due to mechanical stresses but to the vagaries of atomic movements which on rare occasions and for short periods leave a chain of structural defects sufficiently continuous to provide an outward path for the iron ions. If the iron is exposed unwetted to dry air, crack-heal will cause local and intermittent thickening of the film on an atomic scale; possibly the very slow increase of weight noted by Vernon (37) on iron even after 50 days' exposure to air (relative humidity, 10%) may be attributed to a crack-heal mechanism.

Although it is probable that crack-heal goes on even in the absence of liquid, contact with water or aqueous solution will modify the results. In presence of certain anions (e.g., Cl^-), metal cations can enter the liquid, and the film, far from being healed, will be undermined, and attack will accelerate. Even if film-forming substances (oxidizing agents or anions forming sparingly soluble salts) are present, some corrosion may occur before repair is definitely established, since in general the liquid near the metal must first become supersaturated and must then produce nuclei before repair takes place. If the liquid contains an organic substance carrying a polar group, the local electrical fields set up where the molecules are adsorbed will probably either aid or retard movement of cations through the film. This may perhaps explain the results of Holness and Ross (38), who found that such substances sometimes accelerate corrosion and sometimes retard it.

It has sometimes been argued that, if the exact nature of the weak places where corrosion starts could be established, so that these points could be eliminated, corrosion would be avoided altogether; unfortunately, this is not always true; elimination of the most sensitive set of points generally causes attack to start at the second most sensitive set which would otherwise be immune. Britton (39) found that plates of a certain iron, finely ground and baked in air for 30 min at 150°C, and then placed vertically in $N/10$ potassium chloride, corroded only along the edges and bottom; but when these edges and bottom had been protected with baking enamel, attack then started at central points, which had been immune on specimens with unprotected edges owing to the cathodic protection afforded by the anodic attack at those edges.

Oxygen as Inhibitor or Corrodent

Consider a number of drops of water placed on an iron surface and surrounded by air. Where a major weak point occurs on the area covered by the drop, corrosion is likely to occur; where there is only a minor weak point, there will be none. Thus, some of the drops develop much rust, others absolutely none. If we surround the drops with oxygen instead of air, only the drops with exceptionally weak spots will develop rust, but these particular ones will rust quicker than in air, since oxygen arriving at the cathodic areas around the points of anodic corrosion accelerates attack at those points. Mears (40) made a statistical study of drops of water on iron below different oxygen-nitrogen mixtures, and found that the proportion of drops developing rust diminished steadily as the oxygen content increased, but that the rate of corrosion attained by those which corroded at all became higher with increasing oxygen content.

Specimens of iron and zinc placed in distilled water under stagnant conditions usually corrode, but this can be avoided by violent relative movement, which will help the renewal of oxygen. An early paper (41), which I contributed by invitation to an American symposium, described how the whirling of pure iron in distilled water containing oxygen prevented almost entirely the rusting which occurred under stagnant conditions. Davies (29) obtained similar results with zinc in extremely pure water. Here corrosion was completely prevented by whirling, but under stagnant conditions small white dots appeared on the surface with pronounced pits below them. Where a polythene thread was stretched over the surface, so as to shield a thin line of metal from oxygen, there were far more pits on the shielded line than on the surrounding area. Evidently those points which were insufficiently weak to develop corrosion with the slow rate of oxygen supply which occurs under ordinary stagnant conditions were able to start corrosion when there was additional shielding from oxygen by the polythene thread. On a vertical zinc surface, particles of corrosion product falling from a pit which had already developed on the upper part of the surface, and lodging at points below it, themselves caused shielding and started pitting where otherwise it would not have occurred. This explained the curious arrangement of the pits on zinc in vertical lines, a phenomenon noted in 1919 by Bengough and Hudson (42).

Even under stagnant conditions, Davies (29) was able to avoid corrosion of zinc by distilled water if oxygen was applied under a pressure of some atmospheres, so that oxygen solubility was increased. He introduced oxygen under pressure into the vessel while the zinc was still dry; afterwards, when water was introduced, pitting was avoided. This plan followed the method of Bengough and Wormwell (43) who had shown in 1934 that on iron high oxygen pressures tend to oppose corrosion.

Presumably if an oxidizing agent much more soluble than oxygen itself could be used, inhibition of corrosion under stagnant conditions would be easily obtained. This is probably the main cause of inhibition of potassium chromate solution, which, as Mayne and Pryor (44) have shown, produces a film which is mainly iron oxide, even when the specimens were free from oxide on immersion in the chromate solution. Chromium compounds are sometimes present in the film, as shown chemically by Hoar (45); also by Brasher and Stove (46) and by Simnad (47), using radioactive tracer methods. It is not certain whether they contribute to the protection; King, Goldschmidt, and Mayer (48) consider that they detract from it.

Salt Solutions

Let us now consider the case where the water contains chloride. If the supply of oxygen is ample, we may still succeed in arresting any metal ions which start to pass outward through some at least of the weak places in the film, so that the oxide film will merely thicken at such points. If the supply of oxygen is insufficient to prevent emergence into liquid at the weakest points, then corro-

sion will set in (provided that the chloride is soluble). If so, the relatively slow arrival of oxygen at the area around the weak point will stimulate the attack, by using up electrons in the cathodic reaction, so that the emergence of metallic ions at the weak point can proceed continuously without accumulation of electric charge. The higher the concentration of chloride, the greater the effect, since points at a greater distance from the weak point can act as cathodes, owing to the greater conductivity of the liquid. On the other hand, at very high chloride concentrations, the oxygen solubility declines, and this usually depresses the corrosion velocity. Provided the oxygen supply has not reached the level at which it prevents corrosion at weak places, the attack becomes more rapid as the oxygen supply increases. Replenishment of oxygen at the area around the weak point will also have the effect of causing trains of chlorine ions to move toward the weak point, thus favouring corrosion.

This will happen even if the distribution of oxygen to all parts of the surface is uniform. The danger of unequal distribution (differential aeration) is that it tends to intensify corrosion if the shielded (anodic) area is small compared to the exposed (cathodic) area. No one has ever claimed that differential aeration is a necessary condition for corrosion in salt solution. The paper (11) in which differential aeration was first discussed makes this quite clear. Comparative experiments were described on (*a*) zinc specimens with virtually the whole area exposed to the liquid, and (*b*) others with part of the area shielded from oxygen; the total corrosion measured was actually *greater* in the first case but it was more intense in the second case, being largely concentrated on the shielded region.

Now consider that sodium phosphate instead of sodium chloride is the chief salt present. The cathodic reduction of oxygen over the main area will cause phosphate ions, instead of chloride ions, to migrate toward the points where, in chloride solution, corrosion would develop. Now, however, solid iron phosphate will be formed at this point, and the leakage will be repaired. At points somewhat less weak, the oxygen supply may be sufficient to carry out the repairs. This doubtless explains the results of Mayne and Menter (49) who found that the film produced on iron which had remained in a solution of disodium phosphate (Na_2HPO_4) containing oxygen, and had escaped visible attack, consisted largely of gamma ferric oxide, but there were inclusions of hydrated ferric phosphate at certain places. It also explains the results of Pryor and Cohen (50) who found that oxygen is required for inhibition by sodium phosphate although, in the absence of oxygen, corrosion, being of the hydrogen evolution type, is commonly slow in almost any slightly alkaline solution.

If, to a chloride solution, sodium phosphate is added with the intention of inhibiting the corrosion of iron, but in insufficient amount, a protective film may be produced over the greater part of the surface, but at the weakest spots, particularly those situated in shielded places where the inhibitor is not readily replenished, corrosion may start; the iron salts there produced may precipitate the phosphate in membraneous form at a slight distance from the points of attack, so that the inhibitor will subsequently fail to reach those places where it is most needed if attack is to be halted. The combination of large cathode and small anode leads to intense attack (for the same reason that attack is intense at a small bare area on steel elsewhere plated with copper). This intensified attack is met with in chloride-phosphate mixtures where contact of, say, a glass rod with the steel provides a shielded area, and also at the meniscus zone of partly immersed specimens. Recent work by Peers (51) has indicated that the intense water line attack in chloride-phosphate solutions, often leading to perforation of steel sheets which elsewhere remain immune, is due to exhaustion of inhibitor at the meniscus crevice.

Alkali as an Inhibitor

Another way of inhibiting the corrosion of iron is by alkali addition. In this case the conversion of oxygen into OH^- ions over the main part of the surface permits the opposite reaction to occur at the weak points, so that instead of metal ions entering the solution, oxide is formed; thus the oxygen arriving over the large area around the weak point can act, as it were, by proxy, at the weak point in question, which is, therefore repaired; evidently a small supply of oxygen per unit area represents a large total if the cathodic area is large, and oxygen can produce inhibition in alkaline solutions where it would cause corrosion in neutral or weakly acid solutions.

This explains some interesting results obtained at the U. S. Bureau of Standards by Groesbeck and Waldron (52). Increase of the amount of oxygen in water brought to a definite *p*H by means of sodium hydroxide and/or carbon dioxide, was found first to increase corrosion, and then to diminish it, the oxygen becoming an inhibitor at high concentrations. The maximum occurred at a smaller oxygen concentration when the *p*H was high than when it was low. The fact that corrosion first increases and then decreases with increasing oxygen concentration is clearly shown in recent work by Uhlig, Triadis, and Stern (53).

Pitting in Water Containing Salts

Since corrosion usually starts locally, there are three possibilities at each point of attack: (*a*) it may heal up; (*b*) attack may remain localized, producing a pit; and (*c*) attack may spread out, giving general corrosion. If the total attack is even partly controlled by the cathodic reaction, pitting must lead to intensified attack, and it is important to know when it will occur.

Corrosion in a salt solution which is nearly neutral at the outset will produce a strongly alkaline reaction at the cathodic area, since reduction of oxygen provides OH^- ions, while liberation of hydrogen uses up H^+ ions. To a lesser extent it may produce acid at points where anodic attack is starting, although not all anodic reactions produce acidity. On zinc, for instance, of the three anodic reactions:

$$Zn = Zn^{++} + 2e$$

$$Zn + H_2O = ZnOH^+ + H^+ + 2e$$

$$Zn + 2H_2O = Zn(OH)_2 + 2H^+ + 2e$$

only the second and third produce acidity. If corrosion is proceeding slowly, so that the amounts of the three products formed correspond roughly to the equilibria

$$Zn^{++} + 2H_2O \leftrightharpoons Zn(OH)^+ + H^+ + H_2O$$
$$\leftrightharpoons Zn(OH)_2 + 2H^+$$

it would be expected that, starting from a neutral solution, the acid-forming reactions will predominate at first; later, when the liquid has become slightly acid, the first should predominate, and the fall in the *p*H should become very slow. An important question is whether the zinc hydroxide concentration formed by the last reaction will ever become high enough to cause the deposition of solid hydroxide; probably this will not be the case, since the *p*H will start to fall at once, so that the third reaction will soon cease to be important, although the second one, which also produces acidity, may continue. If so, the liquid produced at the anodic points should be capable of dissolving the zinc oxide film present on the face of the specimen, since zinc oxide is slightly more soluble than the γ-hydroxide and much more soluble than the ϵ-hydroxide (29).

On metals like aluminium or tin, forming salts very prone to hydrolysis, the acid-forming reactions are likely to predominate until the liquid has become distinctly acid. In both cases, the formation of solid products at the anodic points may be expected. On aluminium, for instance, we have the following possibilities

$$Al = Al^{+++} + 3e$$
$$Al + H_2O = AlOH^{++} + H^+ + 3e$$
$$Al + 2H_2O = Al(OH)_2^+ + 2H^+ + 3e$$
$$Al + 3H_2O = Al(OH)_3 + 3H^+ + 3e$$

The last reaction may be expected to predominate at about *p*H 7, while the first will probably only become important below *p*H 6. The liquid produced at the anode is likely to become supersaturated with respect to the hydroxide and oxide (both very sparingly soluble substances) and is unlikely to be capable of dissolving the oxide film present on the metal; even if it should become theoretically capable of dissolving the film, the rate of dissolution will be very slow, as explained below.

The gradual development of acidity around an aluminium anode (with current supplied from an outside battery) has been followed quantitatively by Edeleanu (54). He reached the conclusion that, on an aluminium specimen immersed in a neutral salt solution (without any current from an external source), those weak points which start to corrode will develop acidity, and the *p*H will sink from 7 to some lower value (perhaps about 5), beyond which it will sink no further, since most of the change will then follow the first (nonacid-forming) reaction; any small amount of acidity still produced will be used up in secondary reactions, such as a local attack of the hydrogen-evolution type. This establishment of acid conditions at the original weak spot will ensure that corrosion, once fairly started, will continue there, in preference to other places, since the first reaction will produce no film and will undermine and remove the film present already.

It may be urged that the anodic reaction should heal the weak point by building up a film of hydroxide. However, Edeleanu has calculated, that, provided the acidity is allowed to accumulate, the *p*H will have sunk to a range at which the first reaction begins to predominate before enough hydroxide has been produced to cover the entire surface. Sometimes, of course, accumulation of acid may be prevented, and then the weak points will heal up. For instance, Wright and Godard (55) showed that rapid movement of water prevents pitting of aluminium; probably it sweeps away the acid. Even under stagnant conditions, the alkali from the cathodic regions may interfere with the accumulation of acid in incipient pits, for instance, if OH^- ions migrate toward the anodic points. Thus it is not surprising that buffer substances promote pitting, since they prevent any large concentrations of OH^- and thus render small the proportion of current carried by OH^- ions. Porter and Hadden (25) found that waters containing calcium bicarbonate often produce pitting, especially if traces of copper are present; doubtless the reaction with alkali helps to keep low the OH^- concentration outside the pits; mounds (largely aluminium hydroxide formed by interaction between anolyte and catholyte) are formed over the pits, and probably prevent the buffer from entering and destroying the acidity within. Farmery's observation (56) that the addition of small amounts of sodium bicarbonate to sodium chloride solution greatly promote the stress corrosion cracking of certain aluminium alloys—another type of localized attack—has probably a similar explanation. Conversely, the prevention of the pitting of stainless steel in chloride solution by means of sodium hydroxide is attributed by Matthews and Uhlig (57) to the neutralization of acid products formed by anodic action.

Eighteen years ago, Hoar (58) studied the corrosion of tin; he reached the conclusion that the first change was a reinforcement of the natural film at certain weak points, along with the accumulation of acid; when the local conditions had become sufficiently acid, the production of soluble tin salts became the main anodic reaction, leading to intense corrosion. He thus explained the "black spots," an old-standing trouble in dairies where tinned equipment was used.

On iron and zinc, the anodic production of acid may not be necessary to prevent healing (their salts hydrolyze less readily, and the production of Fe^{++} or Zn^{++} ions may become important at *p*H values close to neutrality). However, some acidity is undoubtedly formed, and may have another important effect, namely, a dissolution of the oxide film. It is known that zinc oxide, even in the massive form which mineralogists call zincite, is readily attacked by acids, in contrast to aluminium oxide (corundum) which suffers only an extremely slow attack. The direct attack on ferric oxide, which forms the natural film on iron, is very slow, but in contact with the metal, a ferric oxide film suffers rapid reductive dissolution (59, 60). Thus if plates of iron or zinc are partly immersed in sodium or potassium chloride solution in a vertical or nearly vertical position (22), the corrosion which starts at weak points on the face produces a heavy product (an acid solution of ferrous or zinc chloride) which sinks downward and spreads sideways covering an arch-shaped area;

the acid reaction destroys the film, and soon the whole of the arch-shaped area is suffering anodic attack (Fig. 13). Later similar arch-shaped areas develop from other points higher up and in the end nearly the whole immersed area is suffering corrosion, which, being well distributed, is not intense. Mantles of membranous hydroxide are formed along the borders of the arch-shaped areas where anolyte and catholyte interact, and on some types of iron two or three mantles (1, 2, and 3 in Fig. 13) may be produced at successive stages. The corrosion pattern varies with structure and surface condition, but a rather rapid passage from local to general attack is typical of iron and zinc in salt solutions.[3]

The fact that the anodic product does really destroy the oxide film on iron has been demonstrated by special experiments on heat-tinted iron. Each of the specimens used consisted of two rectangular segments mounted in a single plane so that one formed a continuation of the other, the two segments being out of electrical contact and separated by a 1 mm gap; the compound specimen was placed in a sloping position in $N/10$ sodium chloride solution, so that the upper segment passed through the water line. Vertical scratch lines had been traced through the oxide film on the upper segment, exposing the metal, but not on the lower specimen. In general, corrosion started at the scratch lines, and the colours disappeared over arch-shaped areas, around the scratch lines, as would be expected; but the colours also disappeared on the lower segment over streaky areas forming the prolongation of the scratch lines, the oxide film being here destroyed by the heavy anodic products descending from the upper segment.

On aluminium, the spreading of corrosion over arch-shaped areas has not been observed; it would hardly be expected, since the liquid formed at the anodic points will probably be supersaturated with respect to Al_2O_3, and in any case the direct dissolution of alumina by acid is a very slow process. However, there may be some attack at areas originally immune for other reasons. Thus Schikorr (63), studying aluminium in sodium chloride solution, observed that both the primary products, aluminium chloride and sodium hydroxide, can attack the metal with evolution of hydrogen. The attack by alkali would prevent corrosion being confined to the pits; calcium bicarbonate will remove alkali and help pitting. If the liquid contains a trace of copper (either as an original constituent or through the presence of copper in an aluminium alloy) the cathodic deposition of metallic copper may favour pitting, first, by preventing attack at the areas where alkali is formed, and, second, by providing a surface on which the cathodic reaction proceeds efficiently, increasing anodic attack in the pits. Acid liquids behave differently. Bryan and Morris (64), studying solutions containing both citric acid (0.5%) and sodium chloride (0.2 or 2%), noted

[3] Reference should here be made to two early papers which express similar but perhaps not identical ideas. Atkins (61) showed that ferrous salt solutions become acid on standing with precipitation of ferric hydroxide; the pH value may sink to 2.6. Bengough and Wormwell (62), discussing the spreading of corrosion producing from a susceptible spot downward and sideways over an arch-shaped area, emphasize the fact that alkali cannot exist in regions covered by iron salts.

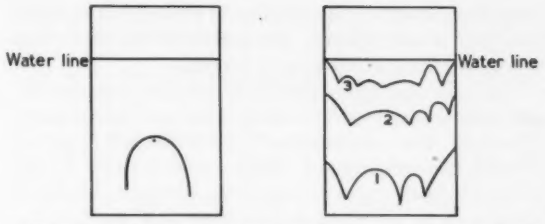

FIG. 13. Arch-shaped extensions of corrosion from a single point (*left*); successive positions of membranes (*right*).

that the attack was most general at the higher chloride concentration and on impure aluminium; the danger of pitting was greatest when the chloride was low and the aluminium "pure" (99.992%).

Other metallic impurities in water may favour pitting. Bird (65) found that small amounts of iron salts reduced the total attack, but tended to localize it as pits; possibly the iron was plated out as a very thin film by simple replacement, which was largely protective, but at discontinuities the combination of large cathode and small anode produced intense attack. Wilkins (66), on theoretical grounds, thinks that all metals more noble than hydrogen will promote pitting, while those less noble than chromium will not do so; the action of intermediate metals is variable.

Pitting in Pure Water

Zinc and iron do not require the anodic production of acid to prevent healing, and since the effect of such acid is to spread out the attack, corrosion is most localized in distilled water. Davies (29) produced very marked pitting of zinc in water of high purity where the formation of acid by traces of foreign anions is extremely unlikely. It might be expected that zinc in distilled water would cover itself with a hydroxide film and suffer no attack. In fact, the attack does tend to stifle itself in time; Bengough, Stuart, and Lee (70) showed that the corrosion-time curve of zinc in distilled water, or even in very dilute potassium chloride, was asymptotic, the corrosion rate ultimately becoming very slow, in contrast to the curves in more concentrated chloride, which were straight. However, the stifling of corrosion only becomes reasonably complete after a lengthy period and meanwhile the attack, becoming increasingly localized, bores down into the metal, producing deep pits. Much of the zinc compound appears, not as a surface film, but as colloidal particles in the liquid; in Davies' work the water acquired the power to produce a good Tyndall cone, and the particles showed cataphoresis in an electric field. The failure to build a protective film rapidly is probably connected with the high nucleation energy of the zinc hydroxides; this is well shown by the fact that the ϵ-hydroxide, which, being the least soluble, should be the most stable, is, under ordinary circumstances, never produced at all (68).

Corrosion of iron seems to show more tendency to spread than that of zinc, although an exact study under comparable conditions of purity seems to be lacking. The author's observations (41) refer to steel in distilled water containing small amounts of carbon dioxide; there seems to have

been some tendency for corrosion to extend, but certainly less than in salt solution. The extension may have been due to reductive dissolution of the film.

The behaviour of aluminium in carefully prepared distilled water has recently been studied at Cambridge by Hart (69). The essential result is film formation; pitting is rare, but intergranular attack, another form of relatively localized corrosion, is met with. Pitting produced on aluminium in hot chromic-phosphoric acid has been examined by Pearson, Huff, and Hay (70) whose electromicrograms suggest that the attack is controlled by crystallographic factors, since the surfaces exposed by it are cube faces; the attack tunnels into the metal along passages which from time to time turn sharply at right angles. Extensive tunnelling of this nature was photographed with the electron microscope in 1951 by Harris and Tull in thin aluminium foil treated anodically in a hot dilute solution of hydrochloric acid and sodium chloride (71).

Final Remarks

The fact that pitting is a form of corrosion having more serious results than general attack has produced the belief that it is an extreme form, and due to some adverse factor not operative in well-distributed corrosion. In fact, however, pitting is an intermediate form standing between general corrosion and immunity; it is essentially a type of "oxidation from a distance" where the collecting area for oxygen is large, the areas where cations leave the metal are small, and where the oxide (hydroxide or basic salt) collects as nodules over the rapidly forming pits. In almost all cases, corrosion starts locally, and if the conditions are such that there is neither healing nor spreading, it remains localized, producing pits which extend inward and/or sideways. The factors deciding the geometry of the advance being essentially crystallographic, are mainly physical, but in some cases the segregation of noble impurities or sulphide inclusions in certain regions may increase the probability of pit-development, while the cathodic deposition of noble metals from the water can increase the severity of pitting and prevent spreading. Thus the situation is often complicated. Nevertheless, pitting is not something mysterious and peculiar, and it is believed that the mechanism of corrosion presented above is capable of explaining the three phenomena—general corrosion, pitting, and immunity.

I commenced my lecture with an appeal for clear thinking; I would end by saying that it should also be broad thinking, not confined to phenomena which happen to be catastrophic, sensational, or financially remunerative. The key to a better understanding of corrosion science may be found in the study of cases of corrosion possessing minor industrial importance. If, for that reason, the experimenter, lacking financial support on a grand scale, has to make do with inexpensive equipment and simple methods, his results may be none the worse on that account. Indeed, simple methods may often give more value than the showy ones, provided always that full use is made of the human brain—a far finer instrument than any produced by stringing together valves or transistors.

Any discussion of this paper will appear in a Discussion Section to be published in the December 1956 Journal.

References

1. D. Eurof Davies, U. R. Evans, and J. N. Agar, *Proc. Roy. Soc. London*, **A225**, 443 (1954).
2. T. Mills, Unpublished work.
3. R. K. Hart, Unpublished work.
4. U. R. Evans, *Rev. Pure and Appl. Chem.* (*Australia*) **5**, No. 1, 1 (1955).
5. N. B. Pilling and R. E. Bedworth, *J. Inst. Metals*, **29**, 529 (1923).
6. U. R. Evans, *Trans. Am. Electrochem. Soc.*, **46**, 247 (especially p. 269) (1924).
7. K. Fischbeck (with L. Neundeubel and F. Salzer), *Z. Elektrochem.*, **39**, 316 (1933); **40**, 517 (1934).
8. C. Wagner and K. Grünewald, *Z. physik. Chem.*, **B40**, 455 (1938).
9. K. Feitknecht (with H. Weidmann and E. Häberli), *Helv. Chim. Acta*, **26**, 1911 (1943); **32**, 2294 (1949); **33**, 922 (1950); R. Petermann, Dissertation, Berne (1945); F. M. Aebi, Dissertation, Berne (1946).
10. C. W. Borgmann and U. R. Evans, *Trans. Electrochem. Soc.*, **65**, 249 (1934).
11. U. R. Evans, *J. Inst. Metals*, **30**, 239 (1923).
12. J. N. Agar, quoted by U. R. Evans, *J. Iron Steel Inst.*, **141**, 220P (1940).
13. U. R. Evans and T. P. Hoar, *Proc. Roy. Soc. London*, **A137**, 343 (1932).
14. G. S. Noordhof, quoted by U. R. Evans, *Proc. International Congress Pure and App. Chem.* (*London*), **5**, 743 (1947).
15. R. H. Brown and R. B. Mears, *Trans. Electrochem. Soc.*, **74**, 495 (1938); **81**, 455 (1942).
16. U. R. Evans, *Nature*, **136**, 792 (1935).
17. R. S. Thornhill and U. R. Evans, *J. Chem. Soc.*, **1938**, 614.
18. U. R. Evans, *J. Soc. Chem. Ind.*, **43**, 315 T (1924).
19. E. Chyżewski and U. R. Evans, *Trans. Electrochem. Soc.*, **76**, 215 (1939).
20. B. L. Cross and N. Hackerman, *Corrosion*, **10**, 407 (1954).
21. U. R. Evans, *J. Soc. Chem. Ind.*, **47**, 55T (1928).
22. U. R. Evans, *J. Chem. Soc.*, **1929**, 111.
23. U. R. Evans, *ibid.*, **1929**, 92.
24. P. M. Aziz and H. P. Godard, *Corrosion*, **10**, 269 (1954).
25. F. C. Porter and S. E. Hadden, *J. Appl. Chem.*, **3**, 385 (1953).
26. C. E. Homer, *Iron Steel Inst. London, Carnegie Schol. Mem.*, **21**, 35 (1932); *Rep. Corr. Com. Iron Steel Inst.*, **2**, 225 (1934).
27. T. P. Hoar, D. Havenhand, T. N. Morris, and W. B. Adam, *J. Iron Steel Inst.*, **133**, 239P (1936); **140**, 55P (1939); **144**, 133P (1941).
28. R. B. Mears, *Iron Steel Inst. Carnegie Schol. Mem.*, **24**, 69 (1935).
29. U. R. Evans and D. Eurof Davies, *J. Chem. Soc.*, **1951**, 2607.
30. U. R. Evans, *J. Soc. Chem. Ind.*, **45**, 37T (1926).
31. R. Seligman and P. Williams, *J. Inst. Metals*, **23**, 159 (1920).
32. P. J. E. Forsyth, *Phil. Mag.*, **45**, 344 (1954).
33. S. C. Britton and D. G. Michael, *J. Appl. Chem.*, **5**, 1 (1955).
34. T. K. Ross, *J. Appl. Chem.*, **5**, 10 (1955).
35. U. R. Evans, "Symposium on Internal Stresses on Metals and Alloys" (Inst. Met.) p. 291 (1948).
36. U. R. Evans, *Nature*, **157**, 732 (1946).
37. W. H. J. Vernon, *Trans. Faraday Soc.*, **31**, 1668, esp. p. 1671 (1935).
38. H. Holness and T. K. Ross, *J. Appl. Chem.*, **1**, 158 (1951); **2**, 520, 526 (1952).
39. S. C. Britton and U. R. Evans, *Trans Electrochem. Soc.*, **61**, 441, esp. p. 454 (1932).
40. R. B. Mears and U. R. Evans, *Trans. Faraday Soc.*, **31**, 527, esp. p. 530 (1935).
41. U. R. Evans, *Ind. Eng. Chem.*, **17**, 363 (1925).

42. G. D. Bengough and O. F. Hudson, *J. Inst. Metals*, **21,** 37, esp. p. 59 (1919).
43. G. D. Bengough and F. Wormwell, *Report Chem. Res. Board 1935–37* (H.M.S.O.) p. 17 (1938).
44. J. E. O. Mayne and M. J. Pryor, *J. Chem. Soc.*, **1949,** 1831.
45. T. P. Hoar and U. R. Evans, *ibid.*, **1932,** 2476.
46. D. M. Brasher and E. R. Stove, *Chem. Ind.*, **1952,** 171.
47. M. T. Simnad, "Properties of Metallic Surfaces," Inst. Met. p. 23 (1953).
48. C. V. King, E. Goldschmidt, and N. Mayer, *This Journal*, **99,** 423 (1952).
49. J. E. O. Mayne and J. W. Menter, *J. Chem. Soc.*, **1954,** 103.
50. M. J. Pryor and M. Cohen, *This Journal*, **98,** 263 (1951); **99,** 542 (1952); M. J. Pryor, *Corrosion*, **9,** 467 (1953).
51. A. M. Peers and U. R. Evans, *J. Chem. Soc.*, **1953,** 1093.
52. E. C. Groesbeck and L. J. Waldron, *Proc. Am. Soc. Testing Materials*, **31,** II, 286 (1931).
53. H. H. Uhlig, D. N. Triadis, and M. Stern, *This Journal*, **102,** 59 (1955).
54. C. Edeleanu and U. R. Evans, *Trans. Faraday Soc.*, **47,** 1121 (1951); C. Edeleanu, *J. Inst. Metals*, **80,** 187 (1951–52); *also* C. Edeleanu, Private communications.
55. T. E. Wright and H. P. Godard, *Corrosion*, **10,** 195 (1954).
56. H. K. Farmery, Dissertation, Cambridge (1955).
57. J. W. Matthews and H. H. Uhlig, *Corrosion*, **7,** 419 (1951).
58. T. P. Hoar, *Trans. Faraday Soc.*, **33,** 1152 (1937).
59. U. R. Evans, *J. Chem. Soc.*, **1930,** 478.
60. M. J. Pryor and U. R. Evans, *J. Chem. Soc.*, **1949,** p. 3330; **1950,** 1259 (4 papers).
61. W. R. G. Atkins, *Trans. Faraday Soc.*, **18,** 310 (1922–23).
62. G. D. Bengough and F. Wormwell, *Proc. Roy. Soc.* **A140,** 399 (esp. p. 405) (1933).
63. G. Schikorr, *Mitt. Mat. Prüfungs-anstalten, Sonderheft*, **22,** 22 (1933).
64. J. M. Bryan and T. N. Morris, *J. Soc. Chem. Ind.*, **59,** 159 (1940).
65. C. E. Bird, Dissertation, Cambridge (1955).
66. N. J. M. Wilkins, Atomic Energy Research Establishment M/R 1296, (Nov. 1953). Abstract in Bulletin of British Non-ferrous Metals Research Association, p. 156, April 1955.
67. G. D. Bengough, J. M. Stuart, and A. R. Lee, *Proc. Roy. Soc.*, **A116,** 425 (1927); **121,** 88 (1928); **127,** 42 (1930).
68. F. M. Aebi, Dissertation, Berne (1946); W. Feitknecht and E. Häberli, *Helv. Chim. Acta*, **33,** 922 (1950).
69. R. K. Hart, Unpublished work.
70. E. C. Pearson, H. J. Huff, and R. H. Hay, *Can. J. Tech.*, **30,** 11 (1952).
71. A. L. Williams, Private communication.

THE ELECTROCHEMICAL SOCIETY, INC.

The Electrochemical Society is an international organization of individuals and companies concerned with or interested in Electrochemistry and allied subjects.

The Society is dedicated to the advancement of the theory and practice of Electrochemistry and related subjects, as shown in the following divisions:

Battery	Electro-Organic
Corrosion	Electrothermics and Metallurgy
Electric Insulation	Industrial Electrolytic
Electrodeposition	Theoretical Electrochemistry
Electronics	

Among the means to this end are the holding of meetings for the reading and discussion of professional and scientific papers on these subjects, the publication of such papers, discussions, and communications as may seem appropriate, and cooperation with chemical, electrical, and other scientific and technical societies.

It is an incorporated society without capital stock. The affairs of the Society are managed by a Board of Directors under a Constitution and Bylaws. Officers are nominated by a nominating committee appointed by the Board of Directors and elected by the members.

Direct all general correspondence and inquiries regarding membership to Society headquarters at 216 West 102nd Street, New York 25, N. Y.

Officers of the Society

President ..... HERBERT H. UHLIG
Past President ..... MARVIN J. UDY
Vice-President ..... HANS THURNAUER
Vice-President ..... NORMAN HACKERMAN
Vice-President ..... SHERLOCK SWANN, JR.
Treasurer ..... LYLE I. GILBERTSON
Secretary ..... HENRY B. LINFORD

Ulick Richardson Evans[1]

R. B. Mears[2]

Tonight we are assembled to honor a great man—a leader in his chosen field of science. Dr. Evans is outstanding as an experimental electrochemist. His genius is to plan and carry out critical experiments on fundamental mechanisms without using involved or complicated equipment. With a minimum of apparatus, he obtains a maximum of precise data. His experimental findings he presents in papers of great lucidity and clarity.

Whence came his love of the experimental approach? Whence came his ability to express his results in an interesting and precise fashion?

We learn that Dr. Evans' father, Richardson Evans, was a lead writer on the "Standard" and the author of several books, some devoted to political and economic subjects and others dealing with the preservation of natural beauty. His mother's family was also literary. His maternal grandfather, uncle, and cousin were all associated with the "Birmingham Daily Post." Thus, Ulick Evans was exposed at an early age to the precise and interesting expression of ideas in words.

Ulick Evans' father also delighted in chemical experiments, which he sometimes performed for the entertainment of his family. Consequently, as a youth, Ulick Evans was introduced to chemistry in a particularly fascinating form.

Richardson Evans had several scientific friends, so that while still a young man Ulick Evans became familiar with laboratory work in electricity, physics, and other sciences. During a visit to the laboratory of Professor C. V. Boys, Ulick Evans was first caused to consider metallic corrosion. Professor Boys had well-fitting tool cupboards in his laboratory, and he pointed out to Ulick Evans that "It is not the damp that causes tools to rust, it is the dust."

From 1902 to 1907 Ulick Evans attended Marlborough College. Here he had his initial formal training in science under Mr. Reginald Durrant, an enthusiastic chemist. Here, also, Ulick Evans was introduced to the subject of probability by Mr. J. J. Taylor, the mathematics master. Thus, at an early age he became accustomed to think "in terms of probability."

Between 1907 and 1911, Ulick Evans was at King's College, Cambridge. His subjects were chemistry, physics, geology, and mineralogy. He was particularly interested in geology, but finally decided to specialize in chemistry. As an undergraduate, he did no official research, but unofficially he worked in Mr. Heycock's laboratory on the separation of metals by electrochemical means. He took the B.A. degree in 1910 and the M.A. in 1914.

After leaving Cambridge he studied for a year with Professor Fresenius at Wiesbaden, then worked from 1912 to 1914 in the laboratory of Dr. Samuel Rideal in London. During this period, he started writing the book "Metals and Metallic Compounds." World War I interfered with this project, so that the book was not published until 1923. During the writing of this book, it became evident to Ulick Evans that scientific knowledge of corrosion processes was sadly lacking. Therefore, even before the book was published, he started experimental work in this field at Cambridge. His researches in corrosion were described in a series of technical papers, which attracted the attention of workers in electrochemistry and corrosion all over the world. This work also attracted a series of research students who wished to continue their training under Dr. Evans' guidance. The first of these was L. C. Bannister. Later, S. C. Britton, T. P. Hoar, A. J. Gould, C. W. Borgmann, H. A. Miley, Paul Queneau, F. W. Fink, K. G. Lewis, Michael Pryor, J. E. D. Mayne, M. T. Simnad, Morris Cohen, and your present speaker were among those who had the privilege of working under Dr. Evans' direction.

We all found it an extremely valuable experience. Dr. Evans was a stimulating and understanding supervisor. He treated each of us as an equal, and as a result we all tried to do the very best we could to live up to his expectations. His thoughtfulness and wisdom made our time at Cambridge the most pleasant and active period in our lives.

His devotion to science could not help but make a deep impression on us. Here was a man who was world renowned in his field, yet who would cheerfully spend his own income to further scientific experiments, instead of using his technical ability to build up a large personal fortune. To Dr. Evans, science is its own reward, not merely a means of attaining an appropriate standard of living.

In 1932 Ulick Evans was awarded the Sc.D. at Cambridge, and in 1949 an Honorary Sc.D. was conferred on him by the University of Dublin. The Royal Society awarded him the Armourers' and Brasiers' Research Fellowship in 1933, and in 1950 he was elected a Fellow of the Royal Society.

In 1948, he received the Willis Rodney Whitney Award from the National Association of Corrosion Engineers for contributions to the science of corrosion.

Dr. Evans has written several books and over two hundred technical papers. His researches have covered the entire field of reactions of metals with their environment. He early espoused the electrochemical theory of

[1] Banquet Address before presentation of the Palladium Medal to U. R. Evans at the Pittsburgh Meeting, October 11, 1955.

[2] Applied Research Laboratory, United States Steel Corp., Monroeville, Pa.

corrosion, and in 1932 his work provided the first experimental proof of this theory. He also proved that the bright colors that formed on metal surfaces exposed to air or to sulfur compounds at elevated temperatures were caused by light interference, just as are the colors of oil films on water. In experiments of great ingenuity and beauty, he succeeded in isolating and studying in detail these fragile films.

He pointed out and proved the influence of oxygen concentration cells—differential aeration—in causing much of the commonly encountered and severely localized corrosion of metal structures. He established in critical experiments the value of inhibitive pigments in paint primers, and did much to resolve the mechanism of inhibitor action. In the field of cathodic protection, he was the first to show that there was a sharp change in slope in the current-potential curve when the critical current density for cathodic protection was attained. He was the first to apply statistical methods to corrosion studies.

In no other field of scientific endeavor has one man exerted such a dominant influence. It is impossible to discuss any phase of corrosion research without conidering the contributions of Dr. Evans. There is probably no research worker in this field whose outlook has not been influenced by direct or indirect contact with Dr. Evans' work.

In addition to his intense devotion to science, Ulick Evans has many other interests. He has long been active in organizations devoted to preservation of the beauty of the English countryside. One of the organizations in which he has been particularly interested is the Scapa Society, which was founded by his father. This society has done much to limit the disfigurement of the landscape by advertising billboards. The activities of such a society in the United States would also be greatly appreciated.

Dr. Evans has also been a keen cross-country runner, swimmer, and mountaineer. He has served as an officer of the Cambridge Hare and Hounds Club and has devoted considerable time and energy to climbing the Austrian and Swiss Alps. In a word, he has been as active physically as he is mentally.

The Palladium Medal Committee and The Electrochemical Society are to be congratulated on the selection of this world-famous scientist to receive the 1955 Palladium Medal.

MANUSCRIPTS AND ABSTRACTS FOR FALL MEETING

Papers are now being solicited for the Fall Meeting of the Society, to be held at the Statler Hotel in Cleveland, September 30, October 1, 2, 3, and 4, 1956. Technical sessions probably will be scheduled on Batteries, Corrosion, Electrodeposition, Electrothermics and Metallurgy, and Theoretical Electrochemistry; (joint symposium with Electrodeposition).

To be considered for this meeting, triplicate copies of abstracts (not to exceed 75 words in length) must be received at Society Headquarters, 216 West 102nd St., New York 25, N. Y., *not later than June 15, 1956. Please indicate on abstract for which Division's symposium the paper is to be scheduled.* Complete manuscripts should be sent in triplicate to the Managing Editor of the JOURNAL at the same address.

***

The Spring 1957 Meeting will be held in Washington D. C., May 12, 13, 14, 15, and 16, at the Statler Hotel. Sessions will be announced in a later issue.

Current Affairs

San Francisco Meeting—April 29 to May 3, 1956

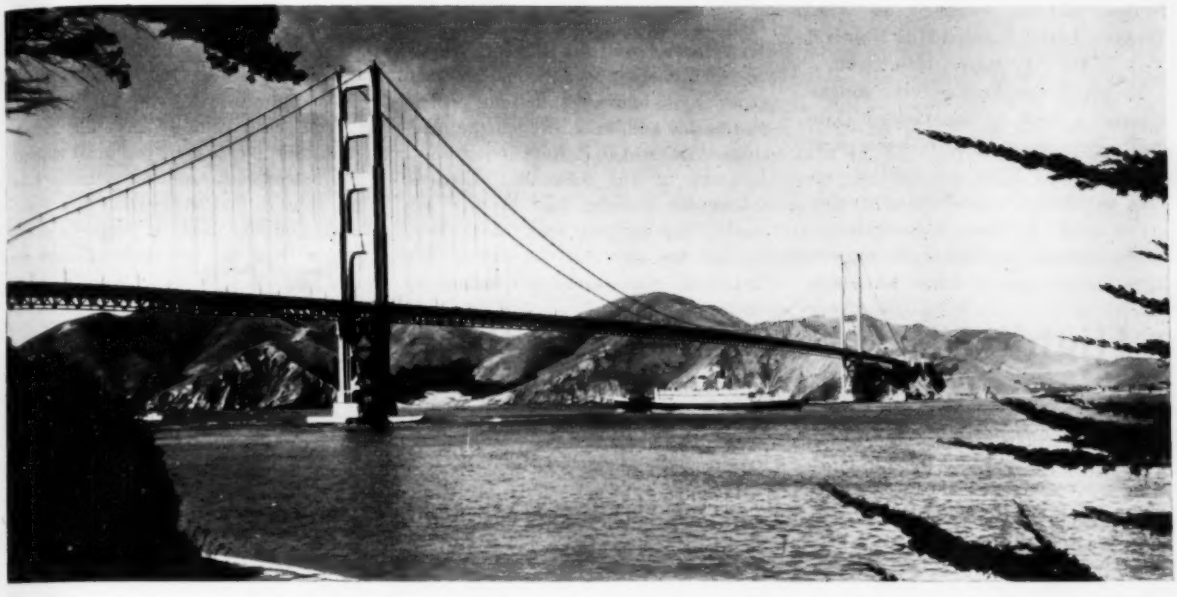

San Francisco's Golden Gate Bridge, the world's longest single span

The spring meeting of the Society will be held April 29 to May 3 in San Francisco, Calif., at the Mark-Hopkins Hotel. When making reservation requests, which should be sent directly to the hotel, please be sure to mention The Electrochemical Society.

The members of the Local Committee in charge of the convention are: R. L. Baldwin, Honorary Chairman; R. F. Bechtold, General Chairman; M. Feinleib, Arrangements; D. V. Doub, Entertainment; R. L. Zimmerly, Finance; C. W. Tobias, Plant Trips; H. F. Myers, Publicity; J. F. Aicher, Registration and Hotel; and Mrs. R. L. Baldwin, Honorary Chairman, and S. L. Dreisbach, Arrangements, Ladies' Entertainment.

Technical Program

The following Divisions have planned technical sessions: Corrosion (joint symposium with Theoretical), Electric Insulation, Electronics (including Instrumentation, Luminescence, Oxide-Cathodes, Phosphor Application, and Semiconductors), Industrial Electrolytics, Electrothermics and Metallurgy, and Theoretical Electrochemistry.

Special Symposia

Three special symposia are planned: (*a*) semiconducting materials, surface controlled phenomena, and chemical process technology, sponsored by the Semiconductor Group of the Electronics Division; (*b*) "Rare Earths" and "Electric Arcs in Inert Atmospheres and Vacuum," sponsored by the Electrothermics and Metallurgy Division; (*c*) "Adsorption Phenomena at Electrode Surfaces," sponsored by the Theoretical Electrochemistry and Corrosion Divisions.

Plant Trips

A plant trip is scheduled for Stanford Research Institute, Stanford, Calif., located adjacent to the campus of Stanford University near Palo Alto. It is the outstanding installation of its kind in the West and is rated very highly throughout the nation. Another trip is scheduled for the Radiation Laboratory at the University of California, Berkeley. Here much of the most important work on nuclear developments and atomic energy has been done.

Other Activities

It is planned to offer a few post-convention tours such as Yosemite Park and Monterey Peninsula (including Carmel, Calif., and the Seventeen Mile Drive). Plans on these functions are not yet complete; further information will appear in a subsequent issue of the JOURNAL. Information on other trips will be available at the registration desk at the meeting and can also be obtained by writing to the San Francisco Convention and Visitors Bureau, Civic Auditorium, San Francisco 2, Calif.

A well-rounded Ladies' Program is now in the process of being worked out.

Further details on the meeting will appear in the February JOURNAL.

What to See and Do in San Francisco

There is much to see and do in this fascinating metropolis. Here are a few of the things you must not miss.

Swing aboard one of the cable cars and high you go, up the hills. Buy flowers from the colorful sidewalk flower stands. Explore fabled Chinatown—where America suddenly seems to be 6000 miles away. Visit the Oriental telephone exchange where calls are given by the subscribers' names instead of by numbers.

Don't miss the Fisherman's Wharf—a bit of Naples to the eye, a bit of heaven

to your nostrils if you like fresh seafood. Drive on down the Marina, view the gay boats in Yacht Harbor. Survey the city by night atop Telegraph Hill where you can see both the Golden Gate Bridge and the San Francisco Bay Bridge, Alcatraz seemingly so close! Treasure Island, Russian Hill, Nob Hill —all of the city spread before you.

No trip to San Francisco is complete without a visit to the Golden Gate Park whose thousand acres are a paradise reclaimed from the sand dunes. This, the place where, a local newspaper in 1880 said, "a blade of grass cannot be raised without four posts to support it," is now a garden of drives, lakes, and groves. Here can be found the De Young Museum, rare and colorful tropical fish in the Steinhart Aquarium, the remarkable African collection of animals in the adjoining Academy of Sciences Building. You would not want to miss a walk through the nearby Oriental Tea Garden. We suggest that you stop there for a cup of tea. If you have the time, drive out to Fleishhacker Pool (the largest outdoor swimming pool in the world) and walk through the magnificent zoo next to it. Return downtown by way of the residential districts, taking the winding road up to Twin Peaks—the lookout spot that shows you all the city and the surrounding Bay and Mt. Davidson, highest of San Francisco's peaks. Stop at Mission Dolores, the church where San Francisco was born, for a quiet restful visit to the past.

Fine food is traditional in this city. Every nation is represented. One may truly "eat around the world" here. Enrico Caruso, saturated in San Francisco food once, sighed: "There is a diabolical mystery to your San Francisco. Why isn't everyone fat?"

You will have to discover the restaurants that please you, you must explore the magnificent hotels, you must take the time to find the part of San Francisco you like best. It requires much longer than the few days allotted for this visit.

Highlights of the Meeting of the Board of Directors

Held October 9, 1955, at the Hotel William Penn, Pittsburgh, Pa.

Communications from the President

President H. H. Uhlig announced that The Electrochemical Society of Japan will start, on January 1, 1956, to publish abstracts of their papers in English. This will materially assist American scientists in utilizing the information contained therein.

President Uhlig also reported on efforts he is making to arrange a joint symposium on passivity with the Faraday Society.

Communications from the Treasurer

Dr. L. I. Gilbertson reported that his policy as Treasurer would be to make periodic reports on the cash and bonds of the Society, as shown below, and that each January 1 all principal securities will be listed.

TOTAL CASH AND BONDS

Acheson Fund, Guaranty Trust Co.			
Principal Securities 1/31/55		$36,486.50	
Income Account Balance 8/31/55		1,696.82	
Total Fund Value, 8/31/55			$38,183.32
Weston Fund, The Hanover Bank			
Principal Securities 1/1/55	$13,548.33		
Principal Account Balance 1/1/55	72.51	13,620.84	
Checking Account Balance 8/31/55		1,228.69	
Total Fund Value, 8/31/55			14,849.53
Consolidated Fellowship Fund			
Wellington Fund Securities 8/31/55		10,674.44	
Fundamental Investors, Inc., Securities 8/31/55		10,985.86	
National City Bank Balance 8/31/55		21.95	
Total Fund Value, 8/31/55			21,592.25
Corrosion Handbook Fund			
U. S. Savings Bonds, Chemical Corn Exch. Bank		10,471.37	
New York Savings Bank Balance 8/31/55		1,764.45	
Millbury Savings Bank Balance 8/31/55		5,000.00	
Total Fund Value, 8/31/55			17,235.82
Richards Memorial Fund, Central Savings Bank Balance, 8/31/55			769.72
Columbus Convention Fund, U. S. Govt. Bonds, Chemical Corn Exchange Bank			400.00
General Reserve Fund			
Principal Securities, Chemical Corn Exchange Bank		1,000.00	
National City Bank Balance, 8/31/55		24.00	
Total Fund Value, 8/31/55			1,024.00
Publication Reserve Fund, National City Bank Balance, 8/31/55			3,654.52
Electrodeposition Division, National City Bank Balance, 8/31/55			1,587.20
Faraday Society, National City Bank Balance, 8/31/55			462.00
Deutsche Bunsen Gesselschaft, National City Bank Balance, 8/31/55			108.00
General Fund			
U. S. Government Bonds, Chemical Corn Exchange Bank		17,988.63	
Chemical Corn Exchange Bank Balance 8/31/55		1,228.46	
National City Bank Balance, 8/31/55		7,429.83	
Total Fund Value, 8/31/55			26,646.92
TOTAL CASH AND BONDS, AUGUST 31, 1955			$126,513.28

Communications from the Secretary

The current financial situation indicates that we should end this year with a healthy surplus.

The Secretary announced that the 100th anniversary of the birth of Dr. Edward Goodrich Acheson would be celebrated in 1956. It was agreed that the Acheson Award Committee would study the matter of cooperation with Acheson Industries in arranging this celebration.

The Secretary then reported that the American Standards Association had invited The Electrochemical Society to be

represented on the Chemical Industry Advisory Board. On motion of Dr. Hans Thurnauer, it was voted that we be represented on this Board and that Hans Neumark be our representative.

The Secretary then reported on a letter received from the Chairman of the Cleveland Section concerning the problem of payment of first year's dues. In the case of applications for membership made at meetings, the $9 dues would be attached to the application blank.

The request of Mr. Jack Bain that the readers' service card be continued was discussed, and, in the light of the good response so far received, on motion of Dr. Norman Hackerman, it was voted that the readers' service card be continued until further Board action. It was agreed, however, that the topic of the readers' service card would be placed permanently on the agenda for future Board meetings.

Future Meetings

San Francisco

The San Francisco Section requested review of the recent Board action raising nonmember registration fees another $3. On motion of Dr. F. A. Lowenheim, it was voted that, for the San Francisco Meeting, the Board rescind the action to boost nonmember registration fees $3.

Reports of Committees

Palladium Medal Committee

The Palladium Medal Committee, composed of R. M. Burns, W. D. Robertson, J. C. Warner, and H. H. Uhlig, drew up rules that had previously been distributed to the Board of Directors, and, on motion of Dr. Hackerman, it was voted that the rules be accepted. These rules will be published soon.

Ways and Means Committee

With regard to financing conventions, under Plan B there is no question. Under Plan A, the Committee favored a sliding scale for the distribution of excess income. It was the recommendation of the Ways and Means Committee that the Cleveland Meeting be used as a guide in this matter; the Secretary was instructed to draw up a budget, but, at the same time, the Cleveland Meeting would operate on the basis of a $3 head tax for registrants. In other words, the fiscal policy used will be that of the current Plan A of the Bylaws. However, data will be collected to make it possible to set up a sliding scale.

The Ways and Means Committee recommended that the local committee should police sessions to insure that all those attending social and technical functions are registered at the meeting.

On motion of Dr. Lowenheim, it was voted that the Secretary be instructed to prepare a new Directory, so priced as to be self-supporting. It was agreed that both alphabetical and geographical listings are necessary, as well as a list of honorary members and receivers of awards.

The Ways and Means Committee felt that we are losing members by the mechanism of accepting them, and they recommended that two out of three references should be used rather than two out of two. Furthermore, the Secretary pointed out that it was not generally known that, if the sponsor signs the application blank, there is no time delay, since a reference blank is not needed. This information should be publicized. The question of changing the number of sponsors was referred to the Membership Committee.

Constitution and Bylaws

The Committee on Constitution and Bylaws recommended three changes in the Bylaws that were approved: (*a*) the inclusion of the Palladium Medal in the Bylaws, (*b*) giving regional editors Bylaw status, and (*c*) permission to attend Board meetings at the invitation of the President.

Survey Committee

A verbal interim report of the Survey Committee was made by Ralph Schaefer. He reported that conversations were held with Dr. R. M. Burns and Mr. F. L. LaQue, and that the Committee spent two days in the New York office. They felt that their primary duty is to develop the financial and human resources of the Society. Findings indicated that our publication costs are definitely in line with other publications, as are the over-all expenses of the Society. He then pointed out that the Survey Committee felt that an Assistant Secretary should be hired as soon as possible; retired businessmen should be a good source. It is obvious that such people are available since a single insertion in the New York Times elicited 67 replies.

The matter of bonding the office force was discussed and, on motion of Dr. Sherlock Swann, it was voted that the office force be bonded to the extent of $25,000.

Publications Committee

Dr. Burns gave a report on the status of the JOURNAL. He also reported that Dr. C. V. King recently had been made Editor.

Membership Committee

Dr. J. R. Musgrave received approval of the following appointments to this Committee:

Division	*Representative*
Battery	C. K. Morehouse
Corrosion	H. R. Copson
Electric Insulation	A. Gunzenhauser
Electrodeposition	R. A. Wooftер
	Fielding Ogburn
Electro-Organic	Hans Neumark
Electrothermics and Metallurgy	A. C. Haskell
Industrial Electrolytic	Fred Koerker
Electronics	A. E. Middleton
	R. H. Cherry
	A. E. Hardy
Theoretical Electrochemistry	Sigmund Schuldiner

Local Section	*Representative*
New York	P. L. Howard
Niagara Falls	R. P. Stambaugh
Philadelphia	H. J. Strauss
Pittsburgh	Leslie Lancy
Washington-Baltimore	Sigmund Schuldiner
Ontario-Quebec	R. R. Rogers
Cleveland	John Yeager
Pacific Northwest	M. J. Pryor
San Francisco	J. F. Aicher
Detroit	No appointment
Chicago	C. A. Hampel
Midland	F. S. Sibley

Becket Award Committee

Mr. A. C. Haskell reported for this Committee. The rules for regulating this award were discussed, with some changes approved. These rules will be published shortly.

New Business

Mr. N. C. Cahoon announced that the Battery Division

is considering a Battery textbook and Mr. G. W. Heise has been selected as Editor.

The meeting was adjourned at 5:45 P.M.

HENRY B. LINFORD, *Secretary*

Addendum

On Tuesday, October 11, 1955, an informal vote was taken on the following motion:

"That the opportunity be made available to companies to financially support The Electrochemical Society by providing a status of Patron, a fee of $1,000 yearly to be assessed all Patrons."

More than 50% of the members of the Board were contacted, with 100% of those contacted voting affirmatively. It was therefore considered that this motion be passed.

Pittsburgh in Retrospect

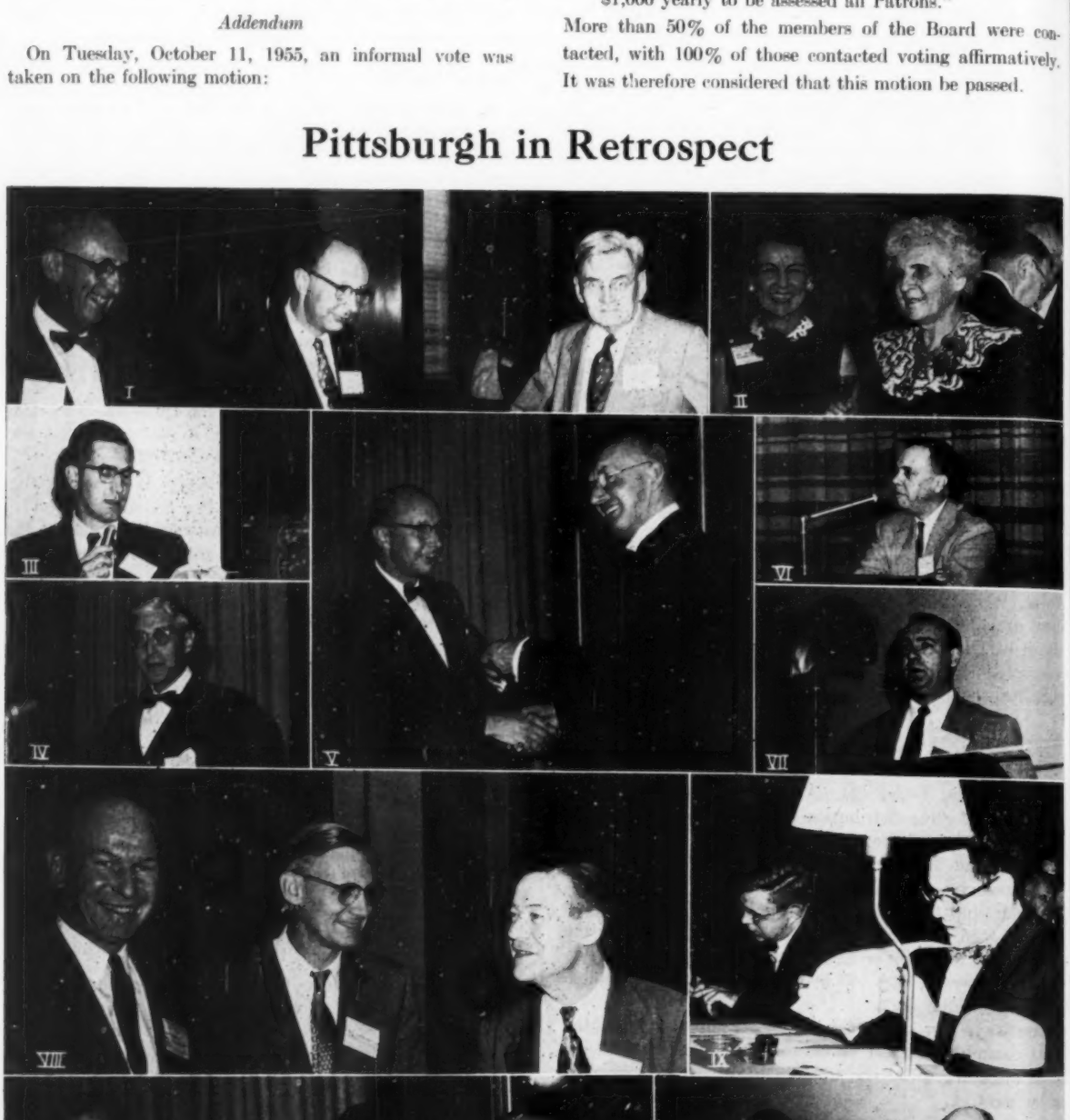

Snapped at the Pittsburgh Meeting. I—R. M. Burns, H. H. Uhlig, and G. W. Heise; II—Mrs. Bruce Bailey and Mrs. Lottie Fink; III—R. B. Hoxeng; IV—R. B. Mears; V—Dr. H. H. Uhlig presenting the Palladium Medal to Dr. U. R. Evans; VI—E. M. Sherwood; VII—M. J. Allen; VIII—C. A. Snavely, P. L. Howard, and C. V. King; IX—J. Kruger and E. W. Johnson; X—H. B. Linford, Norman Hackerman, and J. C. Warner; XI—G. E. Doan and U. R. Evans. (Photographs by Jack Noll, Pittsburgh.)

Registrants at the Pittsburgh Meeting, October 9 to 13, 1955, numbered 546, just 16 less than the total at Boston which was the biggest fall meeting of the Society.

The registration desk, meeting rooms, and Secretary's office were all on the 17th floor of the Hotel William Penn; with this setup it seemed a little easier to find people, deliver messages, and keep up with everything that was going on.

Some meeting rooms reached the S.R.O. status, proving that it's impossible to guess four months ahead of time what session attendance will be; for the most part, meeting rooms were adequate, sessions well attended.

Dr. U. R. Evans' Palladium Medal lecture appears on p. 73 of this issue. One of his former students, Dr. R. B. Mears, introduced (see p. 9C of this issue) the Medalist at the banquet given in Dr. Evans' honor on Tuesday, October 11, at which several of his former students were present. The Tamburitzans from Duquesne University provided the light entertainment for the evening with their colorful Southern Slovakian songs and dances.

The ladies enjoyed a well-planned, interesting program, including a trip to Fort Ligonier. Even the weather was on the Society's side, at least until the last day of the meeting.

The Local Committee for the meeting earned the thanks of members, guests, and ladies; they did a good job.

DIVISION NEWS

Battery Division

The Battery Division held four very successful technical sessions at the Pittsburgh Meeting of the Society. Three of these sessions were round tables with the discussion in each guided by a panel of experts who talked briefly on some aspect of the subject. The general topic of the round tables was the keeping qualities or shelf-life of batteries. This is a problem that is pertinent to all types of batteries. One round table considered the production of "Dry-Charged" lead-acid storage batteries. The other two discussed the reactions at anode and cathode, respectively, which limit or reduce shelf-life. The opening session consisted of four research papers.

The annual Battery Division business meeting was held on October 11, 1955 in the Allegheny Room of the William Penn Hotel following the morning technical session. Presiding at the meeting was the Division Chairman, Dr. N. C. Cahoon. Because this was an odd-numbered year there were no officers to elect and the meeting was brief.

The Secretary-Treasurer reported that the membership in the Division now numbered 223. During the year 31 new members were added, with 3 lost by resignation, and 1, Professor Wendell Latimer, lost through death. A balance of $531.22 was reported in the treasury. The issuing of extended abstracts for the Boston Meeting resulted in all Battery Division members receiving free copies, and enough copies were sold to nonmembers to pay all costs and show a profit of $72.25.

The committee, headed by Dr. E. A. Schumacher, which is studying the question of establishing a Battery Division award for outstanding attainment in the field of Battery Science reported that further study was needed on the details of handling it. There was general agreement that such an award would be beneficial to the Division only if properly organized and administered.

The editor of the Battery Division sponsored book on "Primary Cells," Mr. George Heise, told of the progress made in the preliminary negotiations with publishers, and the other details that precede the actual writing of an edited volume.

Dr. W. H. Stoll, who is to be the General Chairman of the 1956 Society meeting in Cleveland, was introduced and invited all to attend the Cleveland Meeting.

The Division luncheon featured a very timely and interesting lecture and demonstration by Dr. E. J. Stansbury of the Solid State Devices Development Department of the Bell Telephone Laboratories. Dr. Stansbury demonstrated the device popularly called the "Bell Solar Battery." The first use of this device to power a rural telephone line in Georgia was announced in the newspapers only several days prior to this talk. Of special interest to the Battery Division are the rather severe requirements which must be met by the storage battery that stores the energy of the "Solar Battery" during the periods of light and permits operation during the night. The luncheon was attended by 125 members and guests.

E. J. Ritchie,
Secretary-Treasurer

Corrosion Division

The Corrosion Division held its annual meetings, consisting of 8 half-day sessions for the presentation of technical papers, at the fall meeting of the Society in Pittsburgh. Two sessions were devoted to a symposium on Metal Oxidation, two to Kinetics of Corrosion Reactions, two to a third symposium on The Role of Surface Films in Corrosion, and the final two sessions to general papers. The two appointive members of the Divisional Executive Committee, J. E. Draley and R. B. Hoxeng, deserve credit for organizing a considerable part of the excellent program. The meetings were well attended, and interest was maintained until adjournment of the final session.

The annual luncheon was held on October 12, 1955 with U. R. Evans as guest of honor. After a brief talk by Dr. Evans the annual business meeting was convened by Chairman J. V. Petrocelli. The Secretary-Treasurer reported no income or expenditure during the year, with a balance of $32.18 in the treasury. He called attention to the previous distribution of revised Divisional Bylaws and the announcement of a ballot for their adoption. The Chairman announced that plans were under way for a joint symposium with the Theoretical Division at the spring meeting in San Francisco.

The revised Bylaws, with small changes suggested by J. E. Draley, were adopted without dissent. The nominating committee (N. Hackerman, M. C. Bloom, F. Fink) presented the following slate of candidates for office during the coming year:

Chairman—T. P. May
Vice-Chairman—J. E. Draley
Secretary-Treasurer—C. V. King

The candidates were elected without dissent and were installed in office. The incoming Chairman spoke briefly of plans for the coming year.

Cecil V. King,
Secretary-Treasurer

Electrodeposition Division

The Electrodeposition Division held its Annual Business Meeting and Luncheon on Wednesday, October 12, 1955, at the Pittsburgh Meeting. Division Chairman Cloyd Snavely presided.

The first business was a report by Vice-Chairman Sidney Barnartt regarding plans for a joint symposium with the Theoretical Electrochemistry Division to be held at Cleveland in the fall

of 1956. The subjects to be covered are: structure of electrodeposits, kinetics of electrodeposition, and mass transfer in electrodeposition. A keynote speaker will be sought to introduce each of the three subjects. Dr. Barnartt discussed plans to bring at least one of the keynote speakers from Europe by special arrangement. Dr. Wm. Blum moved that a maximum of $500.00 of Divisional funds be made available to help defray the expenses of such a visitor. This was approved by the group, subject to later approval by the Society Board of Directors.

Other topics suggested for symposia at the fall meeting in 1956 are: "Protection of Metals Against High Temperature Oxidation" and "Electrolytic Production of Metal Powders." The Division officers will solicit papers on these topics.

Dr. Snavely reported that the income to the Division from the sale of the revised edition of "Modern Electroplating" was approximately $1,578.00 at the last accounting. This represents 40% of the total income to the Society, the other 60% accruing to the Society treasury.

Various proposed uses for the accumulating funds were discussed. Dr. Frederick Lowenheim suggested consideration of a second volume of "Modern Electroplating" to cover subjects other than both operation and composition. Dr. Leslie Lancy suggested an addendum to bring the revised "Modern Electroplating" up to date. To consider these possibilities, and other publication ventures which the group might undertake, a publication committee was appointed as follows: Frederick Lowenheim, Chairman, Dennis Turner, and Clarence Sample. One of the purposes of the committee is to consider publication and dissemination of technical material not now appearing in the bound JOURNALS.

Chairman Snavely suggested consideration of a Divisional newsletter and offered to try to arrange for starting one if the group so desired. This was approved. Newsletters will be sent to the Division members if and when material is available.

CLOYD A. SNAVELY, *Chairman*

SECTION NEWS

India Section

T. L. Rama Char has taken over as Secretary-Treasurer of the India Section in place of S. Krishnamurthy who has left Bangalore to join the Indian Standards Institution at New Delhi. The officers of the Section are as follows.

Chairman—M. S. Thacker
Vice-Chairman—S. Ramaswamy
Vice-Chairman—A. Joga Rao
Secretary-Treasurer—T. L. Rama Char, Indian Institute of Science, Bangalore 3, India
Representatives on Council of Local Sections—B. K. Ram Prasad and V. M. Dokras

T. L. RAMA CHAR, *Secretary-Treasurer*

New York Metropolitan Section

The first meeting of the season was held at Schwartz's Restaurant on October 20, 1955. It was a joint meeting of the Metropolitan Section and the International Nickel Company Resea Club.

The guest speaker for the evening was Dr. U. R. Evans of Cambridge, England, whose subject was "The Mechanism of Pitting." He stated that, before dealing with pitting, it would be necessary to consider the general field of corrosion. At high temperature metal scales, as the scale becomes thicker, the rate of formation decreases. The rate of scale formation decreases with temperature and at lower temperature the scale formed is thin enough to show interference colors. The scale formed at room temperature is usually too thin to see but can be detected by optical or electrochemical means.

At ordinary temperatures, electrochemical corrosion is important. The scale formed on metal at high temperatures tends to protect the metal from further oxidation. In electrolytic corrosion, since no electrical charge accumulates, corrosion is not stifled and can progress. The metal ions may form a loose precipitate and settle in the solution. The behavior of iron is more complex. The first ions formed are ferrous, and ferrous hydroxide is not stable but is fairly soluble. Ferrous ions may migrate some distance from the anodic area. Oxygen in the solution then oxidizes them and ferric hydroxide precipitates, often on unattached areas of the metal.

Corrosion only starts locally at spots when the physical structure of the metal is imperfect. When a sheet of zinc is exposed to a sodium chloride solution, corrosion starts at the edges where there are stresses, and at a few spots in the strip where there may be defects. Brown and Mears showed that the spots where corrosion would start could be predicted. The way in which local attack is connected with defects or irregularities in the metal surface was shown by Forsyth recently. He subjected a sheet of coarse grained aluminum to a slight deformation. A few slip bands formed and some of them were evident as small steps on the surface of the strip. When subjected to corrosive environment, pits formed at these steps. If the strip was electropolished, pitting did not occur. This shows that the surface irregularity, and not the slip band, was responsible for the attack.

There are two types of salts, those which are corrosive and those which are inhibitors. Consider a metal covered with a thin oxide film and with a point of disarray on the metal surface. A high energy atom may escape through the film, unite with oxygen, and cause a slight local thickening of the film. In a solution containing sodium chloride and abundant oxygen, metal can escape

JUNE 1956 DISCUSSION SECTION

A Discussion Section, covering papers published in the July–December 1955 JOURNALS, is scheduled for publication in the June 1956 issue. Any discussion which did not reach the Editor in time for inclusion in the December 1955 Discussion Section will be included in the June 1956 issue. Those who plan to contribute remarks for this Discussion Section should submit their comments or questions in triplicate to the Managing Editor of the JOURNAL, 216 W. 102nd St., New York 25, N. Y., *not later than March 1, 1956*. All discussions will be forwarded to the author, or authors, for reply before being printed in the JOURNAL.

through the film as ions, without an electrical charge accumulating. When the oxygen in the solution is low, metal can still pass into solution rapidly as ions from a small anodic area, since the cathodic area is very large. If, instead of sodium chloride, the solution contains sodium phosphate, the anodic area will be blocked. Oxygen in solution drives the phosphate ions to the site of attack. There they combine to form insoluble iron phosphate and the precipitate protects the area from further attack. Chlorides, which form soluble salts, increase the rate of solution of metal.

Dr. Evans described experiments where iron was corroded in a solution of sodium carbonate which was mildly corrosive. Corrosion started on a few favorite sites and new sites did not tend to develop. The active anodic area gave sacrificial protection to other possible sites. When the metal was treated so the active areas were healed, corrosion started at other sites.

The conditions for pitting of aluminum have been studied. It has been found possible to have pitting if the solution contains oxygen, chlorine, calcium bicarbonate, and a trace of copper. All of these constituents are often found in city water supplies. Calcium bicarbonate reacts with alkali formed, oxygen makes the anodic reaction possible, and chlorine forms a soluble salt. Copper is deposited around the anodic area and supplies a good cathodic area. It has been found that an aluminum surface is a rather inefficient cathode. Zinc does not usually pit, because the areas of attack spread out to produce a general type of corrosion. In distilled water, however, pitting does occur.

Dr. Evans showed some slides of examples of corrosion cracking. This type of corrosion was not discussed, since it was the subject chosen for a talk at Columbia University the following day. The talk was followed by a discussion period.

K. B. McCain,
Secretary-Treasurer

Ontario-Quebec Section

A Progress Report

1954–1955

Three excellent and well-attended meetings were held during the year. In June, 1954, when the Section was organized, the membership was 35. A year later it had increased to 63. Apparently it is being recognized that the Society is in a position to contribute greatly to the success of our Canadian electrochemical industries; also, that the extent of the contribution which the Society can make will depend on the size of its membership.

1955–1956

The officers and executive committee of the Section for this year are:

Officers

Honorary Chairman—A. F. G. Cadenhead
Chairman—P. J. Ensio
Vice-Chairman (Programs)—A. C. Holm
Vice-Chairman (Membership)—J. Sumner
Chairman, Junior Members Committee—J. U. MacEwan
Secretary-Treasurer—R. R. Rogers

Executive Committee

J. S. Dewar
G. Dodd
A. E. Edwards
N. F. Fasken
T. S. Gamble
L. J. Lichty
W. A. Schaeffer

At the November 18, 1955 meeting of the Section, H. H. Uhlig, President of the Society, spoke on "Corrosion as an Electrochemical Process," and W. C. Gardiner, Olin Mathieson Chemical Corp., spoke on "Brine Impurities and their Effect on the Operation of Caustic-Chlorine Cells."

The meetings for 1956 will be as follows:

February 10—P. E. Cavanagh, Ontario Research Foundation, "A Comparison between Electric and Other Types of Smelting"; a representative of Elektrokemisk, "Smelting of Fine Materials."

May 10—A symposium on "Canadian Power Resources."

The affairs of the parent Electrochemical Society are flourishing. At the end of 1954 the total membership was 2041. The size of the membership is important since it determines the number of technical papers which can be published in the Journal of the Society. These papers are largely in the battery, corrosion, electric insulation, electrodeposition, electronics, electro-organic, electrothermics, metallurgy, industrial electrolytic, and theoretical electrochemistry fields.

There has been a gratifying increase in the attendance at the general meetings of the Society. The attendance at the spring 1955 Cincinnati Meeting was well over 900. A total of 184 technical papers were presented at that time, which is an all-time record for the Society.

R. R. Rogers,
Secretary-Treasurer

Philadelphia Section

The first meeting of the new season, on November 2, 1955, was addressed by Dr. Harry Bloom, graduate of the University of Melbourne and the University of London. Dr. Bloom has been teaching at Aukland University College in New Zealand but is currently devoting a year to research at the University of Pennsylvania. His talk concerned the electrochemistry of molten salts and certain other physical chemical properties of these materials. Dr. Bloom stated that, heretofore, fused salts have been considered to be, at best, only slightly ionized. However, he feels that the unusually high electrical conductivity of many molten salts, especially the alkali and alkali earth halides, contradicts such a view and, in fact, indicates many of them to be nearly 100% ionized. Dr. Bloom conceives a molten salt as made up, perhaps, of simple ions, complex ions, molecules, and holes or spaces between these constituents. His researches, which he described in interesting detail, have been directed toward illuminating the structure of such systems by the study of the electrochemical and other physical properties of pure and mixed molten electrolytes.

A large audience revealed its interest in Dr. Bloom's work by the number of questions asked of the speaker at the close of his talk.

G. W. Bodamer, *Secretary*

San Francisco Section

The regular meeting of the Section was held on October 19, 1955 at the University of California Faculty Club. After dinner and a short business meeting, Dr. Leo Brewer, Professor of Chemistry at the University of California, delivered a talk entitled "New Refractories for Use in the Temperature Range 1500°–3000°K."

The talk was divided into two parts. In the first, Dr. Brewer briefly reviewed the application of electrostatic binding forces as applied to various combinations of atoms, in the light of their positions in the periodic chart. For a number of combinations of atoms, the properties of the resultant material could be predicted from the coulombic

binding forces, the heats of vaporization and ionization, and a knowledge of the lattice energy. For materials made from transition elements and an element like F, O, C, B, N, Si, the number of unpaired *d* electrons in the resultant material (the amount of metallic binding) must be taken into account as well as the coulombic forces.

In the second section of the report, Dr. Brewer pointed out that at high temperatures elements rarely combine in definite stoichiometric proportions, but rather a range of compositions, or solid solutions, exist in which properties change continuously with composition. He indicated that the properties of solid refractories will vary markedly with small changes in the composition of the material. He cited the example of $CeS_{1.50}$, and $CeS_{1.33}$. $CeS_{1.50}$ is an electrical insulator with poor thermal characteristics while $CeS_{1.33}$ is a good electrical conductor with good thermal properties. By varying the ratio of cerium to sulfur in these refractories, a whole range of properties between those exhibited by $CeS_{1.33}$ and $CeS_{1.50}$ could be obtained.

The talk was followed by a lively question and answer period.

BERNARD PORTER

Washington-Baltimore Section

The 34th technical meeting of the Section was held on October 20, 1955 at the National Bureau of Standards. This program was the first of a unique series planned for the year at each of which three different topics will be discussed, extending the scope of the meetings to include all Divisions of the Society. The programs are planned so that there will be a continuity of subject matter throughout a series of three consecutive meetings.

Dr. J. W. Case of the Bureau of Ordnance, U. S. N., spoke on the Preparation of Novel Types of Laminates. Two types of laminates were described, the first a lamination of woven glass fabric impregnated with resin, and the second similarly fabricated from a mat of nonwoven parallel glass fibers. Stress-strain measurements have shown that the strength of the nonwoven variety is superior to the woven fiber. Numerous specimens of the laminates were shown, illustrating the ease of fabrication and exceptional strength of these materials.

Dr. J. J. Lander of the U. S. Naval Research Laboratory spoke of Polarization and the Measurement of the Internal Resistance of the Lead Acid Cell. Dr. Lander described the several a-c and d-c techniques used for measurement of the internal resistance of large submarine storage batteries. Such measurements have indicated that the cause of the inadequacies of these data is concentration polarization occurring at the negative plate. It was concluded that this plate behaves as a lead, lead ion electrode polarized by a degree of supersaturation of lead ion determined by the diffusion rates of the several ionic species, and the rates of neucleation and growth of the lead sulfate crystals.

The third speaker of the evening was Dr. T. N. Yannakopoules, Guest Worker at the National Bureau of Standards from the University of Athens, Greece, whose topic was a Method of Isolating the Solution at the Cathode Interface; Calculation of Concentration Polarization. Dr. Yannakopoules described the necessity for the experimental approach to determination of the true concentration polarization at electrode surfaces, and the most recent technique used in such studies. A porous cup electrode was filled with an inert liquid matched in density to the electrolyte to eliminate the effect of hydrostatic pressure. The solution at the electrode surface passed through the porous wall, and the solution inside the cup was analyzed during polarization studies to determine changes in composition.

JEANNE BURBANK, *Secretary*

NEWS ITEMS

1955 Annual Index

The Annual Index for Volume 102 (1955) of the JOURNAL will appear in the February 1956 issue.

New Assistant Secretary Appointed

Robert K. Shannon has been appointed Assistant Secretary of the Society. Mr. Shannon will be in charge of the secretarial office and will report to the Secretary on all matters of business.

From 1923 to 1954 Mr. Shannon occupied executive staff positions with the National Paint, Varnish and Lacquer Association with headquarters in Washington, D. C. He was Director of the Association's Trademark Bureau for many years and also served as Convention Manager handling arrangements for its large annual meeting. He acted as Secretary of the Association for several years prior to retirement in order to return to his home city of New York.

Aluminum Centenary

The papers presented at the Aluminum Centenary celebration in September 1955 will be published, together with a special Directory of Aluminum, in the *Bulletin of the India Section of The Electrochemical Society*, Vol. 4, No. 4 (1955).

Symposium on Alloy and Special Steels

A symposium on "Production, Properties, and Applications of Alloy and Special Steels" will be held during February 1956 under the auspices of the National Metallurgical Laboratory at Jamshedpur.

T. L. RAMA CHAR,
Regional Editor, India

Nominations for 1956 Acheson Award

William Blum, Chairman of the Acheson Medal Award Committee, would like to receive suggestions for possible candidates for the next Acheson Medal Award, to be made in the fall of 1956.

The procedure to be followed by the membership, taken from the Rules Governing the Award of the Acheson Medal, is given below.

1. Nominations shall be accepted from the membership at large.

2. All nominations, whether made by a member of the Nominating Committee or by any other member of the Society, must be accompanied by a full record of qualifications of the nominee for the award. Such supporting documents from friends of the candidate or from his organization shall be in order.

3. The nominator must assume the responsibility for providing the Chairman of the Nominating Committee with nine copies of the supporting documents, one for each member.

Nominations must be sent to the Chairman not later than March 1 of the year in which the medal is awarded and nominations will be considered closed after that date.

All nominations of candidates for the medal shall be continued in force for a period of two consecutive awards of the medal. Any unsuccessful candidate may be renominated in the usual manner for any subsequent Medal award.

Correspondence should be addressed to William Blum, 2311 Connecticut Ave. N.W., Washington 8, D. C.

English Abstracts of Japanese Papers

The Electrochemical Society of Japan wishes to make its published technical papers available and understandable to English-speaking people throughout the world, and has decided on the following procedure as immediately practical: starting with the January 1956 issue, a full-page abstract in English will be added to all papers printed in Japanese, including translations of captions and legends for tables and figures.

The society is exploring the alternate possibility of publishing a quarterly 40-page journal in English, consisting of abstracts of technical papers printed in Japanese in the regular journal. This would be sold at a price which would defray most of the cost of publication (50¢ per issue has been suggested).

The society would like to know how many subscribers it might expect for such a quarterly journal in the United States, and would also welcome comments on the plan it is actually adopting for 1956. Communications should be addressed to: Dr. Kiichiro Sugino, The Electrochemical Society of Japan, 3, 1-Chome, Yurakucho, Chiyodaku, Tokyo, Japan.

Science Grants and Awards

The National Science Foundation has awarded 18 postdoctoral fellowships for advanced study and research in the natural sciences, under a second award period for postdoctoral fellowships which was inaugurated for the first time in the autumn of 1955. Of the awards announced, 8 were in the life sciences, 3 in chemistry, 1 in engineering, 3 in mathematics, and 3 in physics. These fellowships are in addition to the 715 predoctoral and 70 postdoctoral awards announced by the Foundation in March 1955.

Fellows may attend any accredited nonprofit institution of higher learning in the United States or any similar institution abroad approved by the Foundation. They are permitted to select tenures ranging from six months to 24 months.

The National Science Foundation postdoctoral fellowships carry a stipend of $3,400 with additional allowances for dependents, tuition, and other normal expenses. Results of research carried out by a Fellow during his training may be made available to the public without restriction, except as required in the interest of national security.

Application forms may be obtained from the Fellowship Office, National Research Council, 2101 Constitution Avenue, N. W., Washington 25, D. C.

The National Science Foundation has announced 225 grants totaling about $3,458,140 awarded during the quarter ending September 30, 1955, for the support of basic research in the natural sciences, for conferences in support of science, and for exchange of scientific information. This is the first group of awards to be made during fiscal year 1956. Since the beginning of the program in 1951, over 1,875 such awards have been made, totaling about $20,838,640.

Grants have been made to institutions and scientists in many of the 48 states, Canada, France, and the Netherlands. The research fields included are anthropology, astronomy, chemistry, developmental biology, earth sciences, engineering sciences, environmental biology, genetic biology, mathematical sciences, molecular biology, physics, psychobiology, regulatory biology, and systematic biology.

The research grants were approved by the National Science Board upon the recommendation of Dr. Alan T. Waterman, Director of the Foundation.

Engineering Foundation, New York City, which administers the income from a $1,500,000 fund dedicated to the stimulation of engineering research, has made available its allocations for the 1955–1956 fiscal year. This year's grants total $61,850. They will advance 26 projects, which are receiving estimated outside support of $426,000. The projects, which cover a wide range of research, are being carried out in university laboratories all over the country under sponsorship of the major engineering societies.

Grants are also being made to eight projects under sponsorship of the American Institute of Mining and Metallurgical Engineers. These AIME projects include a newly instituted program for predicting disastrous Storm Surges, which is getting under way at Columbia University's Lamont Laboratories at Palisades, N. Y.

Volumes Wanted

Will anyone who has a copy he no longer needs of Vol. 86 (1944) and 92 (1947) of the TRANSACTIONS please contact Toshio Keta, 4307 Sheridan St., University Park, Hyattsville, Md.

Pennsalt Organic Fluorine Chemicals Plant

The addition of a large organic fluorine chemicals plant at Calvert City, Ky., will inaugurate the Pennsylvania Salt Manufacturing Company's projected expansion program, President William P. Drake has announced.

The new unit will become a major component of Pennsalt's closely integrated chlorine-fluorine production facilities on the Tennessee River. Its initial products will serve the growing refrigerant and aerosol-propellant fields. Future products from this plant and related facilities at the same location are expected to find uses in new and improved plastics, lubricants, metal fluxes, anesthetics, ceramics, agricultural chemicals, and new applications in the growing field of atomic energy.

(Continued on last page of Reader Service Page)

NEW MEMBERS

In November 1955 the following were approved for membership in The Electrochemical Society by the Admissions Committee:

Active Members

ROBERT BAKISH, Sprague Electric Co.; Mail add: 42 Cherry St., North Adams, Mass. (Corrosion)

GEORGE J. BAUMBACH, JR., Sperry Gyroscope, Inc.; Mail add: 93 Shore Blvd., Lindenhurst, N. Y. (Electric Insulation)

JACK BELLE, Westinghouse Atomic Power Div., Bettis Field, P. O. Box 1468, Pittsburgh, Pa. (Corrosion)

HOWARD B. BOMBERGER, JR., Rem-Cru Titanium, Inc.; Mail add: Box 162, R. D. 2, East Liverpool, Ohio (Corrosion)

BORIS N. BOURKE, Yardney Electric Corp.; Mail add: 147 W. 86 St., New York 24, N. Y. (Battery)

GEORGE COMENETZ, Westinghouse Research Labs., Beulah Rd., Churchill Borough, Pittsburgh 35, Pa. (Electrothermics & Metallurgy)

A recent action of the Board of Directors of the Society requires that, commencing January 1, 1956, all prospective members include first year's dues with their applications for membership.

Also, please note that, if sponsors sign the application form itself, processing can be expedited considerably.

WILLIAM S. CORAK, Semiconductor Dept., Westinghouse Electric Corp., 356 Collins Ave., Pittsburgh 6, Pa. (Electronics)

R. A. DAY, JR., Chemistry Dept., Emory University, Ga. (Electro-Organic)

GEORGE A. ELLINGER, National Bureau of Standards, Washington 25, D. C. (Corrosion)

ROBERT F. ENTERS, Yardney Labs., Inc.; Mail add: 42 Elm Ave., Hackensack, N. J. (Battery)

JOSEPH C. FISHER, JR., National Carbon Research Labs., P. O. Box 6056, Cleveland, Ohio (Electrothermics & Metallurgy)

WILLIAM FOWLER, Doehler-Jarvis Div. of National Lead Co., Plant #2, Smead and Prospect, Toledo, Ohio (Electrodeposition)

SHERMAN GREENBERG, Argonne National Lab., P. O. Box 299, Lemont, Ill. (Corrosion)

PAUL M. GRUZENSKY, Northwest Electrodevelopment Lab., U. S. Bureau of Mines; Mail add: Rt. 1, Box 260-A, Corvallis, Oreg. (Electrodeposition)

ARTHUR T. HALPIN, JR., Sylvania Electric Products Inc.; Mail add: 1321 E. 53 St., Brooklyn 34, N. Y. (Electronics)

ANDREW HERCZOG, Central Engineering, P. R. Mallory & Co., Inc., Indianapolis 6, Ind. (Electric Insulation, Electronics, Electrothermics & Metallurgy)

JAMES P. HOARE, Naval Research Lab.; Mail add: 239 Hawaii Ave., N. E., Washington 11, D. C. (Theoretical Electrochemistry)

ALBERT O. HOFFMAN, JR., Electro Metallurgical Co., Mail add: 8472 W. Rivershore Dr., Niagara Falls, N. Y. (Electrothermics & Metallurgy)

W. B. HUGLE, Baldwin Piano Co.; Mail add: R. R. 1, Box 145-8, Newtown, Ohio (Electronics)

EDWIN W. JOHNSON, Westinghouse Electric Corp., Westinghouse Research Labs., Pittsburgh 35, Pa. (Electrothermics & Metallurgy)

HERBERT KAY, Climax Molybdenum Co., 500 Fifth Ave., New York 36, N. Y. (Corrosion)

DAVID T. LAPP, Norton Co.; Mail add: P. O. Box #291, Chippawa, Ont., Canada (Electrothermics & Metallurgy)

THOMAS R. LAWSON, JR., Westinghouse Electric Corp.; Mail add: 536 Windsor Ave., Pittsburgh 21, Pa. (Electronics)

WILLIAM T. LIPPINCOTT, Kedzie Chemical Lab., Michigan State Univeristy, East Lansing, Mich. (Electro-Organic)

WILLIAM G. MARANCIK, Air Reduction Research Lab., Murray Hill, N. J. (Electrothermics & Metallurgy)

RICHARD MCDONALD, Gillette Safety Razor Co.; Mail add: 98 Crescent Ave., Scituate, Mass. (Corrosion)

JOHN W. MCGREW, Mutual Chemical Div., Allied Chemical & Dye Corp.; Mail add: 1348 Block St., Baltimore 31, Md. (Battery, Corrosion, Electrodeposition)

HERBERT E. MCMILLAN, National Carbon Co., P. O. Box 6056, Cleveland, Ohio (Battery)

CARL A. PITHA, Sylvania Electric Products Inc.; Mail add: 74 Pierce Rd., Watertown 72, Mass. (Electronics)

WILLIAM PONG, The Baldwin Piano Co., 1801 Gilbert Ave., Cincinnati, Ohio (Electronics)

ERNEST R. RAMIREZ, Reynolds Metals Co., Richmond, Va. (Corrosion, Electric Insulation, Electrodeposition, Theoretical Electrochemistry)

MERVIN E. RUNNER, Dept. of Chemistry, Illinois Institute of Technology, 3300 S. Federal St., Chicago 16, Ill. (Electro-Organic)

J. K. SARGENT, Jones & Laughlin Steel Corp.; Mail add: 639 Hall St., Aliquippa, Pa. (Corrosion, Electrodeposition)

GEORGE H. SCHIPPEREIT, Battelle Memorial Institute, 505 King Ave., Columbus, Ohio (Electrodeposition)

RALPH J. SCHNEIDER, Bell Aircraft Corp.; Mail add: Box 143, Wilson, N. Y. (Battery, Electric Insulation, Electronics)

ROBERT E. SHEARER, Union Switch & Signal, Div. of Westinghouse Air Brake Co., Pittsburgh 18, Pa. (Electronics)

ROBERT C. SOMMER, Central Research Lab., American Smelting & Refining Co., South Plainfield, N. J. (Electrodeposition)

HAROLD C. TEMPLETON, Lebanon Steel Foundry, Lebanon, Pa. (Corrosion, Electrothermics & Metallurgy)

WILLIAM E. TRAGERT, General Electric Research Lab., P. O. Box 1088, Schenectady, N. Y. (Corrosion)

JAMES K. TRAITT, The Texas Co.; Mail add: 158 N. Walnut St., Beacon, N. Y. (Corrosion)

WILLEM J. VAN DER GRINTEN, Electronics Lab., General Electric Co., Electronics Park, Syracuse, N. Y. (Battery, Theoretical Electrochemistry)

PQ Potassium Silicate Binders
for all Picture Tube Formulas

• Kasil 1 is a clear solution, molecular ratio 1:3.9, 28° Be. Its high quality is uniformly maintained. Excellent performance with sodium and potassium sulphate.

Kasil 22 also a specially clarified potassium silicate has a closely controlled ratio (molecular) of 1:3.4. Kasil 22 is adapted for formulas including barium salts which require less settling time and give good gel strength before baking.

These electronic silicates are available for delivery in packages or in tank cars. In cold weather, drums are shipped in heated trucks and tank cars are specially insulated.

PHILADELPHIA QUARTZ COMPANY
1156 Public Ledger Bldg., Phila. 6, Pa.

1831—125TH ANNIVERSARY—1956

PQ Soluble Silicates

Trademarks Reg. U.S. Pat. Off.

JOHN WAGNER, JR., A. V. Smith Engineering Co.; Mail add: 3343 West School House Lane, Philadelphia 44, Pa. (Corrosion)

PEI WANG, Sylvania Electric Products Inc., Woburn, Mass. (Electrodeposition, Electronics)

G. WORDEN WARING, Raytheon Manufacturing Co., 55 Chapel St., Newton 58, Mass. (Electronics)

MOE S. WASSERMAN, Sylvania Electric Products Inc., 35-22 Linden Place, Flushing 54, N. Y. (Electronics)

GERALD C. WHITNACK, Naval Ordnance Test Station; Mail add: 58 B. Rodman St., China Lake, Calif. (Electro-Organic)

JOHN W. WOOD, E. F. Drew & Co., Inc., 416 Division St., Boonton, N. J. (Corrosion)

Student Associate Members

EDWARD F. DUFFEK, Carnegie Institute of Technology; Mail add: 205 W. Swissvale Ave., Pittsburgh 18, Pa. (Corrosion, Theoretical Electrochemistry)

S. K. PANIKKAR, Dept. of General Chemistry, Indian Institute of Science, Bangalore 3, India (Electrodeposition)

JAWAHARLAL VAID, Dept. of General Chemistry, Indian Institute of Science, Bangalore 3, India (Electrodeposition)

RICHARD A. WHITE, Massachusetts Institute of Technology; Mail add: 67 Inman St., Cambridge, Mass. (Corrosion)

Reinstatements to Active Membership

CHARLES S. LOWE, National Plant, National Carbon Co., Niagara Falls, N. Y. (Industrial Electrolytic)

LAWRENCE M. LIGGETT, Speer Carbon Co., St. Marys, Pa. (Electrothermics & Metallurgy, Industrial Electrolytic)

ARTHUR M. LINN, Metal & Thermit Corp.; Mail add: 6428 22nd Ave., Kenosha, Wis. (Electrodeposition)

Reinstatement and Transfer from Associate to Active Membership

GEORGE SKELLY, North American Aviation; Mail add: 787A Franklin, Columbus 5, Ohio (Corrosion, Electrodeposition)

New Sustaining Members

DOEHLER JARVIS DIV., NATIONAL LEAD Co., 525 Cottage Grove, S. E., Grand Rapids 2, Mich. (Representative: Mr.

Now!

THE 1954 ISSUE OF

ABSTRACTS of the LITERATURE of SEMICONDUCTING and LUMINESCENT MATERIALS and THEIR APPLICATIONS

Compiled by the Battelle Memorial Institute and Sponsored by The Electrochemical Society, Inc.

Here—usefully assembled and collated for you in a single volume—are the year of 1954's literature references to semiconducting and luminescent materials, their properties and their applications.

If you're in any of the fields like transistor electronics, this book can do a valuable job for you. It brings to your attention recent literature of interest and points up the similarities between work you may be doing and what others in related fields are doing.

You'll find each abstracted article described in detail. For example, 53 pages (over 220 abstracted articles) are devoted to germanium and silicon. *The entire volume contains over 750 abstracted articles.*

You'll find that this comment from Electronic Design about the first book in the new series—applies equally to the 1954 Issue:

"The library of every electronic design laboratory that deals with semiconductors or tubes incorporating luminescent materials should include this volume."

1954 Issue—200 pages. 8½ by 11. Handy spiral binding. $5.00

1053 Issue—169 pages. $5.00

Send Coupon Today for Your ON-APPROVAL Copies

JOHN WILEY & SONS, Inc. JES-16
440 Fourth Ave., New York 16, N. Y.

Please send me the book(s) checked below to read and examine ON APPROVAL. Within 10 days I will return the books and owe nothing, or will remit the purchase price(s), plus postage.

☐ Abstracts of the Literature of Semiconducting and Luminescent Materials 1954 Issue, $5.00

☐ Abstracts of the Literature of Semiconducting and Luminescent Materials 1955 Issue, $5.00

NAME

ADDRESS

CITY ZONE STATE

☐ SAVE POSTAGE! Check here if you ENCLOSE payment, in which case we pay postage. Same return privilege. Add 3% City Sales Tax for New York City orders.

Maurice R. Caldwell, Manager, Electroplating & Finishing)

THE CARBORUNDUM CO., Niagara Falls, N. Y. (Representative: Dr. G. M. Butler, Manager, Research Dept.)

Deceased Members

HENRY A. DOERNER, San Francisco, Calif.

R. E. ZIMMERMAN, Short Hills, N. J.

LETTERS TO THE EDITOR

Dear Sir:

I read the fine editorial on Josiah Willard Gibbs and The Hall of Fame in the October 1955 JOURNAL and was surprised to learn that the pedestal to receive the bronze bust of this great scientist of our profession is still empty because of lack of funds. With a sense of personal and collective humiliation I am enclosing a check for $25 as a contribution to The Electrochemical Society Gibbs Fund.

JULES BEBIE
Saint Louis, Mo.

Communication on "Quotes"

Dear Sir:

"Electrochemistry," says a well-known textbook,[1] "...owes its birth to the discoveries of Volta which culminated in the invention of the voltaic pile toward the end of the eighteenth century."

On the contrary, electrochemistry is one of the oldest of our sciences, the pre-Volta literature abounding in references to its theory and practice. The following random citations are offered by way of example.

"...a plate of pure gold"
Exodus, Chap. 28, Verse 36

"The length of the arc shall be three hundred cubits"[2]
Genesis, Chap. 6, Verse 15

"If gold ruste, what shal iren do?"
G. CHAUCER, "Canterbury Tales," Prologue, line 500

"Put you in this pickle"[3]
M. CERVANTES, "Don Quixote," Chap. 5

"And enterprises of great pith and moment with this regard their currents turn awry"
W. SHAKESPEARE, "Hamlet," Act III, Sc. 1, line 56

"You pay a great deal too dear for watts given freely"
Id., "The Winter's Tale," Act I, Sc. 2, line 92

"There is wisdom in this beyond the rules of physics"[4]
FRANCIS BACON

"Watts done we partly may compute, but know not watts resisted"
ROBERT BURNS

Even the principles of the battery, both primary and secondary, seem to have been understood well before Volta's time, thus:

"And he straitly charged them..."
Mark, Chap. 3, Verse 12; *Luke*, Chap. 9, Verse 21

"Alle gute Dinge sind drei[5]"
Mediaeval German proverb

"Discharged, perchance, with greater ease than made."
FRANCIS QUARLES, ca. 1640

No doubt members of the Society will find additional proofs of the ancient origins of Electrochemistry.

(Signed) VERITAS

[1] H. JERMAIN CREIGHTON, "Principles and Applications of Electrochemistry," Vol. I (Principles), 4th Ed., p. 1, John Wiley & Sons, Inc., New York (1943).

[2] *Cf. also*, "Uzzah put forth his hand to the arc ... and there he died ...." *Samuel, II*, Chap. 6, Verse 6, 7

[3] *Cf. also*, W. SHAKESPEARE, "The Tempest," Act V, Sc. 1, line 282.

[4] "Throw physics to the dogs: I'll none of it"
Id., "Macbeth," Act IV, Sc. 3, line 37

[5] Note archaic spelling.

EMPLOYMENT SITUATIONS

Please address replies to box shown, c/o The Electrochemical Society, Inc., 216 W. 102nd St., New York 25, N. Y.

Positions Available

PATENT OFFICE EXAMINERS. Engineers and scientists are needed immediately as Patent Examiners by the U. S. Patent Office, Washington, D. C. Patent Examiners pass upon applications for patents in a wide range of technical fields. The job keeps them in close touch with the latest developments in these fields. Salaries start at $4,345 per year and it is possible to reach $7,570 in 5½ years. Vacations and sick leave and pension benefits are liberal. The positions call for a college degree in engineering or applied science or a college degree with a major in chemistry or physics or with certain combined credits in these fields. There is no examination. For further information, address the Commissioner of Patents, Washington 25, D. C.

ENGINEERS, ELECTRONIC SCIENTISTS, METALLURGISTS, PHYSICISTS, PHYSIOLOGISTS, PSYCHOLOGISTS, TECHNOLOGISTS. The Naval Air Material Center, located at the Naval Base, Philadelphia, Pa., has vacancies in the above engineering and scientific positions which must be filled. The Center is engaged in an extensive program of aeronautical research, development, experimentation, and test operations for the advancement of Naval Aviation. Engineering vacancies exist in the following options: Electrical, Electronics, General, Industrial, Mechanical, Structural, and Aeronautical (various suboptions). Starting salaries range from $3670 to $8990 per annum. Application for Federal Employment, Standard Form 57, should be filed with the Industrial Relations Dept., Naval Air Material Center, Naval Base, Philadelphia 12, Pa. Applications may be obtained from the above address or information as to where they are available may be obtained from any first or second class post office.

Positions Wanted

CHEMIST, 36, 11 years' experience, including batteries, electroplating, general physical and chemical commerical testing, seeks New Jersey, Philadelphia, New York City position. *Reply to Box 357.*

CHEMICAL ENGINEER, 40, B.S. degree, 14 years' experience, including materials engineering and research, electrodeposition processes, product engineering and development work involving capacitors. *Reply to Box 358.*

ADVERTISERS' INDEX

Bell Telephone Laboratories, Inc.	7C
Enthone, Incorporated	Cover 4
Great Lakes Carbon Corporation	Cover 2
Philadelphia Quartz Company	20C
Rapid Electric Company	8C
E. H. Sargent & Company	4C
Stackpole Carbon Company	2C
John Wiley & Sons, Inc.	21C

Journal of the
Electrochemical Society

Literature and New Products

LITERATURE FROM INDUSTRY

CHLORINATOR CATALOGUE. Recently published Catalogue 70-10 illustrates and describes F&P corrosion-resistant chlorination instruments, including: Figure 1050A Chlorinator, high capacity chlorinator (8000 lb/day), chlorine solution distribution panel, hypochlorinator, flow indicating recorder, immersed float vacuum transmitter. Fischer & Porter Co. P-364

HIGH-SPEED POTENTIOMETER. Bulletin describing the new High-Speed Recording Dynamaster Potentiometer has been released. The recorder has a full-scale pen-travel across its 11-in. calibrated chart of only 0.4 sec, without overshoot on long or short traverses. Also featured is a sample chart showing the dynamic characteristics of the instrument. The Bristol Co. P-365

"QUICK-SEAL COUPLINGS." Revised catalogue on the Quick-Seal line of quick connect-disconnect hose couplings features views of the coupling which reveal its unique design and construction. Also described are single-check valve and double-check valve modifications of the coupling. Included are tables and diagrams to facilitate ordering. Titeflex, Inc. P-366

CONSTRUCTION MATERIALS. Fully illustrated catalogue describes Haveg Corp.'s complete line of corrosion-resistant equipment. It features new materials of construction and evaluates equipment molded from polyvinyl chloride, epoxy glass, and polyester glass, at the same time giving data on their resistance to chemicals and heat. Haveg Corp. P-367

DOW PRODUCTS CATALOGUE. A new general products catalogue containing more than 350 basic industrial, agricultural, and pharmaceutical chemicals has been published. Property information is presented in tabular form, along with general use information. A separately printed index, listing each chemical by catalogue name and by synonyms, is provided. The Dow Chemical Co. P-368

LABORATORY APPARATUS. 44-page illustrated Catalogue 55D shows the complete line of laboratory equipment manufactured by Eberbach. This book features the firm's lab shakers, "Hollow Spindle" stirrers, electroanalyzers, slide cabinets, and other apparatus. Eberbach Corp. P-369

PRECISION VOLTAGE DIVIDER. Complete information about L&N's "Precision Voltage Divider" is available is a new data sheet. Included in the sheet are photographs and a line drawing of the Voltage Divider and its circuit. A listing of specifications, accessories, and special voltage dividers is included. Leeds & Northrup Co. P-370

MOLYBDENUM CHEMICAL SYMPOSIUM. First comprehensive review of industrial applications of molybdenum chemicals has been published by the American Chemical Society and is available in reprint form from Climax Molybdenum Co. Comprising 7 different papers, the survey details molybdenum's wide use in diverse chemical fields, and points to new industrial applications resulting from the present increased tempo of molybdenum research. Climax Molybdenum Co. P-371

FISHER CATALOGUE SUPPLEMENT. New Fisher Catalogue Supplement describes, in just over 100 pages, all of the instruments, apparatus, glassware, laboratory furniture, and accessories added to Fisher stocks since the 1952 publication of the major Fisher Catalogue. Fisher Scientific Co. P-372

HORSE HEAD® BULLETIN. Latest issue features a story on a new metal protective paint containing 100% zinc dust and possessing rust inhibitive properties similar to those of the zinc coating on galvanized steel. Another article reports on the progress of the powder metallurgy industry. New Jersey Zinc Co. P-373

LAQUA. Brochure is available on LAQUA, Fidelity's new coating for metals that preserves chemically cleaned

(*Continued on next page*)

It's for You ▶

Send in this postage paid card for further information on the

"LITERATURE FROM INDUSTRY"
and
"NEW PRODUCTS"

listed briefly on the accompanying pages.

Please send manufacturers data on items in January issue indicated by numbers circled:

P-351	P-352	P-353	P-354	P-355	N-223	N-224	N-225	N-226	N-227
P-356	P-357	P-358	P-359	P-360	N-228	N-229	N-230	N-231	N-232
P-361	P-362	P-363	P-364	P-365	N-233	N-234	N-235	N-236	N-237
P-366	P-367	P-368	P-369	P-370	N-238	N-239	N-240	N-241	N-242
P-371	P-372	P-373	P-374	P-375	N-243	N-244	N-245	N-246	N-247

I'd like to have information about products advertised:

By _____
By _____
By _____

Name _____

Address _____

City _____ **State** _____

Title _____

surfaces obtained directly after electroplating or a chemical cleaning operation. Illustrated are LAQUA's many applications in the metal working, electrical, and electronic industries. Fidelity Chemical Products Corp. P-374

NEW PRODUCTS

STAINLESS STEEL FILTERS. A new line of porous stainless steel filters, Poro-Klean, is being produced. The product makes it possible to filter under unusually severe conditions. Physical properties of Poro-Klean elements are: tensile strength (ultimate), 9000–25,000 psi; per cent of elongation (ductility), 3–6%; per cent of porosity, 30–50%. The Cuno Engineering Corp. N-235

WAFER THERMISTORS. A complete series of wafer-type thermistors, suited for temperature compensation of transistors and other temperature dependent devices, is available. The elements are stocked in a complete range of resistance from ohms to megohms, and are available with extremely high temperature coefficients. Thermistor Corp. of America. N-236

MICROVOLT-AMMETER. Model 203 d-c microvoltmeter-ammeter is capable of making accurate measurements of voltages as small as 10 μv and currents as small as 1 $\mu\mu$a. Fifteen voltage ranges cover from 100 μv full scale to 1000 v full scale. Ten current ranges from 100 $\mu\mu$a full scale to 100 ma are provided. Kay Lab. N-237

RADIATION SHIELDING BRICKS. New product, called Raysist Shielding Logs, offers many advantages over conventional lead shielding bricks: weight savings, cost savings, elimination of all vertical radiation leakage, contamination control, simplified shield layout and construction, structural integrity, reduced handling and inventory. Knapp Mills, Inc. N-238

CHEMICAL WIRE STRIPPER. Chemclean #493, an economical stripper simple in operation and nonflammable, chemically removes Formvar, Formex, Isonel, and baked enamel coatings from wire, eliminating mechanical breakage and distortion. It will also remove various other organic finishes and may be used on vertical and overhead surfaces. Chemclean Products Corp. N-239

CERAMIC GRINDING PLATES. To fill the need for chemical, rock, and mineral pulverizing that would produce samples practically free of any contamination, the new Bico Ceramic Pulverizing Plates, made of alumina ceramic, have been developed and tested. According to a test made, the plates were found to produce 100-mesh samples practically zero in contamination. Bico, Inc. N-240

ULTRAPURE REAGENTS. A line of ultrapure chemicals has been developed to help remove the last area of guesswork in spectrophotometry. These "Spectranalyzed Reagents" (Fisher trademark) are all tested on Warren Spectracords, and each bottle bears a facsimile of the actual curve for the 220–360 mμ range. The reagents include acetone, carbon tetrachloride, chloroform, cyclohexane, methyl alcohol, methylene chloride, and isopropyl alcohol. Fisher Scientific Co. N-241

News Items

(Continued from page 19)

ECS Books Available

The following series of books, developed and sponsored by The Electrochemical Society and published by John Wiley & Sons, Inc., 440 Fourth Ave., New York 16, N. Y., is available.

Members of the Society who wish to obtain any of the books at the 33⅓% ECS member discount should send their orders to The Electrochemical Society, Inc., 216 W. 102nd St., New York 25, N. Y. The Society will then forward the orders to John Wiley & Sons, Inc., who will ship the volume with the invoice. To receive the member discount, *orders must* be sent to Society Headquarters.

"Modern Electroplating," edited by Allen G. Gray. Published 1953, 563 pages, $9.50.

"Electrochemistry in Biology and Medicine," edited by Theodore Shedlovsky. Published 1955, 369 pages, $10.50.

"Vapor-Plating; The Formation of Metallic and Refractory Coatings by Vapor Deposition," by C. F. Powell, I. E. Campbell, and B. W. Gonser. Published 1955, 158 pages, $5.50.

"Corrosion Handbook," edited by Herbert H. Uhlig. Published 1948, 1188 pages, $15.00.

"Abstracts of the Literature on Semiconducting and Luminescent Materials and Their Applications," compiled by the Battelle Memorial Institute. *1953 Issue*—published 1955, 169 pages, $5.00. *1954 Issue*—published 1955, 200 pages, $5.00.

Also available is the book entitled "Vacuum Metallurgy; Papers Presented at the Vacuum Metallurgy Symposium of the Electrothermics and Metallurgy Division of The Electrochemical Society, October 6 and 7, 1954, Boston, Massachusetts," sponsored and published by the Electrothermics and Metallurgy Division of the Society. Published 1955, 216 pages, $5.00. Copies of this book in hard paper binding can be obtained from *Society Headquarters*. Society members receive a 20% discount.

Postage Will be Paid by Addressee

No Postage Stamp Necessary If Mailed in the United States

BUSINESS REPLY CARD

FIRST CLASS PERMIT NO. 60024, SEC. 34.9 P. L. & R., NEW YORK, N. Y.

Journal of the Electrochemical Society

216 West 102nd Street

New York 25, N. Y.